A STUDY OF MICROSTRUCTURAL CHANGES IN SYNTHETIC FIBRES RESULTING FROM MECHANICAL DEFORMATIONS

By

Varvara A. Kvaratskheliya

Thesis submitted in partial fulfilment of the requirements for the degree of Doctor of Philosophy

De Montfort University

April, 2001

This thesis is dedicated to

the memory of Pr. O.I. Nachinkin

ABSTRACT

This investigation examines the structure-property relationships of high modulus fibres. Five fibre classes were chosen for examination. These are p-aromatic copolyamide (Armos and SVM) and poly-p-aramids (Terlon and Kevlar) obtained from rigid chain polymers; poly-m-aramids (Phenylon and Nomex) obtained from semi rigid chain polymers, and aliphatic polyamide (Capron and Nylon) and Polyethylene obtained from flexible chain polymers.

The thermo-mechanical properties studied include tensile properties, thermal shrinkage, creep-recovery, stress-relaxation and residual deformation over a range of temperatures.

Results show that mechanical properties are highly related to chain rigidity, orientation and crystallinity of the fibres. The presence of aromatic rings in polymer chains increase the polymer rigidity. The higher the intermolecular attractive force and chain rigidity, the greater the resistance to heat. Study of the creep-recovery properties of polyamide fibres shows that irrecoverable residual deformation for the rigid chain polymers is accumulated within a very short initial period of time (15 seconds) when the load is applied. However for semi-rigid or flexible chain polymer fibres, the residual deformation is accumulated during the whole creep process. The characteristics of tensile stress-strain properties and the accumulation of residual deformation are found to be temperature dependent, especially in the case of Armos and SVM.

The mechanical properties of polyamide fibres are also influenced by moisture which is associated with intermolecular interaction.

Supplementary studies using FTIR, SEM and DSC were also undertaken. FTIR was used for preliminary investigation into the intermolecular hydrogen bonding and associated moisture in fibres. The results support the explanation of the thermo-mechanical properties of polyamide fibres. SEM results show the fibre rupture mechanism related to the fibre structures.

CONTENTS

LIST OF FIGURES

LIST OF TABLES

Acknowledgements

I am very grateful to the following people for their help and advice during this work:

At De Montfort University:

My supervisors Dr. Jinsong Shen and Dr. Jane Wyatt for their suggestions, discussions and hours of reading and correcting of my thesis.

Prof. Ray Harwood for providing an opportunity to study at De Montfort University

Norma Garrington for kind permission their with experimental work to obtain FT-IR and DSC spectra, and for useful discussion.

Ian Fletcher for kind permission to accomplish experimental work to obtain SEM pictures, and for his help throughout experiment.

At Saint-Petersburg State University of Technology and Design:

My supervisor Dr. E.S. Tsobkallo for her support, patience, understanding and kind help during almost four years.

Prof. V.G. Tiranov for providing an opportunity to carry out my PhD research and his support throughout this work.

Prof. K.E. Perepelkin, Prof. S.F. Grebennikov and Dr. O.A. Andreeva for their useful discussions.

I am also very grateful to the following companies for provision of samples for successful completion of this research project:

J.-S. Co Klinvolokno, Russia; VNIISV, Tver, Russia; VNIIPolymervolokno. J.-S. Co Tverchimvolokno, Russia; VNIIPolymervolokno. J.-S. Co St.Petersburg NIIChimvolokno, Russia; VNIIPolymervolokno, Russia; VNIITverchimvolo, Russia; and Dupont de Nemour, USA.

INTRODUCTION

Fibres and fibrous materials play an important role in our life. They not only provide requirement of the man for clothes, but also are widely applied in various household and technical products. Polyamide fibres/yarns occupy a special place among all chemical fibres, because these types of fibres, especially aromatic polyamide fibres can be used for special purposes due to their range of unique properties. Special attention is given to their high and super high mechanical and thermal properties. Significant increasing applications of high performance fibres and yarns are found in various areas of industry, in both textile products for technical purposes and reinforcing elements of constructional materials. Polyamides such as Kelvar, Armos, Terlon, Nomex, and Phenylon are of particular interest as initial raw material for the production of high strength high modulus and heat resistant fibres and yarns. There are increasingly interests for the development of polyamide fibres in order to further expand the range of properties to meet consumer requirements. These fibres, yarns and their products are intended, first of all, for use in conditions of high temperatures and loads. The major parameters of these fibres are: high strength, rigidity and thermal resistance. Thus, the study of these properties in extreme conditions is very important.

It is known that the mechanical properties of fibres depend highly on their structure. One of the main factors contributing to change in these properties is the accumulation of residual deformation. It is noticed that, despite an abundance of literature on the study of deformation and strength properties of these fibres, there are few publications related to the residual component of deformation. Therefore a study of structural changes occurring in the process of deforming of fibres is of importance and forms the main field of investigation in this study.

Objectives

This research investigates the relationship between structures of polyamide fibres and their deformation properties. Hydrogen bonds and Van der Waals forces play very important role

in fibre strength properties. They also significantly influence their deformation. In order to analyse intermolecular interaction contribution in the mechanical characteristics experiments were carried out on the typical types of polyamide and polyethylene fibres; mechanical properties were strongly influenced by their intermolecular interaction: hydrogen bonds and Van der Waals forces.

Summary of the experiments described in this thesis

The Aromatic polyamide is distinctly different in properties from the conventional aliphatic polyamide. There are two types of commercially successful aramids available which can be classified as high-performance fibres. They are para-aramid such as Terlon and Kevlar, and meta-aramid such as Phenylon. In the present work, polymer fibres of varying chain rigidity were chosen as objects of research. These were Terlon, Armos and SVM, formed from rigid chain polymers; Phenylon, formed from semi-rigid chain polymers; and Capron, formed from flexible chain polymers. These fibres represent a wide range of chain rigidity, orientation and crystallinity.

In the experiments described in Chapter 3, tensile stress-strain properties of these yarns were determined. The tangent modulus was analyzed in order to classify the deformation for these fibres. Preliminary stretching is an important factor affecting the mechanical properties of polyamide fibres. The mechanical properties during creep - relaxation process of these fibres are very important to the aromatic fibres, because these fibres are often used under some load over long period of time. Their residual deformations after creep-relaxation were analysed. The relationship between the mechanical properties of these fibres and their structure was discussed.

Chapter 4 studied the mechanical properties of the gel-spun high strength, high modulus Polyethylene yarn, because Polyethylene fibres are different from aliphatic polyamide fibre due to their different type of intermolecular interaction. The intermolecular interaction for polyethylene is defined by Van der Waals bonds, which are weaker than the hydrogen bonds associated with polyamides. The gel-spun high strength high modulus Polyethylene

yarn has high strength and rigidity due to a highly oriented structure of macromolecular chains, despite being formed from a flexible chain polymer. Therefore the mechanical properties of Polyethylene were compared to that of Capron and other highly orientated fibres. The understanding of structure-property relationships of fibres has been improved.

In the experiments described in Chapter 5, the thermo-mechanical properties of polyamide fibres were studied. Aromatic polyamide is significant different in heat resistance from the conventional aliphatic polyamide. First of all, thermal shrinkage of varying polyamide fibres was determined. Effect of temperature on the mechanical properties such as tensile stress-strain property, creep relaxation, residual deformation was studied. The chemical structures and intermolecular interactions of polyamide fibres were related to these thermal properties for different types of polyamides.

Chapter 6 described the use of FTIR, SEM and DSC to investigate the fibre structures and their change during the deformation to break. The structure of new Russian Armos was compared with SVM using FTIR. An attempt was made to investigation of degree of intermolecular hydrogen bonding and asscioated moisture in the polyamide fibres by FTIR. Rupture mechanism of polyamide and gel-spun Polyethylene fibres was studied using SEM. The effect of the microstructure of fibres on the fibre rupture was discussed. DSC experiments were carried out to study heat degradation of the rigid, semi-rigid and flexible aromatic polyamide fibres. Their resistant to heat was related to their chemical structures.

CHAPTER 1

LITERATURE REVIEW

1.1 General introduction

Polyamide fibres, their derived yarns and products have a broad application contributing to different areas of the national economy. Because of the uniqueness and universality of their properties, these fibres are indispensable for household application and technical purposes. The commercial production of polyamide fibres began in 1938, when the pilot production of Nylon 6.6 fibre was undertaken in USA. The production of fibres like Nylon is at the forefront of polyamide fibre production (Kudriyavtsev *et al.*, 1976). Currently, a lot of work on the synthesis of polyamide fibres is carried out in Germany, France and Russia.

The requirements of the aeronautic, rocket and motor industries have resulted in the intensive development of construction materials technology. These industries require high strength, high modulus and heat resistant fibre applications. Aromatic rings were introduced into the polymer molecule. These may be incorporated into the diamine, diacid or both. Many aromatic polyamides (aramids) have been made experimentally, and some are now of commercial importance as special purpose polyamide fibres. The effect of introducing aromatic rings is particularly marked when phenylene groups are incorporated in the molecule through the para-aromatic positions. The high rigidity of polymer chains and strong intermolecular interaction including hydrogen bonds and Van der Waals forces can be achieved in the polymer fibres to contribute to their high strength and high modulus. Meta substitution provides polymers of lower melting point, intermediate between that of the para substituted polymers and those of normal straight-chain constitution. The sources and chemical structure of commercially available aramid fibres such as Kevlar, Terlon, SVM, Armos, Nomex and Phenylon are shown in Table 1.1. These fibres and yarns have unique mechanical (Table 1.2) and thermal characteristics (Machalaba, 1999; Volokhina, 1997; Perepelkin, 1987, 1992; Perepelkin *et al.*, 1999[a]).

Table 1.1 Major types of aramid fibres

Trade name	Chemical structure	Producer
Kevlar®	Poly-*p*-phenyleneterephthalamide	USA, "DuPont de Nemour"
Terlon®	Copolymer similar to poly-*p*-phenyleneterephthalamide	Russia, VNII Polymervolokno
SVM®	*p*-aromatic heterocyclic polyamide	Russia, JS NII Chimvolokno and Kamenskchimvolokno
Armos®	*p*-aromatic heterocyclic copolyamide	Russia, VNIIPolymervolokno. J.-S. Co Tverchimvolokno
Nomex®	Poly-*m*-phenylene isophthalamide	USA, "DuPont de Nemour"
Phenylon®	Poly-*m*-phenylene isophthalamide	Russia, VNIISV Tver

Table 1.2 Mechanical properties of main types of aramid fibres (Machalaba, 1999; Volokhina, 1997; Perepelkin, 1987, 1992; Perepelkin *et al.*, 1999[a])

Yarns	Density, g/cm^3	The modulus of elasticity, GPa	Tensile strength, GPa	elongation at break, %
Kevlar	1.44	140-170	3.3-3.8	2.5-3.5
Terlon	1.44	140-170	3.3-3.8	2.5-3.5
SVM	1.43	135-150	4.2-4.5	3.0-3.5
Armos	1.43	140-160	4.5-5.5	3.0-4.0
Phenylon	1.38	-	0.6-0.8	15-30

Aramid fibres have good textile properties and are used for the production of fabrics. Fabrics made from aramid fibres such as Nomex and Kevlar are lustrous and attractive, with good draping characteristics and handle. Shape retention and wear resistance are

excellent, but the high strength of the fibres can cause pilling similar to other nylon fabrics. Aramid fabrics wash easily and drip-dry quickly. Dry cleaning does not present a problem. Ironing may be carried out safely at temperatures up to 300°C.

Compared with steel, a para-aramid fibre such as Kevlar has a much higher breaking strength, but is about six times lighter, thus providing a tremendous weight saving. This makes for ease of handling and it can be used as cables for mooring lines, for offshore drilling platforms, for parachute lines, fishing lines, mountaineering ropes and pulley ropes. The applications of aramids for ropes and cables in oceanic systems are reviewed by Riewald (1980). Other uses include cord for reinforcing car tyres, and in protective clothing and body armour. Modern light-weight bullet-proof vests contain up to 18 layers of woven Kevlar cloth. Data analysis by Matveev *et al.*, (1993) has shown that Armos and SVM fibres are very effective for use as protection against a ballistic lesion.

The aramids are very resistant to heat and only begin to decompose and char at temperatures in excess of 400°C. They are widely used in the production of heat-resistant paper and related products. Aromatic polyamide films are recommended for application to aircraft and motor vehicles cabins, because they are able to provide electrical insulation at high temperatures in transformers and condensers, etc (Sokolov *et al.*, 1975).

Aramids also have ecological application. The use of SVM fibres as a filter materials is reviewed by Avrorova *et al.*, (1993). In recent years, 20-25% and even up to 40% of the total volume of *p*-aramid yarns produced in the world were used in the replacement of toxic asbestos. *P*-aramid yarns, fibres and pulp provide an ideal alternative to a unique natural material (asbestos), although they are quite an expensive substitute (Volokhina *et al.*, 1993).

An extension of the use of aramid fibres is for composite materials (Machalaba, 1999; Kudriyavtsev *et al.*, 1992; Katz and Milewski, 1978; Wang, 1997), especially for particular constructional uses in extreme conditions (Sokolov *et al.*, 1975). New synthetic composite materials can be reinforced by high strength high modulus fibres. Aramid fibres are

embedded in synthetic resins to form rigid lightweight material for use in the bodies of racing cars, in yachts, and in aerospace.

The high performance characteristics of highly oriented aramid fibres are related to their elastic-strength properties, which have led to their use as power absorption materials for various purposes. These fibres can be used as construction materials, which can withstand high vibration and acoustic loads (for example as required in aeroplane and helicopter engines).

Nylon and Capron have a lower melting temperature so that they may not be used at elevated temperatures. At temperatures below their melting points, however, they have somewhat better resistance to the effect of prolonged heating. Therefore the high strength and abrasion resistance of Nylon and Capron, coupled with other properties such as resistance to moisture and heat, good fatigue resistance and high work of rupture, enabled them to make rapid headway in the tyre cord market (Kudriyavtsev *et al.*, 1976).

In the case of the polyamide fibres, Nylon 6 and Nylon 6.6, the inherent characteristics of the fibres meet the needs of a wide range of important textile applications, and the fibres are produced on a large scale to meet the resulting demand. Capron and Nylon fibres are widely used in the manufacture of sportswear, jersey and carpet products, tights and socks.

Capron yarns are also used in the production of composite materials. Despite the broad application of aramid fibres for composite materials production, their implementation is hindered due to difficulties associated with the impregnation materials by high viscosity thermoplastics. In a report by Volokhina, (1997) one of the achievements in the area of composite materials is discussed, the so-called "fibre" technology of composite materials production. In this technology two types of fibre are used; the reinforcing type (SVM, Terlon, Armos, Kevlar) and template type (thermoplastic Capron yarns). A bar of the materials is produced by the alternation of continuous reinforcing fibres and template fibres. In the structure of a such bar, the thermoplastic fibre comes as close as possible to the surface of a reinforcing fibre, thus providing a decrease in porosity of the product and increasing its mechanical properties.

1.2 Formation of polyamide fibres

Fibres can be produced by using a number of spinning techniques. Spinning is mainly carried out either with a molten polymer (melt spinning) or with a polymer solution. In the case of melt spinning, the filaments are cooled rapidly by cold air in the process tank. If a polymer solution is used, the solvent is removed in the process tank by evaporation with heat (dry spinning) or the solubilizing agent is removed by leaching with another liquid (wet spinning).

The industrial process for production of polyamide fibres such as Nylon and Capron involves three main stages. These are: (1) the synthesis of the polymer, (2) the melt spinning, (3) stretching process and aftertreatment. Polyamides for fibre production can be obtained by following reactions:

- heteropolycondensations of diamines with dicarboxylic acids;
- homopolycondensations of ω-amino acids or their derivatives;
- solution or interphase polycondensation of diamines with dichloranhydride of dicarboxylic acids;
- polymerization of lactams.

Fibres are made by melting spinning from granular polymer or directly from molten polymer. The aftertreatment of polyamide fibres consists of a number of technological processes depending on the final end product. The process of formation of polyamide fibres such as Nylon 6.6 and Capron is reviewed by Kudriyavtsev *et al.*, (1976), Zazulina *et al.* (1985) and Riyauzova *et al.* (1974).

The main ultrahigh strength and high modulus fibres are based on para-polyamides, polyheteroarylenes and some similar copolymers. The fibre-forming and high mechanical properties achieved are based on the ability of rigid chain linear polymers to transform in a liquid-crystalline state. This fact leads to self-ordering effects even at small preliminary orientation at both the stage of fibre spinning and the following thermal treatment (Perepelkin *et al.*, 1999[b]).

Aromatic polyamide fibres or lyotropic liquid crystalline polymers are prepared by condensation polymerization in a powerful solvent or strong acids, owing to their nonfusibility. The chemical structures of several of the commercially significant aramids are shown in Table1.1. Two types of initial solutions are used for Poly-*para-aromatic*-amides moulding:

- solutions of polymer in sulphuric acid, for example 15-25% solutions of Poly-*p*-phenylenterephtalamide or other aromatic copolymers in sulphuric acid. In solutions of the rigid, rod-like aramids, random coil structures do not form and instead the rigid chains pack in quasi-parallel bundles when the polymer concentration is increased.
- 5-6% poly-*p*-amides with heterocycles in the chain or other similar copolymers in a solvent particularly comprising dimetylacetamide (DMAc) and a lyophilic salt such as LiCl. This solvent combination keeps the growing polymer in solution longer, thereby increasing the molar mass of the product to levels which make it suitable for fibre formation. This is achieved by reducing the intermolecular hydrogen bonding while DMAc acts as an acid acceptor and good solvator of the polymer chain.

The technological process of obtaining a solution for spinning can involve separate stages of polymer synthesis and its subsequent dissolution. Direct processing of solutions obtained as result of polymer synthesis can be also used. Before spinning, the filtration and degasification of polymer solutions are very important. These processes guarantee the purity and therefore stability of the spinning process. In all cases, decreasing the time from obtaining a solution of the polymer up to the moment of fibre spinning is necessary to lower the possibility of polymer destruction and spurious processes. These fibres are spun using a wet spinning method (often through air layers (Shorin *et al.*, 1999)). Usually water-spinning baths are used, but the application of organic spinning baths is also possible. Spun fibres are washed to remove residual solvent and dried. During the stretching process, a primary orientation of the structure in the fibres occurs.

Further heat treatment provides a means of regulating the properties of fibres and yarns. The heat treatment is carried out at a temperature not exceeding the glass transition

temperature at approximately 100°C. It is also possible to use minor thermal stretching to increase the modulus of elasticity and make fibres stronger (Machalaba, 1999).

1.3 Structure and properties of polyamide fibres

1.3.1 Structural features

The properties of polyamide fibres are determined by their initial structure at different levels, which are classified into two groups of structure factors. These are:

- morphology, i.e. the geometrical characteristics of structural parts and their positional relationship;
- energy characteristics of structure.

Considering the molecular structure, it is necessary to study the chemical composition of the polymer, i.e. the chemical macromolecule recurring link. The fibres studied in this work are polyamide and olefin polymer types. The most important parameters of polymer molecular structure to be considered are the characteristic of flexibility (rigidity) of macromolecules, i.e. the capability to change the molecular conformation as a result of intermolecular thermal motion of links (equilibrium or thermodynamic flexibility) and the capability to change the conformation as result of external mechanical forces (kinetic or mechanical flexibility). The flexibility of a single macromolecule depends on:

- capability of hindered rotation of monomeric bonds around a single bond of main polymer chain;
- presence of cyclical structures, oxygen bridges, double bonds etc in the polymer chain;
- the sizes of functional groups of a chain and/or lateral substituents resulting in suppression of rotation of links;
- formation of intramolecular hydrogen or other bonds resulting in labile cyclical structures.

The notion of polymer chain flexibility is related to the mobility of macromolecular segments and with the size of the Cune segment (statistical segment). The Cune segment

has a conditional value dependent on the sequence of n-links, each link behaving independently of other links (Tugov and Kostrikina, 1989). For example, polycaproamide is a flexible chain polymer for which the Cune segment is 2.0-2.2nm. Poly-*p*-phenylenterephtalamide and other *p*-aromatics, from which Kevlar, Terlon, SVM and Armos fibres are formed, are rigid chain polymers, for which the Cune segment is about 30-40nm. Poly-*m*-phenylenisophtalamide, from which Phenylon and Nomex fibres are produced, is a semi-rigid chain polymer. The Cune segment for these polymers is about 3-10 nm (Perepelkin, 1985). However it should be noted, that as the intermolecular interaction exerts an influence on the flexibility of macromolecule chains, flexibility is not solely dependent on the constitution of the macromolecule, and nearest neighbouring groups will also exert on influence (Kargin and Slominskii, 1967).

Although the supermolecular structure of polymers will vary, the fibrillar structure is generally characteristic for oriented polymers, including fibres (Tadokoro, 1979; Marikhin and Myasnikova, 1977; Hearle, 1963; Sikorski, 1963; Slutsker, 1974; Morton and Hearle, 1975).

The fibrillar structure of oriented amorphous–crystalline polymers is characterised by longitudinal heterogeneity with sequences of areas having high molecular orderliness (crystallites) and areas with low molecular orderliness (amorphous parts). The macromolecular structure of fibrillar formations in oriented amorphous polymers is characterised by the availability of three-dimensional (often disturbed) distant order in the arrangement of links and macromolecular chains (Perepelkin, 1985). In the crystalline region of structure there are two types of polymer chain packing. There are crystallites on rectified chains (CRC) and crystallites on folded chains (CFC). CRCs are crystallites with chains crossing normal to the fibre axis, CFCs are crystallites with primarily chain fold. The occurrence of such folds depends on the macromolecular flexibility, the degree of intermolecular interaction and the conditions of crystallisation. In flexible chain polymers the degree of folding may be large. The macromolecules of rigid chain polymers are packed with a minimum fold formation or it may be absent (Kargin and Slominskii, 1967; Marikhin and Myasnikova, 1977; Keller, 1963; Mandelkern, 1964; Pakhomov, 1999).

The crystalline-amorphous ratio in a polymer is characterised by the degree of crystallinity, which is dependent on the type of molecular structure, the conditions under which the polymer was obtained and other factors (Perepelkin, 1985). In contrast to the typical aramid fibres, which have an amorphous-crystalline structure, Armos and SVM fibres do not have the obvious three-dimensional order. Perepelkin (1999[a]) suggests that the three-dimensional order is smaller, and that the one-dimensional order is more typical for these fibres. Table 1.3 shows the degree of crystallinity for different polyamide fibres.

Table 1.3 The crystallinity of fibres (Kudriyavtsev *et al.*, 1992, Kuz'min, 1988, Fukuda *et al.*, 1991, Sokolov, 1975)

Fibre	Crystallinity
Terlon	up to 80%
Kevlar	72 ~ 91%
Phenylon, Nomex	30 ~ 40%
Capron, Nylon	20 ~ 50%
Armos, SVM	semi-crystalline

The structure of poly(p-phenylene terephthalamide)(PPTA) fibres under the trade name Kevlar has been investigated extensively. The following are among the models that have been proposed for common PPTA fibres. Warner (1995) suggested the schematic model structure of Kevlar fibre, shown in Fig. 1.1. It is a near-ideal structure of liquid crystalline polymers, with most of the molecules virtually completely aligned.

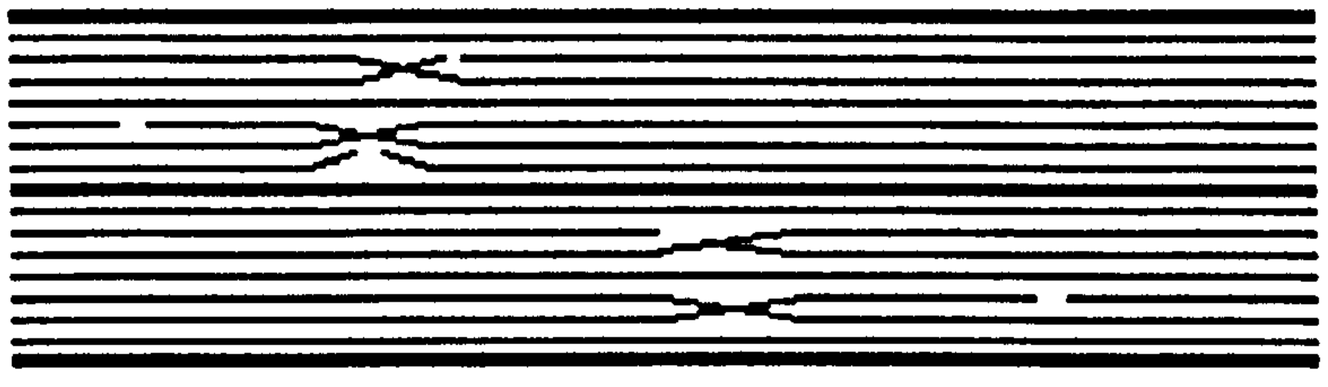

Fig. 1.1 Structure model of Kevlar fibre (Warner, 1995).

Dobb *et al.* (1977) have suggested that Kevlar 49 fibres consist of a series of sheets regularly pleated along their axis and arranged radially. The model structure of Kevlar fibre suggested by Riewald *et al.* (1987) is shown in Fig. 1.2. The fibres comprise several levels of superimposed microscopic and macroscopic structure, including the crystal lattice, pleat structure, fibrillar structure, and skin-core differentiation. Molecular chains are hydrogen-bonded in the radial direction within the layers. Van der Waals forces act between layers in the direction perpendicular to the fibre axis. Covalent bonds give the molecules high strength in the fibre axial direction. Oriented Kevlar chains have very low flexibility. Small angle x-ray scattering studies confirm the absence of chain folding and suggest a fully extended chain conformation.

The microstructure of fibres is characterised by heterogeneity and often includes not less than two or three layers with different supermolecular orderliness. The quantity of structure defects at all levels is very important. These may be chemical dislocation, microflaws of a constitution, pore, disturbance of a surface *etc.* (Koitova, 1992).

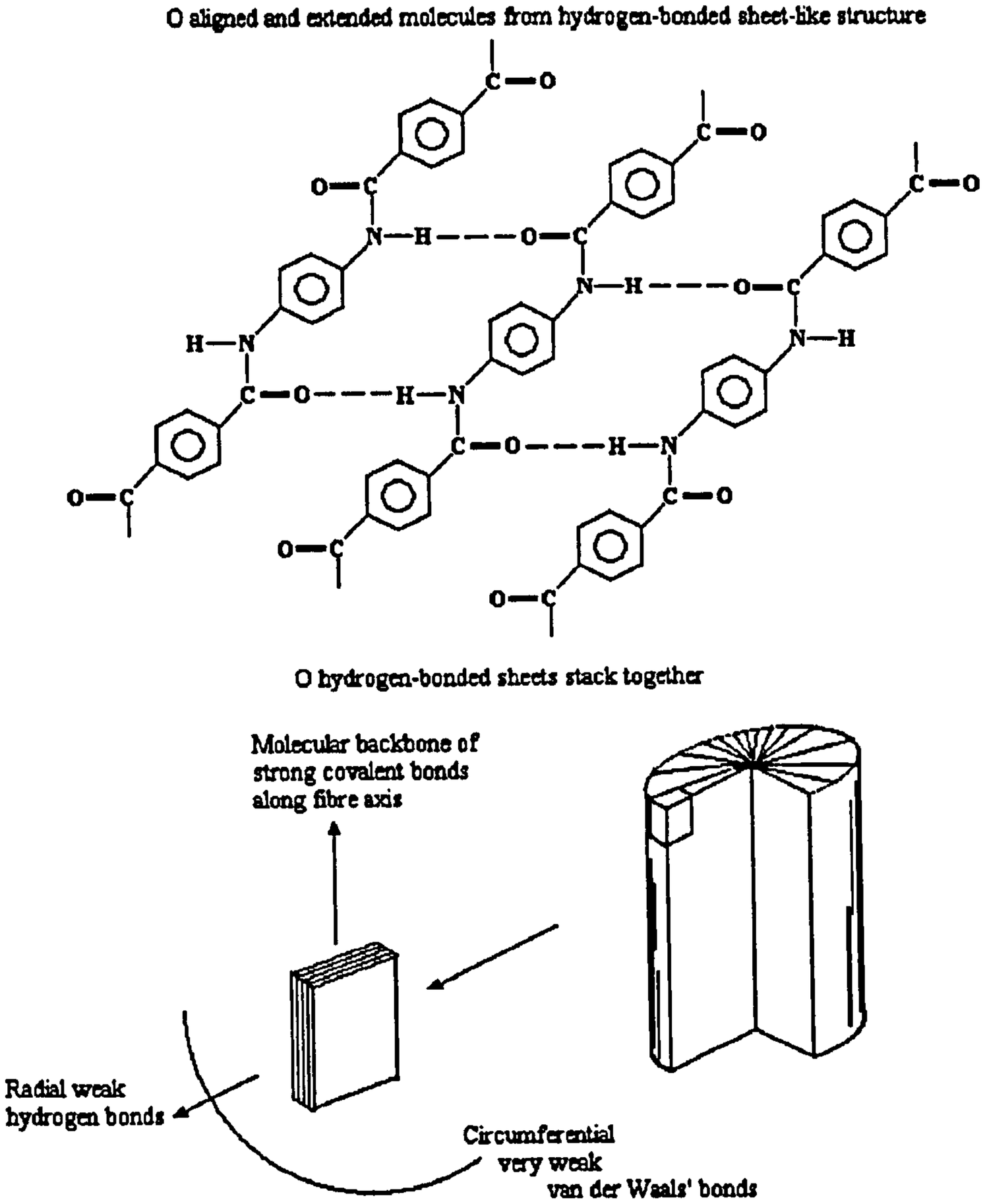

Fig. 1.2 Kevlar aramid fibre structure (Riewald, 1987)

Dobb *et al.* (1977) proposed a structure exhibiting a differentiation between core and skin regions. The core region consisted of stacked layers of crystallites made up of individual macromolecules of average length 220 nm, which were enclosed in a skin with random chain-end distribution. TEM oblique section through Kevlar fibre shows a skin region with extensive micro-voids and a core with a few macroscopic defects (Fig. 1.3). The skin region varies in thickness between the various types of the aramid fibres .

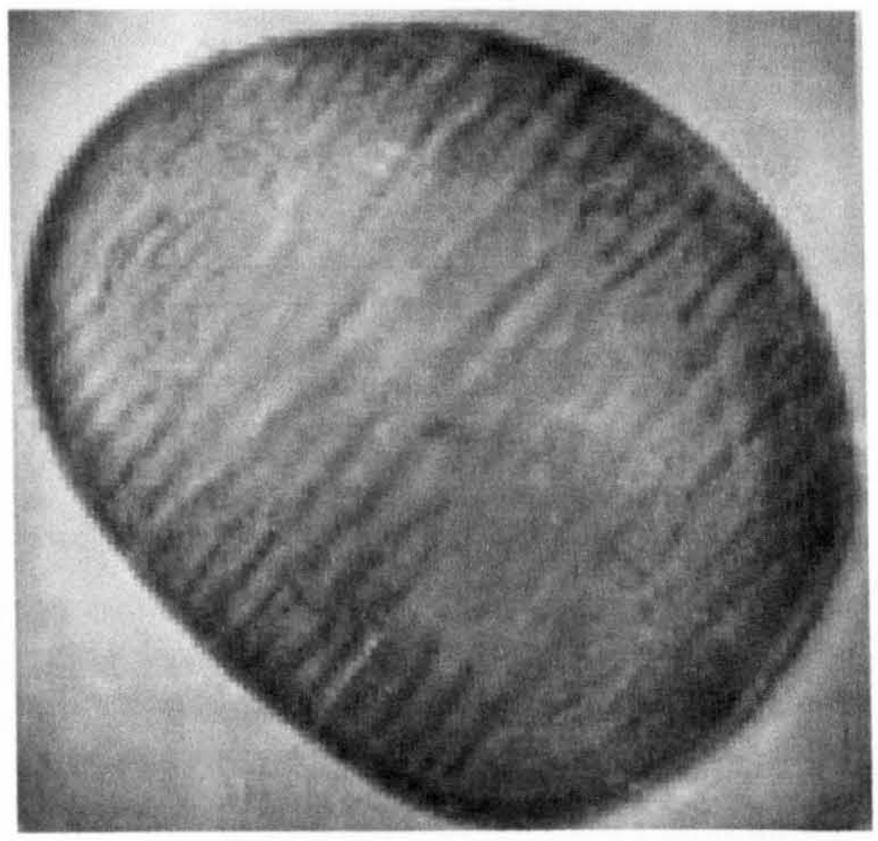

Fig. 1.3 Cross section of Kevlar fibre (Dobb, *et al.*, 1977)

Nomex fibre is a meta-substituted aromatic polyamide which is polymerized from m-phenylenediamine and isophthaloyl chloride. Hydrogen bonding is sterically hindered, therefore the high degree of crystalline order does not occur.

SVM and Armos are heterocyclic para-copolyamides. The elementary links contain very polar groups - peptide and tertiary nitrogen atoms. The structure of this copolymer is characterised by less regularity and less rigidity in comparison with poly-p-phenyleneterephthalamide. This heterocyclic copolymer cannot create liquid crystalline domains in solution. Therefore it is possible to regulate the structure-building during fibre-formation and thermal treatment processes in the direction of the maximal orientation order (Perepelkin, *et al.* 1999[b]).

Fibrillar structure is also usual for traditional polyamides such as Nylon 6.6 and Capron. The schematic structure of Nylon 6 fibre is shown in Fig. 1.3 (Prevorsek *et al.*, 1977; Harget and Ocswald, 1977).

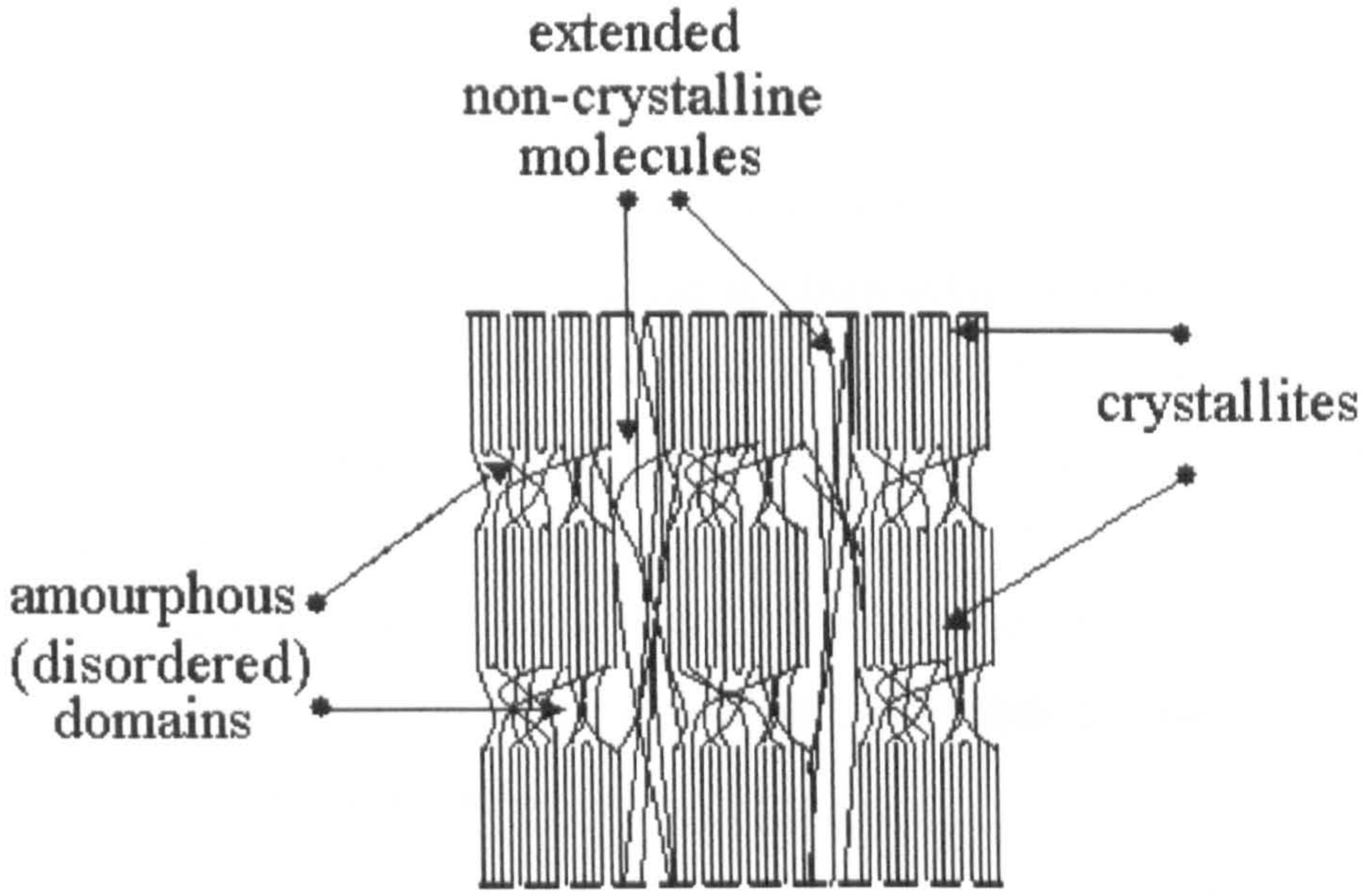

Fig. 1.4 Structure model of Nylon fibre (Prevorsek *et al.,* 1977; Harget and Ocswald, 1977)

In addition to the morphological constitution of fibres at supermolecular level, the energy characteristics of the supermolecular structure are also very important. Bond strength is influenced by dispersion, inductive and dipole-dipole (orientation) interactions between functional groups of adjacent macromolecules, as well as low molecular weight compounds. The availability in macromolecules of functional groups, possessing mobile hydrogen atoms, enables the formation of hydrogen bonds (Perepelkin, 1985). These types of bonds are characteristic for polymers of the amide group. The hydrogen bond has dissociation energy up to 50 kJ/mole and is intermediate between a typical chemical covalent bond (about 500 kJ/mole) and a Van-der-Waals bond (about 1-2 kJ/mole) (Tugov and Kostrikina, 1989). It is well established that the length of hydrogen bonds can vary, depending on the functional groups forming the hydrogen bond (Perepelkin, 1985; Pauling, 1960; Eisenberg and Kauzmann, 1969). The length of hydrogen bond is 1.8-2.8 Å for O-H···O, 3.0-3.4 Å for N-H···N, and 2.8-3.0 Å for N-H···O.

The ability to form hydrogen bonds depends on a number of factors including the distance between the groups which are able to form hydrogen bonds (Parker and Lindenmeyer, 1977). Beliaev *et al.,* (1978) report that hydrogen bonds were found to weaken during the crystallisation of aromatic polyamides. The tendency of phenylon rings to parallelise during

crystallisation results in an increase in H···O distance. This leads to a decrease in the hydrogen bond strength. Most strong hydrogen bonds are formed in amorphous, unregulated areas of polymer. This may be due to chain folds, in which one chain covers another. This offers optimum potential for hydrogen bond formation. For samples of aromatic rigid chain polyamides under special conditions (existence of preliminary orderliness) increasing temperature results in an increase in the energy of formation of hydrogen bonds between amide groups. Thus, according to the literature, when the temperature is increased, increasing efficiency of hydrogen bonds formation for rigid chain aromatic polyamides can be seen (Beliaev *et al.*, 1978).

The main distinctive feature of hydrogen bond formation in aromatic polyamides is the existence of molecular groups with weak intermolecular interaction (Shablygin and Pakhomov, 1979). During a crystallisation of aromatic polyamides the energy of hydrogen bond formation decreases in the case of macromolecule orientation. This results in a sharp increase of an intermolecular interaction involving the π-electrons of benzene rings. Thus these so-called π-bonds are also responsible for an intermolecular interaction in aromatic polyamides.

The energy of destruction of rigid chain polymer fibres depends on the energy of an intermolecular interaction (Gul, 1979). Previous workers (Perepelkin and Chereiskii, 1977; Zarin, 1991) suggest the theoretical capability for the strength improvement for rigid chain polymers can be achieved to a greater degree than for flexible chain polymers.

Perepelkin *et al.* (1999[b]) suggested that the specific position is for Armos fibre, which is a heterocyclic para-copolyamide. An extended chain conformation with irregular elementary link positions creates 1-D order regularity enabling axial movement. This facilitates the structural transformation of fibres during thermal treatment and improves the axial order in super-molecular structures. Therefore, a less regular molecular chain structure leads to a higher proportion of stress-holding molecular chains and hence to Armos fibre's maximal mechanical properties compared to other para-aramid fibres.

crystallisation results in an increase in H···O distance. This leads to a decrease in the hydrogen bond strength. Most strong hydrogen bonds are formed in amorphous, unregulated areas of polymer. This may be due to chain folds, in which one chain covers another. This offers optimum potential for hydrogen bond formation. For samples of aromatic rigid chain polyamides under special conditions (existence of preliminary orderliness) increasing temperature results in an increase in the energy of formation of hydrogen bonds between amide groups. Thus, according to the literature, when the temperature is increased, increasing efficiency of hydrogen bonds formation for rigid chain aromatic polyamides can be seen (Beliaev *et al.*, 1978).

The main distinctive feature of hydrogen bond formation in aromatic polyamides is the existence of molecular groups with weak intermolecular interaction (Shablygin and Pakhomov, 1979). During a crystallisation of aromatic polyamides the energy of hydrogen bond formation decreases in the case of macromolecule orientation. This results in a sharp increase of an intermolecular interaction involving the π-electrons of benzene rings. Thus these so-called π-bonds are also responsible for an intermolecular interaction in aromatic polyamides.

The energy of destruction of rigid chain polymer fibres depends on the energy of an intermolecular interaction (Gul, 1979). Previous workers (Perepelkin and Chereiskii, 1977; Zarin, 1991) suggest the theoretical capability for the strength improvement for rigid chain polymers can be achieved to a greater degree than for flexible chain polymers.

Perepelkin *et al.* (1999[b]) suggested that the specific position is for Armos fibre, which is a heterocyclic para-copolyamide. An extended chain conformation with irregular elementary link positions creates 1-D order regularity enabling axial movement. This facilitates the structural transformation of fibres during thermal treatment and improves the axial order in super-molecular structures. Therefore, a less regular molecular chain structure leads to a higher proportion of stress-holding molecular chains and hence to Armos fibre's maximal mechanical properties compared to other para-aramid fibres.

The structures of aramid fibres have been investigated by other workers (Kudriyavtsev *et al.*, 1976; Perepelkin, 1985; Hearl, 1963; Reimschuessel and Prevorsek, 1976; Lewin and Pearce, 1985).

1.3.2 Moisture sorption mechanism of polyamide fibres

All polyamide fibres are hydrophilic. The most important factors to be considered due to the interaction of fibres with moisture are polarity, quantity and availability of functional groups, and solvated molecules of water. Interaction with water will depend on features of sample orderliness, as sorption will occur in the amorphous areas of the polymer structure. The aromatic polyamide fibres have an amorphous-crystalline structure (Kevlar, Terlon, Phenylon, and Nomex) or a semi-crystalline structure (Armos, SVM). They contain polar functional groups (-NH and -CO) which are capable to associate with water molecules by H-bonding.

In Nylon 6 water molecules are bound on two neighbouring amide groups in an accessible region. The first water molecule forms two hydrogen bonds between the carbonyl groups of neighbouring chains. In this step a large amount of heat is evolved. Therefore, this water may be defined as firmly (or strongly) bound water whose activity is low. In practice, it is nearly impossible to remove it completely. The second and third water molecules join the already existing H-bonds from the NH groups to other CO groups with a negligible thermal effect. Consequently, this water is denoted as loosely (or weakly) bound (Fig 1.5). The incorporation of loosely bound water leads to a plasticization, that means a weakening of already existing H bonds (Deopura *et al.*, 1983).

This two-step model was later extended by Starkweather (1980, 1981), who considered a clustering of water molecules. Additional water molecules attach to firmly or loosely bound water and form structures generally called "clusters". A possible alternative to clustering is the existence of freezable unbound water in cavities (microvoids).

Several authors have suggested the existence of inter- and/or intrafibrillar microvoids. Northolt (1981) reported elongated microvoids in Kevlar from small-angle X-ray scattering

(SAXS). Dobb *et al.* (1979) estimated the size of the microvoids in Kevlar 29 and Kevlar 49 to several tens of angstroms in width from Guinier analysis of equatorial SAXS intensity distribution.

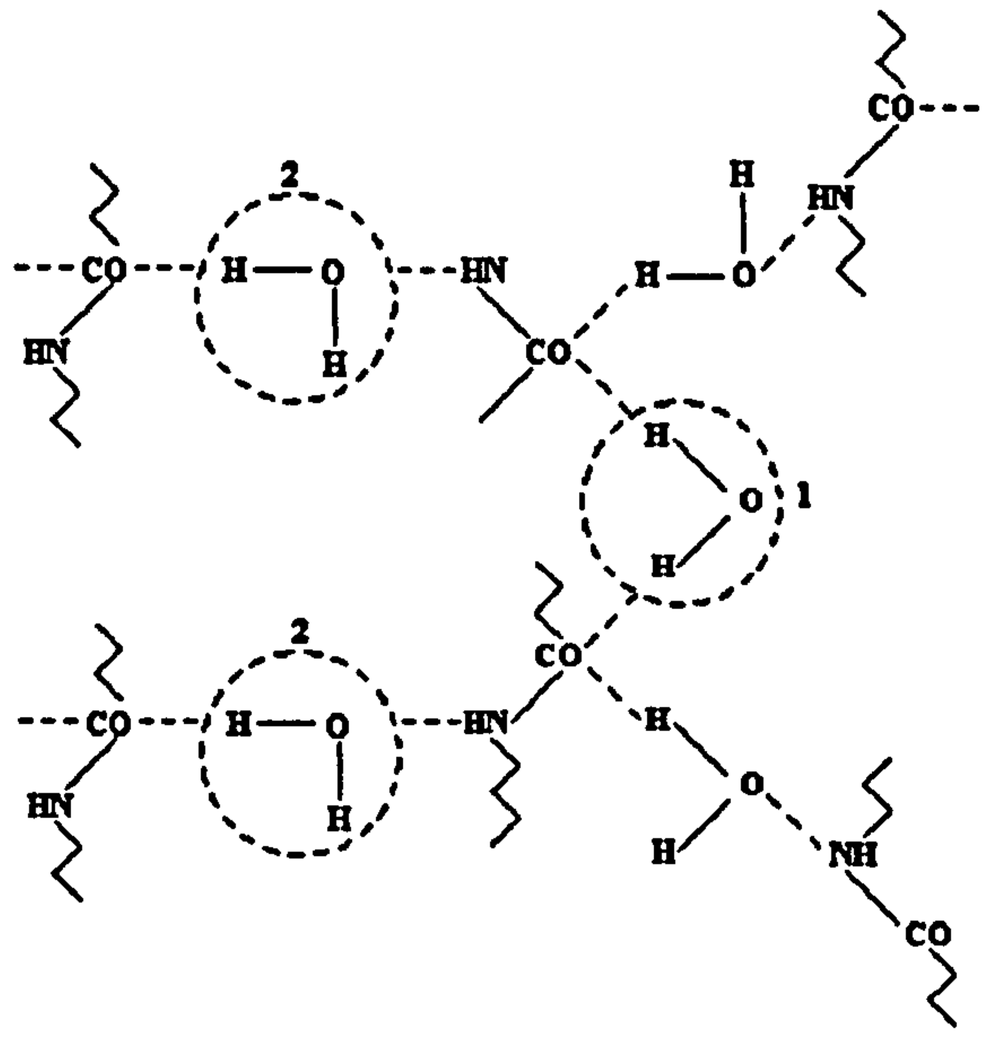

Fig. 1.5 The interaction of water with nylon; (1) strong coupled water, (2) weakly coupled water (Deopura *et al.*, 1983)

Saijo *et al.* (1994) have observed the moisture sorption rate in a bone-dry regular Kevlar at 25°C at saturated vapour pressure by the Time-resolved SAXS technique. They also suggested the picture of the build-up of two kinds of water cluster: at first the water molecule is sorbed to form a strong bond with the adsorption site (monolayer adsorption), additional water molecules form a "micro-water cluster" (multilayer adsorption); and then, if space is available, the micro-water cluster grows to a "macro-water cluster" until the space (microviod) is filled with condensed moisture.

Kurzemnieks (1980) has established that moisture is accessible to semi-crystalline areas, as well as amorphous areas, and that the interplay of water molecules in certain parts of the chains can result in the amorphization of the material structure. It was supposed that these

parts of the chain are amide groups and the effect of amorphization is explained by the destruction of hydrogen bonds, caused by these groups.

The isotherm of a sorption characterises material absorptivity, the condition of fibre surface, the degree of crystallinity etc. For most fibres an S-shaped isotherm of a sorption is characteristic. As the analysis of isotherms of sorption is quite a simple and effective way of estimating different material properties, the reports of its analysis are rather widely shown in the literature (Koitova *et al.*, 1993; Grebennikov *et al.*, 1984; Rowlend, 1980; Belokurova and Reitlinger, 1978). It should be noted, however, that most refer to traditional kinds of fibres.

The water sorbed in a series of poly(para-phenylene terephthalamide) (PPTA) fibres (regular Kevlar, Kevlar 49, Kevlar 149, and a heat treated PPTA fibre) was characterized by analyzing the moisture sorption isotherm and thermodynamic quantities derived from calorimetric measurements of the heat of moisture sorption. The results indicate that the bulky and rigid phenyl ring in the aromatic polyamide chain opens the space for each peptide site to adsorb moisture more efficiently than the site in the aliphatic polyamide chain (Fukuda *et al.*, 1991).

Zarin and co-workers (Zarin, 1991; Zarin *et al.*, 1983) present data relating to the interaction of fibres with water vapour. There are three stages to this process: (1) the sorption of water by free amide groups in the polymer at 0-2% sorption of a yarn; (2) breakage of hydrogen bonds between adjacent chains of polymer at 2-3% sorption of a yarn; and (3) when the hydrogen bonds are weak, the intermolecular bonds which are of a "polymer-water-polymer" type relax and the mobility of molecules is augmented when the sorption is above 3%. The analysis of NMR spectra of SVM yarns by Shuster (1988) confirms the supposition about the formation of hydrogen bridges by water molecules.

1.3.3 Deformation and strength properties of polyamide fibres

The mechanical properties of solid-state oriented polymers are directly related to the degree of orientation developed. For each polymer there are limits to the amount of orientation

possible, based on the molecular weight and crystallization of the polymer. The properties of interest include tensile strength, modulus, impact strength, creep resistance, elongation-to-break, and upper use temperature.

The modulus of aramid fibres correlates with structure depending on the alignments induced. The correlation could be with: (a) crystallite perfection, (b) lateral crystallite size, and (3) degree of pleating. In the case of crystallite perfection, chain alignment would be induced through the elimination of chain-bending defects. In the case of lateral crystallite size, additional chain alignment would occur by the (fibre-aligned) crystallization of previously noncrystalline material. In the case of pleating, increased chain alignment occurs through the removal of pleat creases, thereby aligning each former pleat with the fibre axis. But from the present work, it is suggested that the chain stiffness might be an additional parameter for fibre modulus.

Intensive studies have been carried out to analyse the deformation and strength properties of polyamide yarns such as Nylon and Capron (Kunugi *et al.*, 1982; Kveder and Rijavec, 1994; Felthan, 1966; Becht *et al.*, 1971;). However, the deformation and strength properties of aramid yarns become most interesting because they are capable of maintaining considerable loads and are intended for use in extreme conditions. The properties of many types of *p*-aramid fibres are described in the literature in detail (Springer *et al.*, 1998; Budnitskii, 1990; Yang, 1989; Yang, 1993; Duobinis, 1993;).

In real technological conditions the yarns are subjected to different mechanical loads, for example the sample is stretched up to some value of elongation or stress, and then is fixed. It can be expected that the deformation and strength properties of yarns at different stages of stretching will vary due to some change in their structure. These changes will obviously depend on the nature of the fibre. Fig. 1.6 shows typical schematic creep curve. A load is applied at to initial extension ε_0, extension slowly increases while load is applied (t_0 t_1), at t_1 the load is removed and there is an initial elastic contraction (ε_e), followed by creep recovery (ε_{he}) to leave a final extension (ε_p) due to plastic deformation. So the behaviour of polymer materials during stretching is characterised by three types of deformation. These

are elasticity (ε_e), retarded high elasticity (ε_{he}) and plastic deformation (ε_p) (Kargin and Slominskii, 1967; Gul', 1979).

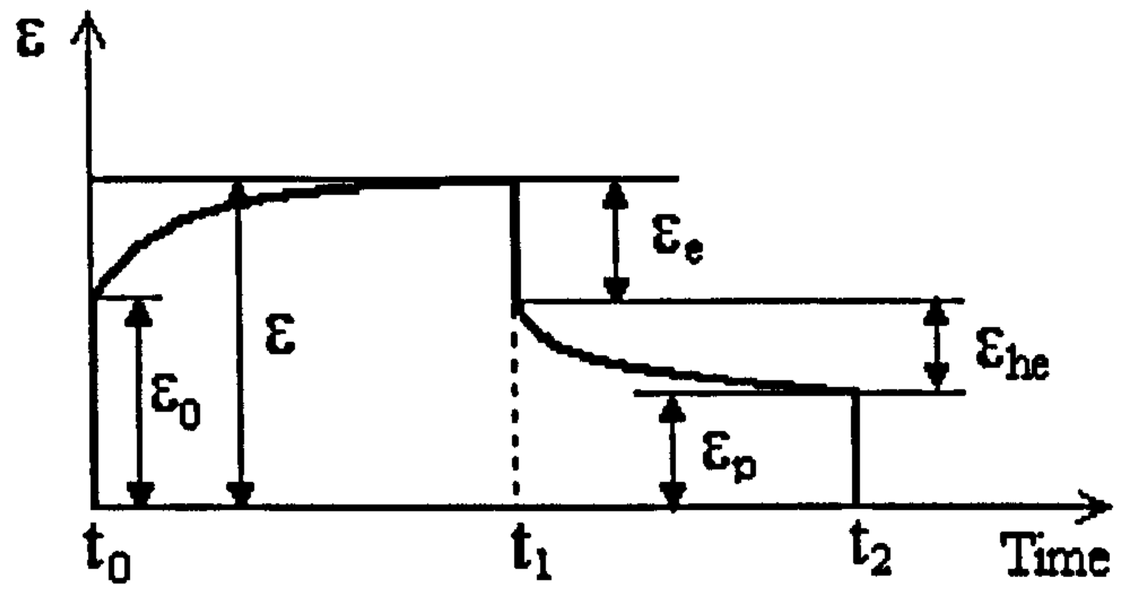

Fig. 1.6 Schematic representation of a creep curve (Pakhomov, 1999)

The elastic deformation is a result of bond stretching and flexing, and it is completely reversible. This region characterizes Hookean elastic deformation which is stored in internal bond energy.

The retarded highly elastic deformation is a characteristic of polymers composed of flexible convoluted molecules and has an entropic nature. At retarded highly elastic deformation there is a decrease in entropy owing to leaning of conformation set in molecular chains. This deformation is slowly recovered upon removal of the stress. The residual mechanical energy is dispersed in the form of heat when overcoming internal friction.

The plastic deformation of polymers involves chemical bond breakage, so-called "chemical flow", or by the sliding of molecular chain segments past one another, so-called "physical flow" (Askadakii, 1973). The plastic deformation is irreversible. In most cases, it is very difficult to separate the irreversible deformation from the retarded highly elasticity deformation because the retarded highly elasticity deformation need a very long relaxation time to complete recovery. Therefore residual deformation is often used for evaluation.

The deformation of polymers can be explained by two mechanisms: intermolecular and

intramolecular mechanisms. The combination of both mechanisms is also possible. Deformation as a result of the intermolecular mechanism includes the sliding of molecules or molecular segments and other elements of the structure. In case of intramolecular mechanism, the deformation is caused by rearrangement and change within polymer chain molecules (Pakhomov, 1999). Penn and Milanovich (1979) have found that breakage of chemical bonds are not characteristic for aramid fibres, or characteristic to a minimum degree. The destruction of the fibres occurs in a cascade fashion, the breakage of chemical bonds occurring only on a narrow part of the fibre before fibre breakage (Pakhomov *et al.*, 1986).

The most important characteristics of a polymer molecular structure which influence on mechanical properties are: (1) molecular regularity, (2) availability of specific groups in the polymer chain which can increase intermolecular interaction; and (3) the conformation structure of the polymer (Pakhomov, 1999; Perepelkin, 1966). All these properties have an influence on the deformation behaviour of yarns and fibres. Shablygin and Pakhomov (1979) have found that the conformation structure of a polymer strongly influences the mechanical properties of aramid fibres. The deformation and strength properties depend on the quantity of hydrogen bonds between neighbouring chains responsible for the intermolecular interaction.

Haraguchi *et al.*, (1979) investigated the effect of the uniplanar orientation on the mechanical properties of PPTA thin film from the viewpoint of orientation of the hydrogen-bonded sheet. It was found that the hydrogen-bonded sheet plays a primary role as a slip plane during tensile deformation

There is a direct relationship between the molecular structure and mechanical properties. Para-linked aramid fibres show higher molecular alignment and better mechanical performance than the meta-linked aramid fibres. For example, poly(p-phenylene terephthalamide) in the form of Kevlar has the structure of parallel, densely packed chain molecules with a high degree of orientation and crystallinity. Though the chemical structure of poly(m-phenylene isophthalamide) (Nomex) is somewhat similar to that of Kevlar, the

meta links of the monomer unit introduce kinks into the polymer backbone and thus hinder a high degree of structural organization. In consequence, Kevlar is an example of a highly elastic polymeric fibre with a high elastic modulus and a low breaking strain. Nomex shows the stress-strain behaviour typical for a partially crystalline fiber, similar to that of aliphatic polyamides.

The relationship between structure and mechanical properties has been explicitly reviewed by several workers (Perepelkin, 1985; Ward, 1971; Stoeckel *et al.*, 1978; Bodor, 1984; Pakhomov and Shablygin, 1982). Only a few publications are related to accumulation of residual deformation for nonoriented polyethylene (Tsobkallo, 1988; Tsobkallo, 1996; Tsobkallo *et al.*, 1997). The recovery properties and accumulation of deformation for aramid fibres have not been extensively studied. Such an investigation will give further insight into the relationship between the deformation mechanism and the structure of fibres.

Aramid fibres usually have a low resistance to light. Fibres do interact with ultraviolet light and sunlight, with accompanying degradation. Table 1.5 indicates the amount and magnitude of change in the tensile properties of Kevlar 149 when exposed to ultra-violet radiation for various periods of time. It is therefore recommended that the surface of the fibre should be covered by some other material when used for outdoor applications.

Table 1.4 Effect of ultra-violet radiation on tensile properties of Kevlar 149 (Dobb and Robson, 1993)

Days exposed	Tensile Strength (GPa)	Strain to failure (%)	Initial Modulus (GPa)
0	2.48	1.40	144
1	1.80	1.04	147
2	1.35	0.82	147
4	1.03	0.67	143
7	0.81	0.61	137
14	0.70	0.54	134

1.3.4 The temperature effect on deformation and strength properties of polyamide yarns

The temperature dependence of mechanical properties is important, because many end-uses involve operation at elevated temperatures. It is especially true for aramid fibres and yarns, which are intended for use in extreme conditions (high temperature and load).

Highly flexible chains will be able to rotate easily into the various available conformations, while the internal rotations of bonds in a stiff chain are hindered and impeded. Variations in chain stiffness can be brought about by incorporating different groups in linear chains and the results can be appraised by following the changes in T_m (melt transition temperature) and T_g (glass transition temperature). Chain stiffness is greatly increased when an aromatic ring is incorporated in the chain, as this restricts the rotation in the backbone and reduces the number of conformations a polymer can adopt. This is an important aspect, as fibre properties are enhanced by stiffening the chain. The effect of aromatic rings on chain stiffness is shown in Table 1.5.

Table 1.5 The thermal characteristics of some polymer fibres (Machalaba, 1999; Volokhina, 1997; Perepelkin, 1987, 1992)

Fibre	Temperature (°C)	
	Glass transition	Decomposition
Kevlar	345-360	450-550
Terlon	345-360	450-550
SVM	270-300	500-550
Armos	270-300	500-550
Nomex	275-300	370-400
Fenilon	275-300	370-400
Polyethylene	-	≈220

It should be noted that the glass transition temperature of rigid chain polymers is different from the usual glass transition temperature of flexible chain polymers. Askadskii *et al.*, (1990) suggested that when a certain temperature known as the glass transition temperature is reached, a partial mobility is started. This mobility is attributable to the restricted torsion vibrations of repeat units or the vibration of the whole macromolecule. The segmental mobility is characteristic of flexible chain polymers, but the segmental mobility of rigid chain polymers is almost absent. However, even restricted mobility can be sufficient to allow a phase change in liquid crystal polymers. Therefore, under certain conditions, the temperature for first signs of restricted mobility of rigid chain fibres is used as glass transition.

Lee and co-workers (1995) studied the kinetics of Kevlar structural and mechanical property changes during heat treatment under tension using an interrupted heat-treatment method. In this work, heat treatment was interrupted after different treatment times, with the specimens immediately quenched to room temperature. Results indicated that the tensile modulus was strongly sensitive to the level of temperature of treatment and to tension, both parameters causing an increase in modulus. However, very low tension resulted in a small decrement in modulus. The kinetics shown by the tensile modulus were found also for crystallite reorientation (toward the fibre axis) and for the removal of pleating, suggesting that molecular reorientation is responsible for the modulus improvement and that this reorientation occurs through the removal of pleats. The responses of other structural features (paracrystalline axial distortion parameter, axial and transverse crystallite size) to change in temperature and tension deviated significantly from that of the tensile modulus, indicating that these features are not primary determinants of stiffness improvement during heat treatment.

The thermostability of aramid fibres depends both on chemical structure and the method of fibre formation. As a rule, the strength of fibres is lowered as the temperature of test is increased. The strength of many aramid fibres is 50-55% from initial value at 300°C (Kudriyavtsev *et al.*, 1992).

In the case of aramid fibres noticeable structural rearrangements occur in the temperature range above the glass transition temperature, and the beginning of thermochemical processes (250-300 °C) (Kudriyavtsev *et al.*, 1992).

There are many reports which discuss the effect of thermal ageing on the deformation properties of aramid fibres and yarns (Askadskii *et al.*, 1990; Perepelkin *et al.*, 1993; Perepelkin *et al.*, 1995; Hinderlich and Abdo, 1989; Hudosheev *et al.*, 1981). This is well documented and the generic processes, describing structural changes of *p*-aromatic fibres and yarns at very high temperatures, are discussed by Wu *et al.* (1990) and Radusch *et al.* (1994). From these reports, it is certain that the extent of internal stress in poly-para-phenylene terephtalamide fibres after annealing is one of the most important factors affecting the ultimate thermal mechanical properties. It can now be quantitatively measured using the concept of a thermal shrinkage stress. The correlation of the microscopic crystal structure parameters with annealing conditions, and therefore, with internal stress, has been established. Changes in the mechanical properties of aramid fibres at temperatures below the glass transition temperature are much less studied. The data presented in the literature is concerned mainly with strength properties, creep processes and stress relaxation, and does not discuss the problem of residual deformation (Hudosheev *et al.*, 1982; Tiranov *et al.*, 1976; Stalevich *et al.*, 1981).

All polyamide fibres are hydrophilic. Penn (1979) reported that the Kevlar fibre interacts reversibly with water, releasing water more slowly than it absorbs it. Equilibrium moisture content shows great variability at 50% r.h., and 23°C, the values ranged from 1.6% to 35%. For hydrophilic fibres the temperature effect on deformation and strength properties essentially depends on moisture. The importance of the interaction of water with textile fibres and yarns is associated with the fact that moisture is the most widespread medium affecting materials under real conditions of processing and exploitation.

Wang and co-workers (1992) found that the creep rates of these fibres under cyclic moisture variations are much higher than those under constant moisture conditions. When an aramid fibre is undergoing repeated drying and wetting cycles while under a constant

load, creep strain of the fibre increases continuously, rather than cycling between high and low strain levels, as might be expected. They believed that aramid fibres contain hydrogen bonds between rodlike crystallites oriented at small angles relative to the fibre axis. The hydrogen-bonded water molecules may exist between the crystallites in a monolayer fashion (Fig. 1.7 (a)) under low relative humidity or in a multilayer fashion (Fig. 1.7 (b)) under high relative humidity. Transient moisture conditions may cause slippage of hydrogen bonded elements and result in accelerated crystallite rotations due to breakage of hydrogen bonds, thus causing increases in logarithmic creep rate.

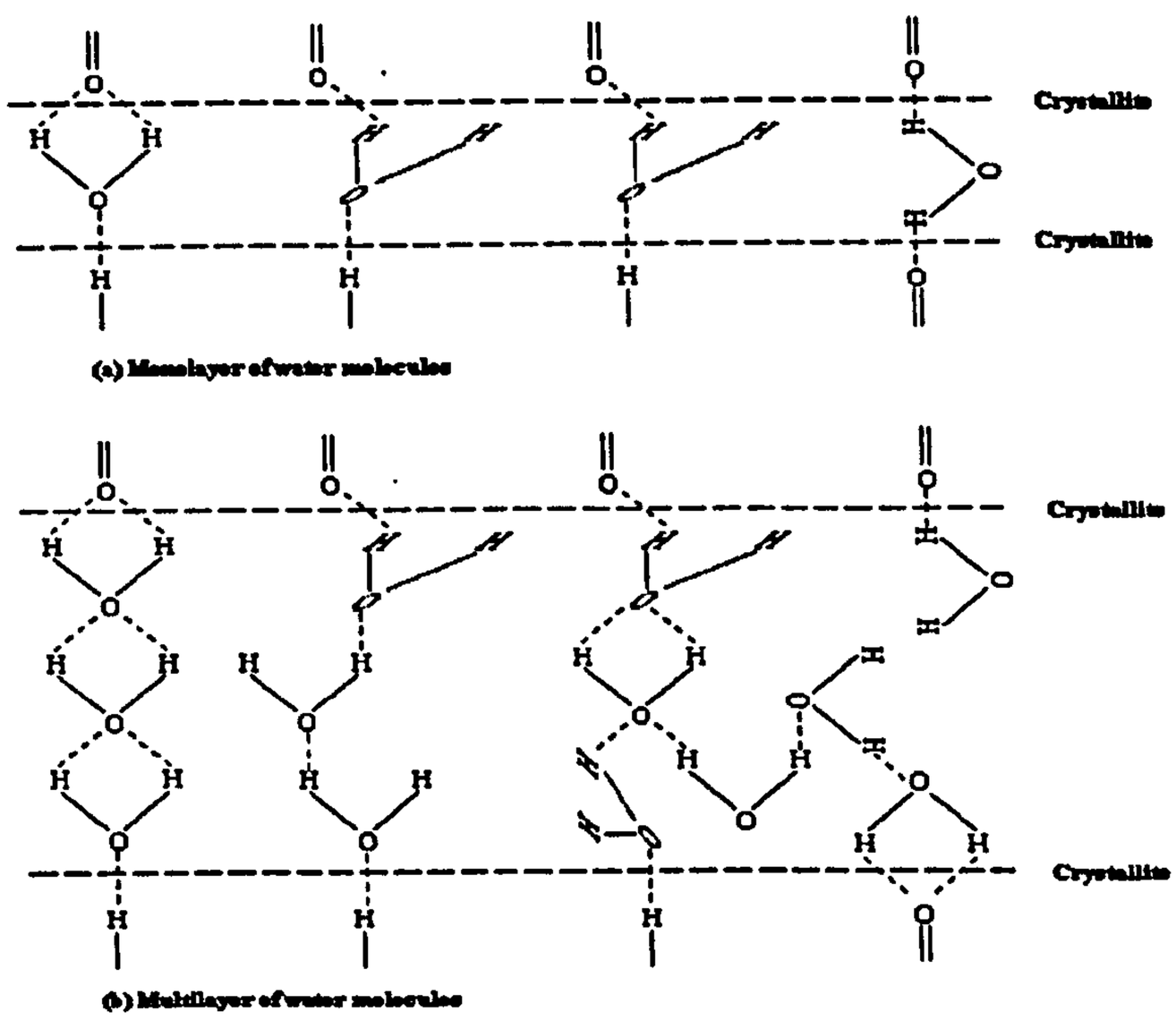

Fig. 1.7 Illustration of water molecules between crystallites (Wang *et al.* 1992)

Some Authors (Volkov *et al.*, 1990; Kozlov and Papkov, 1982) suggest that moisture can behave as plasticizer under certain conditions, however in rigid chain polymers, which are subjected to orientation processes, the effect of antiplasticization can also be observed. Both plasticization and antiplasticization can render strong influences on the deformation and strength properties of yarn. For traditional amide yarns (Capron, Nylon) the influence of moisture and hydrogen bonds on the deformation and strength properties of fibres are very interesting. As shown by previous workers (Vanderschueren and Linkens, 1978;

Kollross and Owen, 1982; Frank *et al.*, 1996), the availability or absence of moisture, and the quantity and type of hydrogen bonds, influence the mechanical properties of fibres. Kettle (1977) reports that the glass transition depends on the moisture content. The wide scatter of the reported data on glass transition in the literature can be explained by this fact.

Therefore absorption of moisture with consequent changes in some mechanical properties are characteristic for many polymers, due to on intermolecular interaction, caused by hydrogen bond formation. As reported by Machalaba (1999) the strength of aramid fibres is dependent on the moisture content and there are two reason for this: (1) the quantity of intermolecular bonds is increased at the expense of hydrogen bonds, which form by water bridges, (2) water can cause a plastification effect.

1.4 Structure and properties of gel-spun high strength high modulus polyethylene

1.4.1 Fibre formation and its application

In the production of high strength and high modulus Polyethylene fibres, melt spinning or solution spinning may be used. Melt spinning is restricted from a practical viewpoint to comparatively low molecular weight polymers (Mean Mol. Wt. <200,000) because of the requirement of a comparatively low melt viscosity. This disadvantage has been overcome by the solution spinning route which uses very high molecular weight polyethylene (Mean Mol. Wt. >1,000,000). The process comprises three main stages:

(1) the continuous extrusion of the solution of ultra-high-molecular weight polyethylene,
(2) spinning of the solution followed by gelation/crystallization which can be done either by cooling and extraction or by evaporation of the solvent, and
(3) ultradrawing and removal of remaining solvent.

The polymer is dissolved in a suitable solvent above its crystalline melting point, approximately between 150 and 220°C, followed by cooling to below 90°C, when a semicrystalline gel is formed. The most commonly used solvents include decalin, paraffin

Kollross and Owen, 1982; Frank *et al.*, 1996), the availability or absence of moisture, and the quantity and type of hydrogen bonds, influence the mechanical properties of fibres. Kettle (1977) reports that the glass transition depends on the moisture content. The wide scatter of the reported data on glass transition in the literature can be explained by this fact.

Therefore absorption of moisture with consequent changes in some mechanical properties are characteristic for many polymers, due to on intermolecular interaction, caused by hydrogen bond formation. As reported by Machalaba (1999) the strength of aramid fibres is dependent on the moisture content and there are two reason for this: (1) the quantity of intermolecular bonds is increased at the expense of hydrogen bonds, which form by water bridges, (2) water can cause a plastification effect.

1.4 Structure and properties of gel-spun high strength high modulus polyethylene

1.4.1 Fibre formation and its application

In the production of high strength and high modulus Polyethylene fibres, melt spinning or solution spinning may be used. Melt spinning is restricted from a practical viewpoint to comparatively low molecular weight polymers (Mean Mol. Wt. <200,000) because of the requirement of a comparatively low melt viscosity. This disadvantage has been overcome by the solution spinning route which uses very high molecular weight polyethylene (Mean Mol. Wt. >1,000,000). The process comprises three main stages:

(1) the continuous extrusion of the solution of ultra-high-molecular weight polyethylene,
(2) spinning of the solution followed by gelation/crystallization which can be done either by cooling and extraction or by evaporation of the solvent, and
(3) ultradrawing and removal of remaining solvent.

The polymer is dissolved in a suitable solvent above its crystalline melting point, approximately between 150 and 220°C, followed by cooling to below 90°C, when a semicrystalline gel is formed. The most commonly used solvents include decalin, paraffin

oil, and xylene (Savitskii *et al.*, 1989; Smith and Lemstra, 1980; Pennings, 1986; Hoogsteen *et al.*, 1988). The concentration of polymer in solution depends on the polymer molecular weight and level of mechanical properties, and can vary from 2 to 15%. Because the polymer solution is very dilute, it reduces the molecular entanglement of the polymer in the condensed state (Alekseev, 1994). The concentration of polymer in the solution controls the degree of molecular entanglement, and it must be reduced as the molecular weight of the polymer increase. The principle difference of gel-technology from other solution methods of chemical fibre formation is that the fibre is formed from solution spinning as a result of a decreasing of temperature, instead of vaporisation of solvent or replacement by a precipitant (Alekseev, 1994). The spinning is conducted by dry or dry-wet spinning through special conical spinners (Savitskii *et al.*, 1989; Pennings *et al.*, 1986; Hoogsteen *et al.*, 1988).

The gel is essentially a solid material with a very high microvoid content. Because it has few entanglements per molecule it can be drawn to very high degree. The high density polyethylene used in the production of high modulus gel-spun fibres has a molecular weight in excess of 1,000,000 to provide strength and creep resistance.

The gel can be drawn with the solvent or after removal of the solvent (Smith and Lemstra, 1980; Savitskii *et al.*, 1984; Smook and Pennings 1982). If the solvent is not removed prior to drawing, it emerges during the drawing process, and the resulting fibres are very porous. If the solvent is removed prior to drawing, the fibres are less porous, but equally as strong and stiff.

High strength, lightness, water- and rot-resistance Polyethylene fibres have enabled them to become established in the marine cordage field. There are great advantages in ropes and nets that float, do not rot and do not absorb water. The reinforcement of elastomers (conveyor belts, high pressure hose pipes *etc.*) and plastics (sking, boats and yachts *etc.*) (Alekseev, 1994) are other applications.

1.4.2 Structure and properties of high strength high modulus polyethylene

Cooling of polyethylene solutions during drawing (stirring, pressing through a capillary tube *etc.*) (Pennings, 1967), produces crystals such as the shish-kebab type (Fig. 1.8) in which there is a central core consisting of more or less extended polyethylene molecules (shish) with folded-chain type crystals deposited on the core (kebabs) (Bigg, 1988).

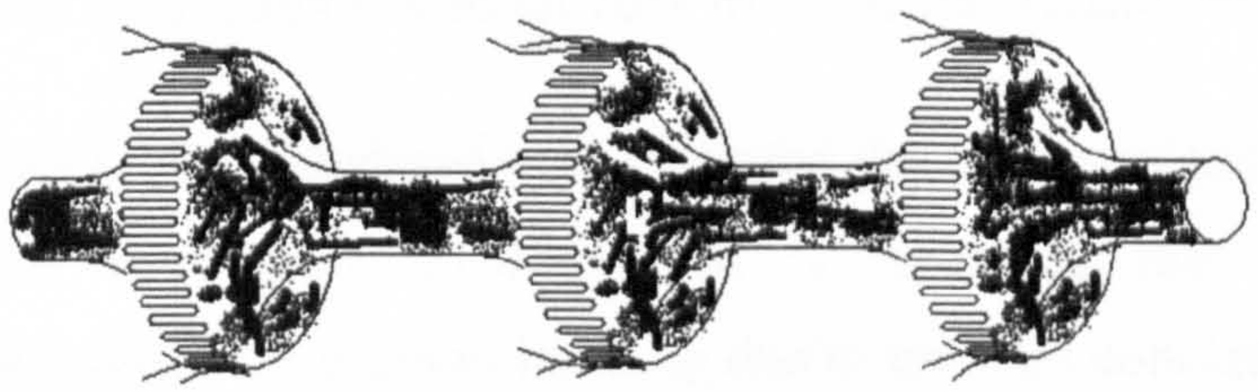

Fig. 1.8 The shish kebab type of structure (Bigg, 1988)

This shish-kebab structure can be transformed into extended smooth fibrils at a very high draw ratio. A schematic representation of a Polyethylene fibre microfibril is shown in Fig.1.9 (Bigg, 1988). Analysis of the structure by different methods has shown that the diameter of fibrils for a polyethylene fibre is approximately 0.5 μm. The fibrils in turn consist of microfibrils (15-20 nm diameter), which are constructed from alternating crystalline and unregulated areas of length accordingly 50-70 and 4-10 nm (Zubov *et al.*, 1986; Bakeev *et al.*, 1986).

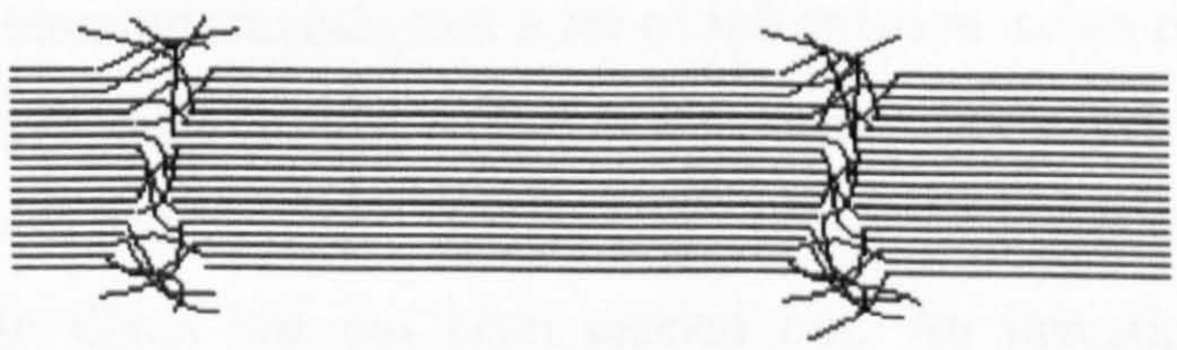

Fig. 1.9 The Polyethylene fibre microfibril (Bigg, 1988)

It should be noted that the so-called "unregulated" areas for this fibre have a larger packing density than amorphous areas of usual chemical fibres (Prevorsek, 1989). Polyethylene has

a degree of crystallinity of up to 70%, depending on the conditions of crystallisation. As a rule, a crystallisation of polymer from melts and solutions produces crystals with folded chains or lamel. The lamel represent flap-type crystals, inside which chains are in a folded formation (Alekseev, 1994).

The intermolecular interaction in polyethylene is not strong due to weak Van der Waals forces (Pullman, 1978). Polyethylene fibres have a quite high strength and modulus elasticity, though now even for the best Polyethylene fibres the strength is about 10% of the theoretical value and the modulus is about 70% from the theoretical value (Ward, 1986).

Termonia and Smith (1986) discussed and compared the modes of failure of PPTA and of polyethylene under fixed-strain conditions. It is suggested that for PPTA, a high concentration of stress rapidly starts to build up due to the high concentration of chain ends resulting from the small number of PPTA units per macromolecule. As a result, catastrophic failure occurs and the specimen breaks in a brittle fashion. In polyethylene, on the other hand, the concentration of chain ends is much lower and the local stress concentration arising from the few initial primary bond breakings are distributed among the numerous neighbouring Van der Waals bonds. However, as these primary bond fractures increase in number, the stress concentration in the Van der Waals bonds also increases and secondary bond fracture occurs. As a result, failure of the specimen is accompanied by a creep-like mode of deformation.

1.5 The current research interests

The review of the literature reveals that a lot of information exists relating to the structure and properties of individual polyamide fibres. However a systematic approach to study the relationship between structure and the property of creep deformation for aromatic and aliphatic polyamide fibres has not been carried out. An investigation the relationship between intermolecular iteration, creep-recovery and residual deformation of polyamide fibres has not been found in publication. Therefore, the study of polyamide fibres is very interesting, and it is proposed to research the properties of fibres and yarns belonging to

different groups. These are:

- the conventional polyamide fibres obtained from flexible chain polymers, for example Capron and Nylon 6.6;
- Phenylon and Nomex fibres, obtained from semi rigid chain polymers;
- fibres with unique mechanical and thermal properties such as Armos, SVM, Terlon and Kevlar obtained from rigid chain polymers.

The deformation and strength properties of fibres are dependent upon intermolecular interaction. Therefore it is interesting to compare the properties of high strength high modulus fibres having different type of intermolecular interaction. It is proposed to compare the mechanical properties between types of polyamide fibres (for which the intermolecular interaction is defined by hydrogen bonds) and also to compare with Polyethylene fibres (the intermolecular interaction is defined by Van der Waals bonds).

CHAPTER 2

MATERIAL AND EQUIPMENT

2.1 The characteristic of research objects

The polyamide yarns produced from polymers with different chain rigidity were chosen as subjects for research. These were Terlon, Armos, SVM and Kevlar yarns from rigid chain polymers; Phenylon and Nomex yarns from semi-rigid chain polymers; Capron and Nylon yarns from flexible chain polymers. In addition, the high strength high modulus Polyethylene yarn produced by gel-technology was chosen for comparison. The characteristics of these yarns are shown in Table 2.1.

The polymer materials chosen in the present work represent different chemical structures and different types of intermolecular interaction. It is known that the intermolecular interaction of a polyamide is defined by hydrogen bonds, but in the case of polyethylene the intermolecular interaction is mainly due to the weaker Van-der-Waals forces. It is interesting to relate tensile strength, deformation and recovery properties to the polymer structure by studying the mechanical properties of polymers with similar chemical nature and intermolecular bonds, but with different rigidity of the molecular chain.

The rigidity of molecular chains renders a large influence on the elastic properties of polymers. The concept of rigidity of polymer chains as a rule relates to the mobility of macromolecular segments and the size of a Cune segment (Perepelkin, 1985). Therefore polycaproamide, from which the Capron fibre is produced, can have flexible chain polymers (Cune segment is 2.0-2.2 nm). Poly-*p*-amides from which SVM, Armos, Terlon, Kevlar fibres are produced, can have rigid chain polymers (Cune segment is about 30-40 nm). Polymetaphenilenizoftalamide (PMFA) from which Phenylon and Nomex fibres are produced, has a Cune segment about 3-10 nm, therefore they are semi-rigid chain polymers.

Kevlar, Nomex and Nylon 6.6 yarns, supplied by "DuPont de Nemour", USA were used for comparison.

Table 2.1 Characteristics of polymer yarns used in the present work

Polyamide Yarns			
Trade name	**Chemical structure**	**Linear density (tex)**	**Producer**
Capron	Polycaproamide $[—NH—(CH_2)_5—CO—]_n$	91	Russia, J.-S. Co Klinvolokno
Phenylon	Poly-*m*-phenyleneisophthalamide 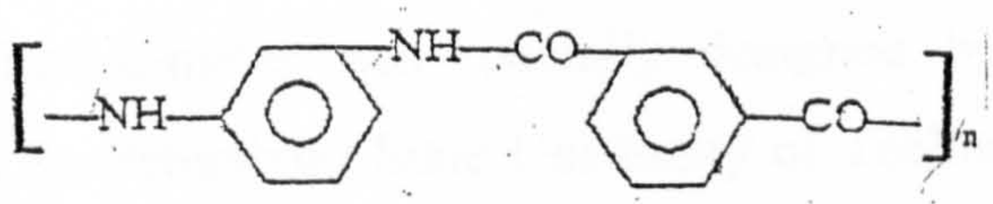	93.5	Russia, VNIISV, Tver
Armos	*p*-aromatic heterocyclic copolyamide	100	Russia, VNIIPolymervo-lokno. J.-S. Co Tverchimvolokno
SVM	*p*-aromatic heterocyclic polyamide 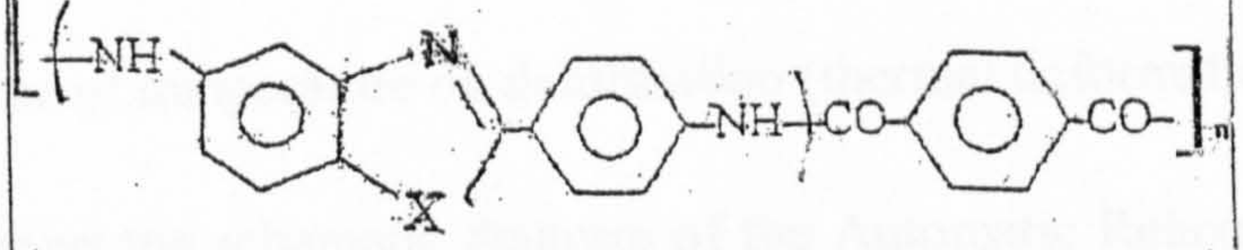	58.8	Russia, VNIIPolymervo-lokno. J.-S. Co St.Petersburg NIIChimvolokno
Terlon	Similar to Poly-*p*-phenyleneterephthalamide 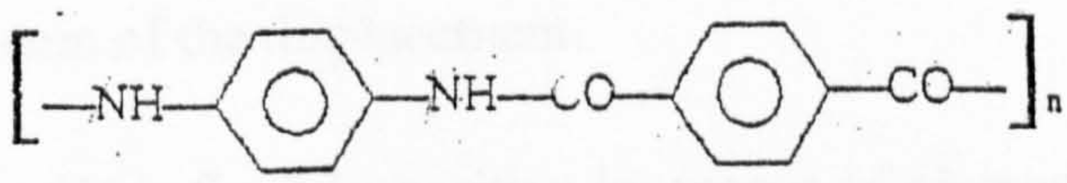	58.8	Russia, VNIIPolymervo-lokno
Polyethylene Yarn			
Polyethy-lene	high molecular polyethylene $[—CH_2—CH_2—]_n$	45.5	Russia, VNIITverchimvo-lokno

2.2 Equipment

2.2.1 Instron tensile tester

The research of deformation and strength properties of yarns such as stress-strain properties and stress-relaxation were carried out on a universal "Instron-1122" Tensile Tester. This equipment allows to a stretching speed from 0.05 mm / min up to 1000 mm / min with a range of loads from 1 mN up to 5 kN.

2.2.2 Automatic relaxometer for creep-recovery

The Automatic Relaxometer was specially designed by the Department of Material Resistance of the St.-Petersburg State University of Technology and Design in Russia for determination of the creep-recovery properties of yarns. This device can be used for measuring deformation properties of polymer yarns such as:

- Deformation with time at constant stretching load (creep),
- Residual deformation with time after removal of loading (elastic recovery),
- Influence of temperature on deformation (thermal deformation properties).

Fig. 2.1 shows the schematic diagram of the Automatic Relaxometer which can be placed on the top of the rigid bench. The device is mainly composed of the steel base (1); the top plate (3) supported by three columns (2) on the base; the loading application system and measuring system of the displacement.

A yarn sample (4) is fixed in position by means of clamps (5 and 6). The bottom clamp is held rigid by attaching to a support (7). The mobile upper clip (5) is connected through draft (10) and a balance beam (11) to the mechanism of a loading force. Because the ratio of the shoulders on the balance is 1:5, the loading force applied to the sample can be five times of the actual load weight. the cargo (24) which can move on direction (25) is necessary for an equilibration of balance serves.

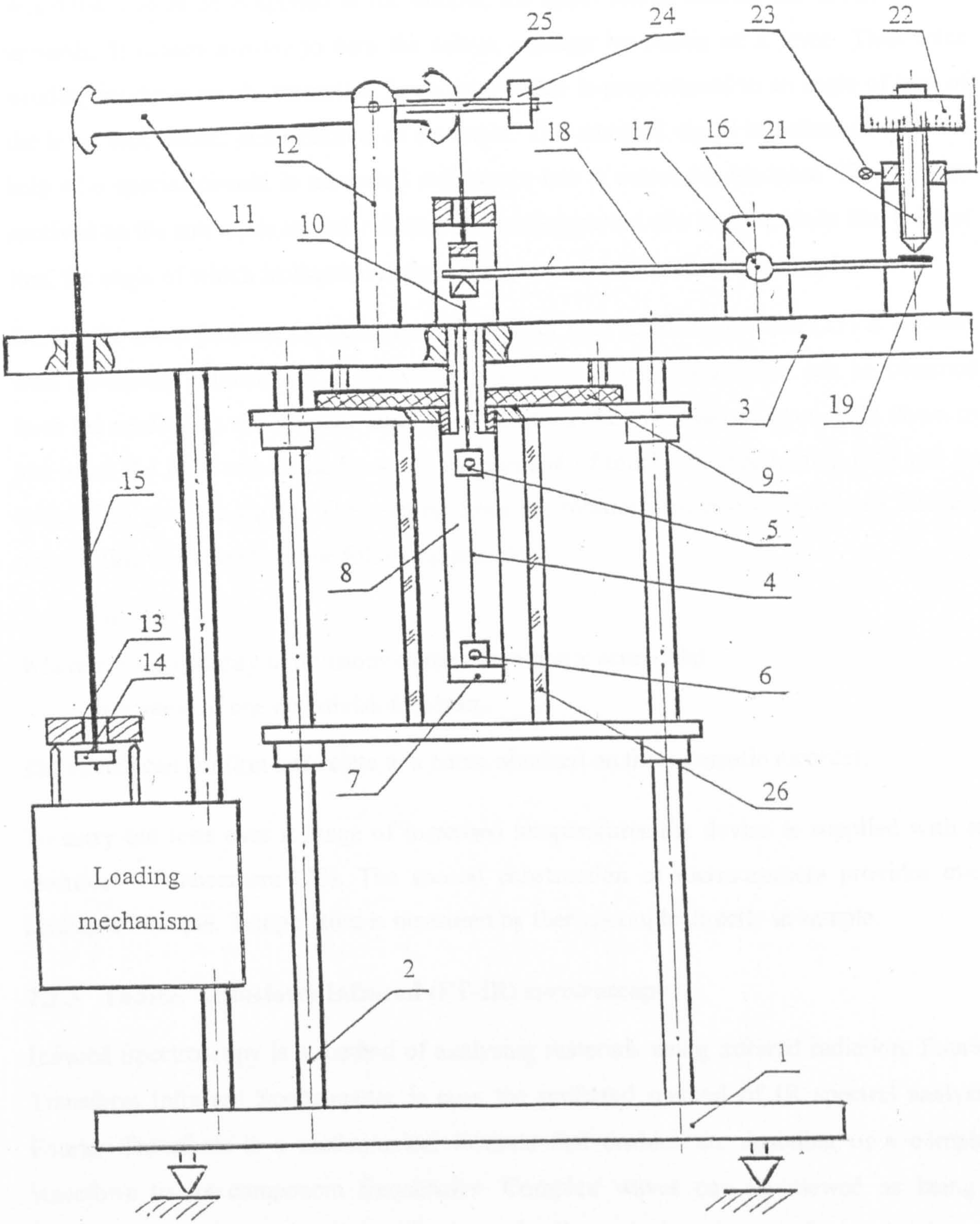

Fig. 2.1 Schematic diagram of Automatic relaxometer

When the load force is applied to the sample, the upper clamp holding the sample moves upwards. It causes a rotor to turn the selsyn - gauge by means of a lever. Thus rotor winding produces an electromotive force, whose size is proportional to an angle of turn of the lever and, hence, deformations of a sample. The received signal transformed with the help of a special circuit, is measured and enters into a automatic recorder. The diagram received on the automatic recorder during the loading period of a sample, looks like a direct line, the angle of which inclination defines the speed of deformation of a sample.

During the creep process, the right arm of the lever (18) fixed on the rack (17) is lowered with increasing deformation of the yarns. The level of the deformation can be obtained from the reading on the rotation dial (22) by turning the micrometric screw (21) down to just touch the right end of the lever. At the moment of touch, the electrolamp (23) will be initiated to give the signal. The reading from the rotation dial can be translated into the deformation of a sample in the following equation:

$$\Delta L = n * k$$

Where n = the quantity of divisions of the micrometric screw dial

k = value of one dial division in mm.

The results can confirm and relate to a curve obtained on the automatic recorder.

To carry out tests over a range of increased temperatures the device is supplied with an electrical thermocamera (20). The special construction of thermocamera provides even heating all sample. Temperature is measured by thermocouple directly in sample.

2.2.3 Fourier Transform Infrared (FT-IR) spectroscopy

Infrared Spectroscopy is a method of analysing materials using infrared radiation. Fourier Transform Infra-red Spectrometer is now the preferred method of IR spectral analysis. Fourier Transform is a mathematical formula that enables the decoding of a complex waveform to its component frequencies. Complex waves can be viewed as being a combination of an infinite series of single waves. By analysing any waveform using Fourier Transform, the individual component wave forms can be reconstructed. The principles and

analytical capabilities of Fourier Transform Infra-red Spectrometer are well understood. The coupling of Fourier Transform Infra-Red spectroscopy and microscopy have allowed analysis of samples as small as single fibres to be performed. One major advantage of the infra-red microscope is that the specimen to be analysed can be viewed conventionally and positioned accurately before analysis is carried out. The Spectra Tech FTIR 50XC (Nicolet) with a microscope IR-Plan TM (Fig. 2.2) was used in the present work.

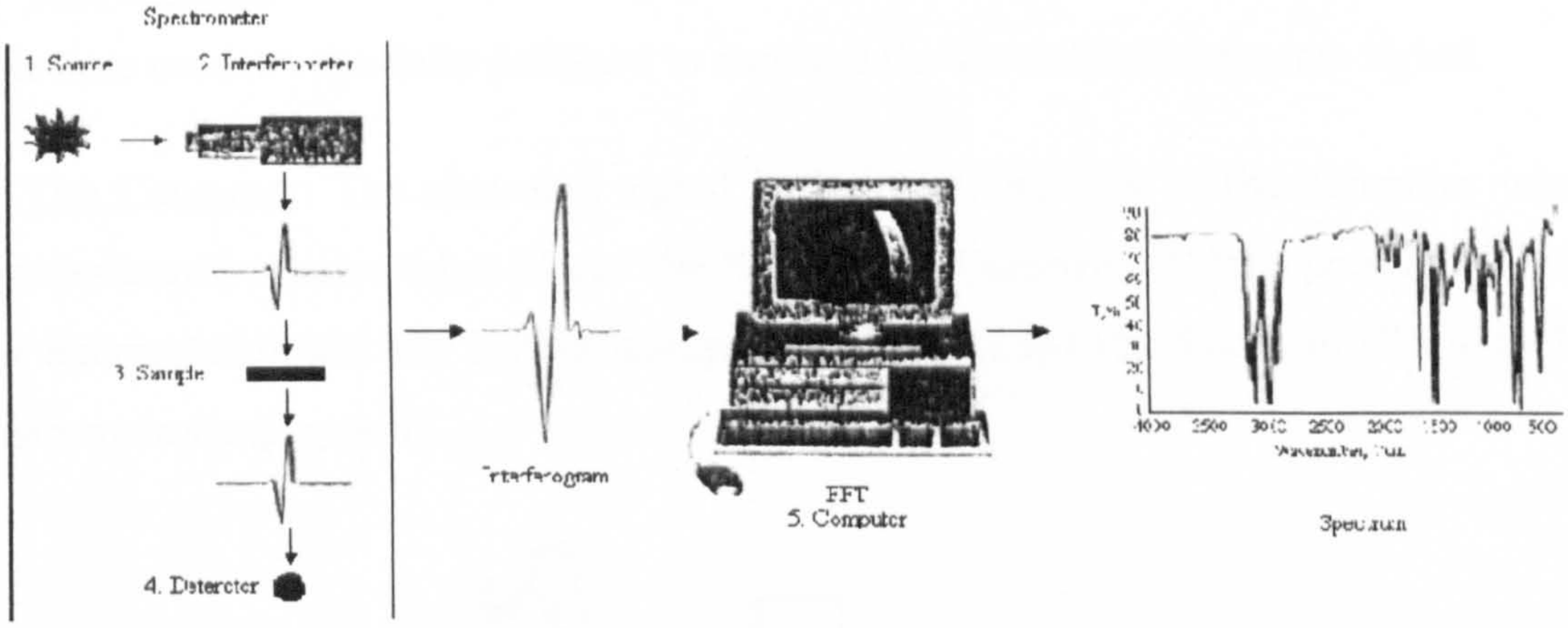

Fig. 2.2 Scheme of the FT-IR process

In infrared spectroscopy, IR radiation is passed through a sample. Some of the infrared radiation is absorbed by sample and some of it is passed through (transmitted). The resulting spectrum represents the molecular absorption and transmission, creating a molecular fingerprint of the sample. Like a fingerprint no two unique molecular structures produce the same infrared spectrum. This makes infrared spectroscopy useful for several types of analysis.

The normal instrumental process is as follows:

1. The Source: Infrared energy is emitted from a glowing black body source. This beam passes through an aperture which controls the amount of energy presented to the sample (and, ultimately, to the detector).

2. The Interferometer: The beam enters the interferometer where the "spectral encoding"

takes place. The resulting interferogram signal then exits the interferometer.

3. The sample: The beam enters the sample compartment where it is transmitted through or reflected off the surface of the sample, depending on the type of analysis being accomplished. This is where specific frequencies of energy, which are uniquely characteristic of the sample, are absorbed.

4. The Detector: The beam finally passes to the detector for final measurement. The detectors used are specially designed to measure the special interferogram signal.

5. The Computer: The measured signal is digitized and sent to the computer where the Fourier transformation takes place. The final infrared spectrum is then presented to the user for interpretation and any further manipulation (Fig. 2.3) (The theory of FT-IR by Nicolet Instrument Corporation).

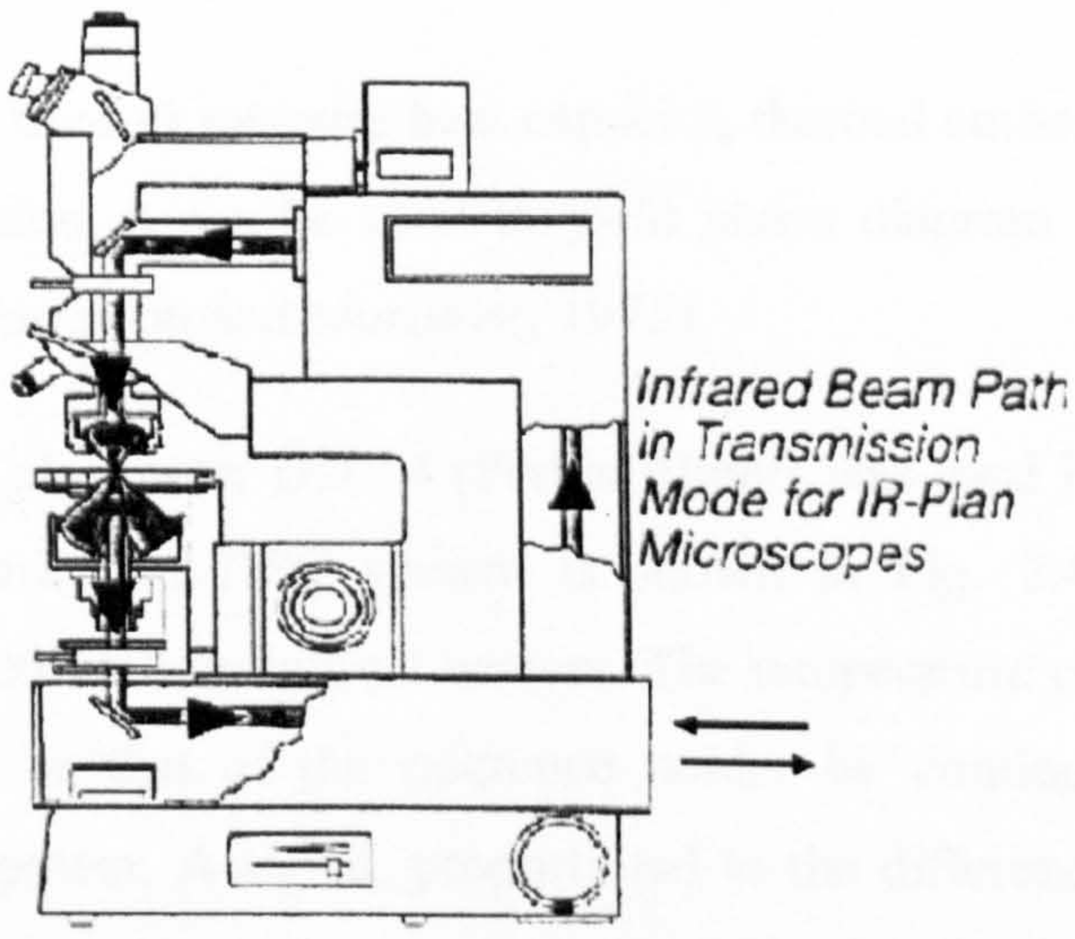

Fig. 2.3 Scheme of microscope for FTIR

The coupling of an IR microscope with an FTIR spectrometer allows the infrared analysis of samples as small as 10μm in diameter. An IR microscope consists of transfer optics, which transmits the IR beam from the interferometer of the spectrometer to the detector. The measured area must be delimited. This achieved by bringing the area of interest to the

centre of the field of view under visible light and delineating this area by means of adjustable apertures (Total Coverage in FT-IR Microscopy).

The FT-IR microscope can be successfully used to quantify the different components of individual fibres.

2.2.4 Differential scanning calorimetery (DSC)

Whenever a material undergoes a change in physical state, such as melting or transition from one crystalline form to another, or whenever it reacts chemically, heat is either absorbed or liberated. Differential scanning calorimeters can be used to determine the enthalpies of these processes by measuring the differential heat flow required to maintain a samples of the material and an inert reference material at the same temperature. This equipment is usually programmed to scan a temperature range by increasing linearly at a predetermined rate.

The apparatus can also be used to measure heat capacity, thermal emissivity and the purity of solid samples. In addition, it can be used to yield phase diagram information and to provide kinetic data (McNaughton and Mortimer, 1975).

A Differential Scanning Calorimeter DSC 4 (Perkin Elmer) was used in the present work. The schematic representation of DSC system is shown in Fig. 2.4. The sample and reference are each provided with individual heaters. The temperature of the sample holder is always kept the same as that of the reference holder by continuous and automatic adjustment of the heater power. A signal, proportional to the difference between the heat input to the sample and that to the reference, dH/dt, is obtained and recorded.

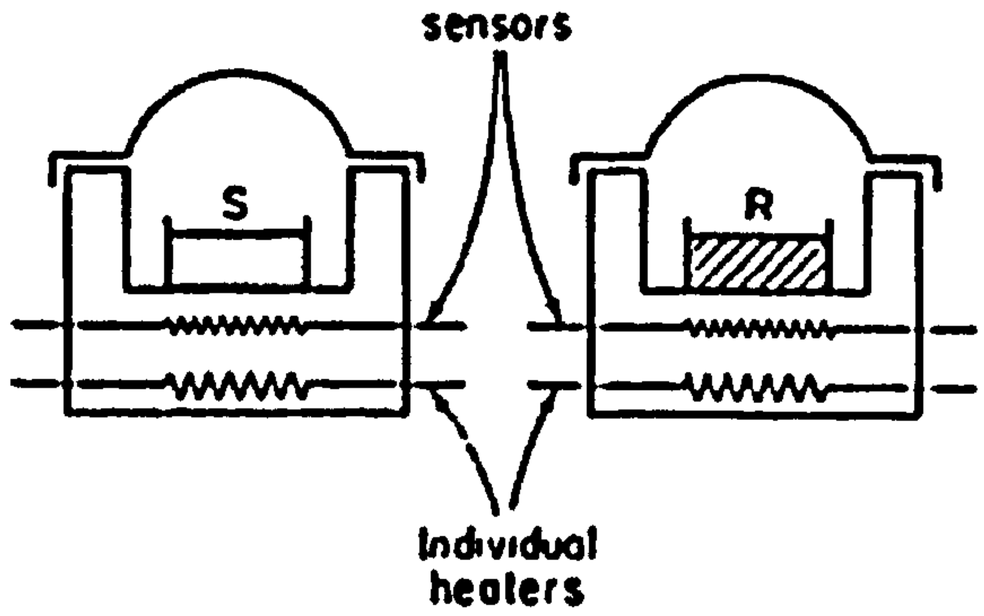

Fig. 2.4 Scheme of DSC system

2.2.5 Scanning Electron Microscopy (SEM)

The Scanning Electronic Microscopy (SEM) was used for the morphological analysis of fibre surface. Fibre samples were fixed on stubs using adhesive tape. The mounted specimens were sputter coated with a gold particle discharge to give better reflection of the electron beam and prevent the accumulation of electric charge on the sample. The SEM analysis was performed on a Scanning Electronic Microscopy S 430, LEICA.

CHAPTER 3

THE STUDY OF DEFORMATION AND STRENGTH PROPERTIES OF POLYAMIDE YARNS AFTER PRELIMINARY STRETCHING

3.1 Introduction

Fibres and yarns are subjected to different loads in their practical and industrial applications, resulting in changes in their mechanical properties. Therefore studying the deformation and strength properties after preliminary deformation is very important. In order to predict the mechanical properties of yarns, the residual deformation must be taken into account. The nature of accumulation of residual deformation is dependent on the rigidity of the molecular chain and intermolecular interactions. For this reason the deformation and strength properties of fibres which have different molecular chain rigidities are compared in this investigation.

The polyamide fibres formed from polymers of varying chain rigidity were chosen as objects of research. These were polyamide fibres formed from rigid chain polymers (Terlon, Armos, SVM, Kevlar); polyamide fibres formed from semi-rigid chain polymers (Phenylon, Nomex); and polyamide fibres formed from flexible chain polymers (Capron, Nylon).

3.2 Experimental

3.2.1 Yarn samples preparation

Armos, SVM, Terlon, Kevlar, Phenylon, Nomex, Capron and Nylon yarn samples were conditioned at 20°C and 65% r.h. before testing. In order to study the effect of preliminary stretching on the tensile properties of yarns, samples were prepared by stretching yarn to different extensions depending on the fibre type for 10 minutes, and then allowed to relax

for 10 min for recovery. Armos yarns were preliminary stretched to a range of extension from 1% to 3%; SVM from 1% to 4%; Phenylon from 4% to 19%; and Capron from 8% to 14% for further tensile testing.

3.2.2 Determination of stress-strain tensile properties

The tensile properties of the original yarns and also preliminary stretched yarns were determined using an Instron-1122 tensile tester equipped with a load cell having a maximum capacity of 5 KN. Yarn gauge lengths of 100 mm and a stretching speed of 100 mm/min were used. The tensile properties were initially expressed by stress-strain curves.

The modulus is calculated by differentiation of the stress-strain curve ($E=\partial\sigma/\partial\varepsilon$). The tangent modulus used in this work was obtained by determining the slope ratio of tangent to point on the stress-strain curve over the total range of deformation (Fig. 3.1), i. e. lower limit and upper limit associated parameters are equal to the point at which tangent modulus is taken.

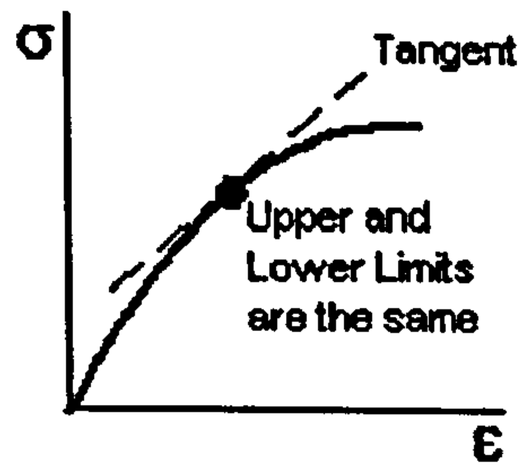

Fig. 3.1 Modulus Examples for Tangent Calculations

The relative modulus of rigidity is determined as the slope ratio of tangent to the most linear part of the stress-strain curve. Because the stress-strain curves of Armos and SVM yarns consist of two zones of deformation, the rigidity of Armos and SVM yarns is characterized by two values of modulus E_1 and E_2. These module correspond to the slopes of the most linear parts of the first and second zones of deformation.

3.2.3 Creep-recovery properties

The process of yarn creep-recovery was investigated using the Automatic Relaxometer as described in Section 2.2.2. Yarn samples were subjected to a range of constant loads for a period of 10 min. The load was then removed. The stress produces an immediate elastic response, which is followed by a time-dependent viscous response. The deformation recovery of the yarn was measured after the removal of the load. The strain with time was monitored throughout the process of creep-recovery and the final residual deformation was determined after 10 min recovery. Deformation (strain) and Residual deformation were calculated as:

Deformation (strain) = $(L_2 - L_1) / L_1$

Residual deformation = $(L_3 - L_1) / L_1$

where L_1 is the original length of yarn

L_2 is the extended specimen length

L_3 is the specimen length measured after recovery

3.2.4 Stress-relaxation properties

The process of stress relaxation was investigated using an Instron 1122 Tensile Tester equipped as described in Section 3.2.2. The yarn samples were extended at a speed of 100 mm/min to a range of strains, and held for a period of 10 min. The stress over a period of time was measured. The values of residual deformation were determined after another 10 min relaxation.

3.3 Results and discussion

3.3.1 Tensile stress-strain properties of Armos, SVM, Terlon and Kevlar yarns at room temperature

Study of the stress-strain relationship for yarns is the simplest and most popular method for determining deformation and strength properties. Stress-strain curves provide information relating to the break characteristics including breaking stress and breaking elongation

(deformation). However, these curves can provide more in-depth information relating to the rearrangements of structure, which occur during deformation (Pakhomov *et al.*, 1986).

It is known that the degree of rigidity of macromolecular chains will influence the elasticity, deformation and strength properties of polymers. The chemical properties of polymers will depend on the rigidity of molecular chains. Poly-*p*-amides, from which SVM, Armos, Terlon and Kevlar fibers are formed, are rigid chain polymers (Cune segment is about 30-40 nm) (Perepelkin, 1985). This rigidity is attributable to the presence of a benzene ring in the structure of the polymer and the para-position of amide groups.

Figs. 3.2 and 3.3 show the effect of preliminary stretching at an extension of 1, 2, and 3% on the stress-strain behaviours for Armos and SVM yarns. It can be seen that the character of Armos and SVM stress-strain curves is similar, therefore the future work will focus on the analysis of Armos yarns in more detail.

From the stress-strain curves for original Armos and SVM yarn (curves 1 in Figs. 3.2 and 3.3), two regions of different curvature can be observed. The tangent modulus was obtained by differentiating these stress-strain curves. Fig 3.4 shows the relationship between the tangent modulus and strain. It can be seen that the tangent modulus decreases with increasing strain up to 1.5% (the first region), thereafter the tangent modulus increases (the second region). But a third region showing the final decrease in the tangent modulus due to breakage of covalent bonds in polymer chains during deformation (Pakhomov *et al.*, 1986) is not observed. Therefore it is suggested that, for Armos and SVM yarns, breaking of covalent bonds in the main macromolecular chain occurs only in a very narrow zone just before yarn breakage. This suggestion agrees with previous work by Tsobkallo (1988), who investigated the relationship between tensile strain and the related concentration of breaking covalent bonds using infrared spectroscopy, during destruction processes for SVM yarns (Fig. 3.5). It was noted that breakage of covalent bonds in this type of polymer fibre occurs only in the narrow area of certain strain at the point of fibre break. The stretching of yarns involves sliding of structural members, and consequent breakage of old, and

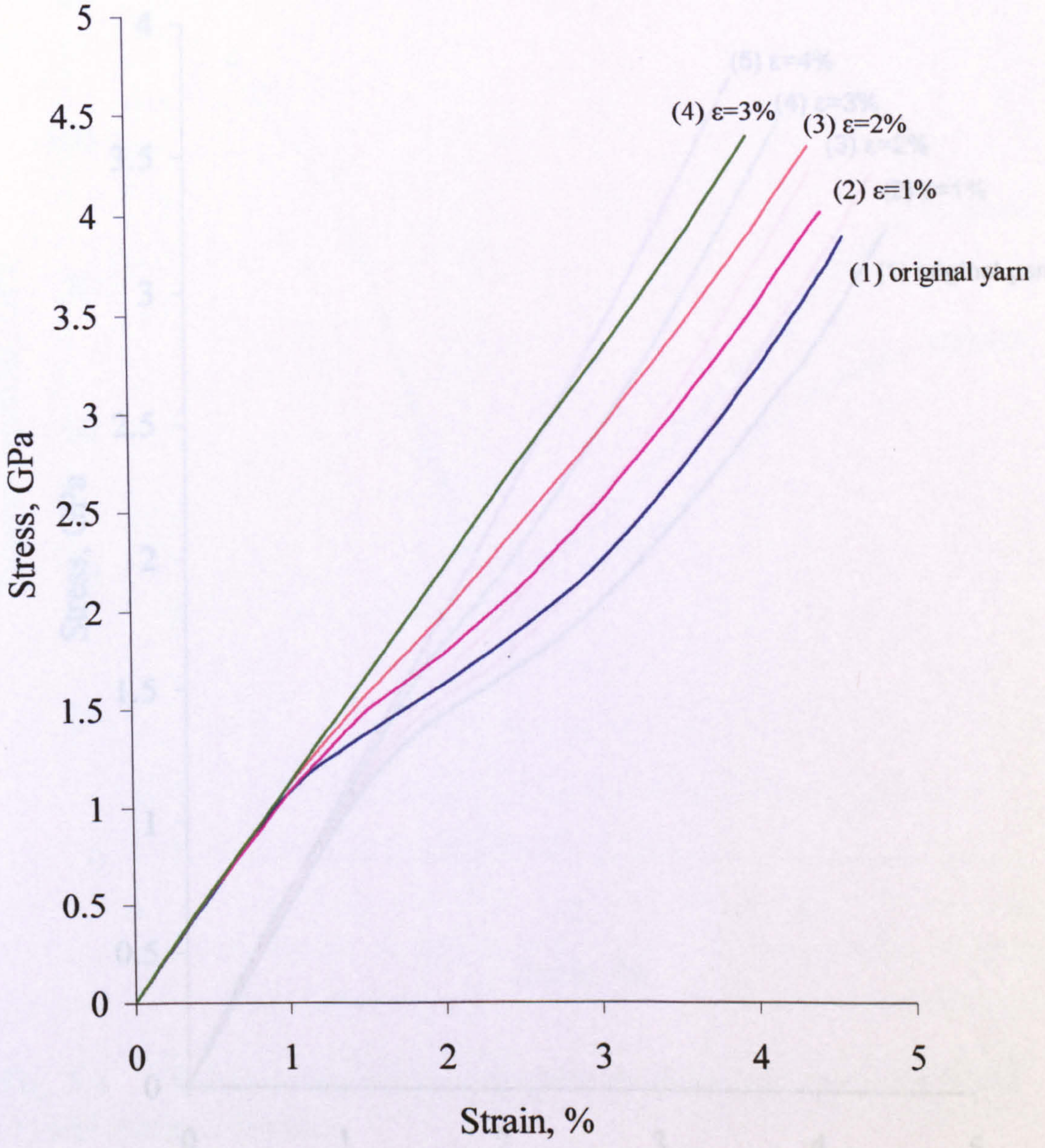

Fig. 3.2 Stress-strain curves of Armos yarn before and after preliminary stretching: (1) original yarn; (2) yarn after preliminary stretching at ε=1%; (3) yarn after preliminary stretching at ε=2%; (4) yarn after preliminary stretching at ε=3%

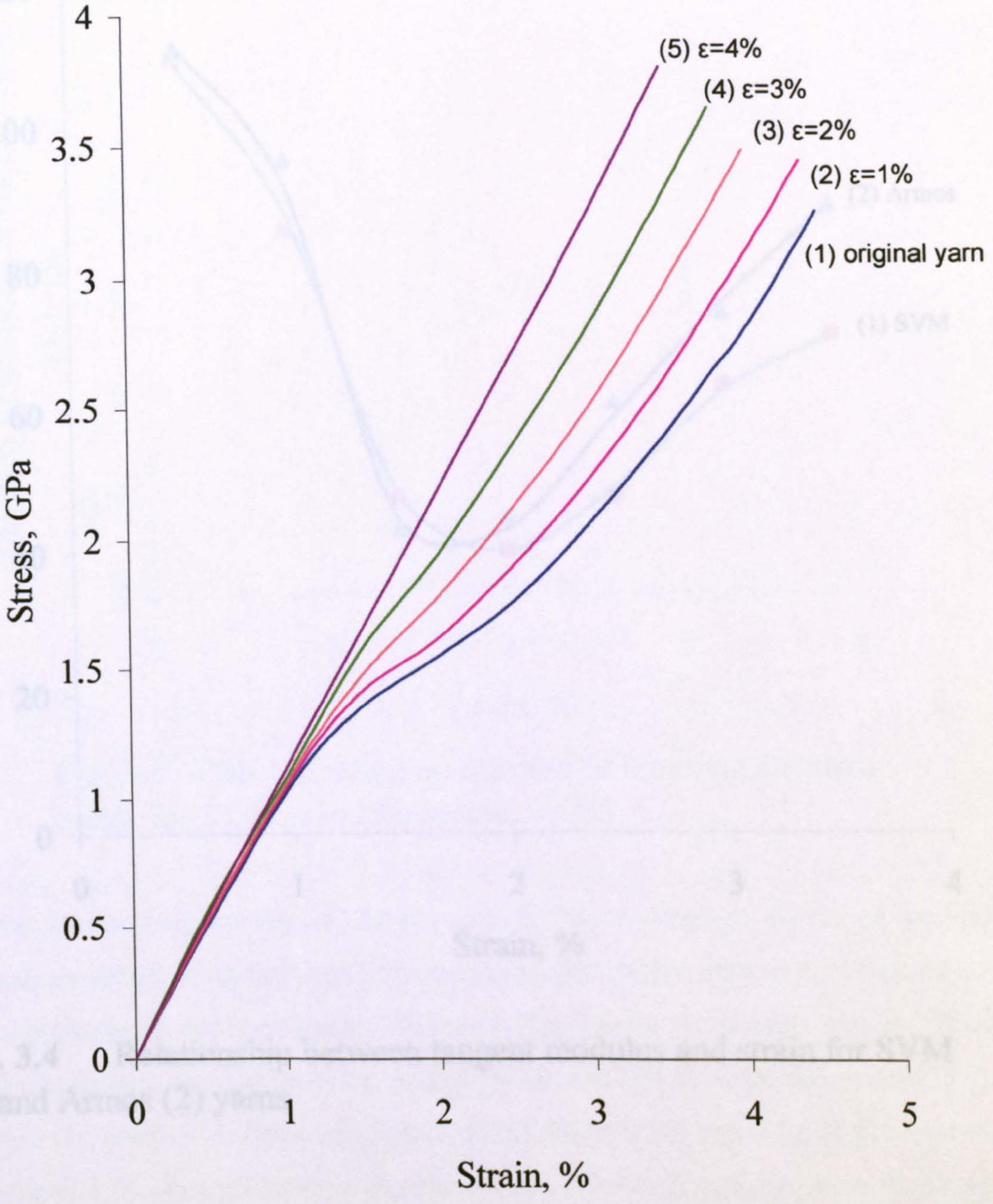

Fig. 3.3 Stress-strain curves of SVM yarn before and after preliminary stretching: (1) original yarn; (2) yarn after preliminary stretching at ε=1%; (3) yarn after preliminary stretching at ε=2%; (4) yarn after preliminary stretching at ε=3%; (5) yarn after preliminary stretching at ε=4%

formation of new, intermolecular bonds accompanied by some conformation and orientation processes.

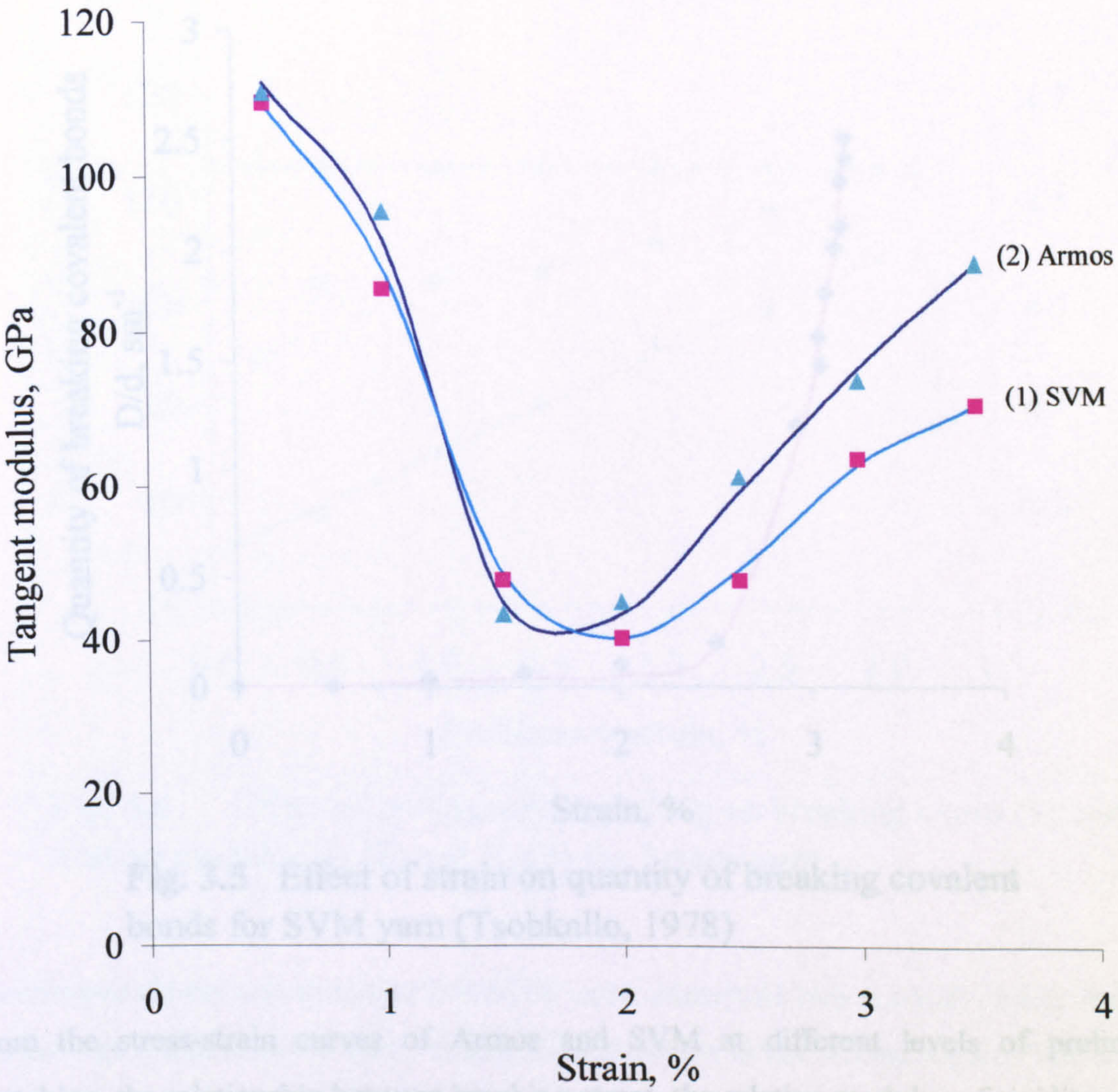

Fig. 3.4 Relationship between tangent modulus and strain for SVM (1) and Armos (2) yarns

From Figs. 3.2 and 3.3 it can be seen that increasing the preliminary deformation causes the characteristic second region of the stress-strain curve of Armos and SVM yarns to disappear. The curves gain linear character beyond 3% preliminary deformation for Armos

and 4% for SVM. Such a change in the stress-strain curves suggests that preliminary stretching of Armos and SVM results in additional orientation of macromolecular chains.

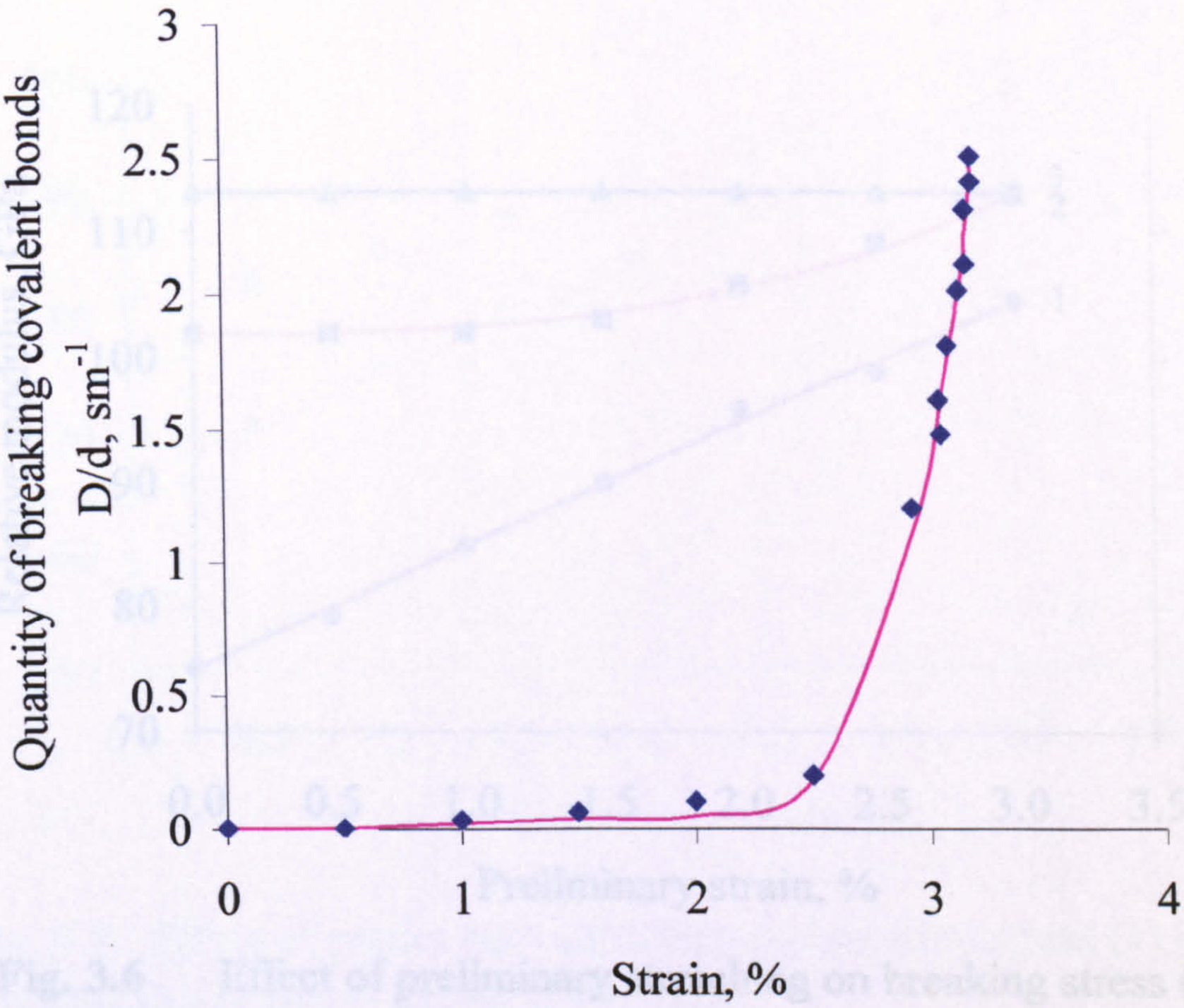

Fig. 3.5 Effect of strain on quantity of breaking covalent bonds for SVM yarn (Tsobkallo, 1978)

From the stress-strain curves of Armos and SVM at different levels of preliminary stretching, the relationship between breaking stress, the relative modulus of rigidity and the value of preliminary deformation are shown in Fig. 3.6 for Armos and Fig. 3.7 for SVM yarns. It can be seen that the breaking strength of Armos and SVM yarns increases by about 10% when the level of preliminary applied deformation is increased up to 4% (curves 1 in Figs. 3.6 and 3.7). Such an increase in strength can be related to an increase in the number of polymer chains subjected to load and the formation of additional intermolecular bonds. It is thought the preliminary stretch results in the formation of structured blocks and orientation along the length of the fibre axis, which both can result in the formation of

additional intermolecular bonds and therefore influence the physical-mechanical properties of polyamide yarns.

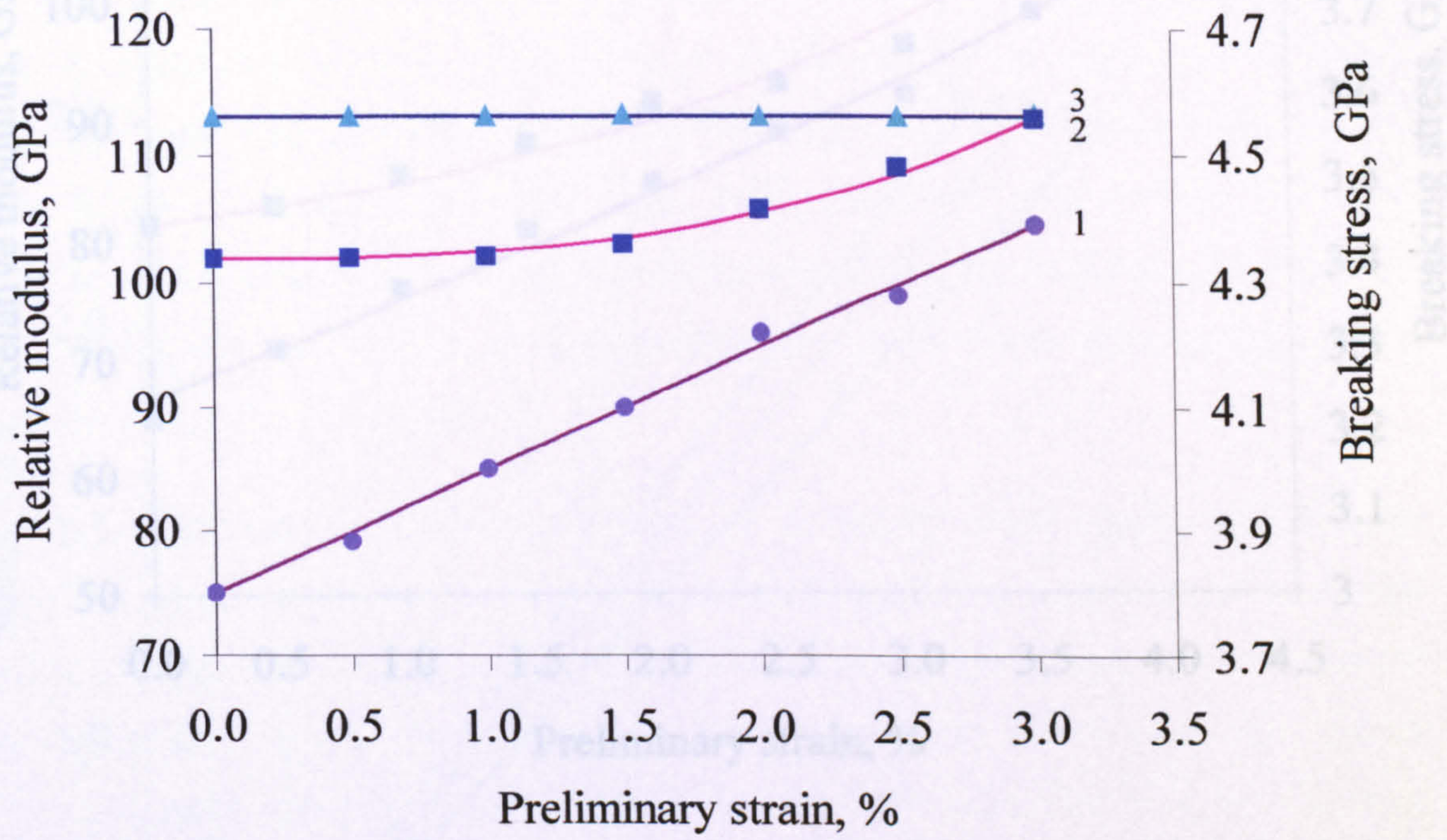

Fig. 3.6 Effect of preliminary stretching on breaking stress (1) and relative modulus E_2 (2) and E_1 (3) for Armos yarn

The stress-strain curves of Armos and SVM yarns consist of two regions: almost linear in the first region and then the curve shape of deformation in the second region. The relative modulus from the first region (E_1) for the yarns preliminary stretched at different levels remains practically constant. The preliminary deformation does not change the slope of the first part of the curve (Figs. 3.6 and 3.7 curves 3). But the relative modulus from the second region (E_2) increases with increasing ordering of the structure by preliminary stretching, and eventually reaches the same level of E_1 (curves 2 in Figs. 3.6 and 3.7). As mentioned previously, such a change of fibre rigidity suggests an increase in macromolecular orientation.

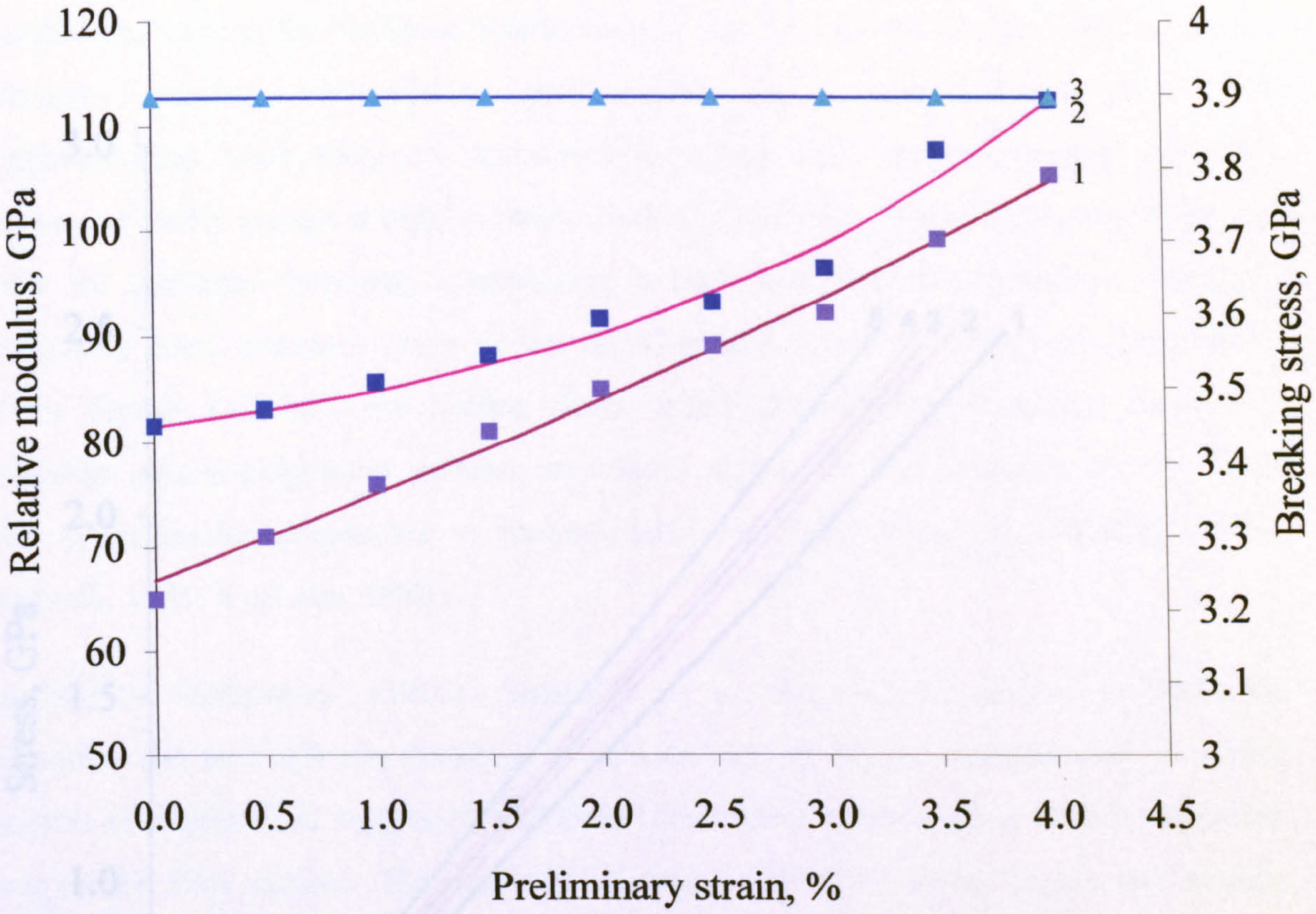

Fig. 3.7 Effect of preliminary stretching on breaking stress (1) and relative modulus E_2 (2) and E_1 (3) for SVM yarn

The almost linear stress-strain relationships of Terlon and Kevlar yarns before and after preliminary stretching are shown in Fig. 3.8. It can be seen that Terlon and Kevlar have an approximately constant tangent modulus with strain up to about 3.5%. It has known that Terlon and Kevlar polymer fibres are structurally and chemically very similar, so the mechanical properties of Terlon yarn will be further studied in the present work.

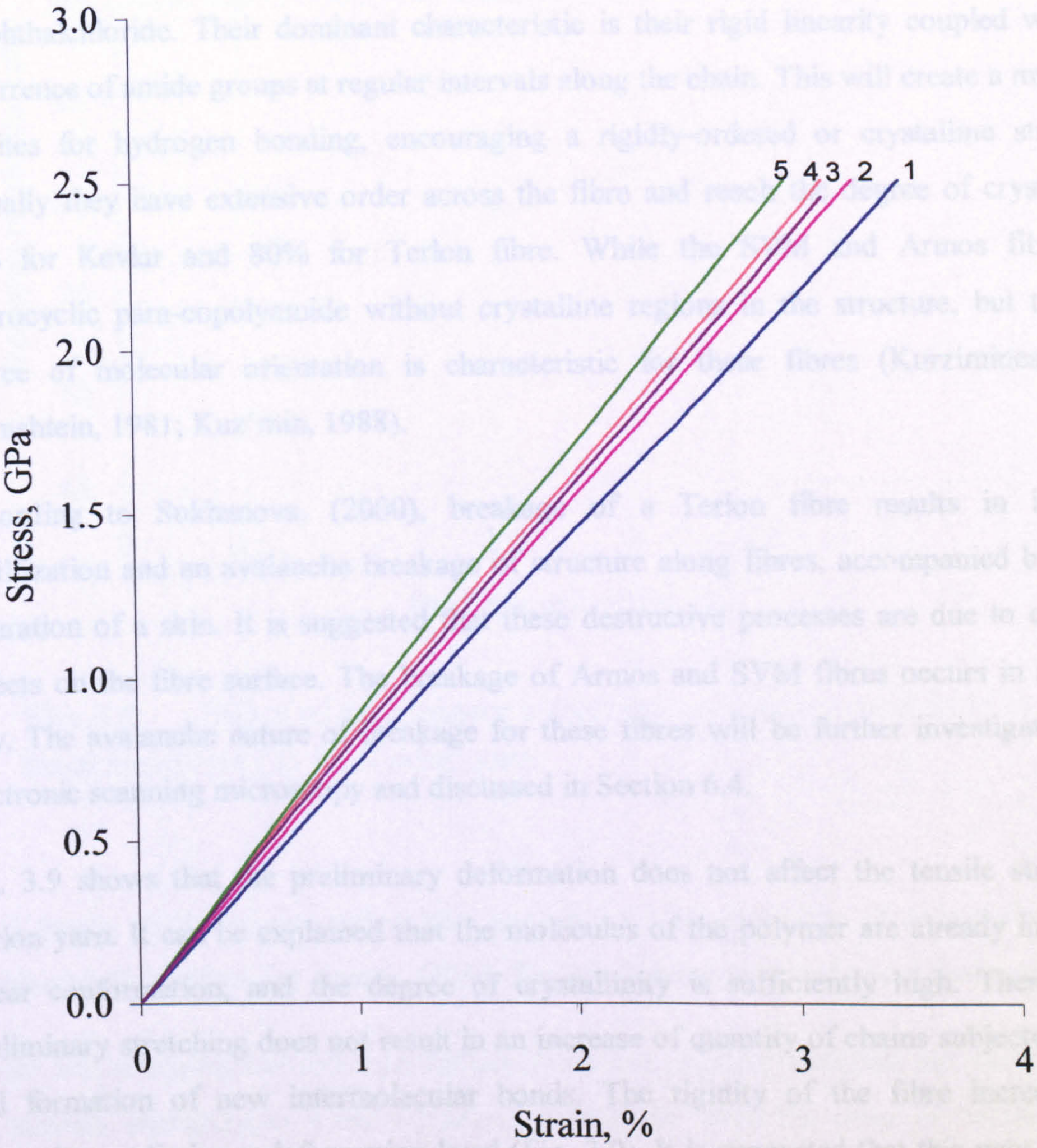

Fig. 3.8 Stress-strain curves of Terlon and Kevlar yarns before and after preliminary stretching: (1) original Terlon yarn; (2) Terlon yarn after preliminary stretching at ε=1%; (3) original Kevlar yarn; (4) Terlon yarn after preliminary stretching at ε=2%; (5) Terlon yarn after preliminary stretching at ε=3%

A possible explanation for the linear relationship is that Terlon and Kevlar fibres are para-substituted aromatic polyamides polymerized from p-phenylenediamine and terephthalchloride. Their dominant characteristic is their rigid linearity coupled with the occurrence of amide groups at regular intervals along the chain. This will create a multitude of sites for hydrogen bonding, encouraging a rigidly-ordered or crystalline structure. Actually they have extensive order across the fibre and reach the degree of crystallinity 90% for Kevlar and 80% for Terlon fibre. While the SVM and Armos fibers are heterocyclic para-copolyamide without crystalline regions in the structure, but the high degree of molecular orientation is characteristic for these fibres (Kurzimines, 1979; Blumshtein, 1981; Kuz'min, 1988).

According to Sukhanova, (2000), breakage of a Terlon fibre results in intensive fibrillization and an avalanche breakage of structure along fibres, accompanied by partial separation of a skin. It is suggested that these destructive processes are due to extensive defects on the fibre surface. The breakage of Armos and SVM fibres occurs in a similar way. The avalanche nature of breakage for these fibres will be further investigated using electronic scanning microscopy and discussed in Section 6.4.

Fig. 3.9 shows that the preliminary deformation does not affect the tensile strength of Terlon yarn. It can be explained that the molecules of the polymer are already in oriented linear conformation, and the degree of crystallinity is sufficiently high. Therefore the preliminary stretching does not result in an increase of quantity of chains subjected to load and formation of new intermolecular bonds. The rigidity of the fibre increases with increasing preliminary deformation level (Fig. 3.9). It is suggested that this may be due to additional orientation of polymer chains in amorphous regions of the polymer or removal of pleat creases, thereby aligning each former pleat with the fibre axis during preliminary deformation.

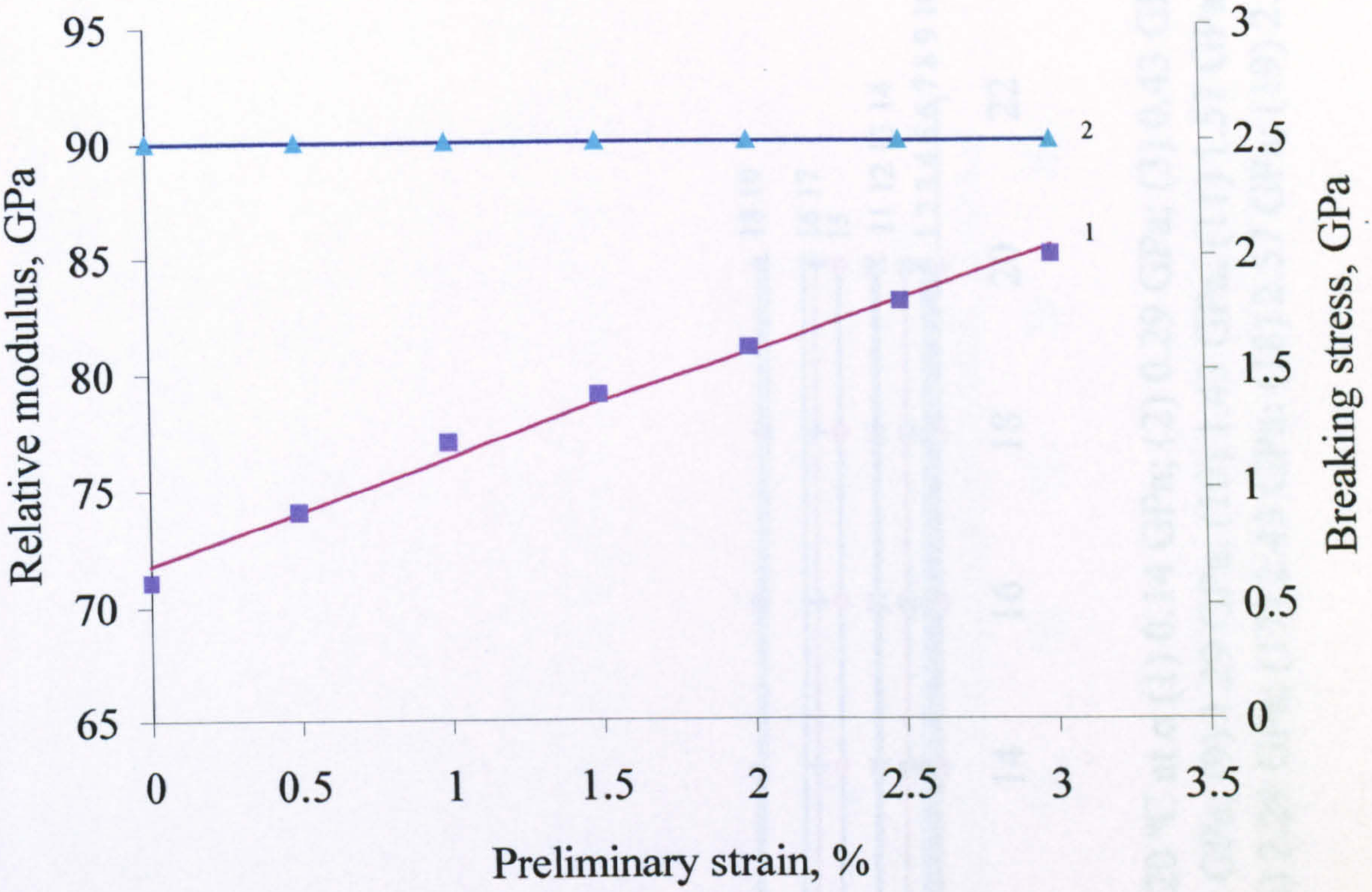

Fig. 3.9 Effect of preliminary stretching on relative modulus (1) and breaking stress (2) for Terlon yarn

3.3.2 Study of elastic and relaxation properties and character of accumulation of a residual deformation for Armos, SVM, Terlon, Kevlar yarns at room temperature

Under real technological and exploitation conditions polymer materials are often subjected to constant stretching at some extension (usually far from the point of breakage) for a period of time before removal of the stretching force. The performance of polymer yarns under such conditions can be studied through the processes of creep - recovery and stress relaxation. Figs. 3.10-3.13 show the creep behaviour of Armos, SVM and Terlon yarns formed from rigid chain polymers. Generally, the residual deformation increases with the stress applied for the first 10 minutes. The characteristics of creep-recovery for these yarns

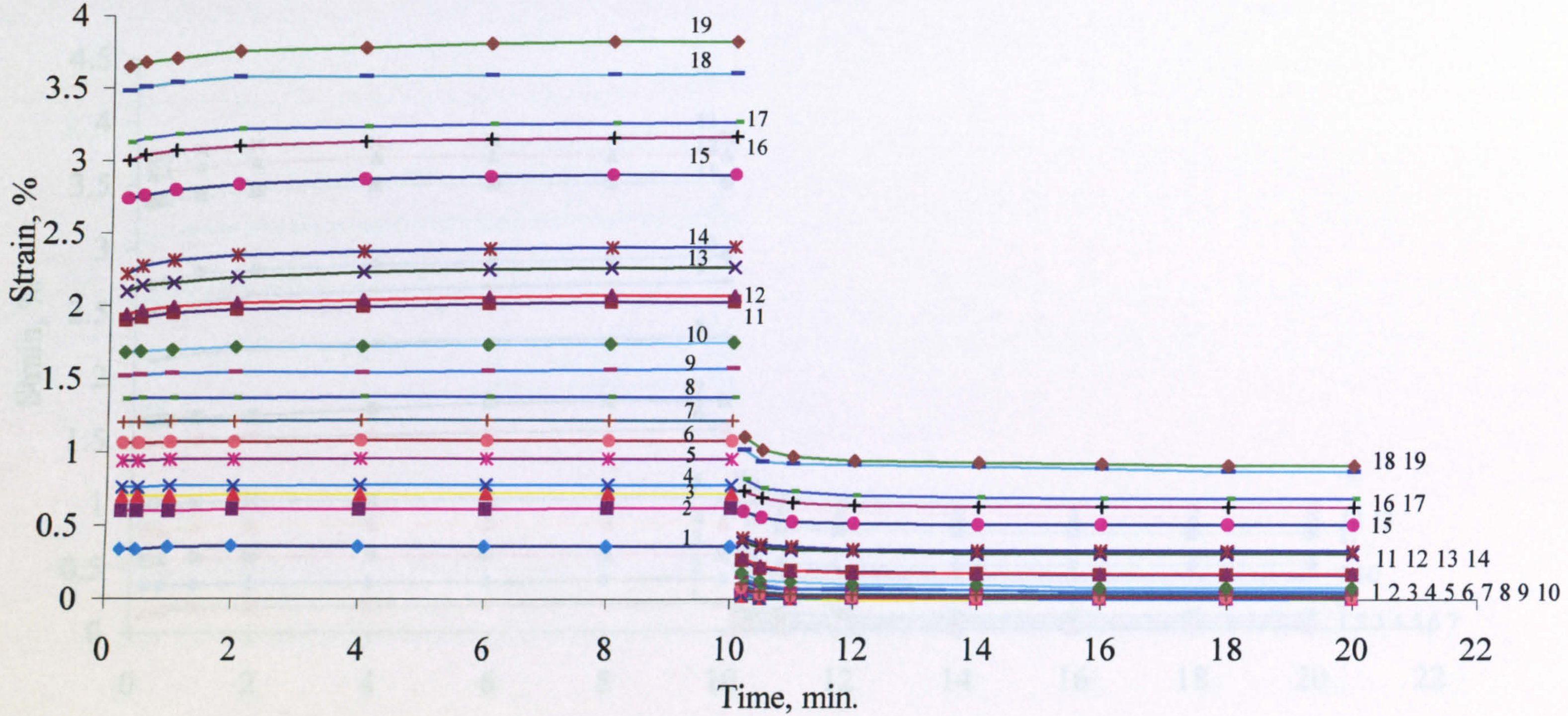

Fig. 3.10 The family of creep-recovery curves for Armos yarn at 20 °C at σ (1) 0.14 GPa; (2) 0.29 GPa; (3) 0.43 GPa; (4) 0.57 GPa; (5) 0.72 GPa; (6) 0.86 GPa; (7) 1.00 GPa; (8) 1.14 GPa; (9) 1.29 GPa; (10) 1.43 GPa; (11) 1.57 GPa; (12) 1.72 GPa; (13) 1.86 GPa; (14) 2.00 GPa; (15) 2.15 GPa; (16) 2.29 GPa; (17) 2.43 GPa; (18) 2.57 GPa; (19) 2.72 GPa

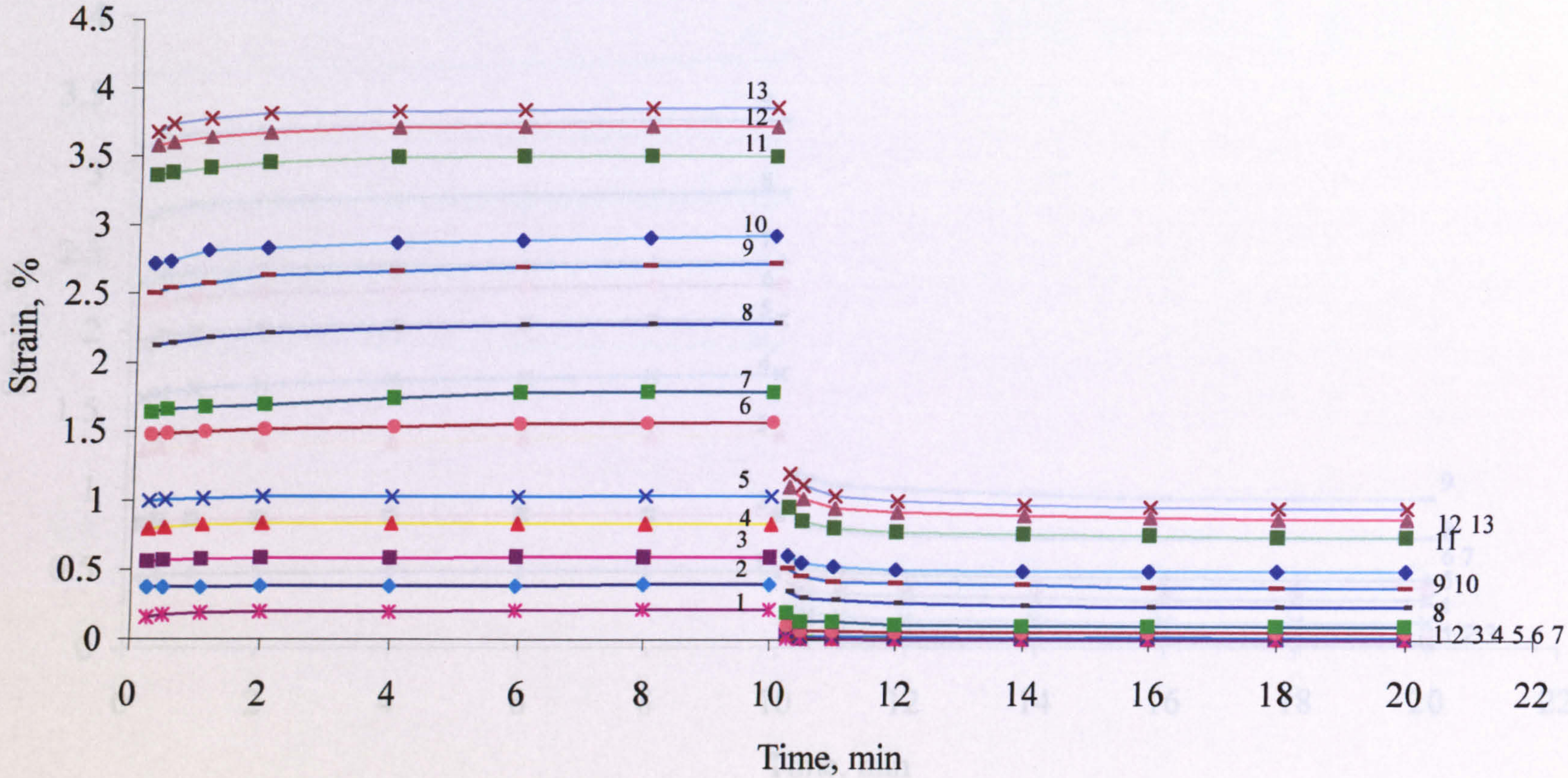

Fig. 3.11 The family of creep-recovery curves for SVM yarn at 20 °C at σ (1) 0.25 GPa; (2) 0.49 GPa; (3) 0.73 GPa; (4) 0.97 GPa; (5) 1.22 GPa; (6) 1.46 GPa; (7) 1.70 GPa; (8) 1.95 GPa; (9) 2.19 GPa; (10) 2.43 GPa; (11) 2.68 GPa; (12) 2.92 Gpa; (13) 3.16 GPa

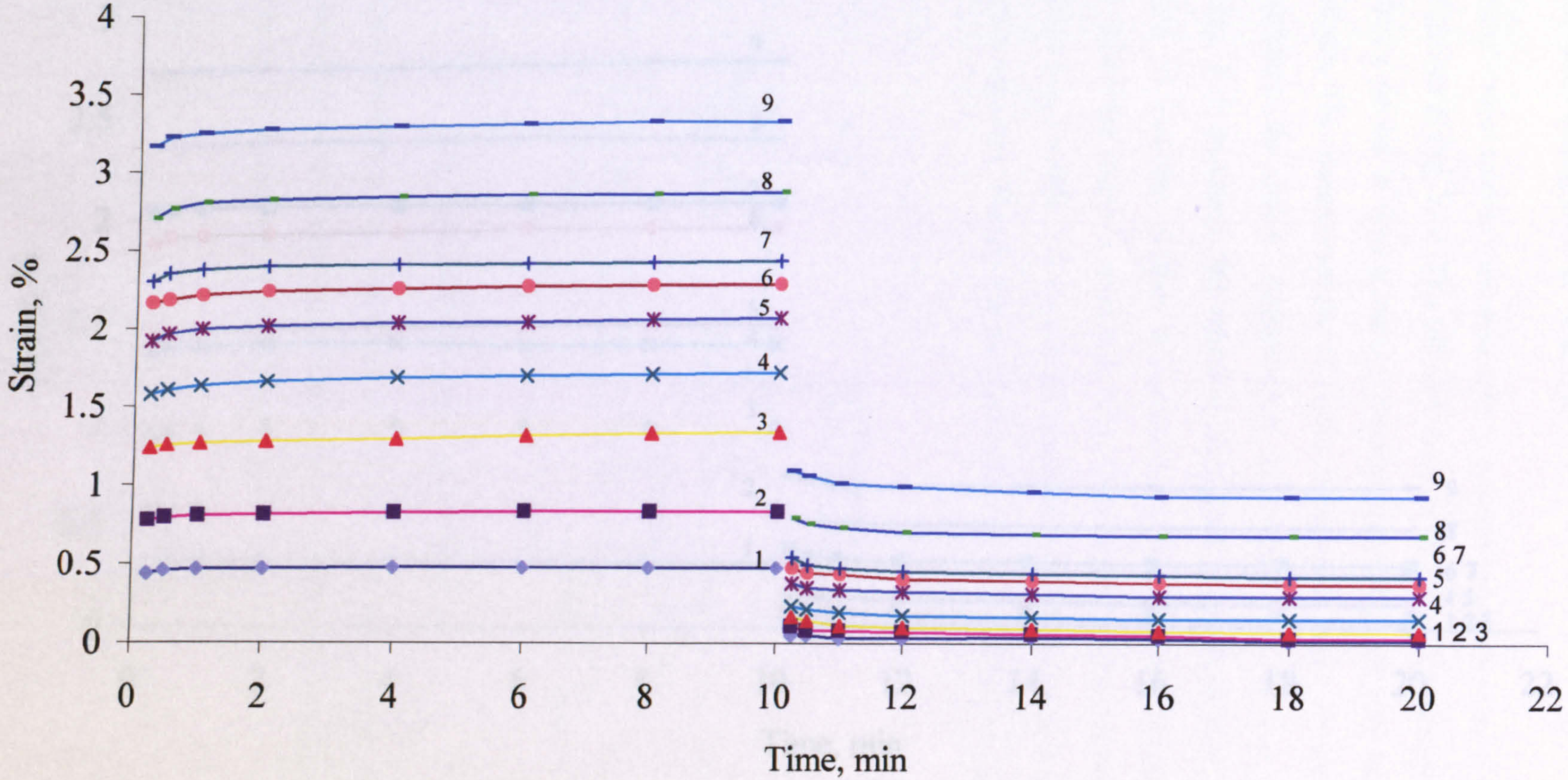

Fig. 3.12 The family of creep-recovery curves for Terlon yarn at 20 ºC at σ (1) 0.25 GPa; (2) 0.49 GPa; (3) 0.74 GPa; (4) 1.23 GPa; (5) 1.36 GPa; (6) 1.48 GPa; (7) 1.73 GPa; (8) 1.98 GPa; (9) 2.10 GPa

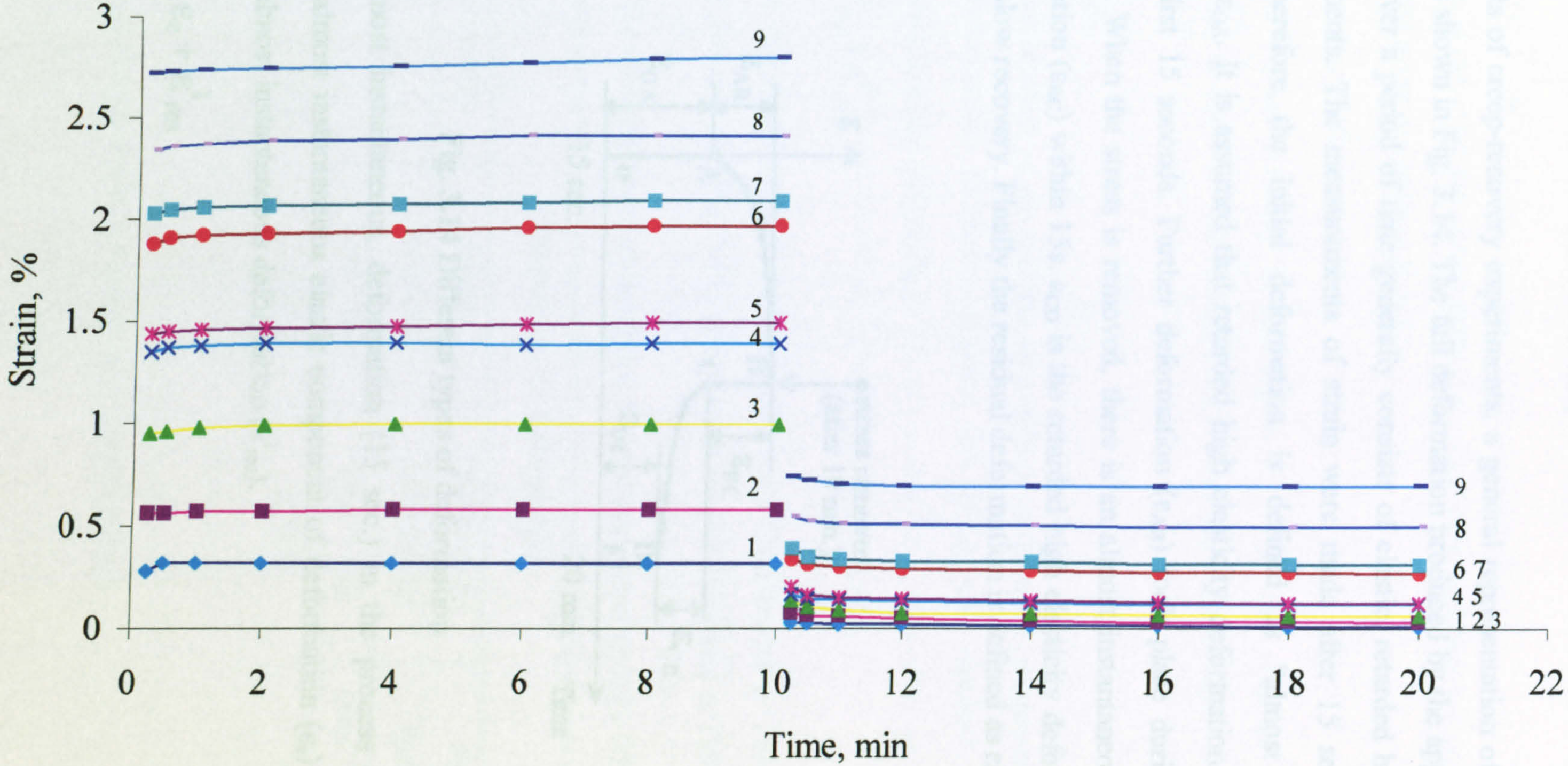

Fig. 3.13 The family of creep-recovery curves for Kevlar yarn at 20 °C at σ (1) 0.16 GPa; (2) 0.32 GPa; (3) 0.63 GPa; (4) 0.78 GPa; (5) 0.94 GPa; (6) 1.10 GPa; (7) 1.25 GPa; (8) 1.41 GPa; (9) 1.57 GPa

are very similar. Only when the deformation is more than 1.5% prior to removal of applied force, does the residual deformation is observed.

From the results of creep-recovery experiments, a general representation of a creep curve can be given as shown in Fig. 3.14. The full deformation produced by the application of the tensile stress over a period of time generally consists of elastic, retarded high elastic and plastic components. The measurements of strain were made after 15 seconds of load application, therefore the initial deformation is defined as "almost instantaneous deformation", ε_{OA}. It is assumed that retarded high elasticity deformation has not taken place during first 15 seconds. Further deformation (ε_{AB}) took place during 10 min. at constant stress. When the stress is removed, there is an almost instantaneous recovery of elastic deformation (ε_{BC}) within 15s. ε_{CD} is the retarded high elasticity deformation during the process of slow recovery. Finally the residual deformation is defined as ε_{DE}.

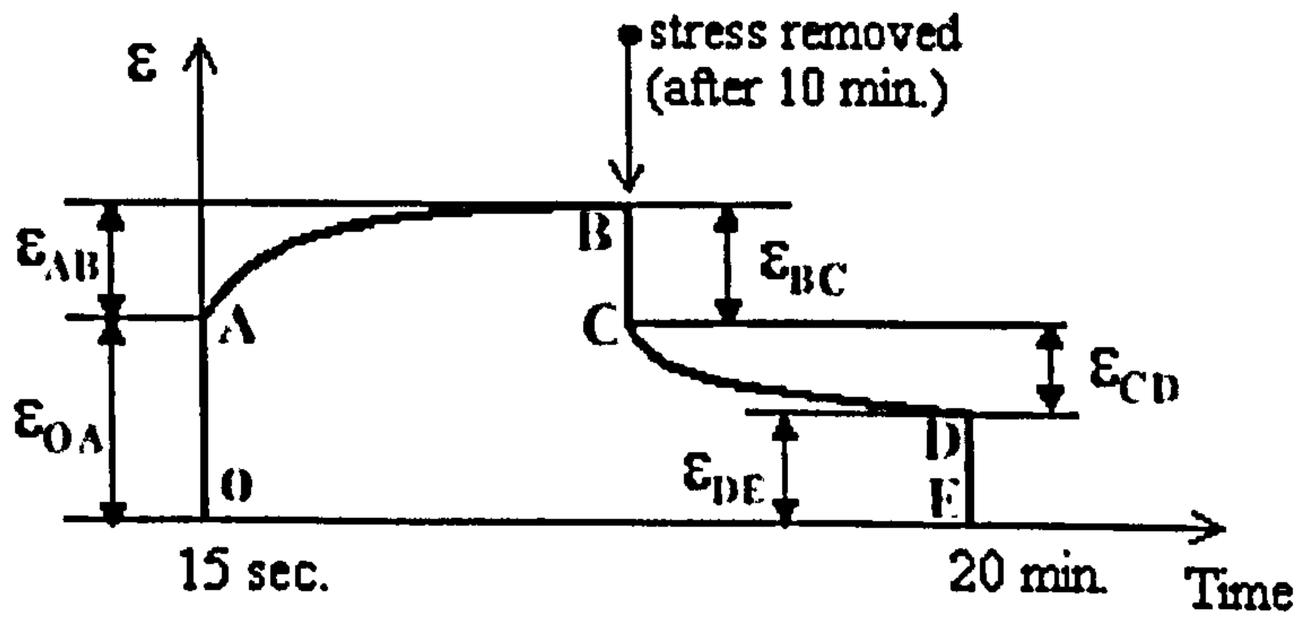

Fig. 3.14 Different types of deformation

The initial, almost instantaneous, deformation (15 sec.) in the process of creep (ε_{OA}) consists of an almost instantaneous elastic component of deformation (ε_e) and a residual component of almost instantaneous deformation (ε^I_{res}).

$$\varepsilon_{OA} = \varepsilon_e + \varepsilon^I_{res} \qquad (1)$$

The creep deformation (ε_{AB}) consists of a retarded high elasticity deformation (recoverable) component (ε_{ve}) and the residual (irrecoverable) component of deformation (ε^{II}_{res}).

$$\varepsilon_{AB}=\varepsilon_{ve}+\varepsilon^{II}_{res} \quad (2)$$

When the stress is removed the almost instantaneous elastic deformation (ε_e) is completely recovered and the curve drops from B to C.

$$\text{Therefore } \varepsilon_{BC} = \varepsilon_e \quad (3)$$

There follows a slower recovery in the region C to D. The retarded high elasticity deformation (ε_{CD}) is equal to the retarded high elasticity deformation (recoverable) of creep (ε_{ve}).

$$\varepsilon_{CD} = \varepsilon_{ve} \quad (4)$$

The residual deformation (ε_{DE}) consists of residual component of almost instantaneous irrecoverable deformation in direct process OA (ε^{I}_{res}) and residual component of deformation during loading (AB) (ε^{II}_{res}).

$$\varepsilon_{DE}=\varepsilon^{I}_{res}+\varepsilon^{II}_{res}. \quad (5)$$

Using the above equations, the deformation components from the creep - recovery curves at σ=2.72 GPa for Armos yarn (Fig. 3.11) were calculated and are given in Table 3.1.

Table 3.1 The components of deformation for Armos yarn at σ=2.72 GPa

Components of deformation				
Creep deformation		Elastic recovery ($\varepsilon_{BC} = \varepsilon_e$)	Viscoelastic deformation ($\varepsilon_{CD} = \varepsilon_{ve}$)	Residual deformation ($\varepsilon_{DE}=\varepsilon^{I}_{res} + \varepsilon^{II}_{res}$)
(ε_{OA})	(ε_{AB})			
3.65%	0.19%	2.73%	0.19%	0.92%

Therefore

The instantaneous irrecoverable deformation in the region OA:

$$\varepsilon^{I}_{res} = \varepsilon_{OA} - \varepsilon_{e} = \varepsilon_{OA} - \varepsilon_{BC} = 3.65\% - 2.73\% = 0.92\%;$$

The residual irrecoverable deformation in the region AB:

$$\varepsilon^{II}_{res} = \varepsilon_{AB} - \varepsilon_{ve} = \varepsilon_{AB} - \varepsilon_{CD} = 0.19\% - 0.19\% = 0\%;$$

The residual deformation in the region DE:

$$\varepsilon_{DE} = \varepsilon^{I}_{res} + \varepsilon^{II}_{res} = 0.92\% + 0\% = 0.92\%$$

It can be seen that the residual deformation ε_{DE} comprises only of the residual deformation ε^{I}_{res} (0.92%) accumulated during the initial 15 seconds, because ε^{II}_{res} is zero. It is therefore suggested that the initial 15 seconds of the creep process cause the irrecoverable deformation, as yarns undergo structural rearrangements resulting in accumulation of residual deformation. Further creep time only causes recoverable retarded high elasticity deformation. The same calculations were applied to SVM and Terlon. It is found that the accumulation of irrecoverable residual deformation during the initial period of time is characteristic for all polymers produced from rigid chain polymers.

Stress relaxation curves for a broad range of tensile strains for Armos and SVM yarns are shown in Figs. 3.15-3.16. It can be seen that for both yarns the stress value decreases in the first minute, thereafter the rate of decrease diminishes. The residual deformation was measured 10 minutes after removal of stress. The results indicate that the values of the residual component of deformation obtained from recovery of creep and stress relaxation processes are identical.

From the creep - recovery and stress relaxation - recovery curves of Armos, SVM, Terlon, and Kevlar yarns, the residual deformations remaining after a 10 min recovery period were determined. The relationship between residual deformation and the strain of the yarn stretched during the initial 10 min. period is shown in Fig. 3.17. It can be seen that the nature of accumulation of residual deformation at room temperature is similar for all yarns formed from rigid chain polymers. The rate of increase in residual deformation for Terlon and Kevlar yarn is slightly higher than that for Armos and SVM yarns. It was also found

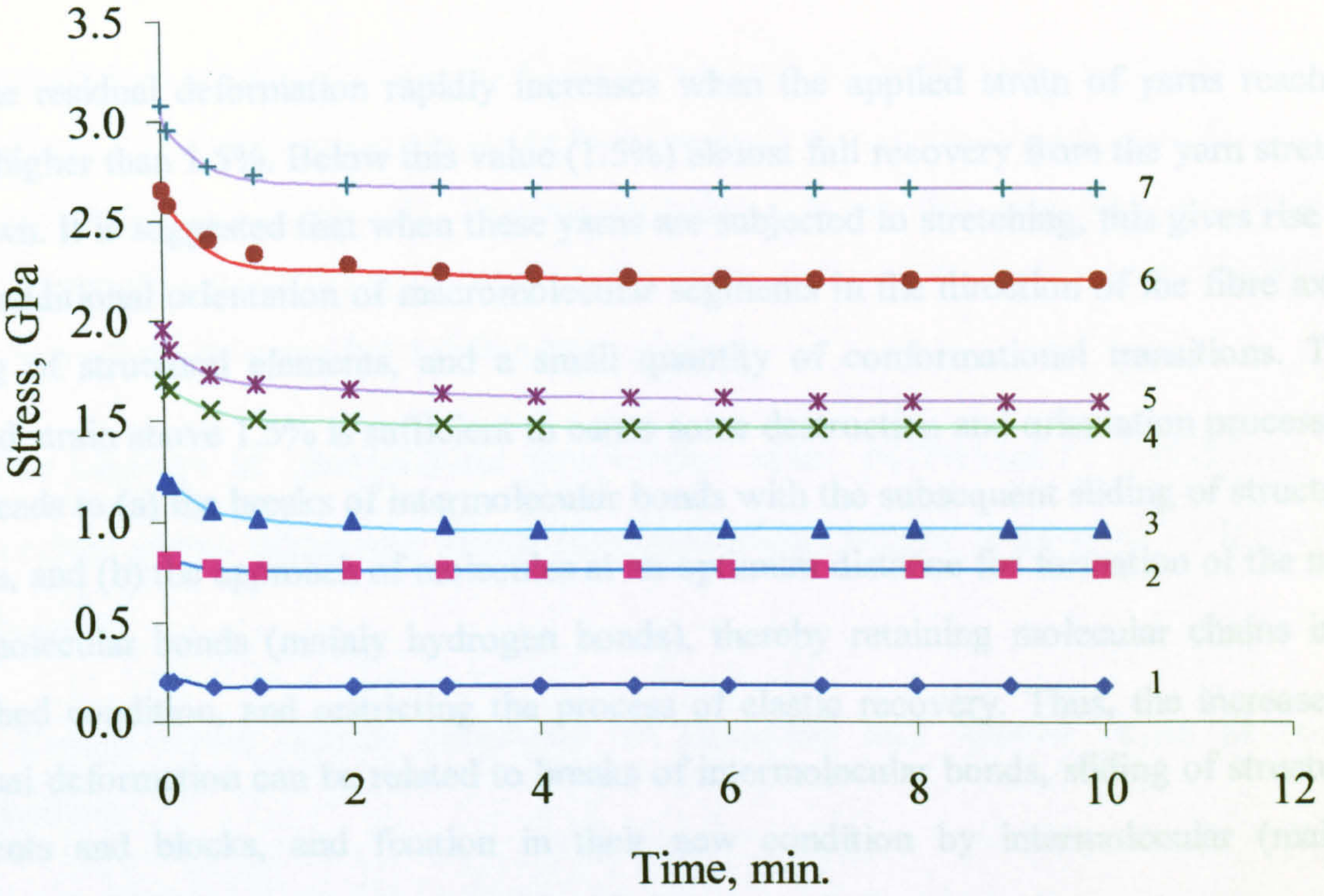

Fig. 3.15 The family of stress relaxation curves for Armos yarn at 20 ºC at ε: (1) 0.5%; (2) 1.0%; (3) 1.5%; (4) 2.0%; (5) 2.5%; (6) 2.5%; (7) 3.5%

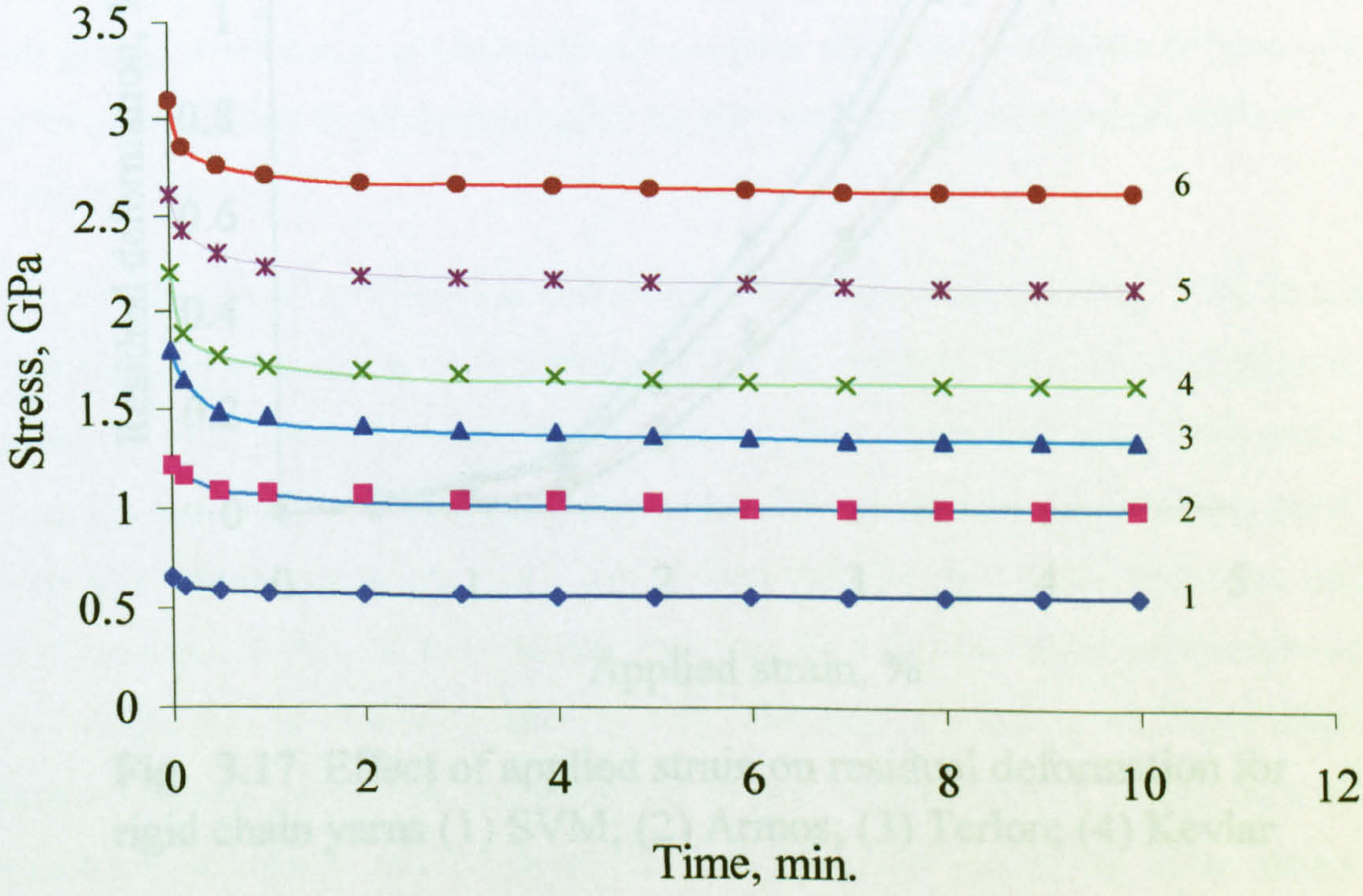

Fig. 3.16 The family of stress relaxation curves for SVM yarn at 20 ºC at ε: (1) 0.5%; (2) 1.0%; (3) 1.5%; (4) 2.0%; (5) 2.5%; (6) 2.5%

that the residual deformation rapidly increases when the applied strain of yarns reaches value higher than 1.5%. Below this value (1.5%) almost full recovery from the yarn stretch is shown. It is suggested that when these yarns are subjected to stretching, this gives rise to some additional orientation of macromolecular segments in the direction of the fibre axis, sliding of structural elements, and a small quantity of conformational transitions. The applied strain above 1.5% is sufficient to cause some destruction and orientation processes. This leads to (a) the breaks of intermolecular bonds with the subsequent sliding of structure blocks, and (b) the approach of molecules at an optimum distance for formation of the new intermolecular bonds (mainly hydrogen bonds), thereby retaining molecular chains in a stretched condition, and restricting the process of elastic recovery. Thus, the increase of residual deformation can be related to breaks of intermolecular bonds, sliding of structural elements and blocks, and fixation in their new condition by intermolecular (mainly hydrogen) bonds.

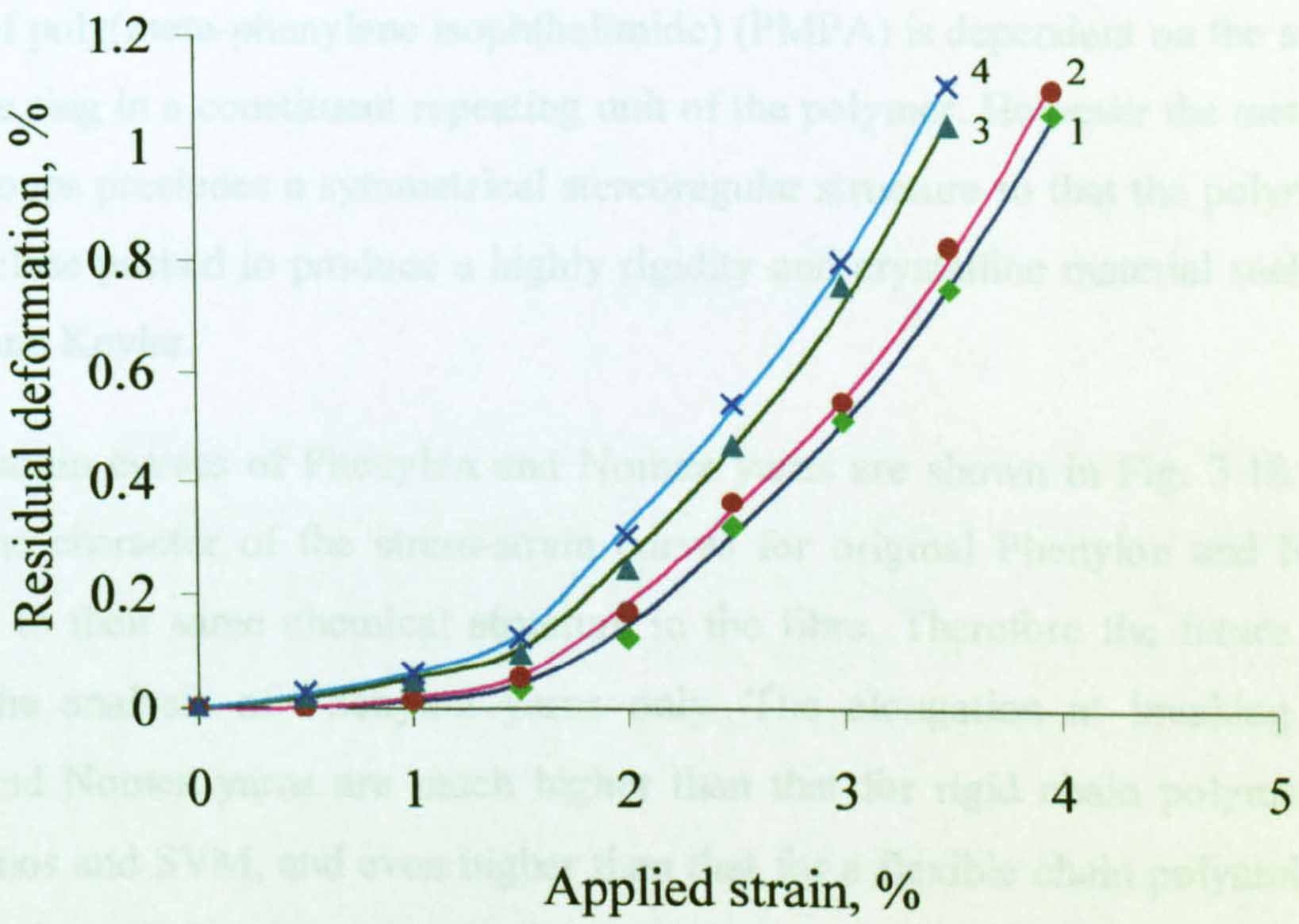

Fig. 3.17 Effect of applied strain on residual deformation for rigid chain yarns (1) SVM; (2) Armos; (3) Terlon; (4) Kevlar

It is noted that at a temperature of 20°C for Armos and SVM yarns the transition zone at the strain of 1.5% is also observed at the "hog-backed" curves, noted earlier on the stress-strain curves (Figs. 3.2 and 3.3). This suggests that it is possible to determine boundary values of applied strain from the stress-strain curve and predict the increase of residual deformation that will occur beyond this point of strain.

3.4 The change of mechanical properties after preliminary stretching of polyamide yarns obtained from medium rigid chain polymers: Phenylon and Nomex

3.4.1 Tensile stress -strain properties of Phenylon and Nomex yarns at room temperature

Phenylon and Nomex fibres are meta-substituted aromatic polyamides with semi rigid polymer chains (Cune segment is about 3-10 nm) (Perepelkin, 1985). The rigidity of molecules of poly(meta-phenylene isophthalimide) (PMPA) is dependent on the availability of a benzene ring in a constituent repeating unit of the polymer. However the meta-position of amide groups precludes a symmetrical stereoregular structure so that the polymer chains can not be close packed to produce a highly rigidity and crystalline material such as found for Terlon and Kevlar.

The stress-strain curves of Phenylon and Nomex yarns are shown in Fig. 3.18. It can be seen that the character of the stress-strain curves for original Phenylon and Nomex are similar due to their same chemical structure in the fibre. Therefore the future work will focus on the analysis of Phenylon yarns only. The elongation at breaking point for Phenylon and Nomex yarns are much higher than that for rigid chain polymers such as Terlon, Armos and SVM, and even higher than that for a flexible chain polyamide such as Capron (results will be shown in Section 3.5). This may be due to the lower degree of orientation of these yarns and the presence of less intermolecular bonds, because the unsymmetrical structures and benzene rings in Phenylon restrict to some extent the formation of short distance H-bonds or Van der Waals force. There are two distinct parts

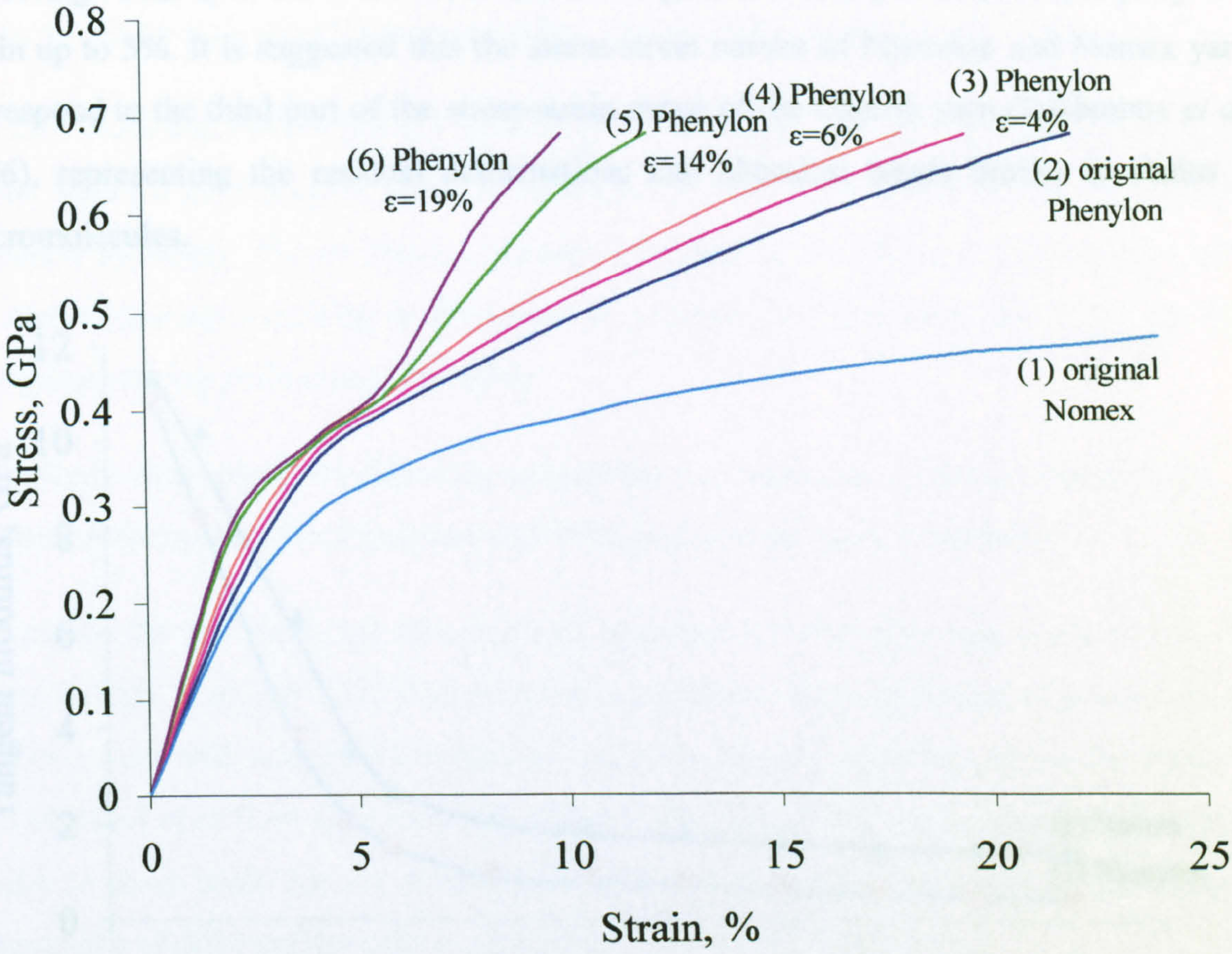

Fig. 3.18 Stress-strain curves of Phenylon and Nomex yarns before and after preliminary stretching: (1) original Nomex yarn; (2) original Phenylon yarn; (3) Phenylon yarn after preliminary stretching at ε=4%; (4) Phenylon yarn after preliminary stretching at ε=6%; (5) Phenylon yarn after preliminary stretching at ε=14%; (6) Phenylon yarn after preliminary stretching at ε=19%

the stress-strain curve of original Nomex and Phenylon (curves 1 and 2 in Fig. 3.18). Differentiation of these curves (Fig. 3.19) shows that the tangent modulus decreases with increasing strain up to 20%. It is seen that the tangent modulus decreases very rapidly with strain up to 5%. It is suggested that the stress-strain curves of Phenylon and Nomex yarns correspond to the third part of the stress-strain curve of the Capron yarn (Pakhomov *et al.*, 1986), representing the residual deformations and chemical bonds breaks in chains of macromolecules.

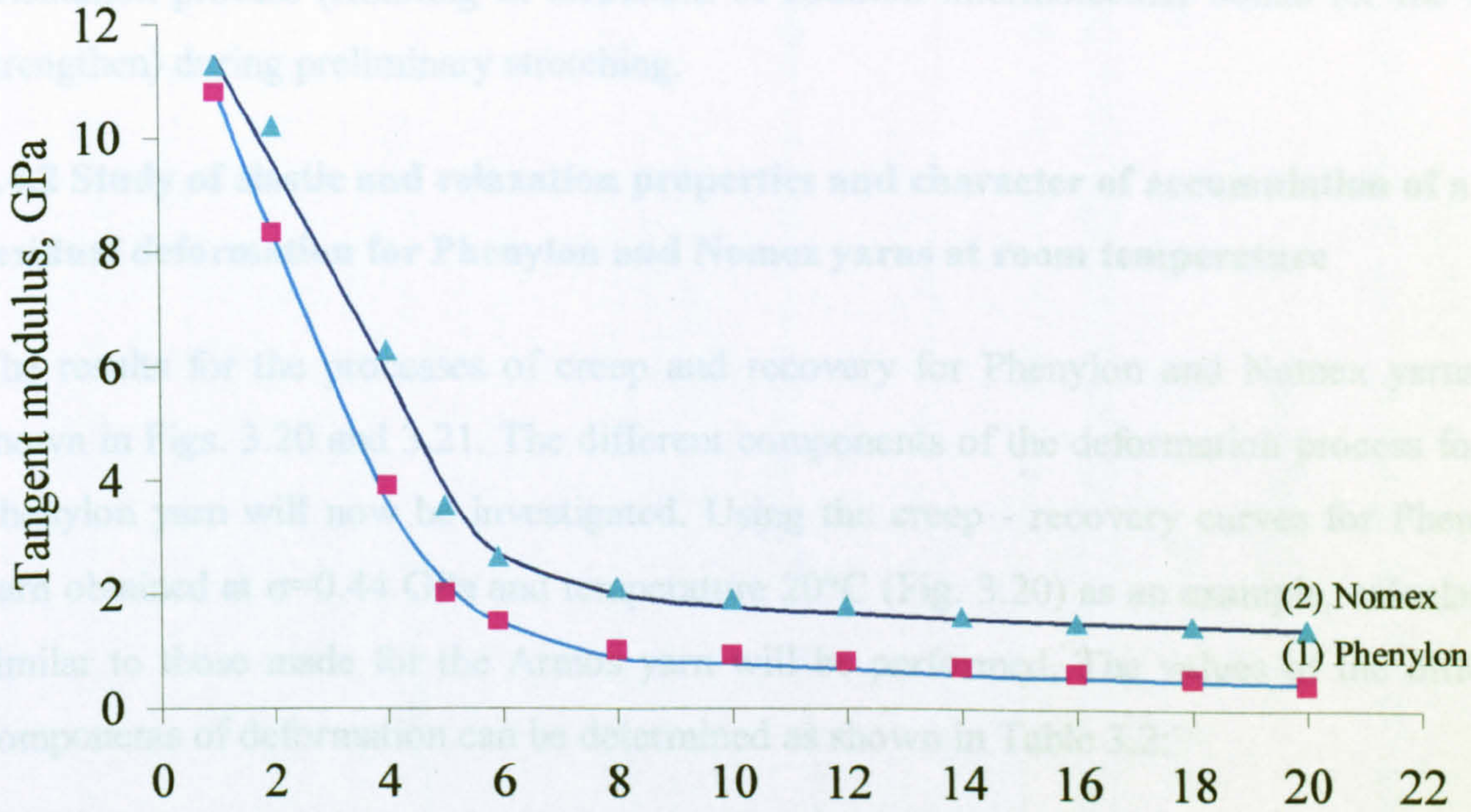

Fig. 3.19 Relationship between tangent modulus and strain for Phenylon (1) and Nomex (2) yarns

Of special interest are the stress-strain curves of Phenylon yarn samples which were preliminary stretched to various extents (Fig. 3.18). After preliminary deformation at ε>5-6%, the shapes of the curves change. This suggests that mechanical effects at deformations >5% result in structural changes. The stress-strain curves of Phenylon yarn subjected to preliminary stretching of 14% and 19% (curves 5 and 6) show 3 distinct areas, with the 3rd area appearing at ε>6%. The shape of these curves are similar to the stress-strain curves of

the Capron yarn (Pakhomov *et al.*, 1986). This change in the character of the stress-strain curves can be related to rearrangements in the structure of an original yarn after preliminary deformation. These stress-strain curves are characteristic of oriented Capron and Nylon yarns, which have an amorphous - crystalline structure (Pakhomov *et al.*, 1986).

It is also found that the preliminary stretch up to 19% strain does not significantly affect the tensile strength of Phenylon yarn. It is suggested that there might be two competitive processes operating. The destructive process (resulting in the decrease of strength) and an orientation process (resulting in formation of addition intermolecular bonds for the fibre strengthen) during preliminary stretching.

3.4.2 Study of elastic and relaxation properties and character of accumulation of a residual deformation for Phenylon and Nomex yarns at room temperature

The results for the processes of creep and recovery for Phenylon and Nomex yarns are shown in Figs. 3.20 and 3.21. The different components of the deformation process for the Phenylon yarn will now be investigated. Using the creep - recovery curves for Phenylon yarn obtained at σ=0.44 GPa and temperature 20°C (Fig. 3.20) as an example, calculations similar to those made for the Armos yarn will be performed. The values of the different components of deformation can be determined as shown in Table 3.2:

Table 3.2 The components of deformation for Phenylon yarn at σ=0.44 GPa

Components of deformation				
Creep deformation		Elastic recovery ($\varepsilon_{BC} = \varepsilon_e$)	Viscoelastic deformation (ε_{CD})	Residual deformation ($\varepsilon_{DE} = \varepsilon^{I}_{res} + \varepsilon^{II}_{res}$)
(ε_{OA})	(ε_{AB})			
12.5%	2.94%	7.86%	0.78%	6.8%

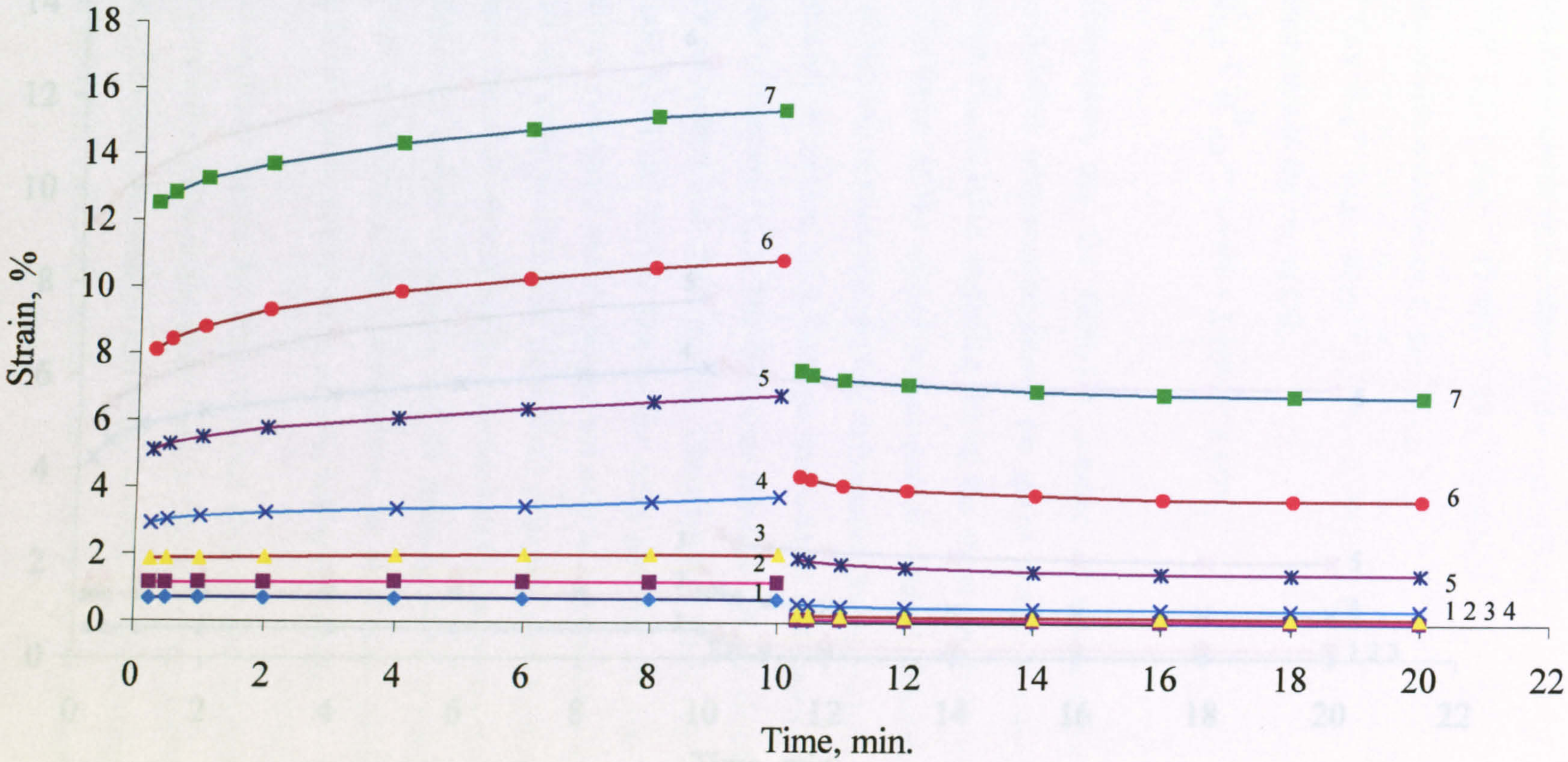

Fig. 3.20 The family of creep-recovery curves for Phenylon yarn at 20 °C at σ (1) 0.07 GPa; (2) 0.15 GPa; (3) 0.22 GPa; (4) 0.29 GPa; (5) 0.37 GPa; (6) 0.38 GPa; (7) 0.44 GPa

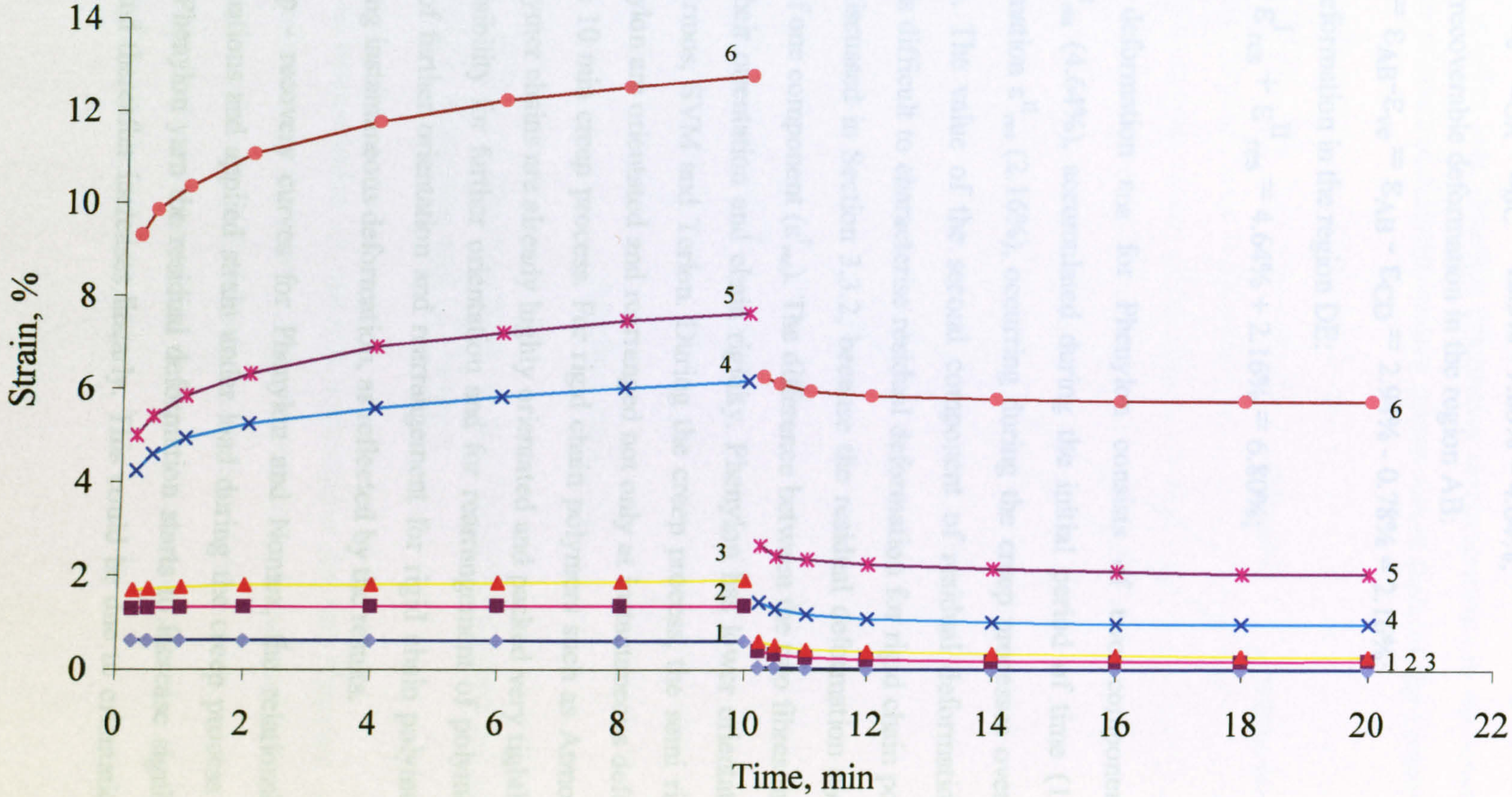

Fig. 3.21 The family of creep-recovery curves for Nomex yarn at 20 °C at σ (1) 0.05 GPa; (2) 0.11 GPa; (3) 0.16 GPa; (4) 0.21 GPa; (5) 0.27 GPa; (6) 0.32 GPa

Therefore

The instantaneous irrecoverable deformation in the region OA:

$$\varepsilon^{I}_{res} = \varepsilon_{OA} - \varepsilon_{e} = \varepsilon_{OA} - \varepsilon_{BC} = 12.5\% - 7.86\% = 4.64\%;$$

The residual irrecoverable deformation in the region AB:

$$\varepsilon^{II}_{res} = \varepsilon_{AB} - \varepsilon_{ve} = \varepsilon_{AB} - \varepsilon_{CD} = 2.94\% - 0.78\% = 2.16\%;$$

The residual deformation in the region DE:

$$\varepsilon_{DE} = \varepsilon^{I}_{res} + \varepsilon^{II}_{res} = 4.64\% + 2.16\% = 6.80\%;$$

The residual deformation ε_{DE} for Phenylon consists of two components: residual deformation ε^{I}_{res} (4.64%), accumulated during the initial period of time (15 sec.); and residual deformation ε^{II}_{res} (2.16%), occurring during the creep processes over a period of time (10 min). The value of the second component of residual deformation (ε^{II}_{res}) is substantial. It is difficult to characterise residual deformation for rigid chain polymers such as Armos as discussed in Section 3.3.2, because the residual deformation ε_{DE} for Armos only consists of one component (ε^{I}_{res}). The difference between the two fibres may be due to difference in their orientation and chain rigidity. Phenylon has lower orientation and less rigidity than Armos, SVM and Terlon. During the creep process, the semi rigid polymer chains in Phenylon are orientated and rearranged not only at instantaneous deformation but also during the 10 min creep process. For rigid chain polymers such as Armos, SVM and Terlon, the polymer chains are already highly orientated and packed very tightly. Therefore there is no possibility for further orientation and for rearrangement of polymer chains. A small amount of further orientation and rearrangement for rigid chain polymers might be completed during instantaneous deformation, as reflected by the results.

From the creep - recovery curves for Phenylon and Nomex, the relationship between residual deformations and applied strain under load during the creep process is shown in Fig. 3.22. For Phenylon yarn the residual deformation starts to increase significantly at a strain of 5 % and thereafter increases linearly. This could be due to orientation processes

occurring during loading, resulting in an increasingly ordered molecular structure in amorphous regions and a consequent increase in the number of intermolecular hydrogen bonds. This stretched condition will preclude elastic recovery. Orientation of the structure of these fibres is rather low, therefore orientation rearrangements in the structure result in an accumulation of residual deformation to a greater extent than for rigid chain polymers.

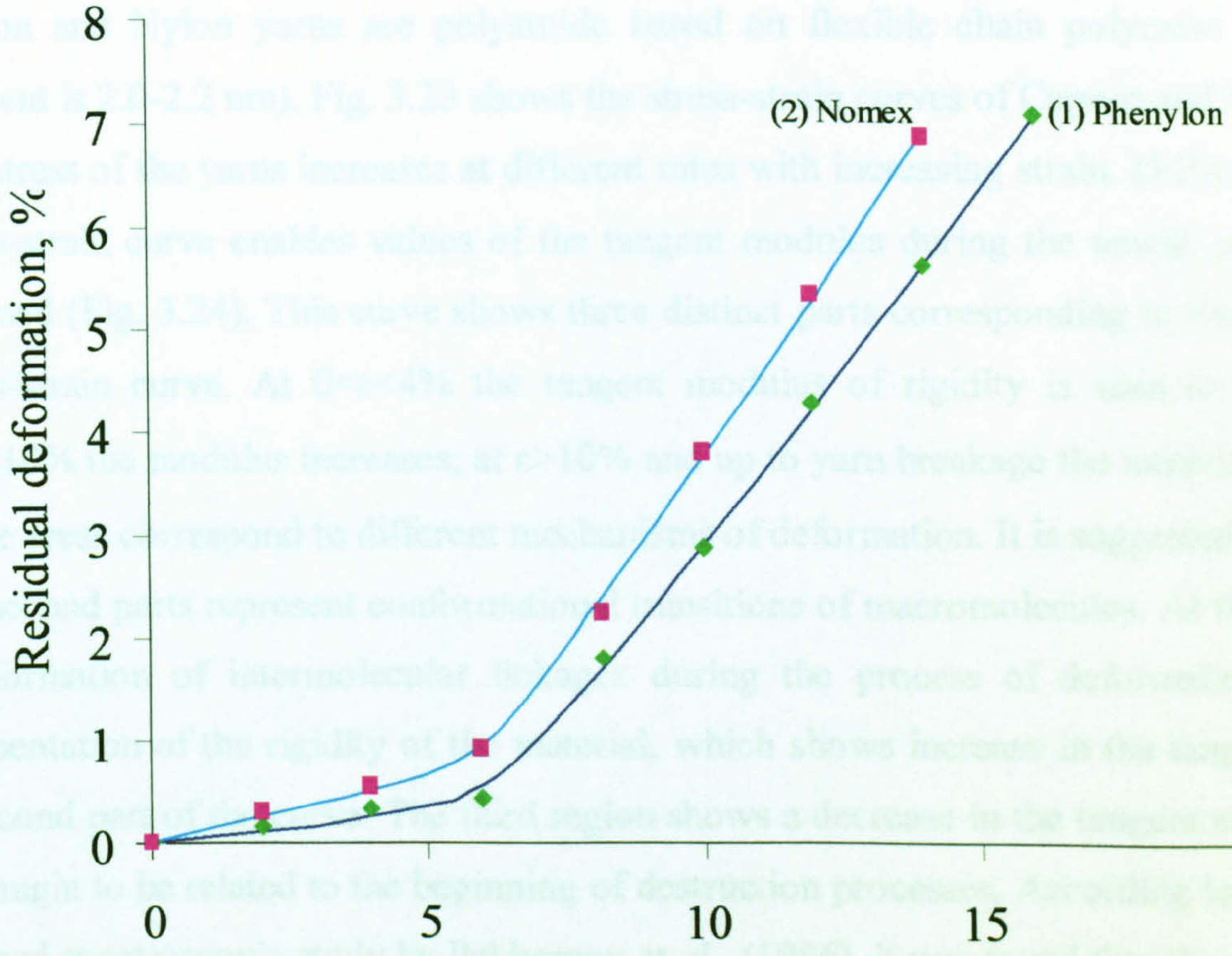

Fig. 3.22 Effect of applied strain on residual deformation for semi rigid chain yarns: (1) Phenylon and (2) Nomex

The character of accumulation of residual deformation for the Phenylon yarns can be related to the tensile curves (Fig 3.18). A significant increase in residual deformation can be observed after a certain value of deformation (about 5 % for Phenylon yarns) which corresponds to the bending point in the stress-strain curves. Therefore it is possible to predict this point from the tensile curves.

3.5 The change of mechanical properties after preliminary stretching of polyamide yarns obtained from flexible chain polymers: Capron and Nylon

3.5.1 Stress-strain curves of Capron and Nylon yarns at room temperature

Capron and Nylon yarns are polyamide based on flexible chain polymers (their Cune segment is 2.0-2.2 nm). Fig. 3.23 shows the stress-strain curves of Capron and Nylon yarns. The stress of the yarns increases at different rates with increasing strain. Differentiating the stress-strain curve enables values of the tangent modulus during the tensile process to be obtained (Fig. 3.24). This curve shows three distinct parts corresponding to the areas of the stress-strain curve. At $0<\varepsilon<4\%$ the tangent modulus of rigidity is seen to decrease, at $4<\varepsilon<10\%$ the modulus increases; at $\varepsilon>10\%$ and up to yarn breakage the modulus decreases. These areas correspond to different mechanisms of deformation. It is suggested that the first and second parts represent conformational transitions of macromolecules. At the same time the formation of intermolecular linkages during the process of deformation results in augmentation of the rigidity of the material, which shows increase in the tangent modulus in second part of the curve. The third region shows a decrease in the tangent modulus. This is thought to be related to the beginning of destruction processes. According to the previous infrared spectroscopic study by Pakhomov *et al.*, (1986), it was found that the concentration of covalent bonds broken increases gradually after strain of 10% (Fig. 3.25) rather than increasing sharply as in the case for SVM (see Fig.3.5). The result infers that, at the third part of the stress-strain curve of Capron yarn, there is an intensive tearing in molecular chains during the breakage of covalent bonds (Fig. 3.25).

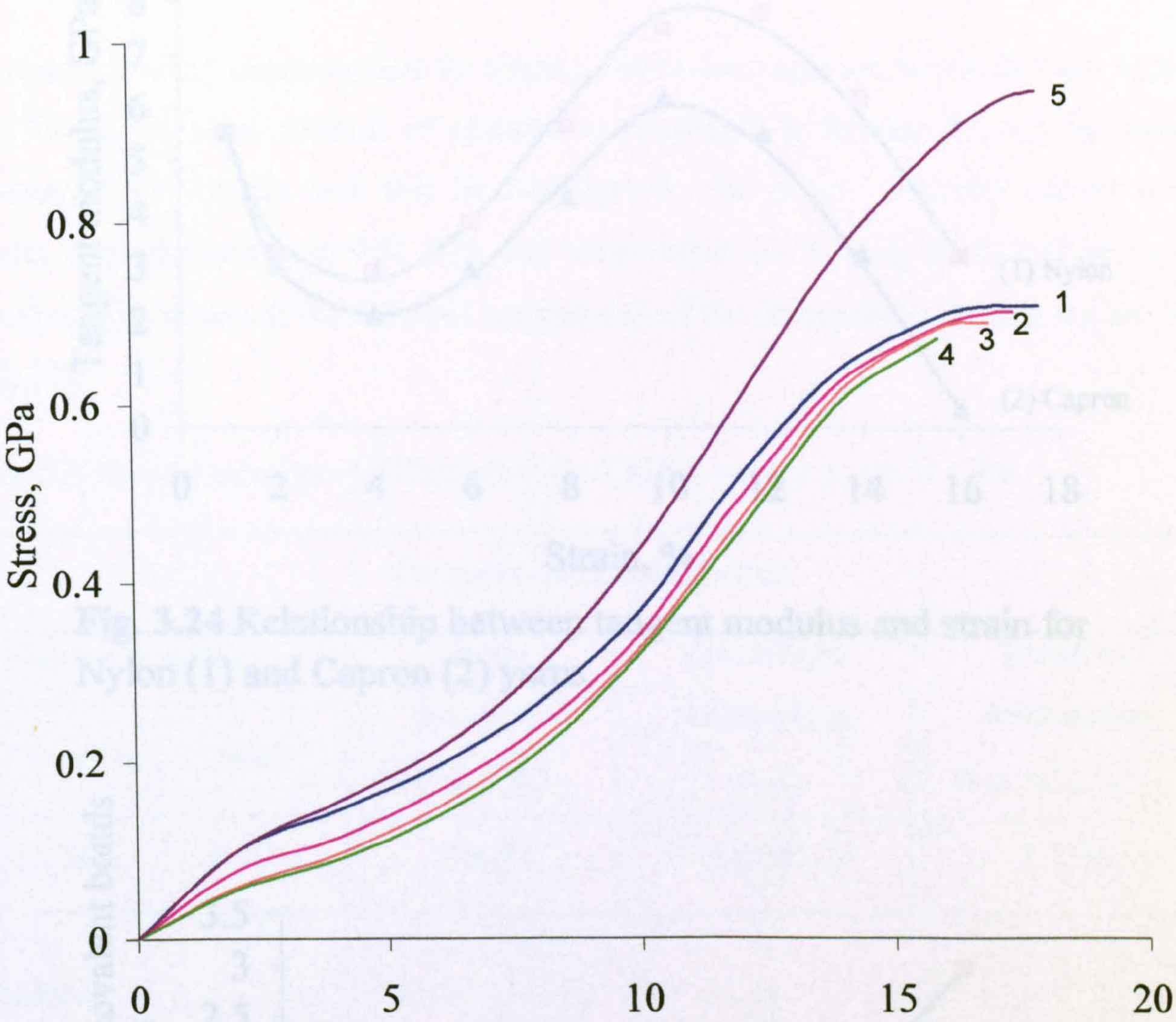

Fig. 3.23 Stress-strain curves of Capron and Nylon yarns before and after preliminary stretching: (1) original Capron yarn; (2) Capron yarn after preliminary stretching at ε=8%; (3) Capron yarn after preliminary stretching at ε=12%; (4) Capron yarn after preliminary stretching at ε=14%; (5) original Nylon yarn

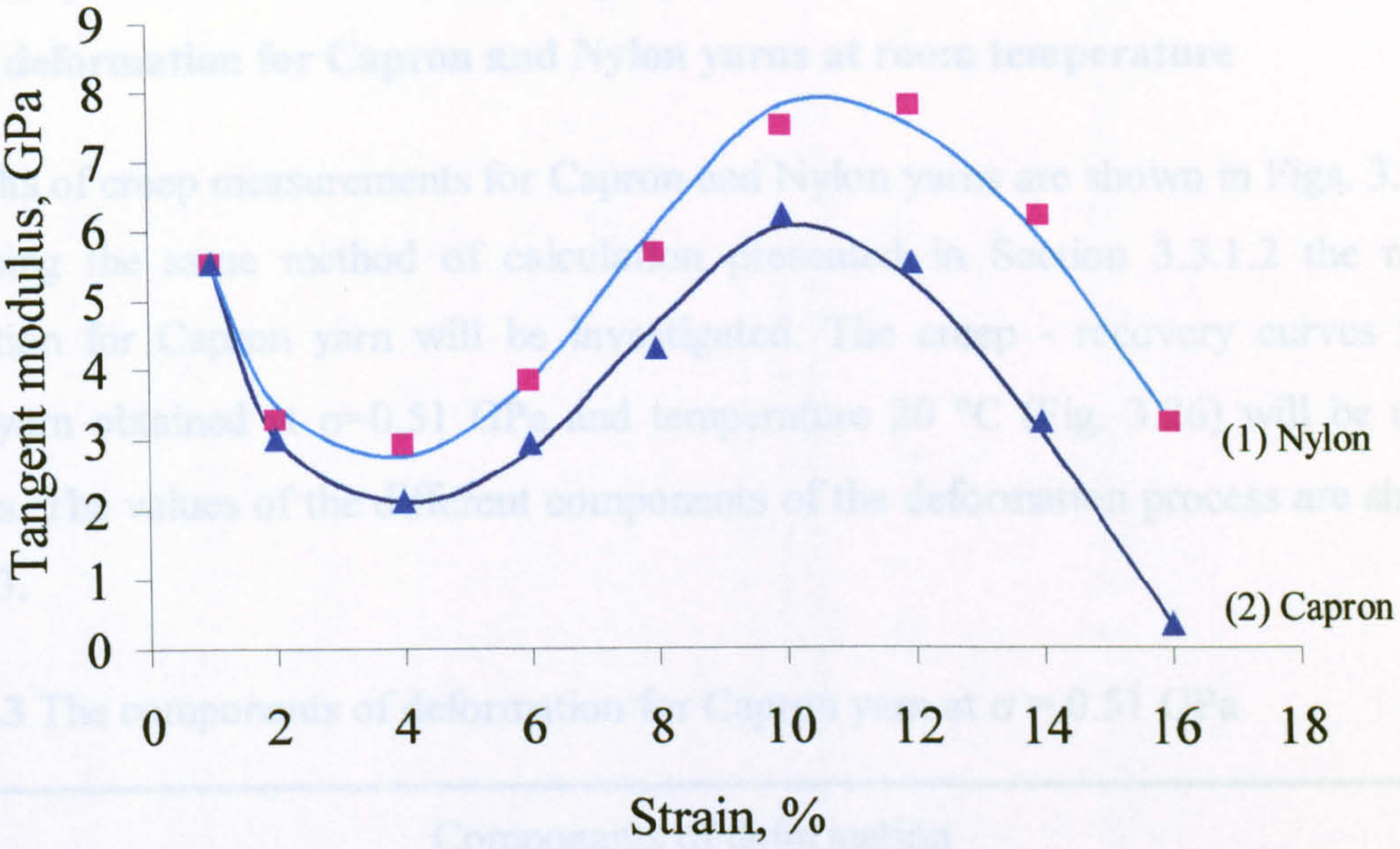

Fig. 3.24 Relationship between tangent modulus and strain for Nylon (1) and Capron (2) yarns

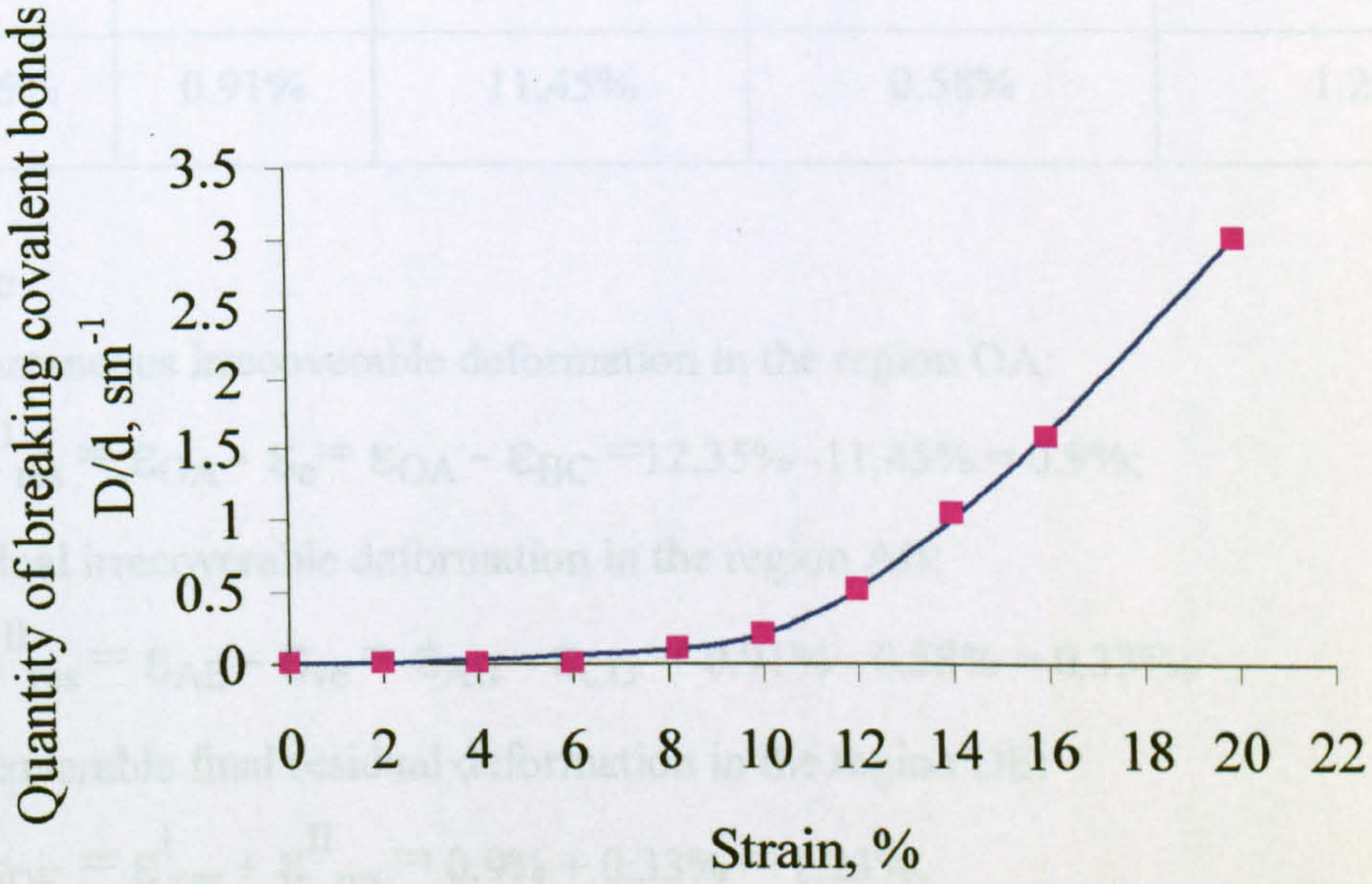

Fig. 3.25 Effect of strain on quantity of breaking covalent bonds for Capron yarn (Pakhomov, 1986)

3.5.2 Study of elastic and relaxation properties and character of accumulation of a residual deformation for Capron and Nylon yarns at room temperature

The results of creep measurements for Capron and Nylon yarns are shown in Figs. 3.26 and 3.27. Using the same method of calculation presented in Section 3.3.1.2 the residual deformation for Capron yarn will be investigated. The creep - recovery curves for the Capron yarn obtained at σ=0.51 GPa and temperature 20 °C (Fig. 3.26) will be used as examples. The values of the different components of the deformation process are shown in Table 3.3.

Table 3.3 The components of deformation for Capron yarn at σ = 0.51 GPa

Components of deformation				
Creep deformation		Elastic recovery ($\varepsilon_{BC} = \varepsilon_e$)	Viscoelastic deformation (ε_{CD})	Residual deformation ($\varepsilon_{DE} = \varepsilon^{I}_{res} + \varepsilon^{II}_{res}$)
(ε_{OA})	(ε_{AB})			
12.35%	0.91%	11.45%	0.58%	1.23%

Therefore

The instantaneous irrecoverable deformation in the region OA:

$$\varepsilon^{I}_{res} = \varepsilon_{OA} - \varepsilon_e = \varepsilon_{OA} - \varepsilon_{BC} = 12.35\% - 11.45\% = 0.9\%;$$

The residual irrecoverable deformation in the region AB:

$$\varepsilon^{II}_{res} = \varepsilon_{AB} - \varepsilon_{ve} = \varepsilon_{AB} - \varepsilon_{CD} = 0.91\% - 0.58\% = 0.33\%;$$

The irrecoverable final residual deformation in the region DE:

$$\varepsilon_{DE} = \varepsilon^{I}_{res} + \varepsilon^{II}_{res} = 0.9\% + 0.33\% = 1.23\%.$$

The residual deformation ε_{DE} consists of two components: the residual deformation ε^{I}_{res} occurred almost instantly over a very short period of time (first 15 seconds) after loading,

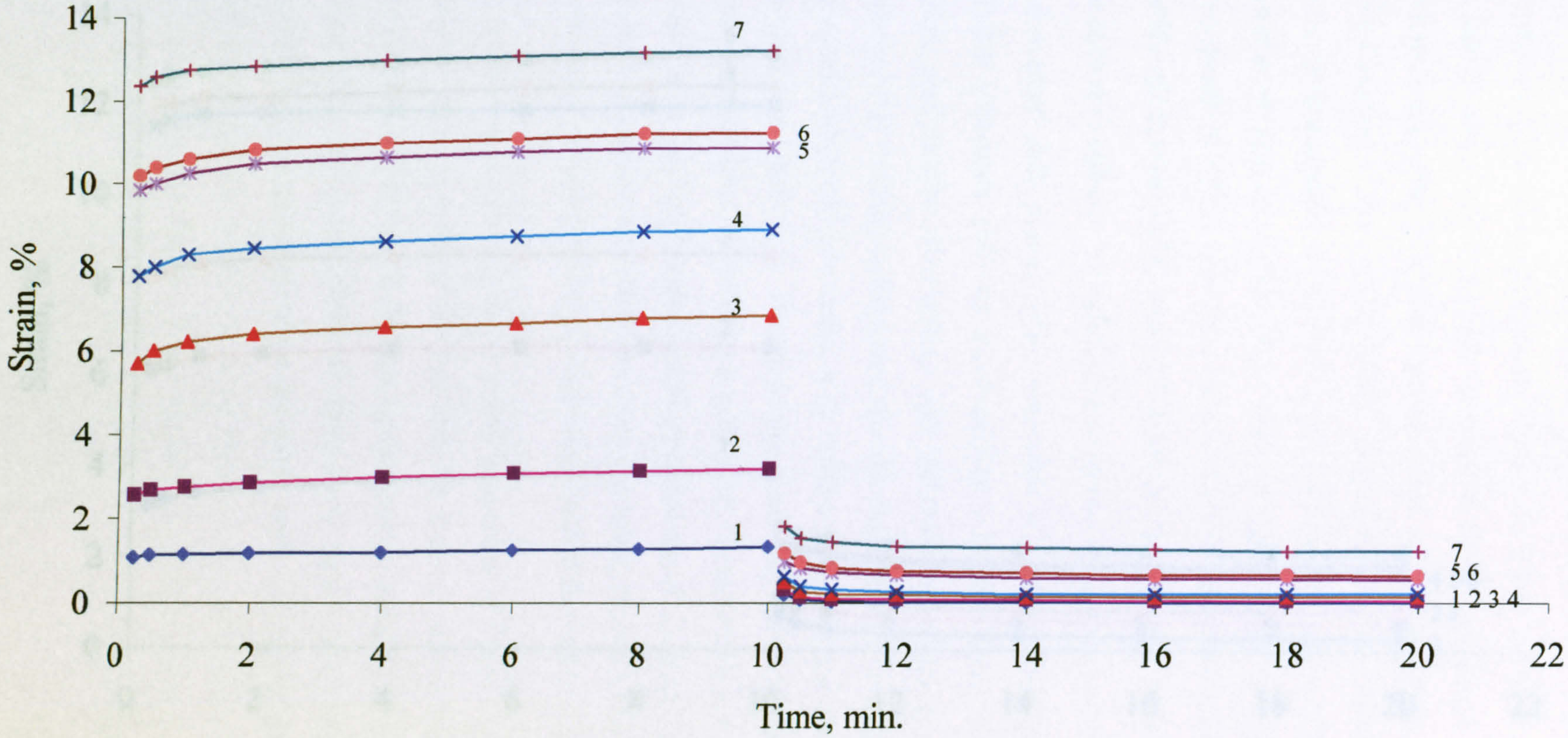

Fig 3.26 The family of creep-recovery curves for Capron yarn at 20 °C at σ (1) 0.08 GPa; (2) 0.12 GPa; (3) 0.16 GPa; (4) 0.24 GPa; (5) 0.32 GPa; (6) 0.48 GPa

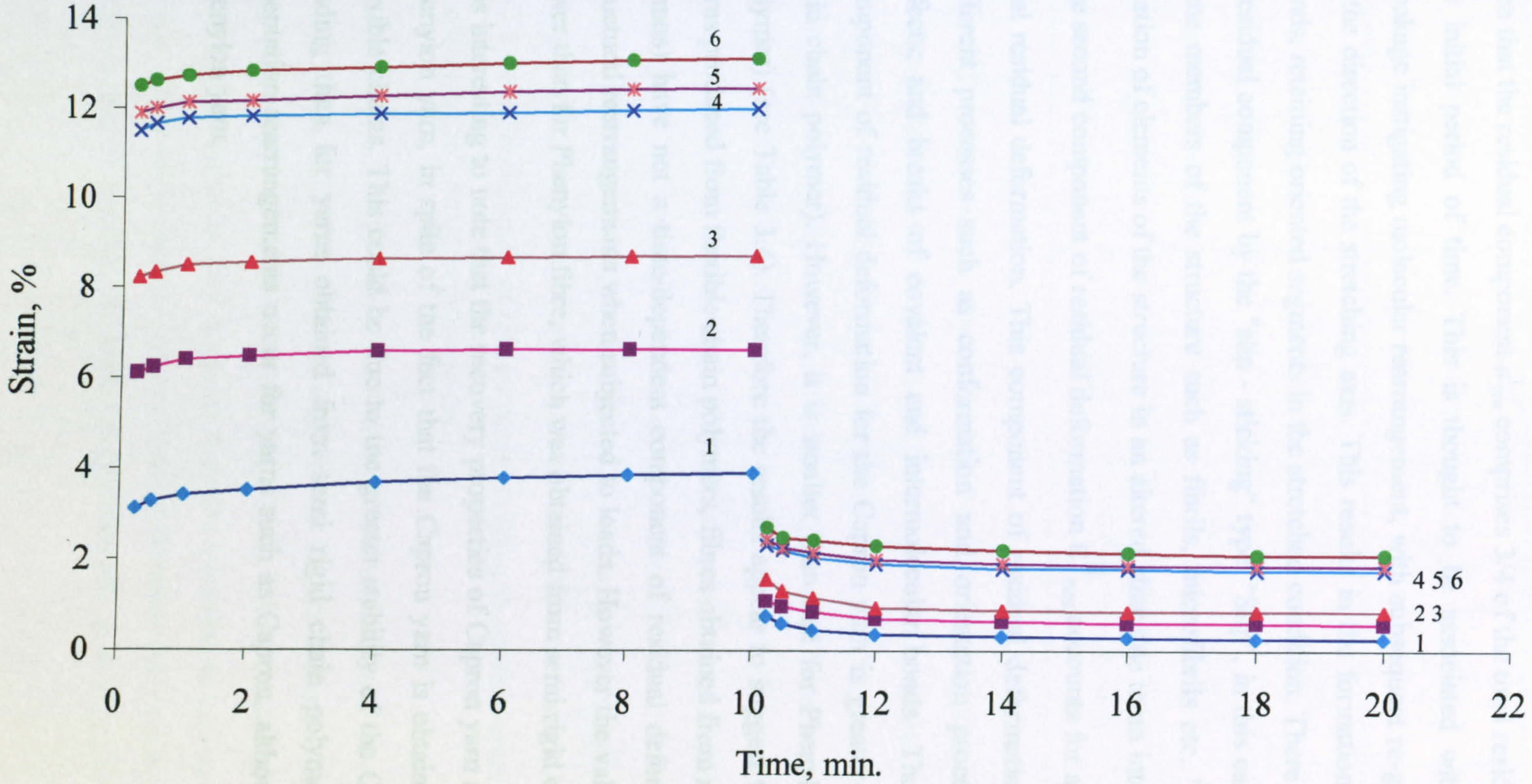

Fig 3.27 The family of creep-recovery curves for Nylon yarn at 20 ℃ at σ (1) 0.08 GPa; (2) 0.16 GPa; (3) 0.24 GPa; (4) 0.41 GPa; (5) 0.49 GPa; (6) 0.53 GPa

and the second residual deformation ε^{II}_{res} during next 10 min in the creep process. It can be seen that the residual component ε^{I}_{res} comprises 3/4 of the total residual deformation during the initial period of time. This is thought to be associated with intermolecular bond breakage instigating molecular rearrangement, with subsequent re-grouping and orientation in the direction of the stretching axis. This results in the formation of new intermolecular bonds, retaining oriented segments in the stretched condition. There is also accumulation of a residual component by the "slip - sticking" type. "Slip", in this case, refers to the shift of some members of the structure such as fibrils, microfibrils etc. "Sticking" refers to the fixation of elements of the structure in an altered state due to an intermolecular interaction. The second component of residual deformation ε^{II}_{res} accounts for approximately 1/4 of the total residual deformation. This component of residual deformation can be explained by different processes such as conformation and orientation processes; accumulation of defects; and breaks of covalent and intermolecular bonds. The value of the second component of residual deformation for the Capron yarn is greater than that for Armos (a rigid chain polymer). However, it is smaller than that for Phenylon (a semi rigid chain polymer) (see Table 3.4). Therefore the results appear to suggest that, compared with the yarns produced from flexible chain polymers, fibres obtained from rigid chain polymer (eg. Armos) have not a time-dependent component of residual deformation conditioned by structural rearrangements when subjected to loads. However the value of this component is lower than for Phenylon fibre, which was obtained from semi rigid chain polymers.

It is interesting to note that the recovery properties of Capron yarn are even higher than for Phenylon yarn, in spite of the fact that the Capron yarn is obtained from polymers with flexible chains. This could be due to the greater stability of the Capron yarn structure at loading than for yarns obtained from semi rigid chain polymers, i.e. at loading no orientation rearrangements occur for yarns such as Capron, although this is the case for Phenylon yarn.

Table 3.4 The components of deformation for different yarns

Sample	Applied deformation (ε)	ε^{I}_{res}	ε^{II}_{res}	ε_e	ε_{ve}
Armos at σ = 2.9 Gpa	3.84%	0.92%	0%	2.73%	0.19%
Phenylon at σ = 0.44 Gpa	15.44%	4.64%	2.16%	7.86%	0.78%
Capron at σ = 0.51 Gpa	13.26%	0.9%	0.33%	11.45%	0.58%

The relationship between the residual deformation and applied deformation (strain) for Nylon and Capron yarns obtained from the creep-recovery curves in Figs. 3.26 and 3.27 are shown in Fig. 3.28. The residual deformations for both Capron and Nylon yarns increase slightly with increasing the applied strain until about 10-11% and thereafter they increase significantly. Pakhomov *et al.*, (1986) have suggested that for values of deformations higher than 10-11%, the breakage of bonds in the main chain (Fig. 3.25) are observed for Capron yarn. The breakage of these covalent bonds in the main macromolecule chain are responsible for the residual deformations. In the area of deformation, where the breaks are absent, the recovery of the yarn strain can take place. In other words, at elongation ε<10-11% reversible structural processes occur, relating to conformation transitions and the high flexibility of polymer macromolecules.

Pakhomov *et al.*, (1986) have also shown that the increase of residual deformation and breaks in the main macromolecule chain for Capron coincide with the beginning of the third part on the stress-strain curve (Fig. 3.23). Thus, for Capron yarn it is possible to determine the values of deformations from the stress/strain curves at which the increase of residual deformation starts. The relationship between the tensile curve and the nature of accumulation of residual deformation is observed. It is suggested that it is possible to

predict the values of given deformation (strain) at which the increase of the irreversible residual component of deformation begins.

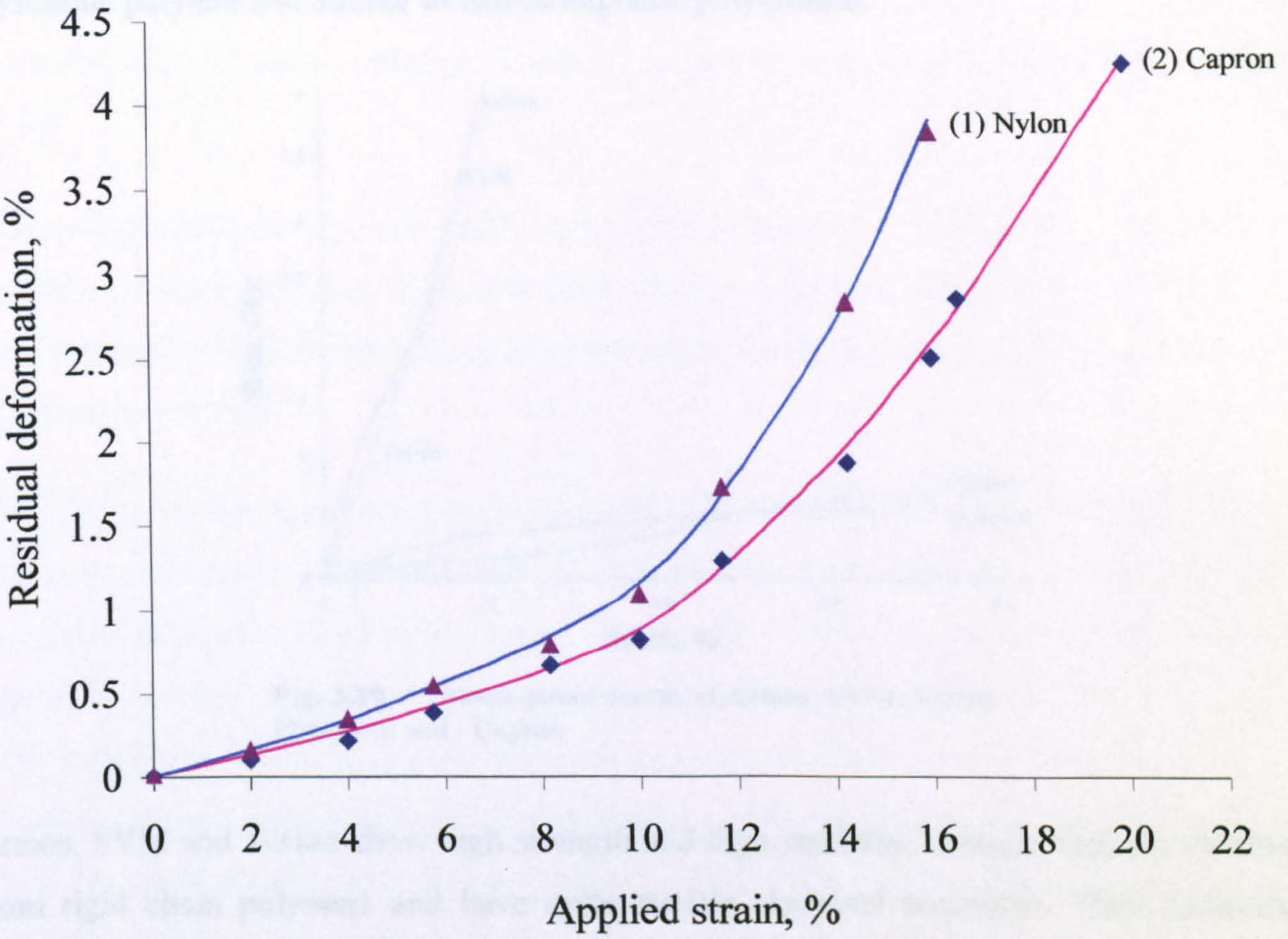

Fig. 3.28 Effect of applied strain on residual deformation for flexible chain yarns: (1) Nylon; (2) Capron

3.5 Conclusion

Polyamide fibres such as Armos, SVM, Terlon, Phenylon and Capron present different performance and characteristic shape of tensile stress-strain curves (Fig. 3.29). Terlon (poly(p-phenylene terephthalamide)) fibres have a very highly symmetrical para-aramid structure with parallel, densely packed chains and this leads to high crystallinity. In consequence, Terlon has a high elastic modulus and a low breaking strain. However the

chemical structure for Phenylon fibres is meta-aramid (unsymmetrical). The meta links hinder a high degree of structural organization. It can not be packed as tightly as rigid chain polymers. In consequence, Phenylon shows the stress-strain behaviour typical of a partially crystalline polymer and similar to that of aliphatic polyamides.

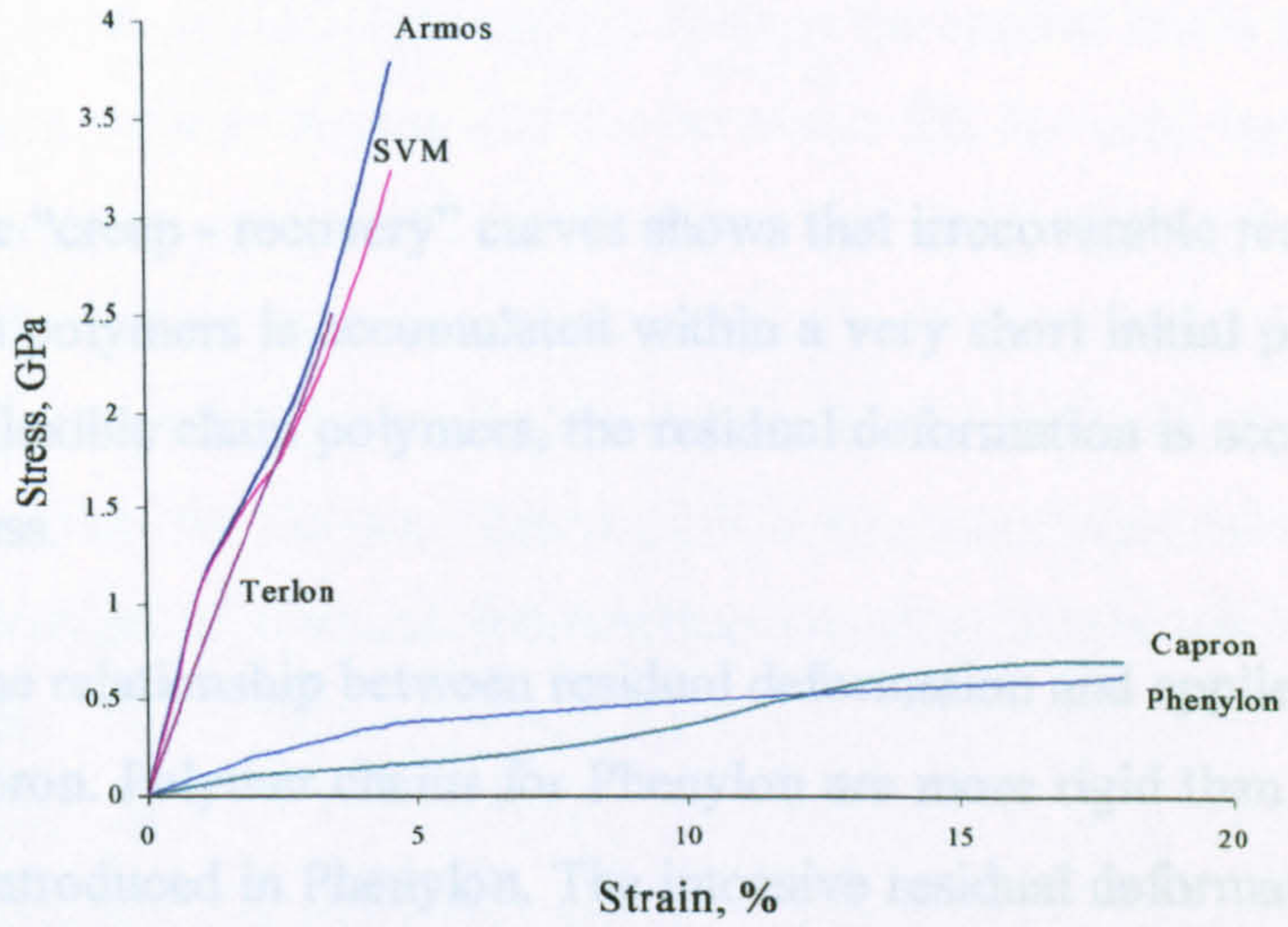

Fig. 3.29 Stress-strain curves of Armos, SVM, Terlon, Phenylon, and Capron

Armos, SVM and Terlon show high strength and high modulus, because they are obtained from rigid chain polymers and have quite similar chemical structures. Their molecular chains are highly orientated. The major factors such as extension of polymer chains, orientation and the possibility of symmetrical structure directly affects strength and modulus of polymer fibres.

SVM and Armos are heterocyclic para-copolyamide. The structure of this copolymer is characterised by less regularity and less rigidity in comparison with poly-p-phenylene terephthalamide. That is the reason that the strength and rigidity of Armos and SVM yarns increase after preliminary stretching. The preliminary stretching of Terlon and Kevlar yarns does not change the character of the stress-strain curves, the strength of these yarns does not vary significantly, and the rigidity increased slightly. Because no further orientation occurred in the preliminary stretching.

Preliminary stretching of Phenylon and Nomex yarns at more then 5% changes the nature of the stress-strain curves due to the rearrangement of the supermolecular structure which occur at this elongation. The preliminary stretching does not result in a significant change of strength. The preliminary stretching of Capron and Nylon yarns due to additional orientation and breaks of chemical bonds in molecular chains influences the stress-strain curves

The analysis of the "creep - recovery" curves shows that irrecoverable residual deformation for the rigid chain polymers is accumulated within a very short initial period of time. But for semi-rigid or flexible chain polymers, the residual deformation is accumulated during a whole creep process.

Fig. 3.30 shows the relationship between residual deformation and applied strain of Terlon, Phenylon and Capron. Polymer chains for Phenylon are more rigid than for Capron due to the phenyl rings introduced in Phenylon. The intensive residual deformation starts at lower applied strain for Phenylon. Polymer chains for Terlon are more symmetric and packed more tightly for achieving higher orientation and crystallinity than that of Phenylon. the intensive residual deformation for Terlon starts at lower applied strain than for Phenylon. There are direct relationships between rigidity of polymer chains, orientation and residual deformation properties. Highly orientated polymer has limited residual deformation.

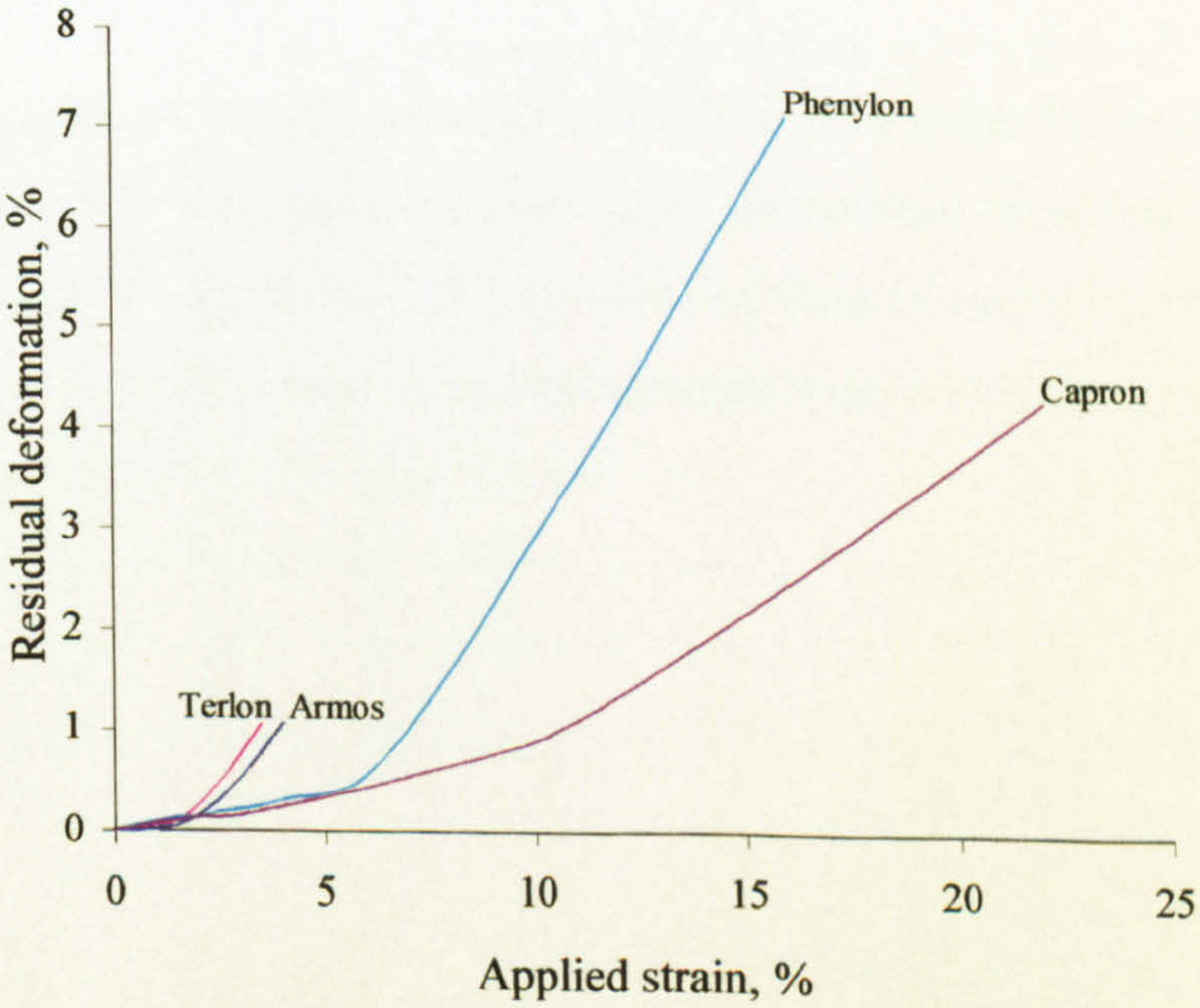

Fig. 3.30 Effect of applied strain on residual deformation for Armos, Terlon, Phenylon, and Capron

The nature of residual deformation is investigated at room temperature for all polyamide yarns. It was shown that all polyamide yarns at room temperature have a zone of preliminary deformation; within these deformations, full recovery from deformation is possible.

Intensive increase in the residual deformation starts at the applied strain about 1.5% for the rigid chain polymers such as Armos and Terlon about 5% for semi rigid chain polymers such as Phenylon and about 10-11% for flexible chain polymers such as Capron. These applied strains at the critical points are corresponding to the bending points on their tensile tress-strain curves except for Terlon, because there is no visible change points on linear stress-strain relationship for Terlon. Therefore, it is suggested that for the critical turning points for accumulation of residual deformation for other fibres can be predicted from stress-strain curves.

CHAPTER 4

STUDY OF DEFORMATION AND STRENGTH PROPERTIES OF HIGH-STRENGTH HIGH MODULUS GEL-SPUN POLYETHYLENE YARN

4.1 Introduction

The gel-spun high strength, high modulus Polyethylene yarn was studied for comparison with polyamide yarns. The reason for this choice is that this yarn has structural similarities with amide yarns but differences in internal intermolecular attraction. The high strength and rigidity properties of this yarn are due to a strongly oriented structure of macromolecular chains, despite being formed from a flexible chain polymer (Cune segment for polyolefine is 2.0-2.2 nm). The intermolecular interaction for polyethylene is defined by Van der Waals bonds, which are weaker than the hydrogen bonds associated with polyamide. The energy of the intermolecular bonds of parapolyamides is about 0.7 kJ/mol, whilst the energy of intermolecular bonds of polyolefines is 0.28-0.37 kJ/mol (Perepelkin, 1985).

4.2 Experimental

4.2.1 Yarn samples preparation

The structure and properties of gel-spun high strength high modulus Polyethylene yarn was described in Section 2.1. The yarn samples were preliminary stretched to a range of extensions from 1% to 3% by loading for 10 min and then releasing the load for 10 min recovery. All original and preliminary stretched samples were conditioned at 20°C and 65% r.h. before further testing.

4.2.2 Determination of stress-strain tensile properties

Tensile testing of the untreated and preliminary stretched high strength high modulus Polyethylene yarns was carried out using the Instron as described in Section 3.2.2. The tensile properties were initially expressed as stress-strain curves. The tangent modulus E was obtained by differentiation of the stress-strain curve as described in Section 3.2.2. The relative modulus was determined as the slope ratio of the tangent to the curve of the most linear part of stress-strain curve as described in Section 3.2.2.

4.2.3 Determination of stress relaxation-recovery properties

The process of yarn stress-relaxation - recovery was investigated using the Instron as described in Section 2.2.1. The residual deformation after 10 min. recovery was measured. The relationship between the residual deformation and applied strain was established as described in Section 3.2.4.

4.3 Results and discussion

4.3.1 Tensile stress-strain properties of gel-spun polyethylene yarn

Tensile stress-strain curves for untreated and preliminary stretched yarns are shown in Fig. 4.1. The characteristic shape of the tensile curve does not change after preliminary stretching up to 3%, because the polymer chains in these fibres have a very high molecular weight, and they are highly extended and possess nearly perfect crystalline alignment.

A smooth decrease of the tangent modulus ($E=\partial\sigma/\partial\varepsilon$) is observed for polyethylene yarn (Fig. 4.2). This can be compared with the third final part of the stress-strain curve of the Capron fibres shown in Section 3.5. The destruction mechanisms play a significant role in the stretching processes of ultra-high strength high modulus Polyethylene fibres. The destruction can involve straightening of few folded chains, sliding of molecular chains through crystallites due to weak Van der Waals intermolecular interaction and eventually breakage of covalent bonds in the main chain. Such an explanation is in good agreement

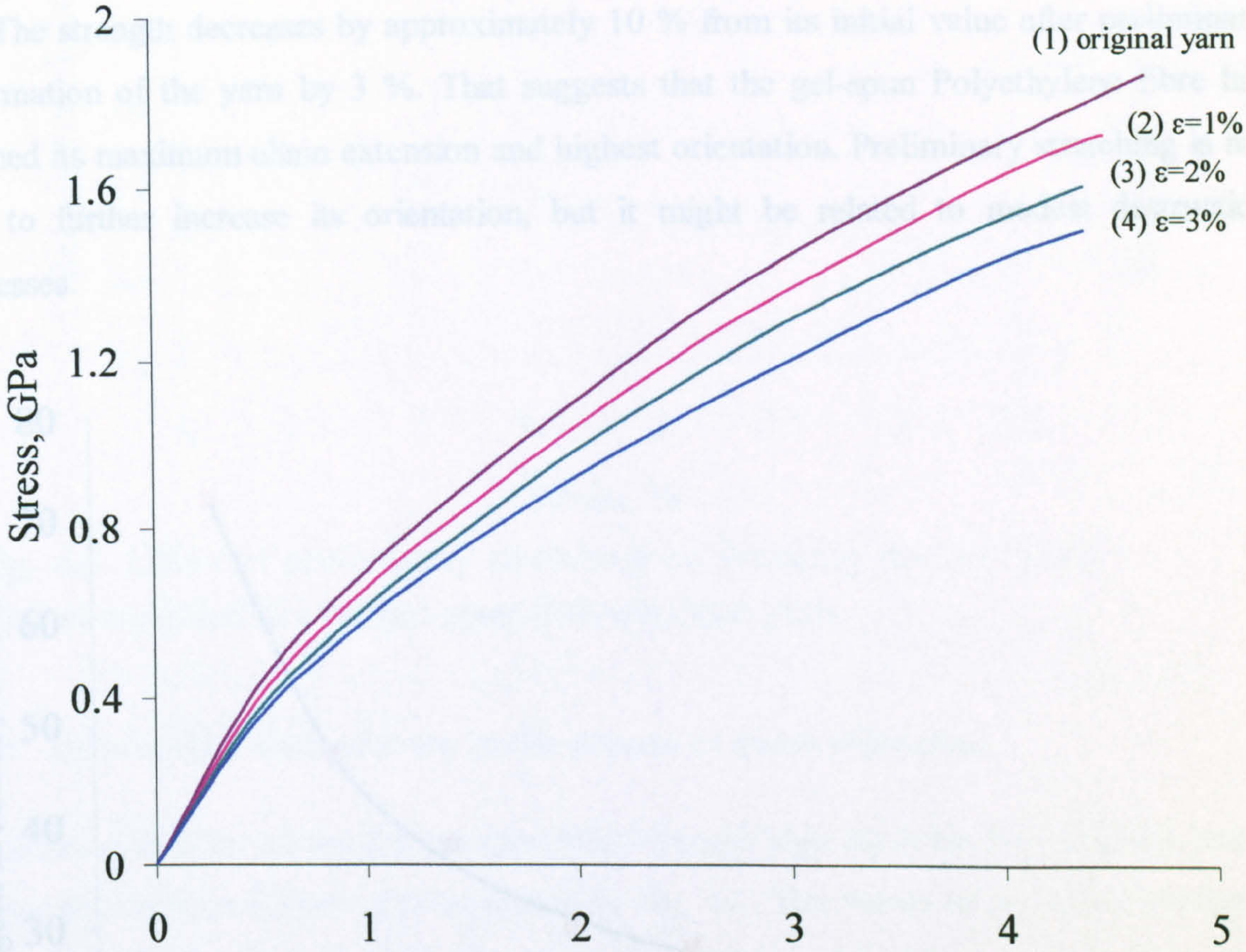

Fig. 4.1 Stress-strain curves of Polyethylene yarn before and after preliminary stretching; (1) original yarn, (2) yarn after preliminary stretching at ε=1%, (3) yarn after preliminary stretching at ε=2%, (4) yarn after preliminary stretching at ε=3%

with the data of Gordeev (1992) and Alekseev (1994). Comparing the stress-strain curves of untreated and preliminary stretched samples, a decrease in break strength and the modulus of rigidity (E) with increasing preliminary stretching is observed as shown in Fig. 4.3. The strength decreases by approximately 10 % from its initial value after preliminary deformation of the yarn by 3 %. That suggests that the gel-spun Polyethylene fibre has attained its maximum chain extension and highest orientation. Preliminary stretching is not able to further increase its orientation, but it might be related to modest destruction processes.

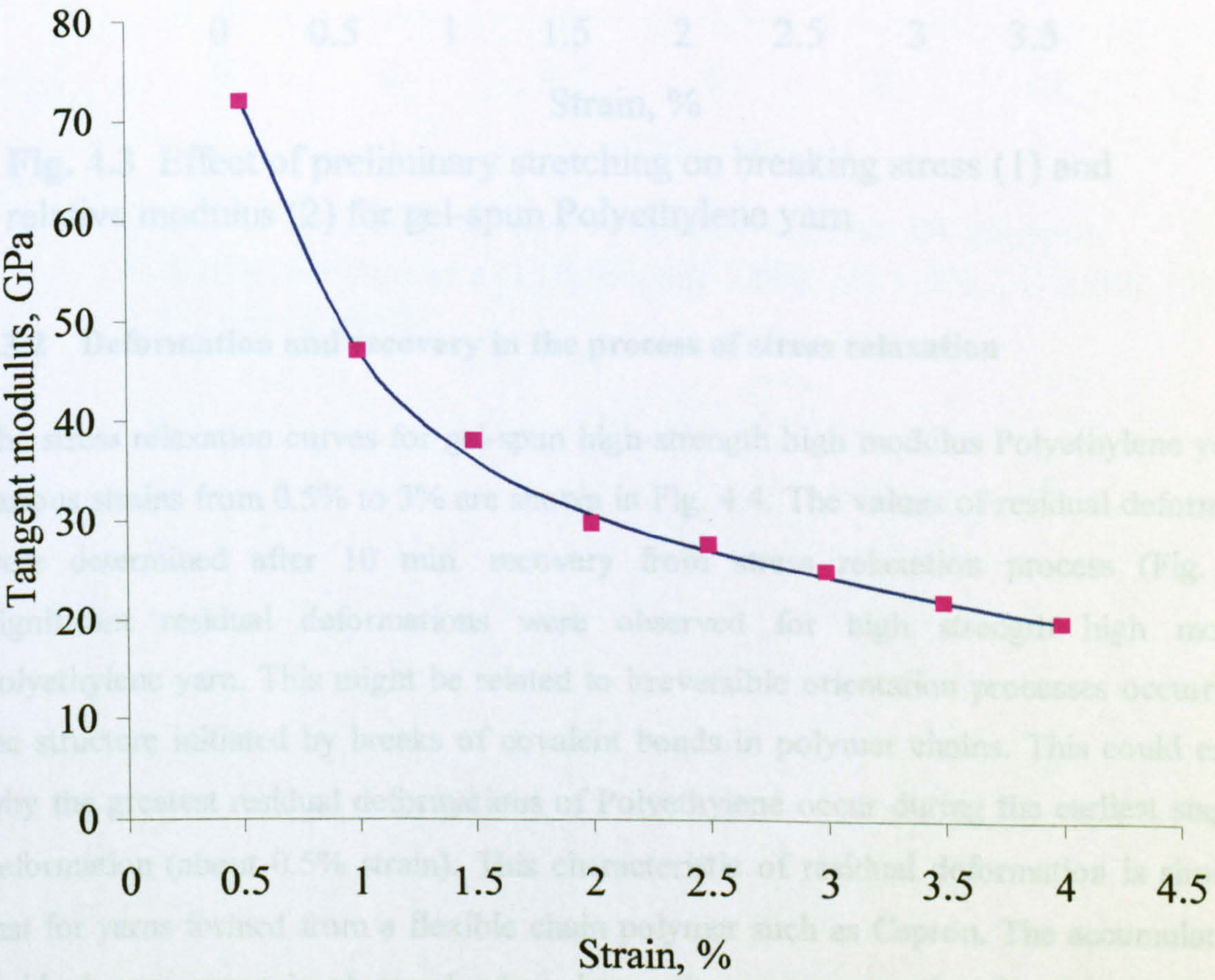

Fig. 4.2 Relationship between tangent modulus and strain for gel-spun Polyethylene yarn

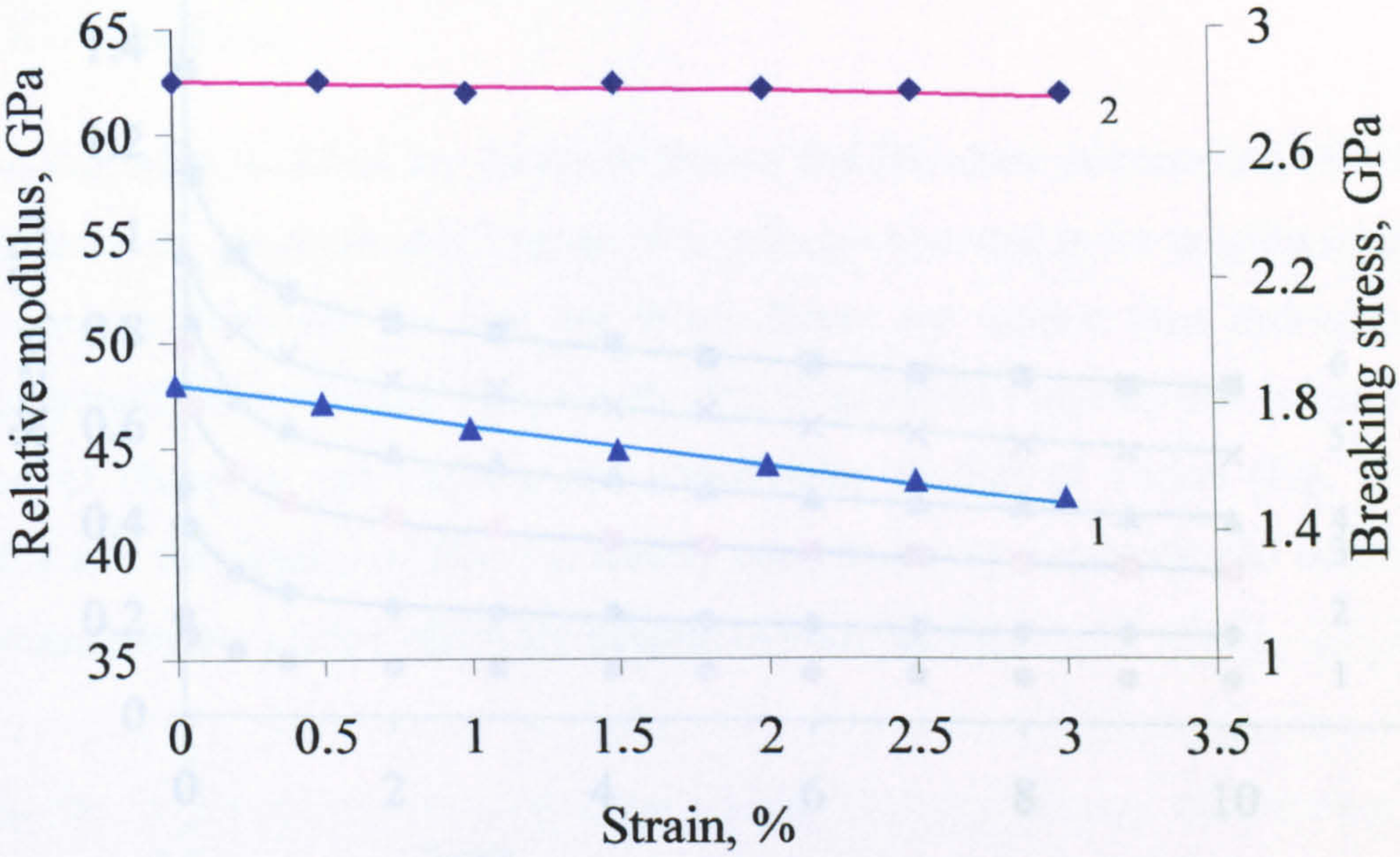

Fig. 4.3 Effect of preliminary stretching on breaking stress (1) and relative modulus (2) for gel-spun Polyethylene yarn

4.3.2 Deformation and recovery in the process of stress relaxation

The stress relaxation curves for gel-spun high-strength high modulus Polyethylene yarn at various strains from 0.5% to 3% are shown in Fig. 4.4. The values of residual deformation were determined after 10 min. recovery from stress relaxation process (Fig. 4.5). Significant residual deformations were observed for high strength high modulus Polyethylene yarn. This might be related to irreversible orientation processes occurring in the structure initiated by breaks of covalent bonds in polymer chains. This could explain why the greatest residual deformations of Polyethylene occur during the earliest stages of deformation (about 0.5% strain). This characteristic of residual deformation is similar to that for yarns formed from a flexible chain polymer such as Capron. The accumulation of residual component is observed when destruction processes of molecular structure are possible.

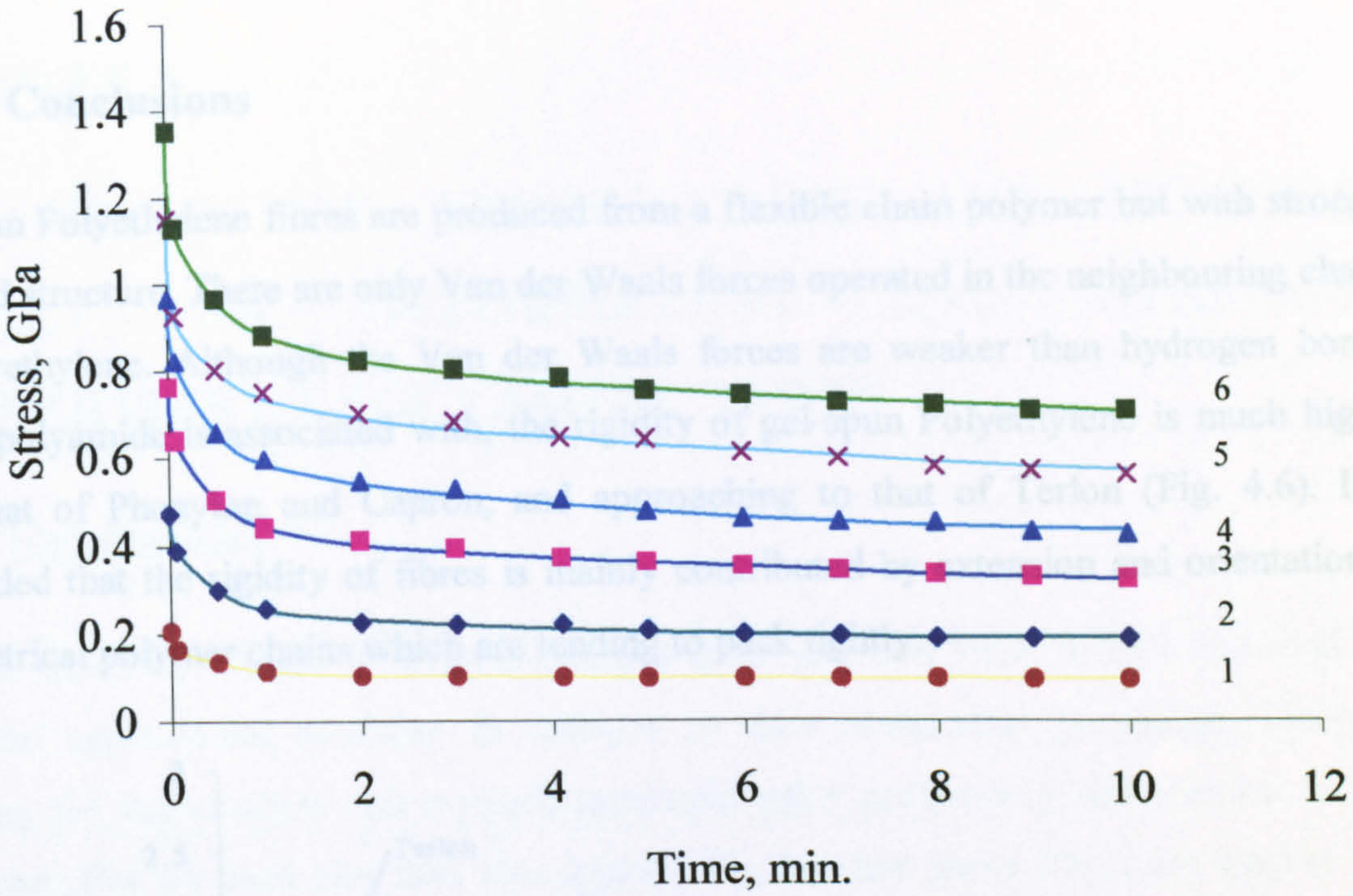

Fig. 4.4 The family of stress relaxation curves for gel-spun Polyethylene yarn at ε (1) 0.5%, (2) 1.0%, (3) 1.5%, (4) 2.0%, (5) 2.5% and (6) 3.0%

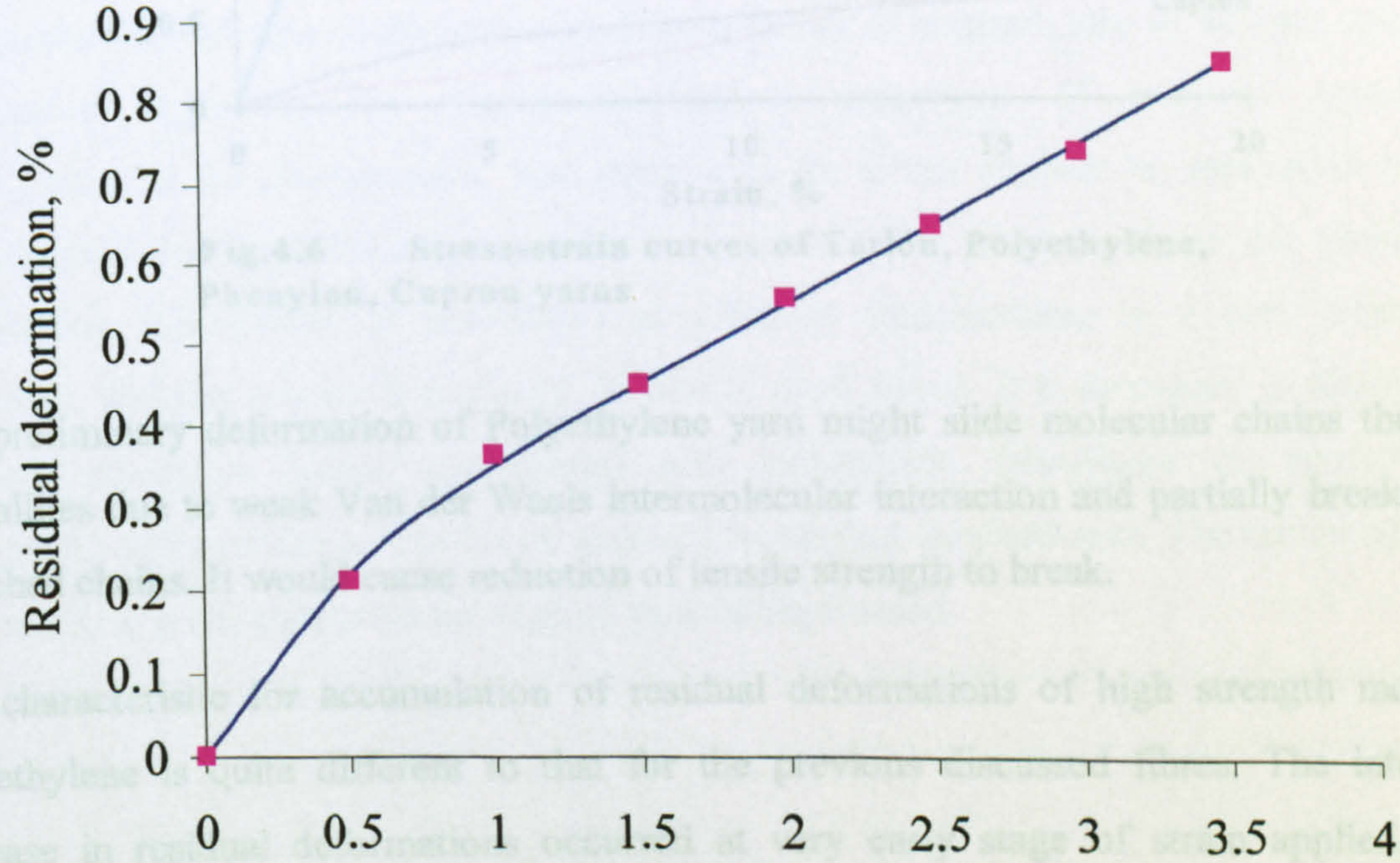

Fig. 4.5 Effect of applied strain on residual deformation for gel-spun Polyethylene yarn

4.4 Conclusions

Gel-spun Polyethylene fibres are produced from a flexible chain polymer but with strongly oriented structure. There are only Van der Waals forces operated in the neighbouring chains in Polyethylene. Although the Van der Waals forces are weaker than hydrogen bonds, which polyamide is associated with, the rigidity of gel-spun Polyethylene is much higher than that of Phenylon and Capron, and approaching to that of Terlon (Fig. 4.6). It is concluded that the rigidity of fibres is mainly contributed by extension and orientation of symmetrical polymer chains which are tending to pack tightly.

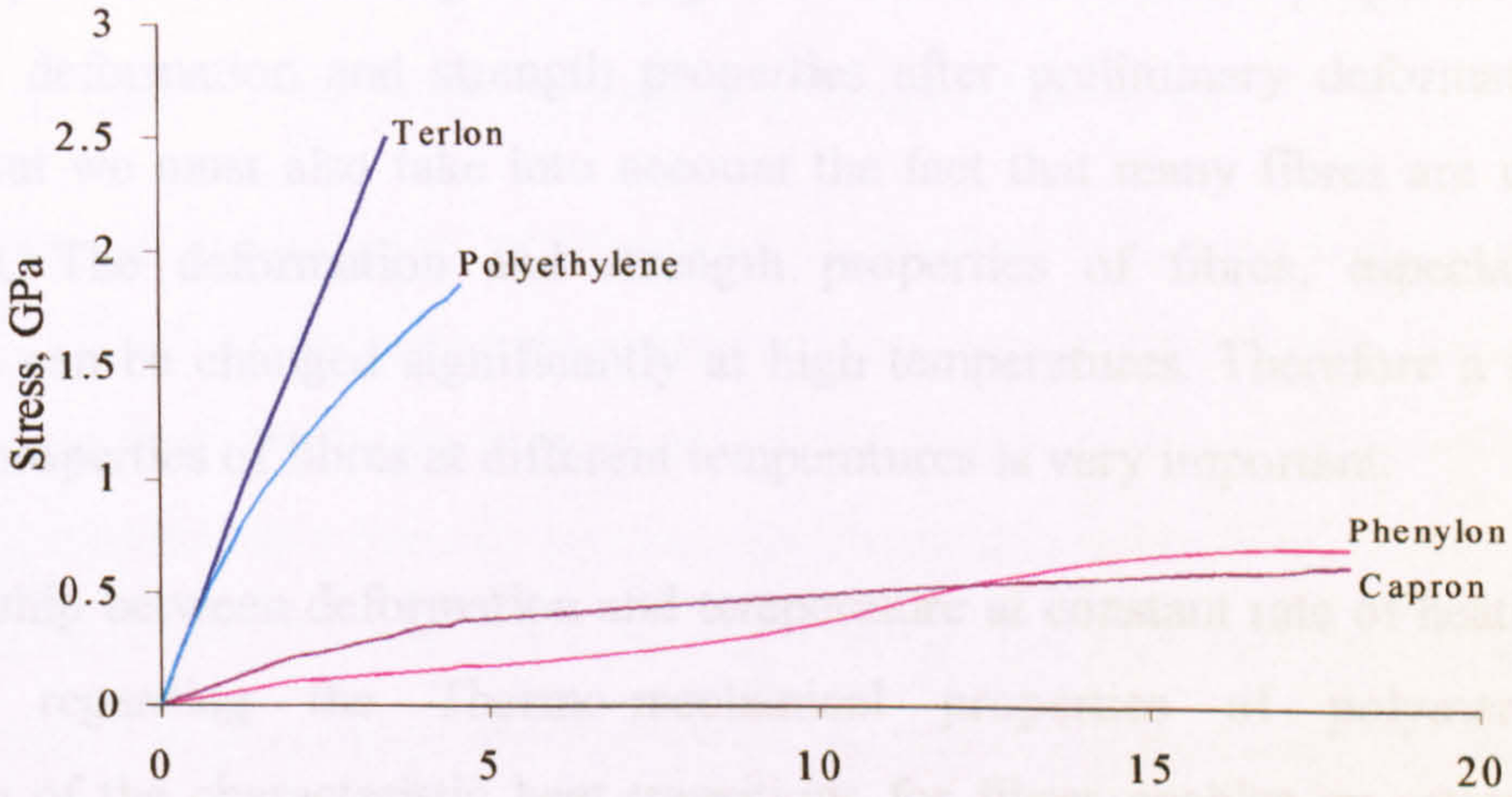

Fig.4.6 Stress-strain curves of Terlon, Polyethylene, Phenylon, Capron yarns

The preliminary deformation of Polyethylene yarn might slide molecular chains through crystallites due to weak Van der Waals intermolecular interaction and partially break fully stretched chains. It would cause reduction of tensile strength to break.

The characteristic for accumulation of residual deformations of high strength modulus Polyethylene is quite different to that for the previous discussed fibres. The intensive increase in residual deformations occurred at very early stage of strain applied. It is believed that this could be related to sliding of molecular chains and breakage of covalent bonds.

CHAPTER 5

THE STUDY OF TEMPERATURE AND MOISTURE EFFECT ON DEFORMATION AND STRENGTH PROPERTIES OF POLYAMIDE YARNS

5.1 Introduction

As was shown in Chapter 3 fibres are subjected to different loads in their practical and industrial applications, resulting in changes in their mechanical properties. Therefore studying the deformation and strength properties after preliminary deformation is very important. But we must also take into account the fact that many fibres are used at high temperatures. The deformation and strength properties of fibres, especially residual deformation, can be changed significantly at high temperatures. Therefore a study of the mechanical properties of fibres at different temperatures is very important.

The relationship between deformation and temperature at constant rate of heating can give information regarding the Thermo-mechanical properties of polymer materials. Investigation of the characteristic heat transitions for fibres enables an estimation of the technological and exploitation properties to be made. For polymer yarns the change of deformation (elongation or shrinkage) at different temperatures is a very important parameter. Heating results in a change of size of most fibres. It is necessary to distinguish between reversible (linear expansion) and irreversible (shrinkage or spontaneous elongation) deformation of a polymer exposed to varying temperatures. The nature of these deformations is dependent on the type of yarn being studied.

5.2 Experimental

5.2.1 Sample preparation

The polyamide yarns spun from polymers with different chain rigidity were selected to study their thermal and deformation properties. These were Armos, SVM and Terlon from rigid chain polymers; Phenylon from semi rigid chain polymers; Capron from flexible chain polymers as described in Section 2.1.

Some yarn samples were further prepared by drying at 105°C to constant weight before testing.

5.2.2 Determination of thermal shrinkage of polyamide yarns

The relaxometer of deformation as described in Section 2.2.2 was operated to measure shrinkage of yarn as a function of temperature. The yarn length change corresponding to shrinkage is monitored by the movement of a probe maintained in contact with the sample. The sample is exposed to a steadily increasing temperature at the heating rate of 10°C/min from 20°C up to 340°C. During the shrinking process, the yarn was kept straight without any load tension. The percentage thermal shrinkage was calculated using the formula:

$$\text{Shrinkage (\%)} = 100 (L_1 - L_2) / L_1$$

Where L_1 is the original length of yarn

L_2 is the length of yarn after shrinkage

5.2.3 Determination of tensile stress-strain properties of polyamide yarns over a range of temperatures

The tensile properties of the yarns at various temperatures were determined using the Instron as described in Section 3.2.2. Multiple measurements of stress-strain curves were undertaken. Samples were subjected to a range of temperatures: 60, 80, 100, 140, 180 and 220°C by controlling the temperature in the sample chamber during the test. The stress-strain responses of yarns were measured over the range of temperatures. The relationships

between breaking stress or breaking elongation and temperature were obtained from the tensile stress-strain curves at varying temperatures.

5.2.4 Determination of creep and stress relaxation properties over a range of temperatures

The creep-recovery and stress relaxation-recovery processes of yarns were investigated as described in Sections 3.2.3 and 3.2.4. Multiple measurements of creep-relaxation and stress-relaxation processes were undertaken. Samples were subjected to a range of temperatures: 60, 80, 100, 140, 180 and 220°C. The response of the yarn sample was measured over this range of temperatures. The relationship between residual deformation and the applied strain prior to removal of load from yarn samples was determined over the range of temperatures.

5.3 Effect of temperature on tensile properties of Armos yarns and their deformation

5.3.1 Thermal shrinkage properties of Armos yarn

The shrinkage-temperature curves for original and dried Armos yarns over a temperature range 20°C to 340°C are shown in Fig. 5.1. It can be seen from curve 1 for the original Armos that the initial minor shrinkage occurred at temperature from approximately 20 to 90°C. Then there is a small spontaneous elongation of the sample in the temperature range 90 to 120°C, after which the shrinkage remained constant. The most significant increase of shrinkage is observed at 150°C upwards. It is believed that during the shrinkage process, the intermolecular bonds formed between neighbouring extended chains become loosened by the thermal energy, allowing contraction along the length of the chain, followed by intermolecular bond re-formation.

It is noticed that the value of shrinkage for the dried yarn is slightly higher than that for the original yarns. The shrinkage of dried yarn also starts to increase intensively at temperatures above 150°C. This difference might be due to the removal of moisture from

the Armos fibre, which results in breakage of hydrogen bonds which were formed as "polymer-water-polymer" type. The neighbouring chains at the broken position might not be sufficiently close to re-form the "polymer-polymer" type hydrogen bonds with the restriction of chain movements at low temperature. Therefore, the easing of intermolecular interaction in the dried Armos is reflected as a thermal shrinkage slightly higher than original Armos yarn. It is noted that the values of shrinkage for both dried and original Armos are actually very small (about 0.6 % at the temperature of 340°C), although temperature does cause some shrinkage for Armos. Therefore the process of shrinkage would not decisively influence the deformation and strength properties of yarns at the investigated temperature range.

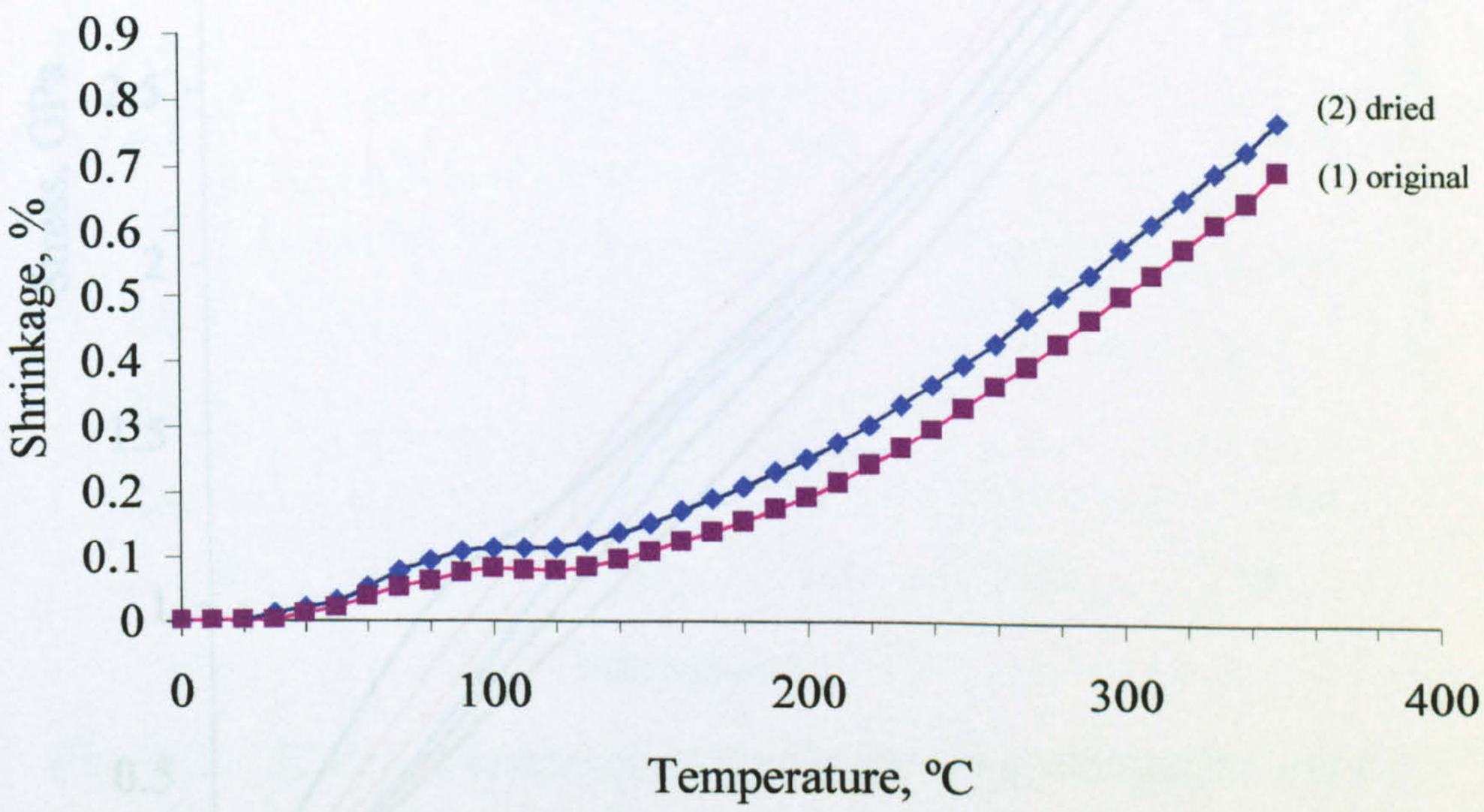

Fig. 5.1 Thermal shrinkage of Armos yarns: (1) original and (2) dried

5.3.2 Effect of temperature on the stress-strain curves of Armos yarn

Typical stress-strain curves of the original Armos yarn at different temperatures are shown in Fig. 5.2. It was found that the shape of the stress-strain curves changes with increasing

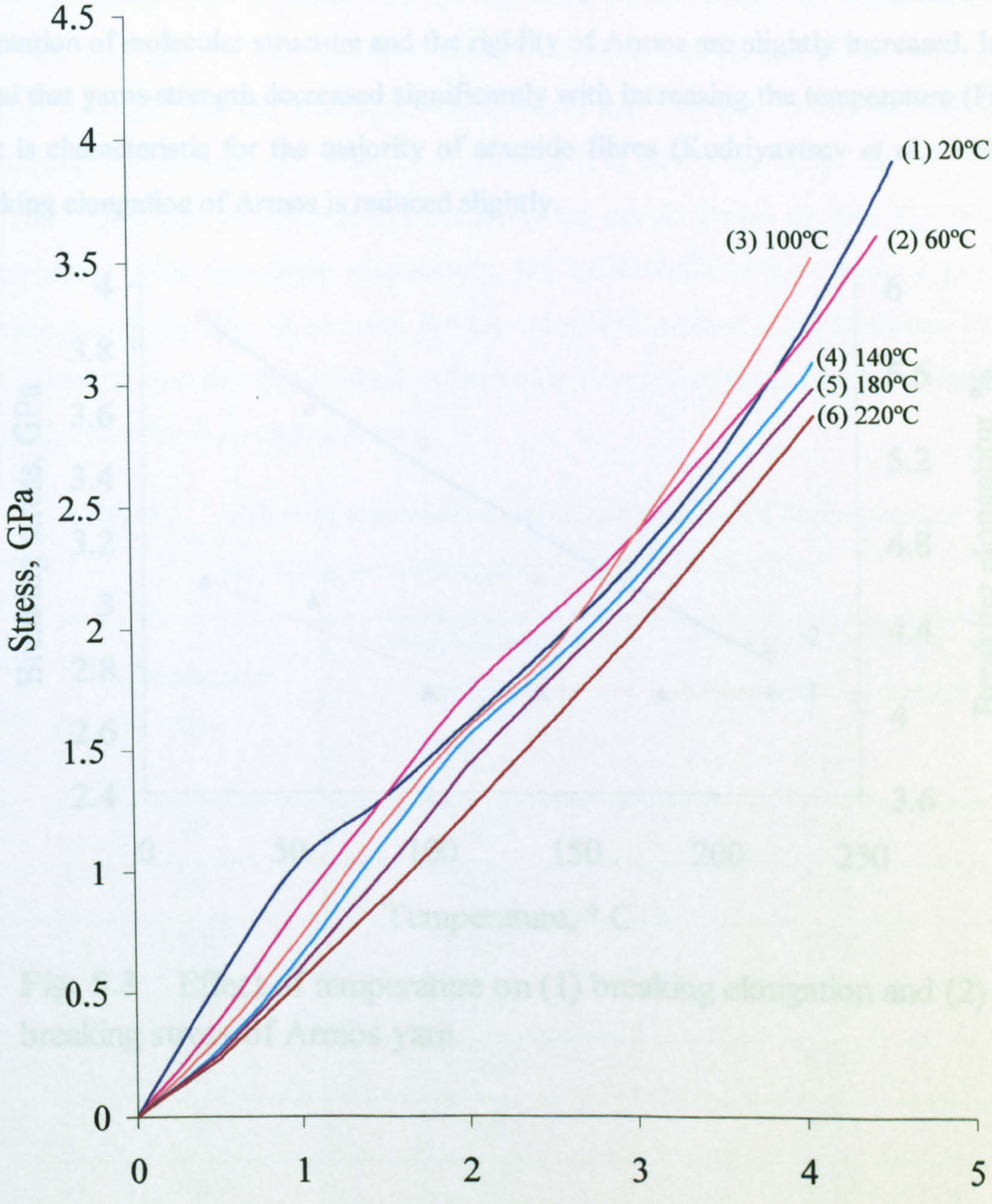

Fig. 5.2 Stress-strain curves of Armos yarn at different temperatures: (1) 20°C; (2) 60°C; (3) 100°C; (4) 140°C; (5) 180°C; (6) 220°C

temperature. A shoulder on the stress-strain curves at approximate 1.5% of strain is found at room temperature, but gradually vanished with increasing temperature. The stress-strain curve becomes almost a straight line at the temperature of 220°C. It testifies that the orientation of molecular structure and the rigidity of Armos are slightly increased. It is also found that yarns strength decreased significantly with increasing the temperature (Fig. 5.3). That is characteristic for the majority of aramide fibres (Kudriyavtsev *et al.*, 1992). The breaking elongation of Armos is reduced slightly.

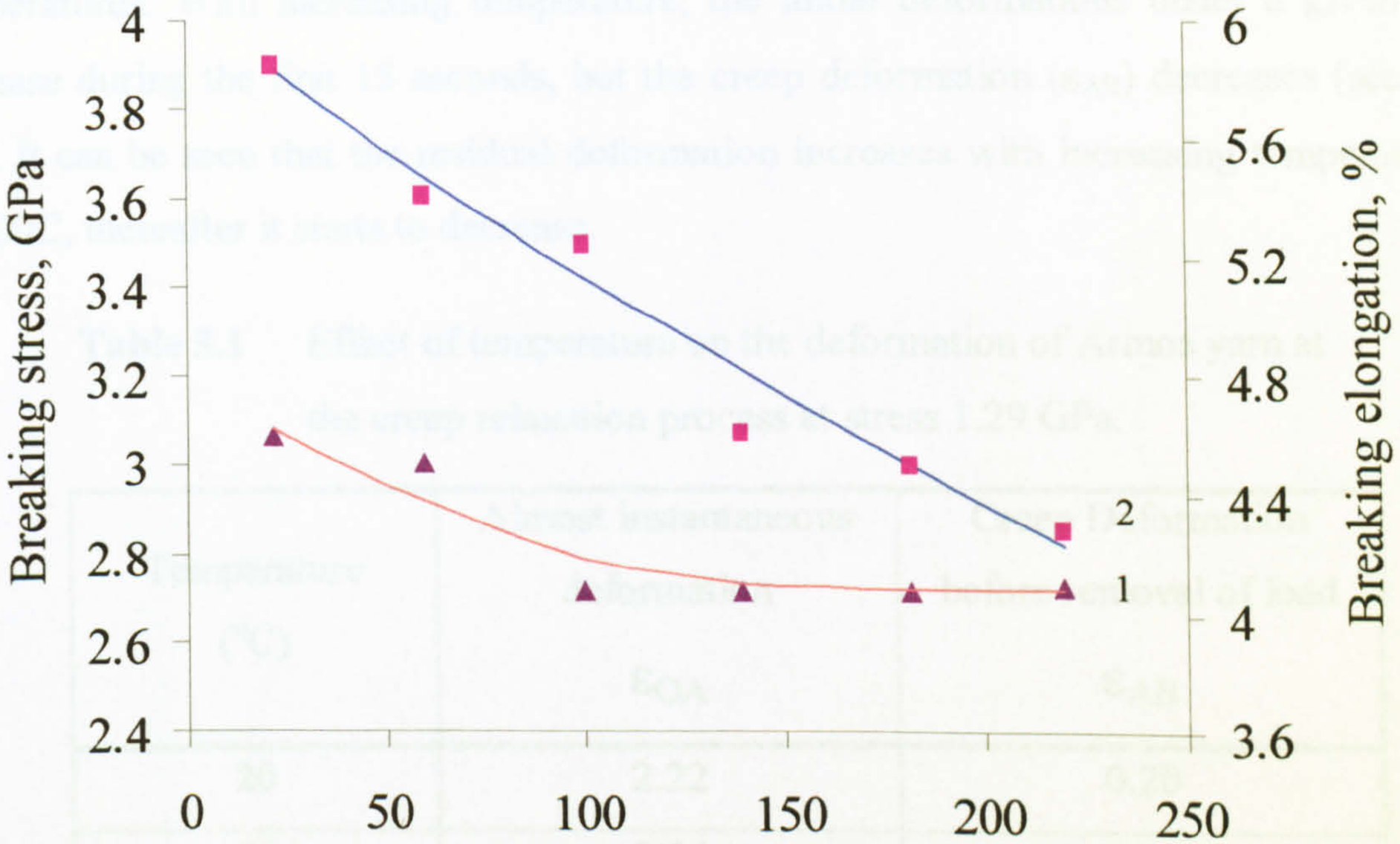

Fig. 5.3 Effect of temperature on (1) breaking elongation and (2) breaking stress of Armos yarn

5.3.3 Influence of temperature on stress relaxation-recovery and creep-recovery properties of Armos yarn and their accumulated residual deformation

The creep and recovery process of Armos was studied over a range of temperatures (60, 80, 100, 140, 180, 220°C). The family of creep – recovery curves are shown in Figs. A_1 – A_6 in Appendix for the individual temperatures and different loads, and the effect of temperature on the creep and recovery property at 2.12 GPa is shown in Fig. 5.4. It is found that the largest part of deformation occurs in an initial period of time (15 sec.) at all temperatures. With increasing temperature, the initial deformations under a given stress increase during the first 15 seconds, but the creep deformation (ε_{AB}) decreases (see Table 5.1). It can be seen that the residual deformation increases with increasing temperature up to 100C, thereafter it starts to decrease.

Table 5.1 Effect of temperature on the deformation of Armos yarn at the creep relaxation process at stress 1.29 GPa.

Temperature (°C)	Almost instantaneous deformation ε_{OA}	Creep Deformation before removal of load ε_{AB}
20	2.22	0.20
60	2.34	0.18
80	2.42	0.12
100	2.60	0.18
140	2.64	0.15
180	2.65	0.14
220	2.71	0.14

The family of stress relaxation curves for original Armos yarns at different temperatures are shown in Figs. A_7 – A_12 in the Appendix. The effect of temperature on stress relaxation

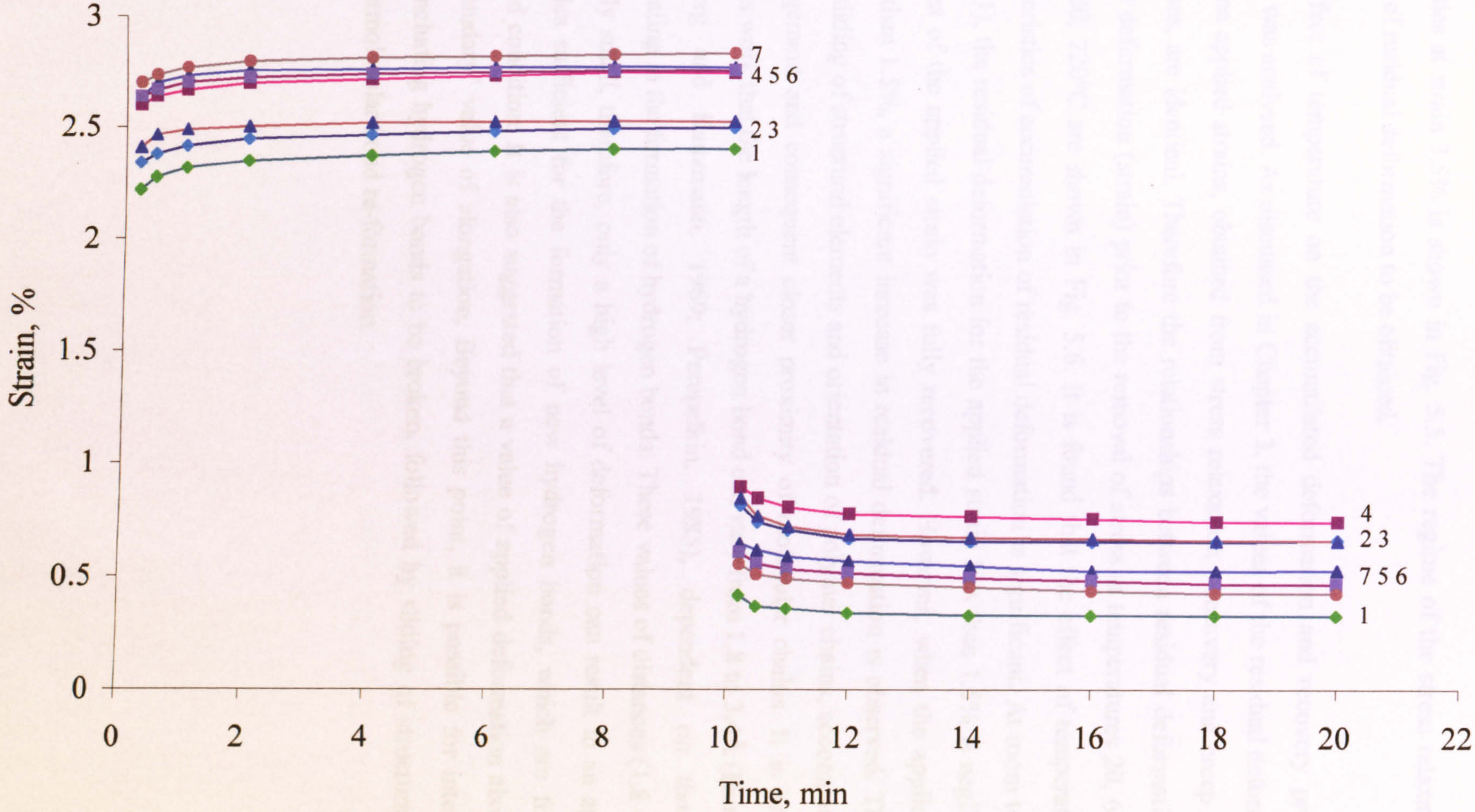

Fig. 5.4 Creep-recovery curves for Armos yarn at σ=2.12 GPa at different temperatures: (1) 20°C; (2) 60°C; (3) 80°C; (4) 100°C; (5) 140°C; (6) 180°C; (7) 220°C

properties at strain 3.5% is shown in Fig. 5.5. The regime of the stress relaxation allows values of residual deformation to be obtained.

The effect of temperature on the accumulated deformation and recovery properties of Armos was analysed. As discussed in Chapter 3, the values of the residual deformations for the same applied strains, obtained from stress relaxation - recovery and creep – recovery processes, are identical. Therefore the relationships between residual deformation and the applied deformation (strain) prior to the removal of stress at temperatures 20, 60, 80, 100, 140, 180, 220°C are shown in Fig. 5.6. It is found that the effect of temperature on the characteristics of accumulation of residual deformation is significant. At room temperature (curve 1), the residual deformation for the applied strain less than 1.5% is negligible, thus the most of the applied strain was fully recovered. However, when the applied strain is higher than 1.5%, a significant increase in residual deformation is observed. This may be due to sliding of structural elements and orientation of polymer chains, accompanied by the rearrangement and consequent closer proximity of molecular chains. It is known from previous work that the length of a hydrogen bond can vary from 1.8 to 3.4Å (Pauling, 1960; Eisenberg and Kauzmann, 1969; Perepelkin, 1985), dependent on those groups participating in the formation of hydrogen bonds. These values of distances (1.8 - 3.4Å) are relatively small, therefore, only a high level of deformation can result in an approach of molecules sufficient for the formation of new hydrogen bonds, which are fixed in the stretched condition. It is also suggested that a value of applied deformation about 1.5% is the "boundary" value of elongation. Beyond this point, it is possible for intermolecular bonds including hydrogen bonds to be broken, followed by sliding of structural elements and intermolecular bond re-formation.

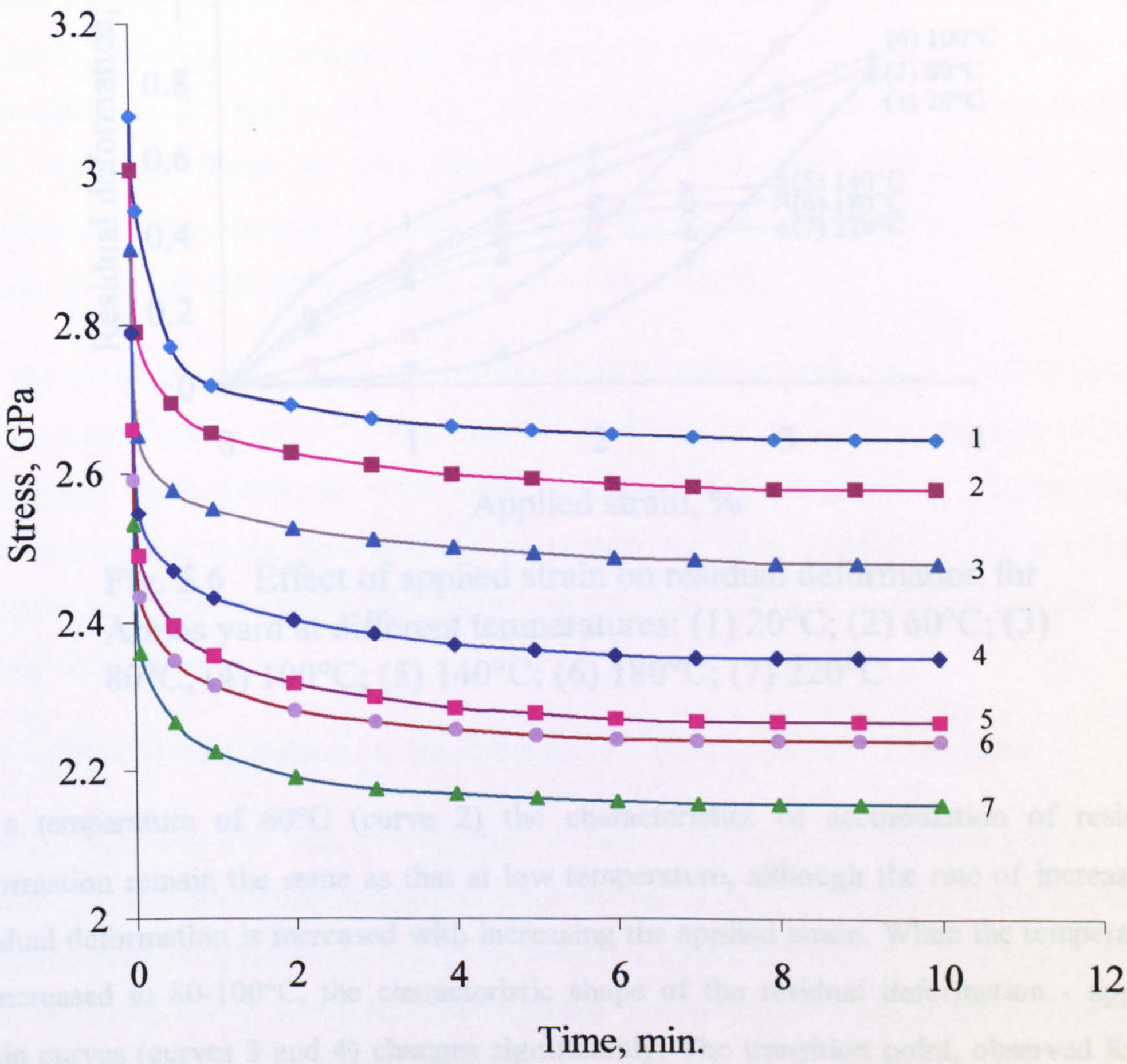

Fig. 5.5 Stress relaxation curves for Armos yarn at ε=3.5% at (1) 20°C; (2) 60°C; (3) 80°C; (4) 100°C; (5) 140°C; (6) 180°C; (7) 220°C

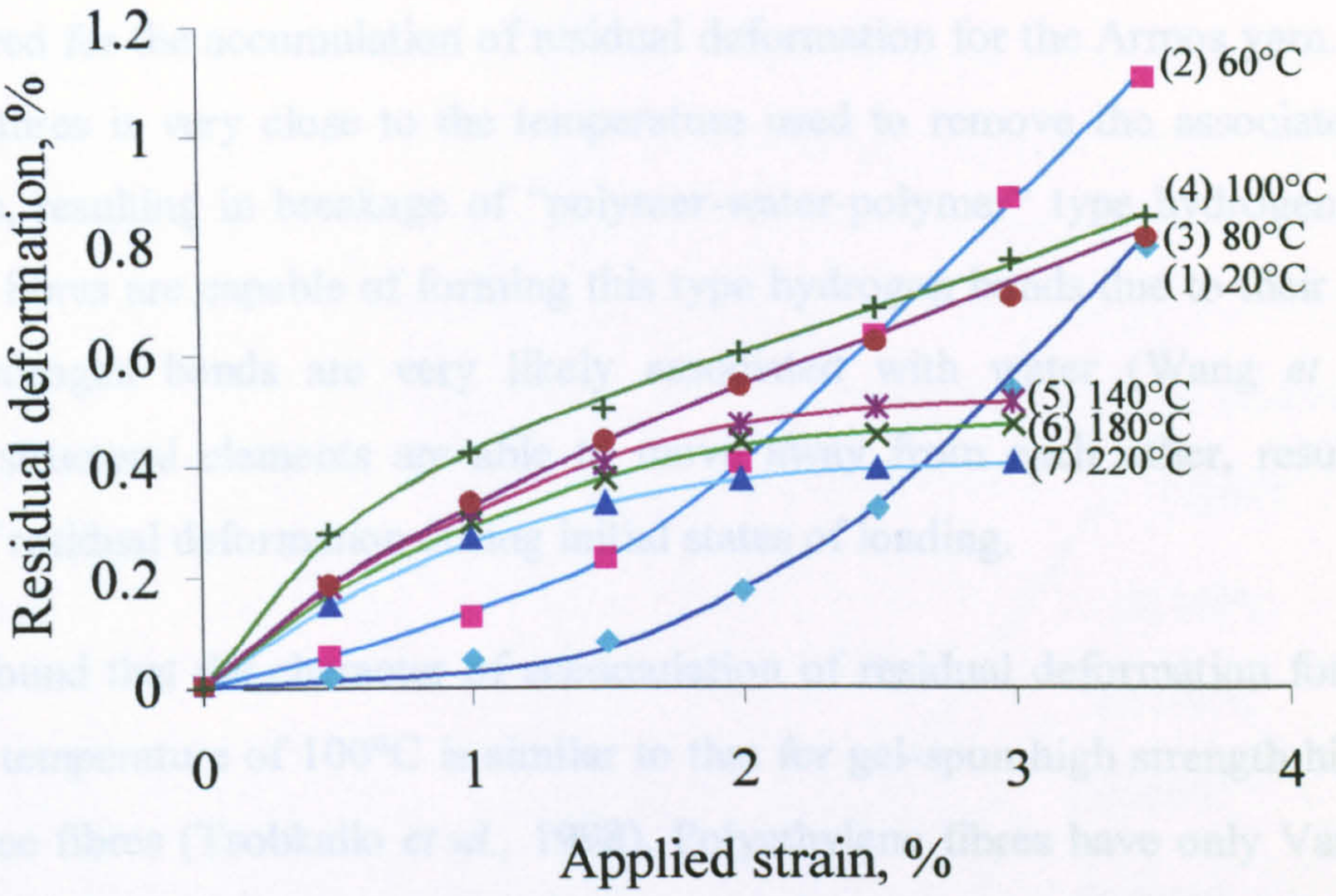

Fig. 5.6 Effect of applied strain on residual deformation for Armos yarn at different temperatures: (1) 20°C; (2) 60°C; (3) 80°C; (4) 100°C; (5) 140°C; (6) 180°C; (7) 220°C

At a temperature of 60°C (curve 2) the characteristics of accumulation of residual deformation remain the same as that at low temperature, although the rate of increase in residual deformation is increased with increasing the applied strain. When the temperature is increased to 80-100°C, the characteristic shape of the residual deformation - applied strain curves (curves 3 and 4) changes significantly. The transition point, observed for an applied strain of 1.5 % at 20°C and 60°C disappears, but the residual component increases for a low value of applied strain.

When the temperature is increased further up to 220°C (curves 5 to 7), the characteristics of accumulation of residual deformation remains same as for a temperature of 100°C, but the rate of increase in residual deformation is reduced after the temperature reaches 140°C. It is suggested this might be due to thermal shrinkage becoming involved beyond this temperature.

From the above discussion, the temperatures around 80-100°C might be the turning point to be considered for the accumulation of residual deformation for the Armos yarn. This range of temperatures is very close to the temperature used to remove the associated moisture from fibres, resulting in breakage of "polymer-water-polymer" type hydrogen bonds. All polyamide fibres are capable of forming this type hydrogen bonds due to their hydrophilic nature. Hydrogen bonds are very likely associated with water (Wang *et al.*, 1992). Therefore structural elements are able to move away from each other, resulting in the increase of residual deformation during initial states of loading.

It is also found that the character of accumulation of residual deformation for the Armos fibres at a temperature of 100°C is similar to that for gel-spun high strength high modulus polyethylene fibres (Tsobkallo *et al.*, 1998). Polyethylene fibres have only Van der Waals bonds contributing to the intermolecular interaction, but their molecular chains are highly orientated and packed tightly. The results suggest that Armos becomes more rigid after removal of moisture.

5.3.4 Effect of temperature on the stress-strain curves of dried Armos yarn

From previous research and investigation of Armos properties at elevated temperatures (Section 5.3.3), it was found that the moisture content in the Armos fibres might affect the yarn properties of deformation to a great extent. Therefore, research on the dried Armos yarn was carried out to investigate this influence. The stress-strain relationship of the dried yarn at room temperature is represented by the almost straight line shown in Fig. 5.7. It might be possible that the polymer molecular chains within the Armos fibre become closer by volatilization of the moisture during drying, so that the rigidity of fibres is increased. The stress-strain relationships of the dried Armos still remain almost linear with increasing temperature, although their initial modulus decreased. It is also found that strength and

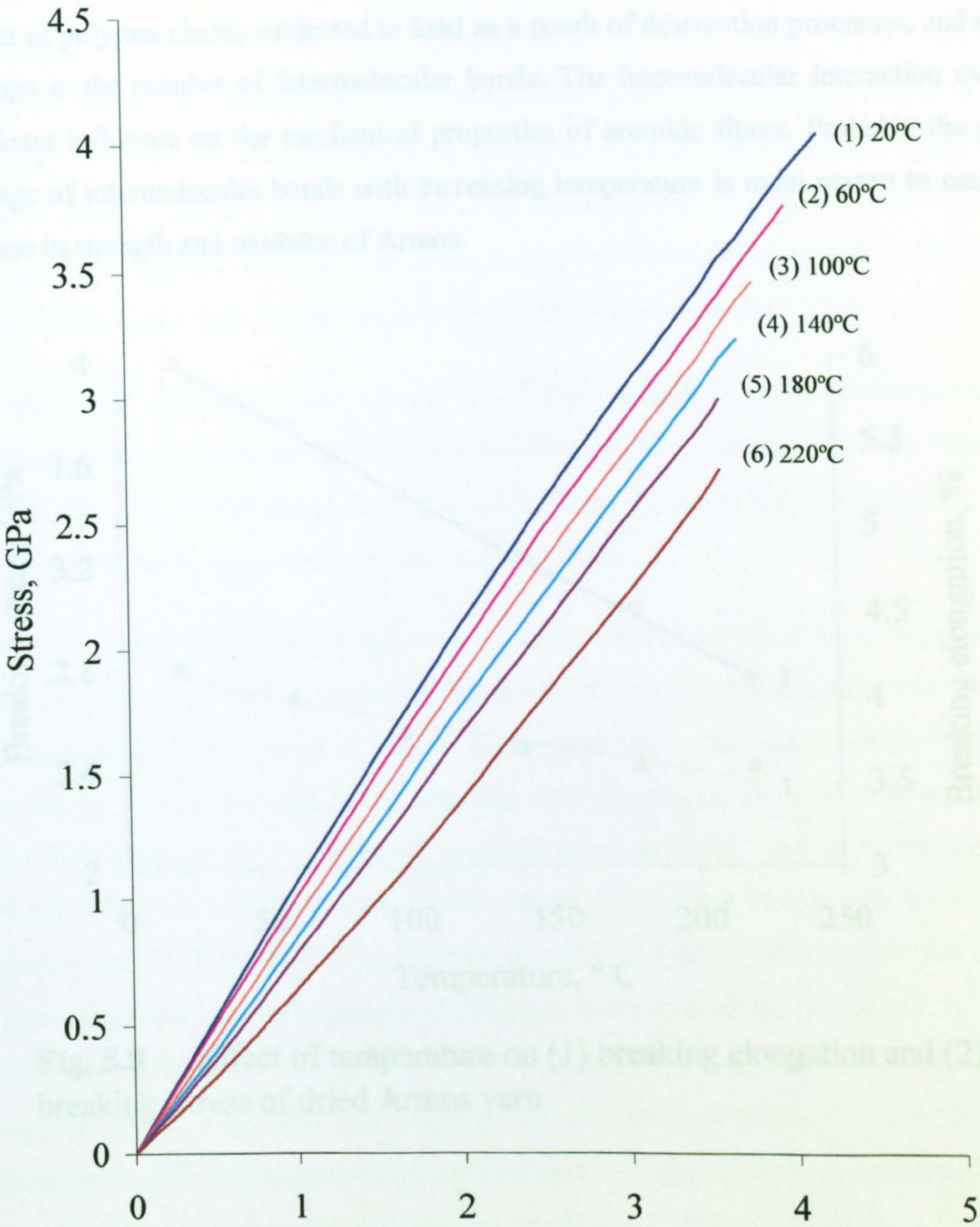

Fig. 5.7 Stress-strain curves of dried Armos yarn at different temperatures: (1) 20°C; (2) 60°C; (3) 100°C; (4) 140°C; (5) 180°C; (6) 220°C

breaking elongation of the dried yarn decrease with increasing temperature (Fig. 5.8). Yarn strength loss is up to 30 % from 20°C to 220°C, while the break elongation did not decrease significantly. The strength decreases with increasing temperature due to decrease in the number of polymer chains subjected to load as a result of destruction processes, and due to a change in the number of intermolecular bonds. The intermolecular interaction exerts a significant influence on the mechanical properties of aramide fibres. Probably the partial breakage of intermolecular bonds with increasing temperature is main reason to cause the decrease in strength and modulus of Armos.

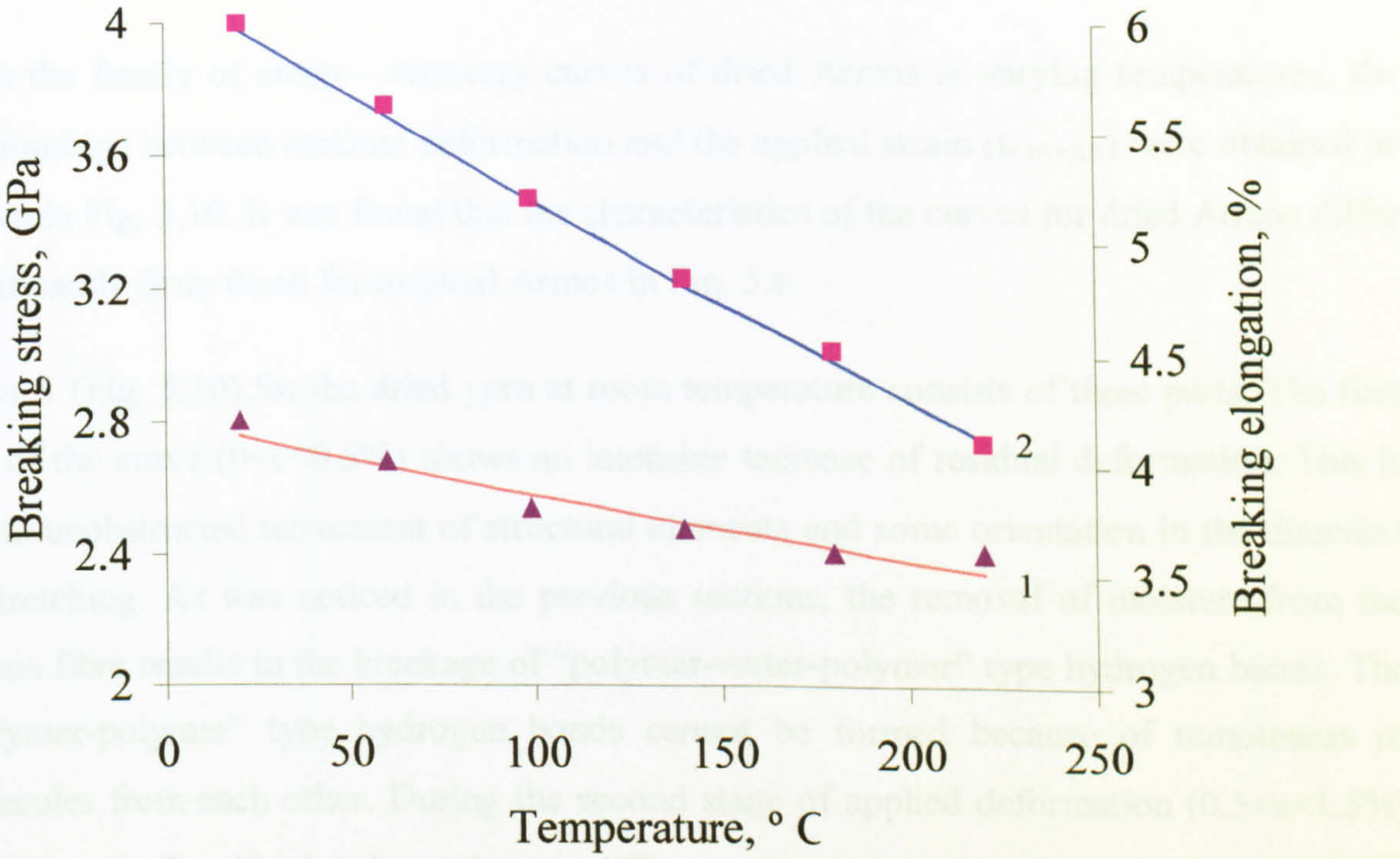

Fig. 5.8 Effect of temperature on (1) breaking elongation and (2) breaking stress of dried Armos yarn

5.3.5 Influence of temperature on creep-recovery properties of dried Armos yarn and their accumulated residual deformation

For the dried Armos yarn the family of creep - recovery curves were obtained at temperatures 40, 60, 80, 100, 120°C over a range of loads (Figs. A_13 – A_18 in Appendix). Fig. 5.9 shows the effect of temperature on the creep-recovery property at stress 2.52 GPa. The increase of temperature up to 220°C does not influence the characteristic shapes of creep – recovery curves for the dried Armos yarns. During the first 10 minutes when load was applied, most of the strain for dried Armos accumulated in the first 15 second similar to the case for the original yarn as discussed in Section 5.3.3.

From the family of creep – recovery curves of dried Armos at varying temperatures, the relationships between residual deformation and the applied strain (ε_{OA+AB}) were obtained as shown in Fig. 5.10. It was found that the characteristics of the curves for dried Armos differ significantly from those for original Armos in Fig. 5.6.

Curve 1 (Fig. 5.10) for the dried yarn at room temperature consists of three parts. The first part of the curve ($0<\varepsilon<0.5\%$) shows an intensive increase of residual deformation. This is due to unobstructed movement of structural elements and some orientation in the direction of stretching. As was noticed in the previous sections, the removal of moisture from the Armos fibre results in the breakage of "polymer-water-polymer" type hydrogen bonds. The "polymer-polymer" type hydrogen bonds cannot be formed because of remoteness of molecules from each other. During the second stage of applied deformation ($0.5<\varepsilon<1.5\%$) the increase of residual deformations at different temperatures are very small. It might be possible that orientation and new "polymer-polymer" type intermolecular bonds formed during the initial stage preclude slippage of structure elements. At $\varepsilon>1.5\%$ residual deformation at different temperatures accumulated in a similar way. A significant increase in the residual component of deformation is observed. One explanation is that applied deformations above 1.5 % are sufficient to start breaking intermolecular bonds and sliding structure elements in the fibre.

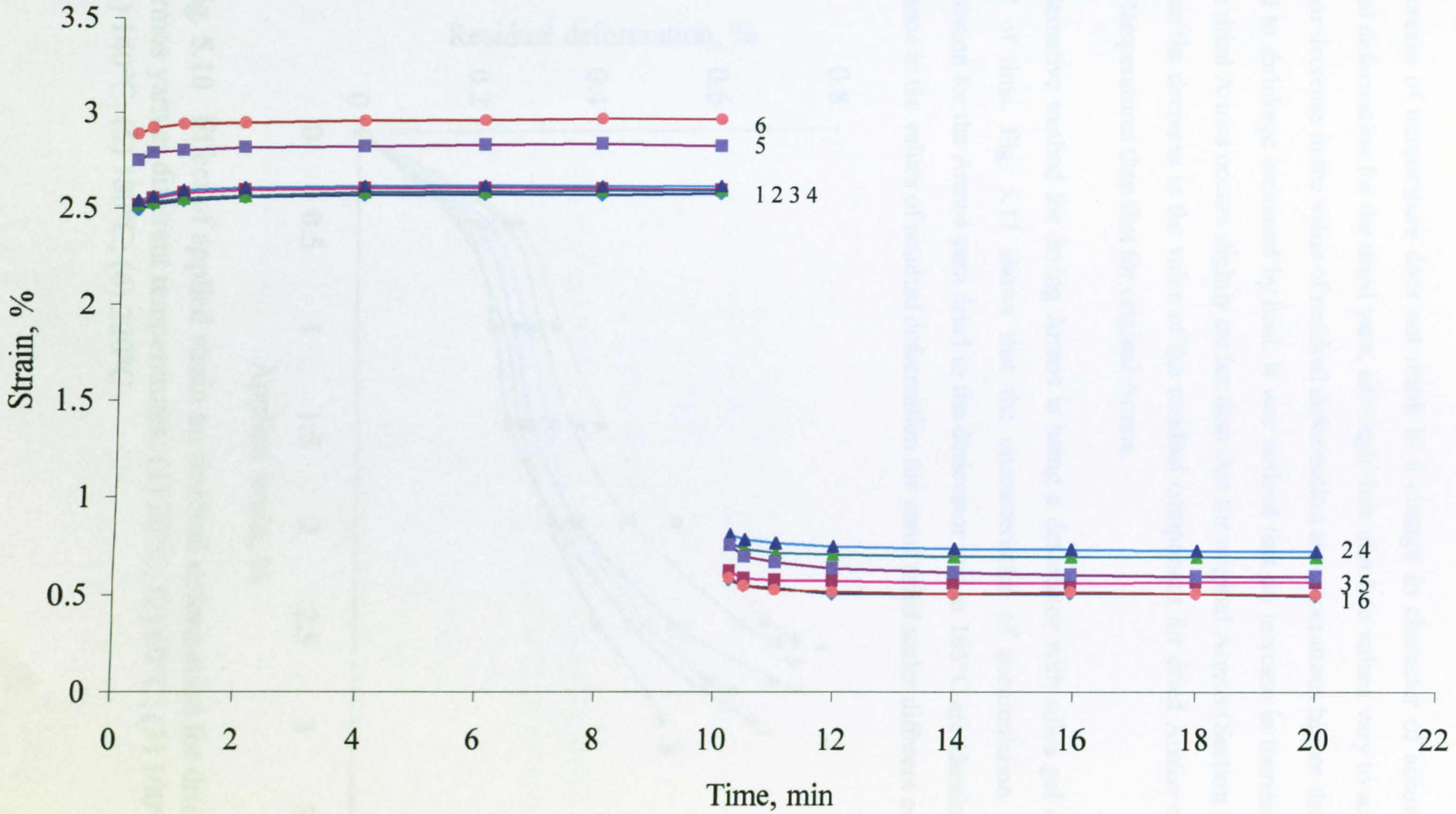

Fig. 5.9 Creep-recovery curves for dried Armos yarn at σ=2.52 GPa at different temperatures: (1) 20°C; (2) 60°C; (3) 100°C; (4) 140°C; (5) 180°C; (6) 220°C

An increase of temperature does not result in a change in character of accumulation of residual deformation for the dried yarn, although their absolute values vary to some degree. A minor decrease in the value of residual deformation at temperatures higher than 140°C is related to shrinkage increased by heat. It was noticed that an increase in thermal shrinkage for the dried Armos occurs slightly earlier than that for original Armos (Section 5.3.1). This explains the decrease in the value of the residual component for dried Armos occurring at lower temperatures than that for original Armos.

An alternative method for drying Armos is using a desiccator with silica gel over a long period of time. Fig. 5.11 shows that the characteristics of accumulation of residual deformation for the Armos yarn dried in the desiccator and at 105°C are identical. There is difference in the values of residual deformation for yarns dried under different conditions.

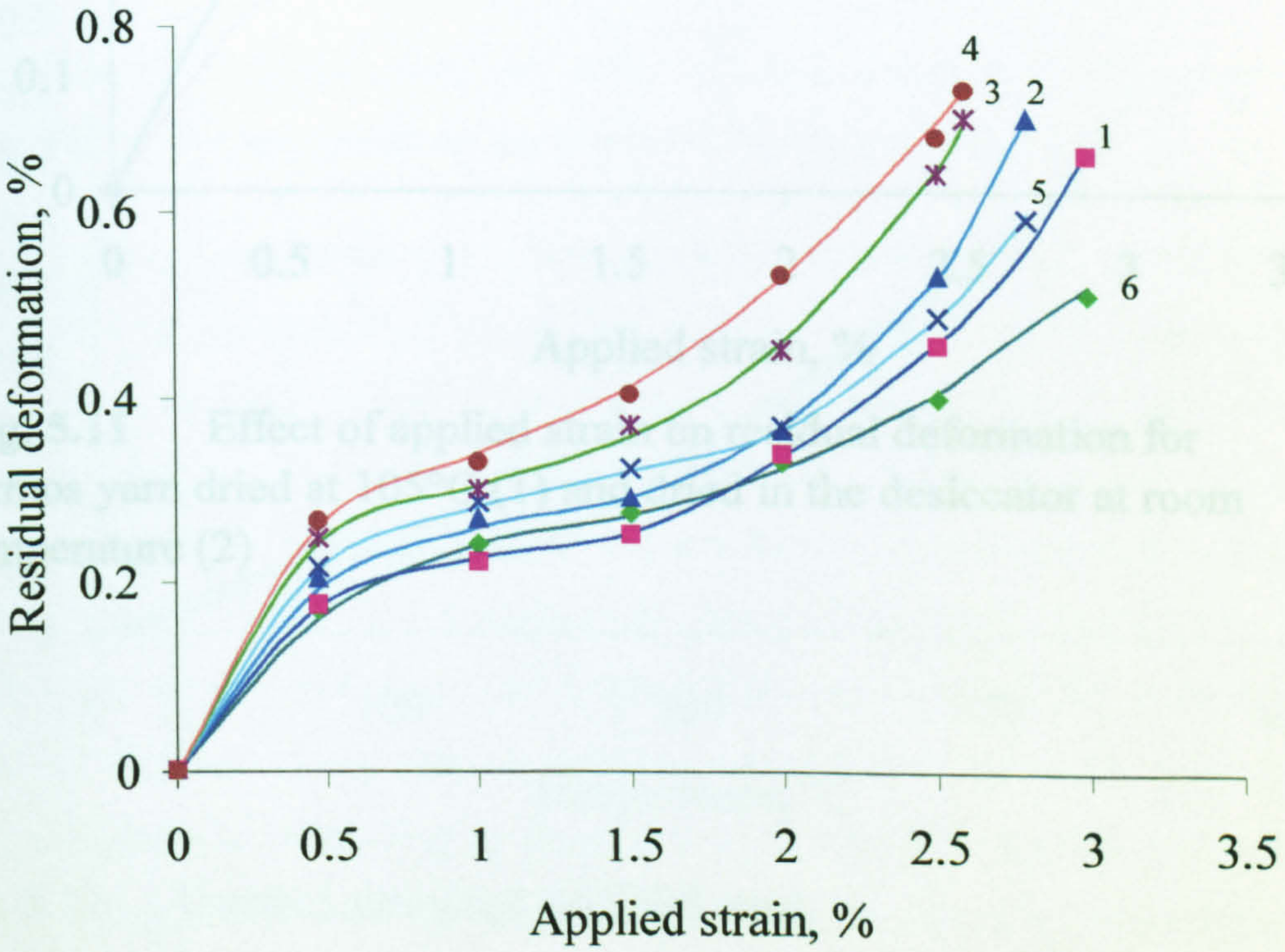

Fig. 5.10 Effect of applied strain on residual deformation for dried Armos yarn at different temperatures: (1) 20°C; (2) 60°C; (3) 100°C; (4) 140°C; (5) 180°C; (6) 220°C

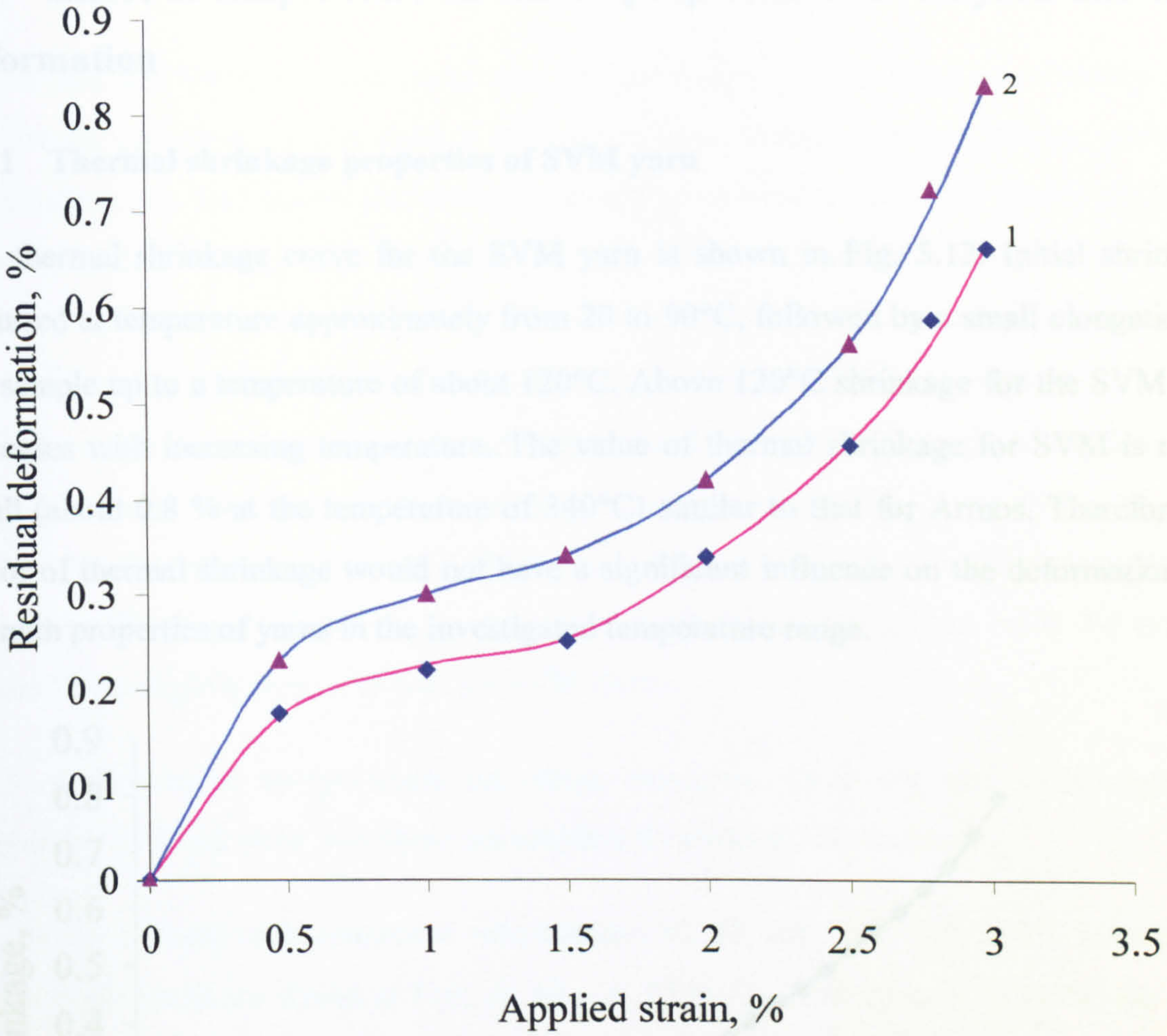

Fig. 5.11 Effect of applied strain on residual deformation for Armos yarn dried at 105°C (1) and dried in the desiccator at room temperature (2)

5.4 Effect of temperature on tensile properties of SVM yarn and their deformation

5.4.1 Thermal shrinkage properties of SVM yarn

The thermal shrinkage curve for the SVM yarn is shown in Fig. 5.12. Initial shrinkage occurred at temperature approximately from 20 to 90°C, followed by a small elongation of the sample up to a temperature of about 120°C. Above 120°C shrinkage for the SVM yarn increases with increasing temperature. The value of thermal shrinkage for SVM is rather small (about 0.8 % at the temperature of 340°C) similar to that for Armos. Therefore the factor of thermal shrinkage would not have a significant influence on the deformation and strength properties of yarns in the investigated temperature range.

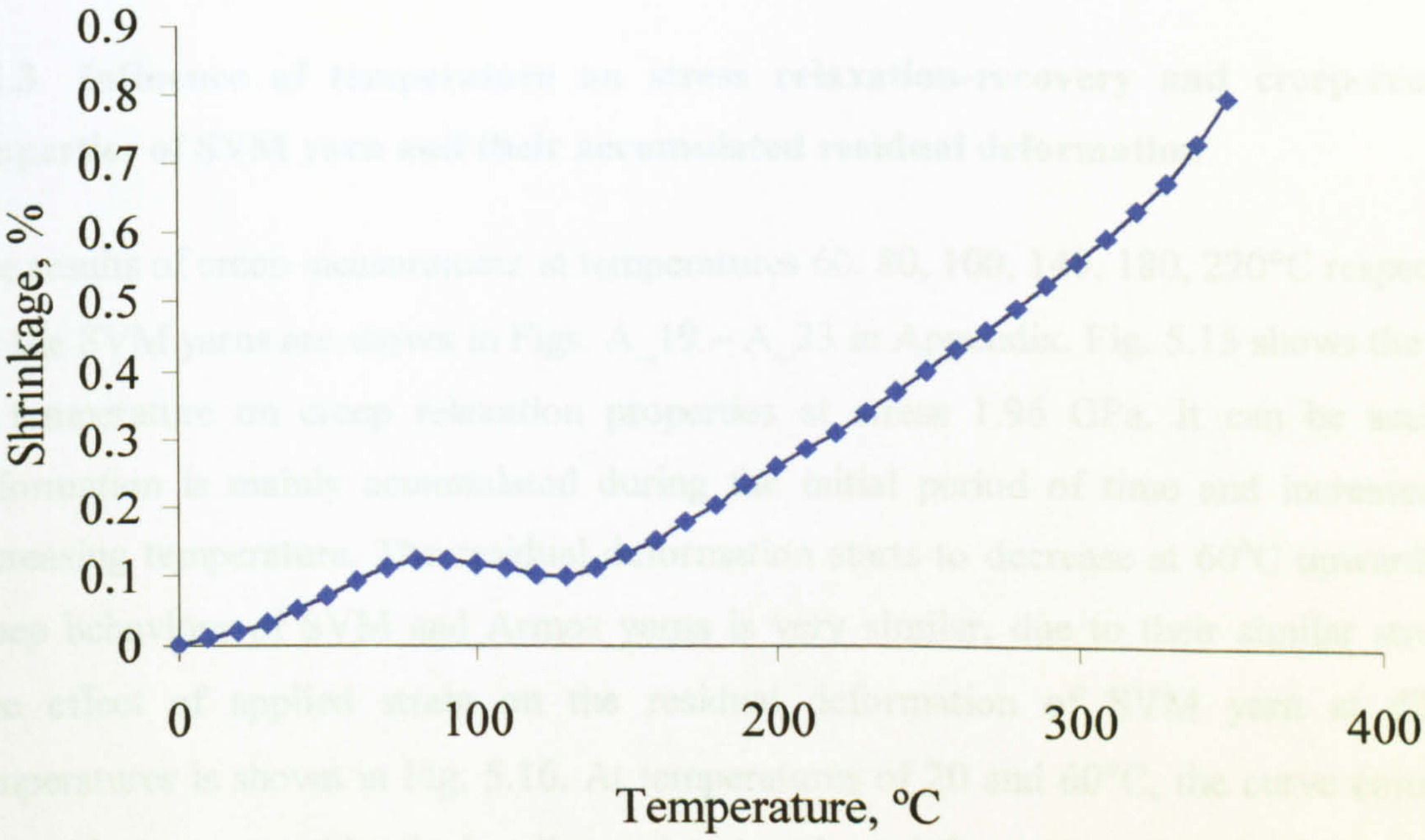

Fig. 5.12 Thermal shrinkage of SVM yarn

5.4.2 Effect of temperature on the stress-strain curves of SVM yarn

The Armos and SVM yarns in many respects are similar. Both fibres are obtained from rigid chain polymers, which have a semi-crystalline structure with a similar chemical constitution. Fig. 5.13 shows that the stress-strain properties of the SVM yarn is similar to that of Armos (see Fig. 5.2). There is a shoulder on the stress-strain curve of SVM at a strain of 1.5% at room temperature, but the shoulder reduces with increasing temperature. The strain-stress relationship obtained at the temperature of 220°C becomes almost linear. From the strain-stress curves at different temperatures, it is found that yarn strength and the break elongation decreases with increasing of temperature (Fig. 5.14). However, it is noticed that the breaking stress for SVM fibres is about 3.4 GPa, but for the Armos fibres is about 3.9 GPa (Figs. 5.2 and 5.13), thus the elongation and strength at break for original Armos fibres slightly surpasses that for SVM fibres.

5.4.3 Influence of temperature on stress relaxation-recovery and creep-recovery properties of SVM yarn and their accumulated residual deformation

The results of creep measurement at temperatures 60, 80, 100, 140, 180, 220°C respectively for the SVM yarns are shown in Figs. A_19 – A_23 in Appendix. Fig. 5.15 shows the effect of temperature on creep relaxation properties at stress 1.96 GPa. It can be seen that deformation is mainly accumulated during the initial period of time and increases with increasing temperature. The residual deformation starts to decrease at 60°C upwards. The creep behaviour of SVM and Armos yarns is very similar, due to their similar structure. The effect of applied strain on the residual deformation of SVM yarn at different temperatures is shown in Fig. 5.16. At temperatures of 20 and 60°C, the curve consists of two regions separated by the bending point at a given deformation of approximately 1.5%. At 80°C, the shape of the accumulation of residual deformation curve alters. This might be due to removal of moisture from the fibre. The decrease in the residual component of deformation at temperatures higher than 140°C could be related to thermal shrinkage occurring. It is also found that the character of accumulation of residual deformation for the original SVM yarn is very similar to that for the Armos yarn (see Fig. 5.6).

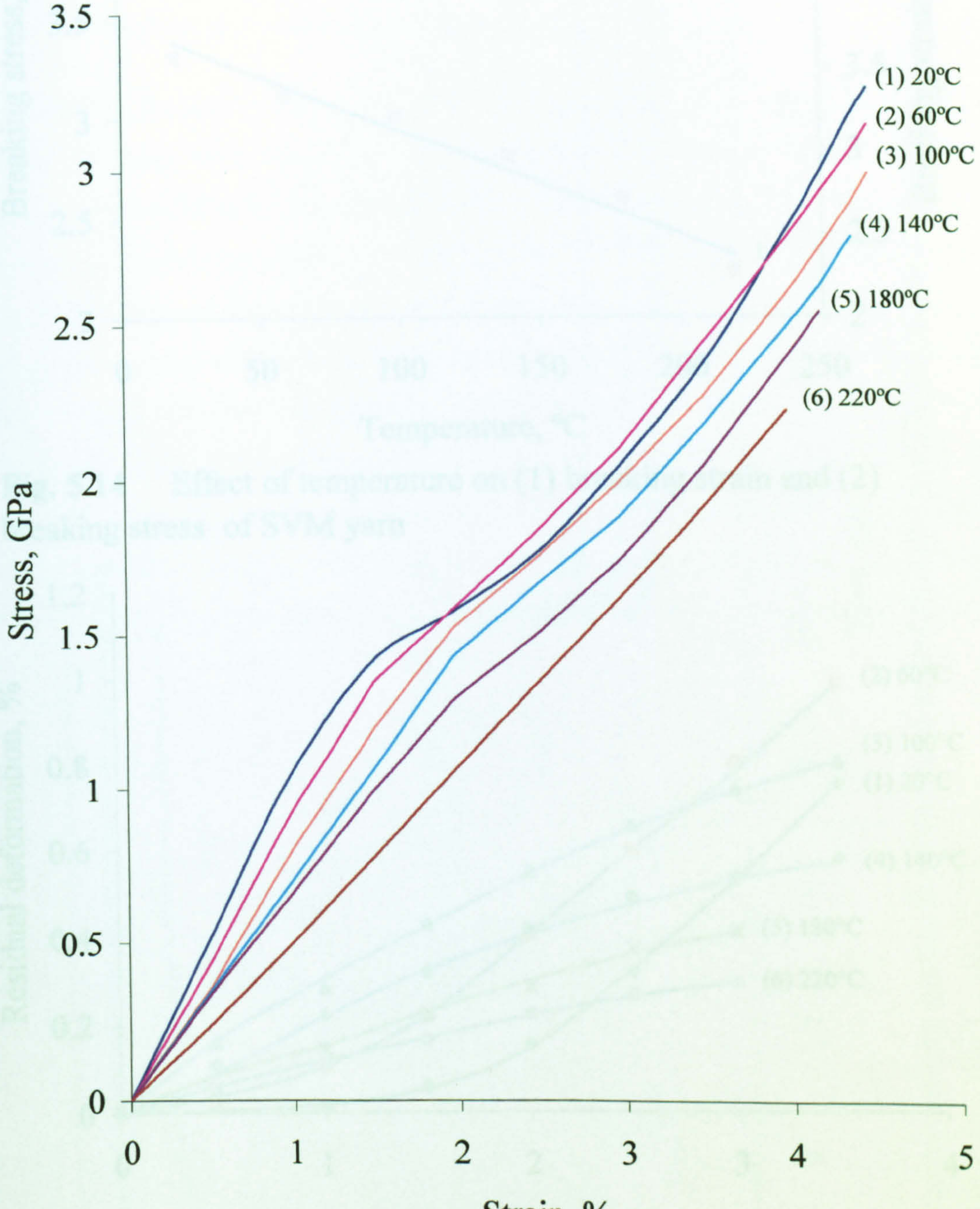

Fig. 5.13 Stress-strain curves of SVM yarn at different temperatures: (1) 20°C; (2) 60°C; (3) 100°C; (4) 140°C; (5) 180°C; (6) 220°C

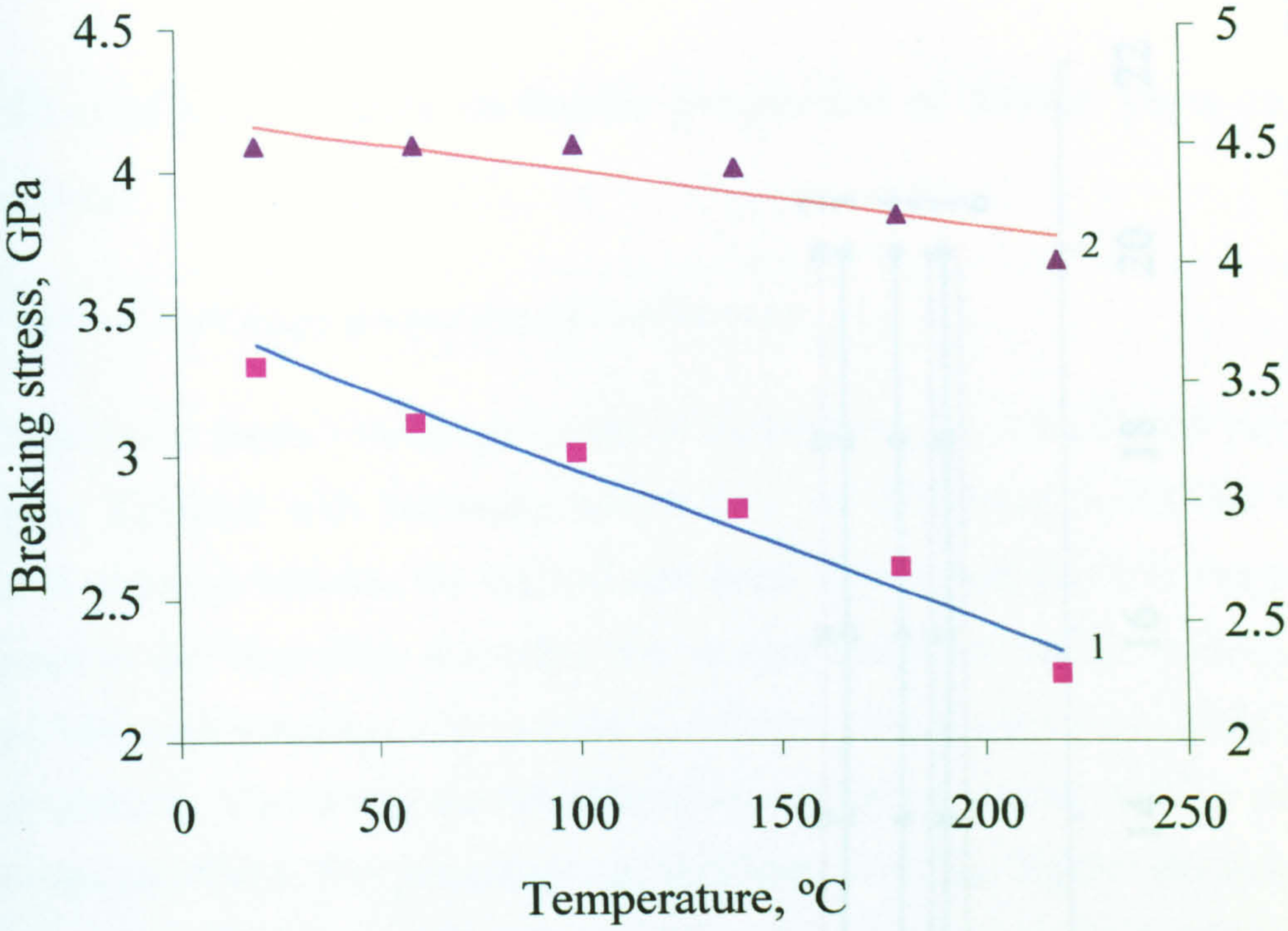

Fig. 5.14 Effect of temperature on (1) breaking strain and (2) breaking stress of SVM yarn

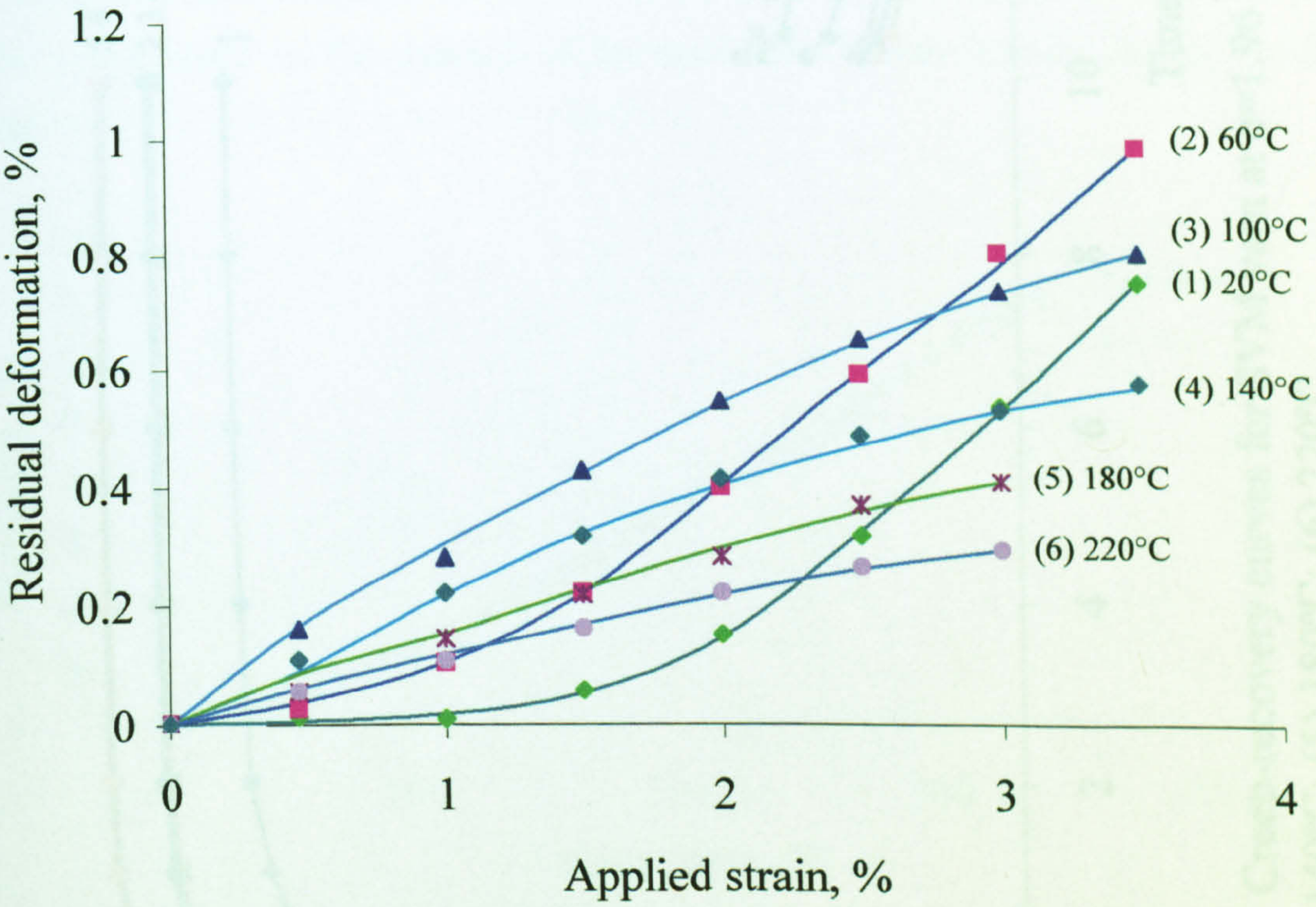

Fig. 5.16 Effect of applied strain on residual deformation for SVM yarn at different temperatures: (1) 20°C; (2) 60°C; (3) 100°C; (4) 140°C; (5) 180°C; (6) 220°C

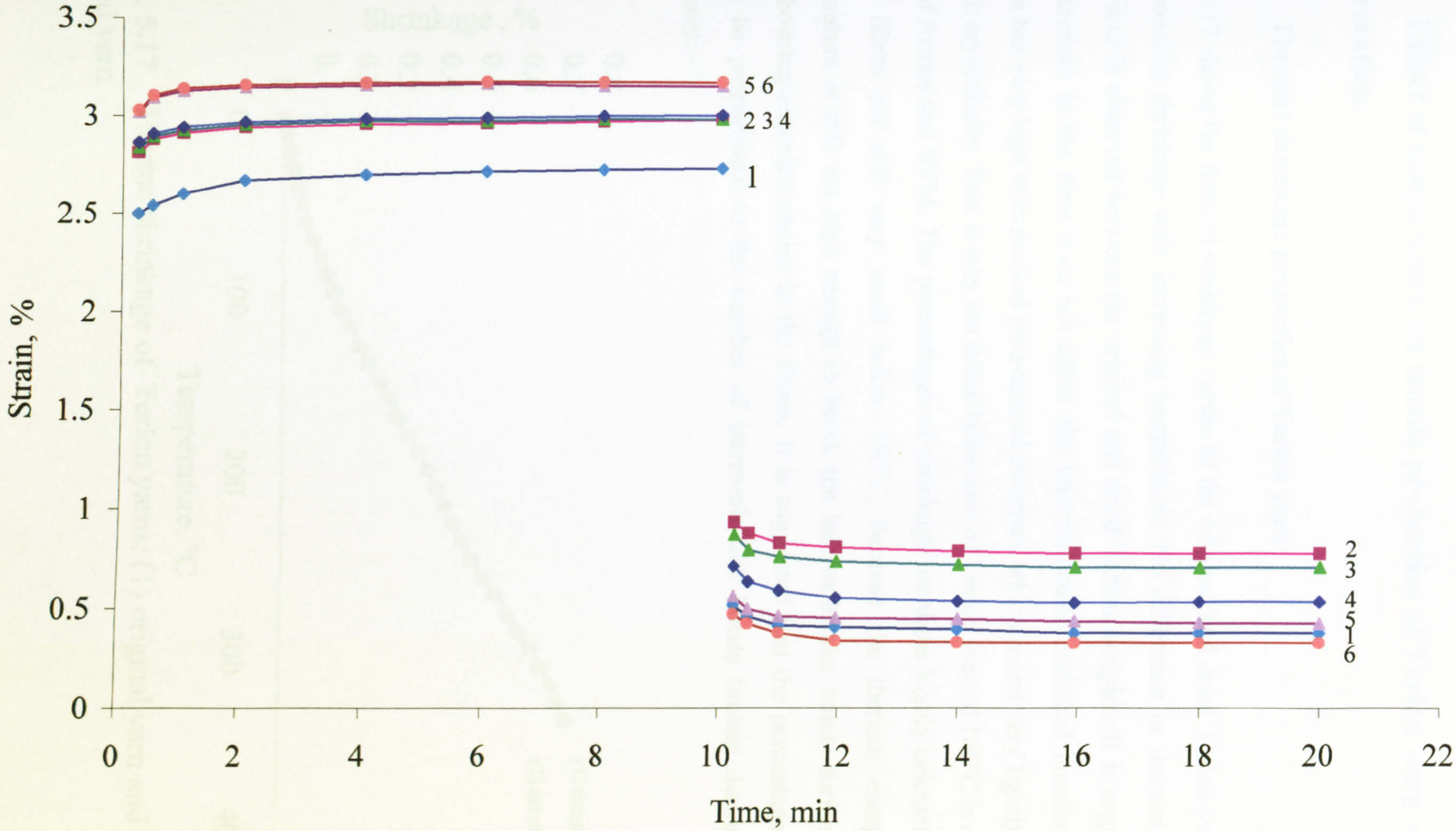

Fig. 5.15 Creep-recovery curves for SVM yarn at σ=1.96 GPa at different temperatures: (1) 20°C; (2) 60°C; (3) 100°C; (4) 140°C; (5) 180°C; (6) 220°C

5.5 Effect of temperature on tensile properties of Terlon yarn and their deformation

5.5.1 Thermal shrinkage properties of Terlon yarn

Fig. 5.17 shows the thermal shrinkage curves of the original and dried Terlon yarns. There is a constant shrinkage with increasing temperature. No difference in thermal shrinkage behaviour is observed between the original and dried Terlon samples. It is suggested that the moisture in the fibre does not affect the intermolecular chemical bonding, because Terlon has very high symmetrical para-aramid structure which packs very tightly and leads to high crystallinity. That is why the initial behaviour of Terlon around 100°C is different to that of Armos and SVM. The percentages of shrinkage for these highly oriented and rigid chain fibres are still very small below 350°C, because the thermal energy at that temperature is still not high enough to break the intermolecular bonds formed between neighbouring extended chains in the fibres. It is suggested that the percentage shrinkage might be proportional to the number of intermolecular bonds broken during the heat treatment.

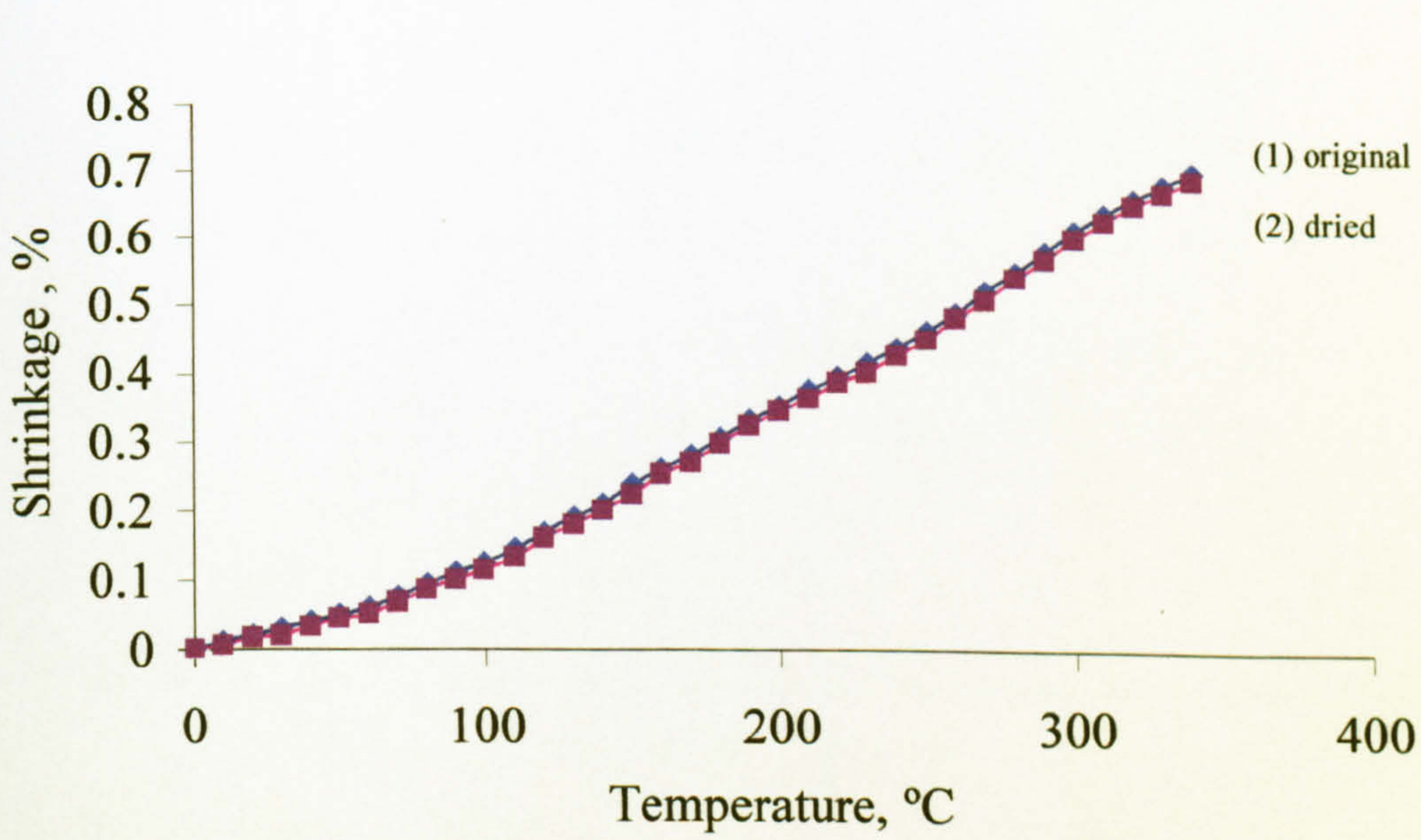

Fig. 5.17 Thermo shrinkage of Terlon yarns: (1) original yarn and (2) dried yarn

5.5.2 Effect of temperature on the stress-strain curves of Terlon yarn

The effect of temperature on the stress-strain properties of Terlon yarn is shown in Fig. 5.18. It can been seen that the stress-strain relationship of Terlon yarn at room temperature is almost linear as discussed in Section 3.3.1. With increasing temperature, the character of the stress-strain relationship does not change. However yarn breaking elongation and strength are decreased (Fig. 5.19). It is noticed that there is significantly decrease of strength when the temperature is increased to 80°C, thereafter further reduction in strength was more gradual. The strength reduction with increasing temperature might be due to the decrease in the number of polymer chains subjected to load as a result of destruction processes, and due to a change in the number of intermolecular bonds. The significant strength loss is observed at temperatures up to 80°C, but this temperature isn't high enough for the start of destruction processes. Therefore, partial breaking of intermolecular bonds might be a possible reason for strength and modulus loss. Terlon, Armos and SVM are all para-amides with high orientations, but it is found that their stress-strain curves are slightly different. The differences observed in the stress-strain relationship could be attributed to the fact that Terlon has very high level of crystallinity.

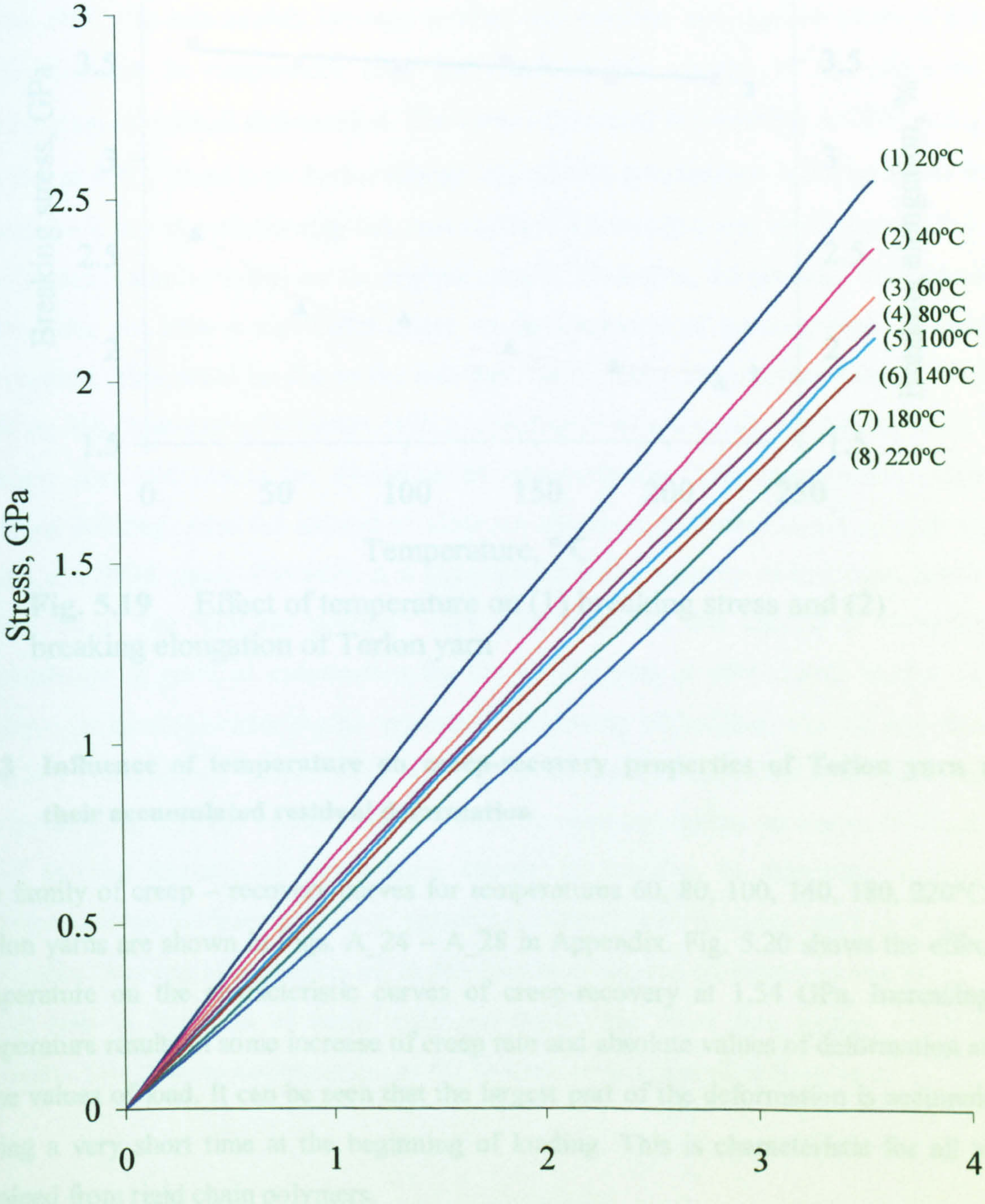

Fig. 5.18 Stress-strain curves of Terlon yarn at different temperatures: (1) 20°C; (2) 40°C; (3) 60°C; (4) 80°C; (5) 100°C; (6) 140°C; (7) 180°C; (8) 220°C

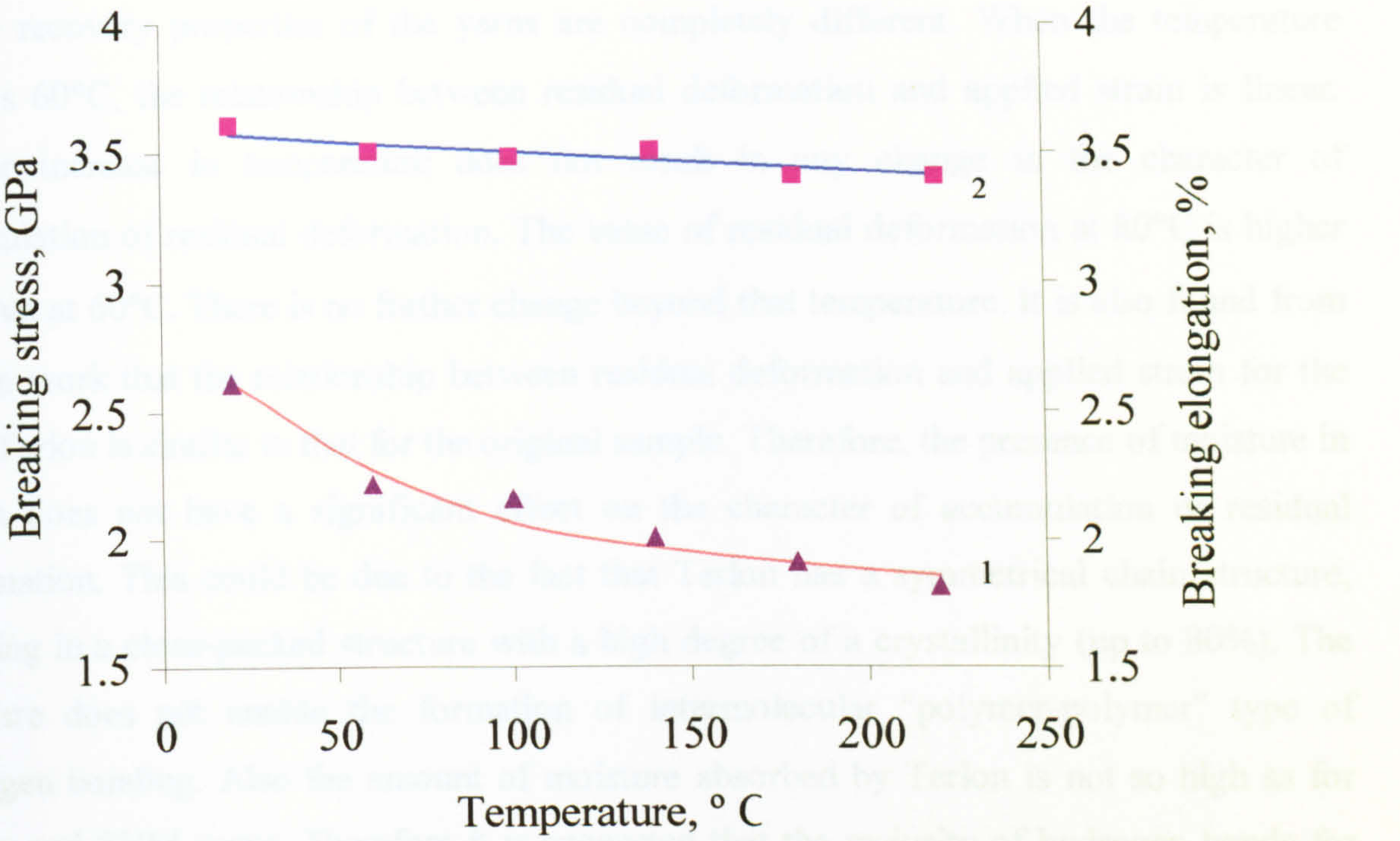

Fig. 5.19 Effect of temperature on (1) breaking stress and (2) breaking elongation of Terlon yarn

5.5.3 Influence of temperature on creep-recovery properties of Terlon yarn and their accumulated residual deformation

The family of creep – recovery curves for temperatures 60, 80, 100, 140, 180, 220°C for Terlon yarns are shown in Figs. A_24 – A_28 in Appendix. Fig. 5.20 shows the effect of temperature on the characteristic curves of creep-recovery at 1.54 GPa. Increasing of temperature results in some increase of creep rate and absolute values of deformation at the same values of load. It can be seen that the largest part of the deformation is accumulated during a very short time at the beginning of loading. This is characteristic for all yarns obtained from rigid chain polymers.

From the family of creep – recovery curves the relationship between of residual deformation and applied strain was obtained for different temperatures (Fig. 5.21). At room

temperature the character of accumulation of residual deformation for the Terlon yarn is very similar to that for the Armos and SVM yarns. However the influences of temperature on the recovery properties of the yarns are completely different. When the temperature reaches 60°C, the relationship between residual deformation and applied strain is linear. Further increase in temperature does not result in any change in the character of accumulation of residual deformation. The value of residual deformation at 80°C is higher than that at 60°C. There is no further change beyond that temperature. It is also found from present work that the relationship between residual deformation and applied strain for the dried Terlon is similar to that for the original sample. Therefore, the presence of moisture in Terlon does not have a significant effect on the character of accumulation of residual deformation. This could be due to the fact that Terlon has a symmetrical chain structure, resulting in a close-packed structure with a high degree of a crystallinity (up to 80%). The moisture does not enable the formation of intermolecular "polymer-polymer" type of hydrogen bonding. Also the amount of moisture absorbed by Terlon is not so high as for Armos and SVM yarns. Therefore it is suggested that the majority of hydrogen bonds for Terlon are of the "polymer-polymer" type. The cause of this change in character of accumulation of residual deformation for the Terlon yarn at 60°C could be due to the breakage of intermolecular bonds; unobstructed moving of building blocks; and fixation them in a new position. Beliaev *et al.*, (1978) has shown that individual hydrogen bonds in crystalline polymers are much weaker than in a semi-crystalline structure. It should be noted that an increase of temperature causes an increase in segmental motility in amorphous areas. Such an increase of segmental motility with load can result in an increase of distance between macromolecules in amorphous areas, and in intermolecular areas. This would lead to breakage of some hydrogen bonds and more free sliding of structure elements. This leads to accumulation of the residual component of deformation.

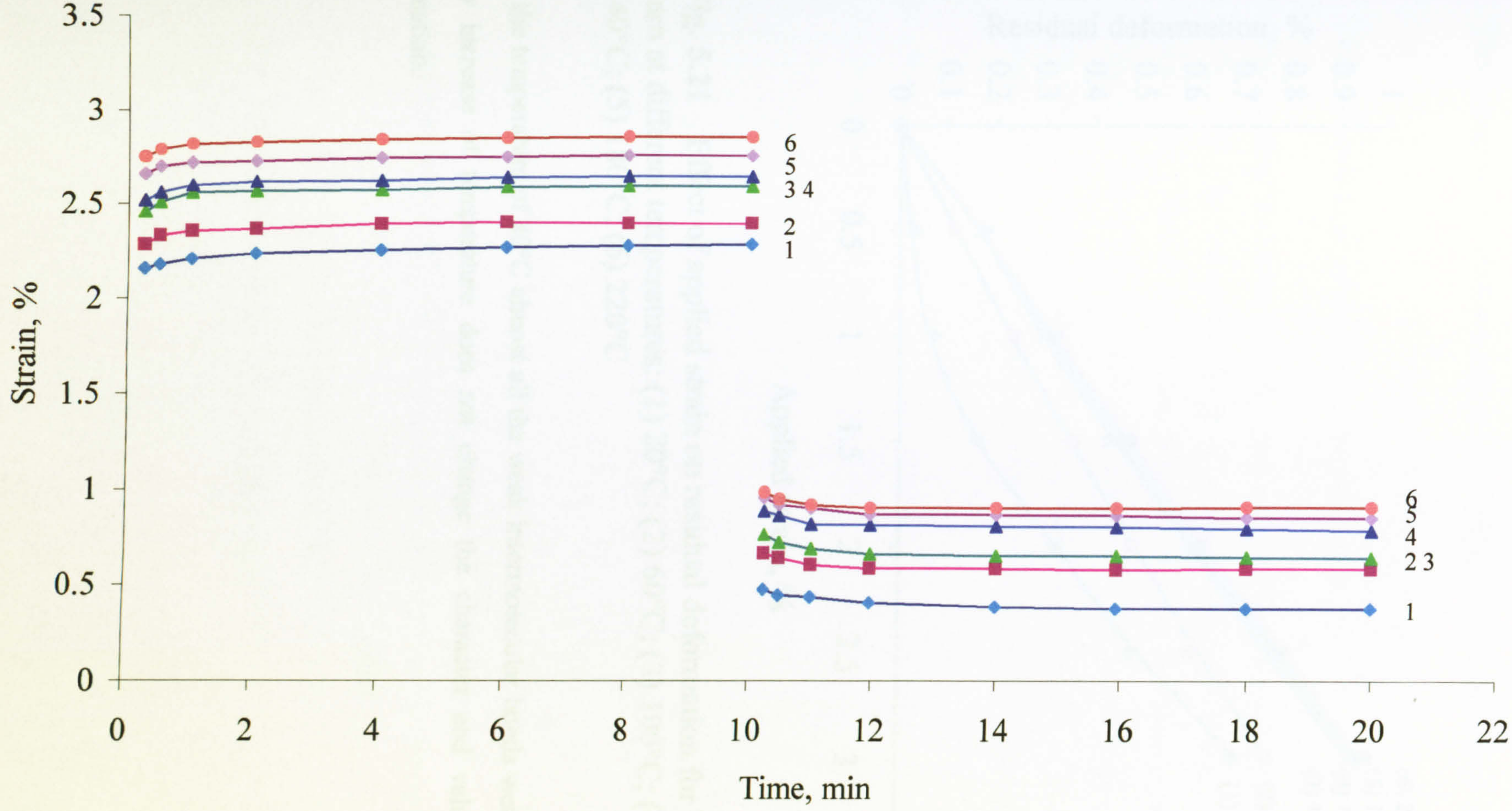

Fig. 5.20 Creep-recovery curves for Terlon yarn at σ=1.54 GPa at different temperatures: (1) 20°C; (2) 60°C; (3) 100°C; (4) 140°C; (5) 180°C; (6) 220°C

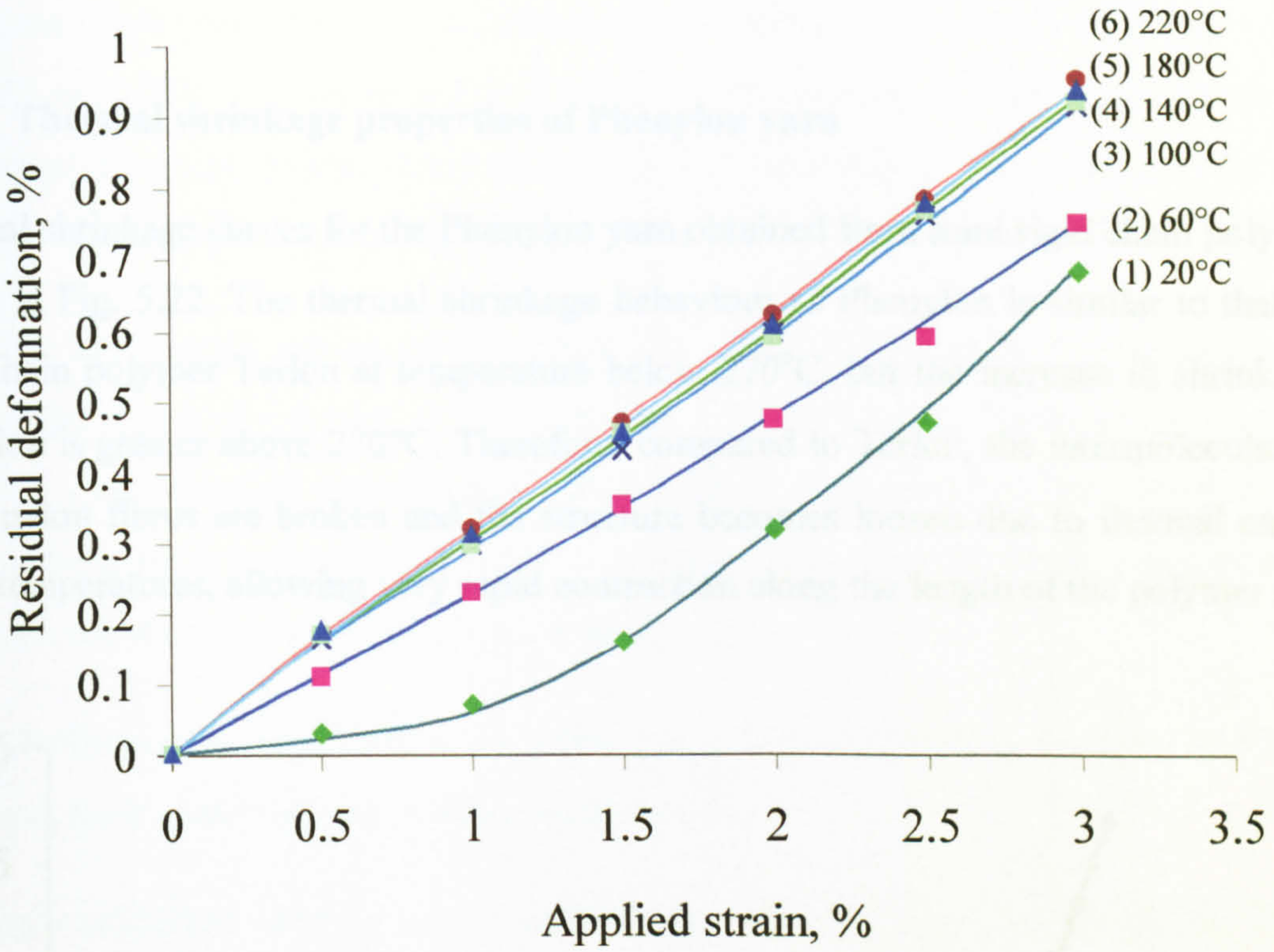

Fig. 5.21 Effect of applied strain on residual deformation for Terlon yarn at different temperatures: (1) 20°C; (2) 60°C; (3) 100°C; (4) 140°C; (5) 180°C; (6) 220°C

Up to the temperature of 80°C almost all the weak intermolecular bonds were broken. The further increase of temperature does not change the character and value of residual deformation.

5.6 The change of deformation and strength properties of Phenylon yarn

5.6.1 Thermal shrinkage properties of Phenylon yarn

Thermal shrinkage curves for the Phenylon yarn obtained from semi rigid chain polymers is shown in Fig. 5.22. The thermal shrinkage behaviour of Phenylon is similar to that of the rigid chain polymer Terlon at temperature below 270°C, but the increase in shrinkage for Phenylon is greater above 270°C. Therefore, compared to Terlon, the intermolecular bonds in Phenylon fibres are broken and the structure becomes loosen due to thermal energy at lower temperatures, allowing very rapid contraction along the length of the polymer chain.

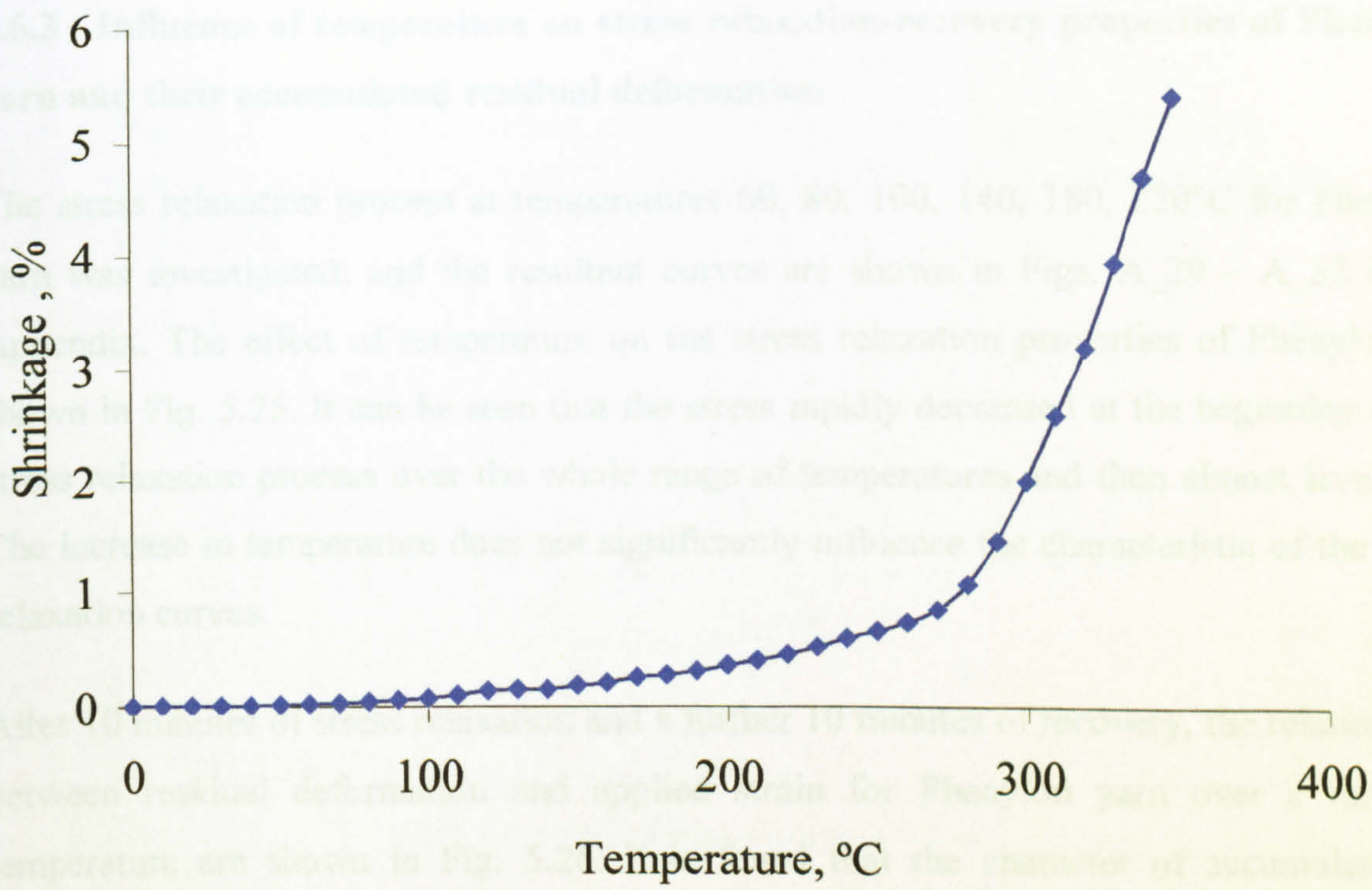

Fig. 5.22 Thermo shrinkage of Phenylon yarn

5.6.2 Effect of temperature on the stress-strain curves of Phenylon yarn

The stress-strain properties for the Phenylon yarn measured at temperatures 20, 60, 100, 140, 180 and 220°C are shown in Fig. 5.23. It is found that an increase in temperature does not change the characteristic shape of the stress-strain curves. The curves can be divided into two regions defined by the turning point at a strain of approximately 5%.

From the stress-strain curves of Phenylon, the effect of increasing temperature on yarn strength and break elongation is shown in Fig. 5.24. It is shown that the strength of the Phenylon yarn decreases significantly with increasing temperature. The reduction of yarn strength from room temperature to 220°C is about 35%. But the break elongation of the yarn does not show any dependence on temperature.

5.6.3 Influence of temperature on stress relaxation-recovery properties of Phenylon yarn and their accumulated residual deformation

The stress relaxation process at temperatures 60, 80, 100, 140, 180, 220°C for Phenylon yarn was investigated, and the resultant curves are shown in Figs. A_29 – A_33 in the Appendix. The effect of temperature on the stress relaxation properties of Phenylon are shown in Fig. 5.25. It can be seen that the stress rapidly decreased at the beginning of the stress relaxation process over the whole range of temperatures and then almost levels off. The increase in temperature does not significantly influence the characteristic of the stress relaxation curves.

After 10 minutes of stress relaxation and a further 10 minutes of recovery, the relationships between residual deformation and applied strain for Phenylon yarn over a range of temperature are shown in Fig. 5.26. It is found that the character of accumulation of residual deformation does not change at high temperatures. As indicated earlier, the structure of the Phenylon is not very oriented. Therefore, the mechanism of deformation for

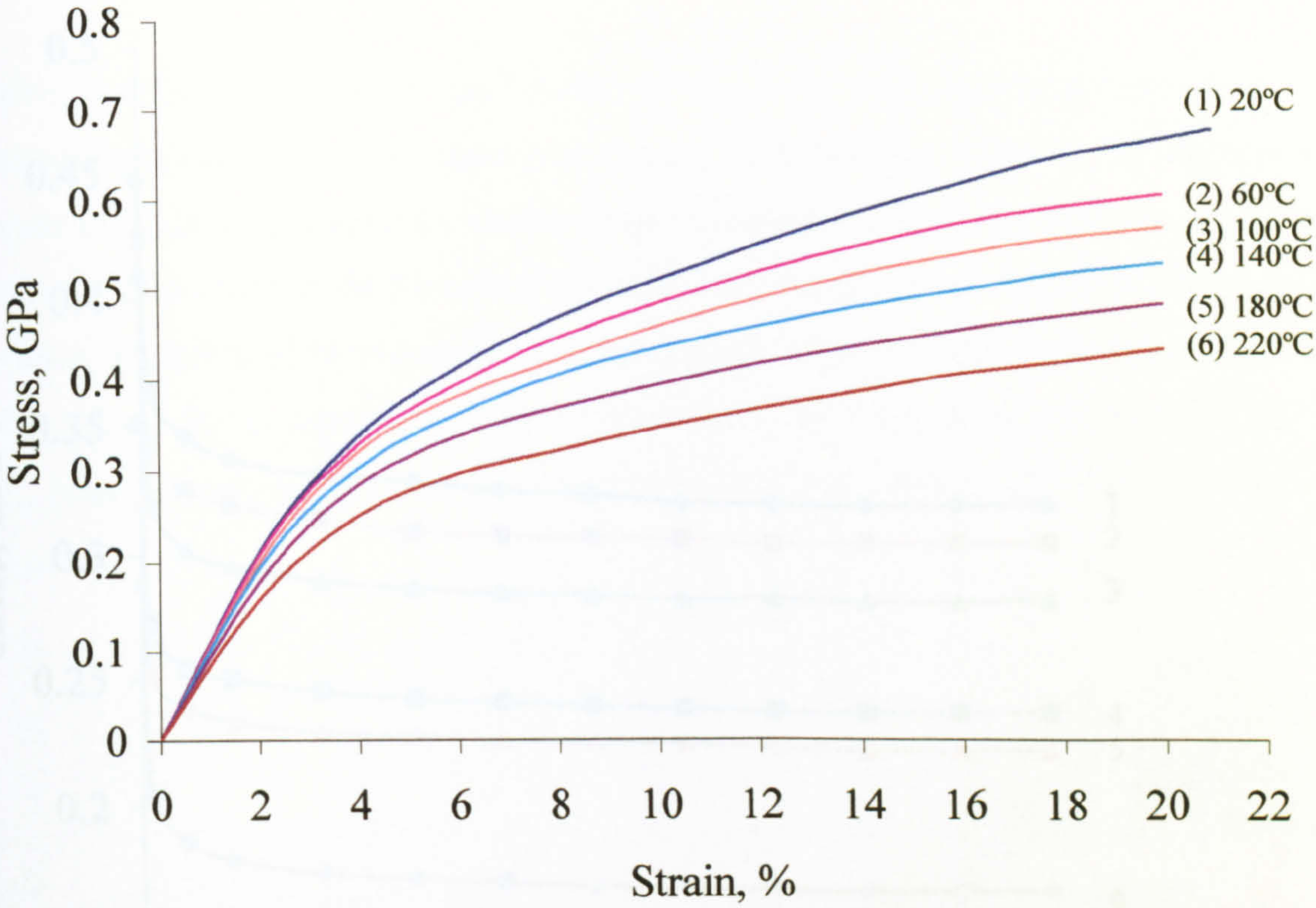

Fig. 5.23 Stress-strain curves of Phenylon yarn at different temperatures: (1) 20°C; (2) 60°C; (3) 100°C; (4) 140°C; (5) 180°C; (6) 220°C

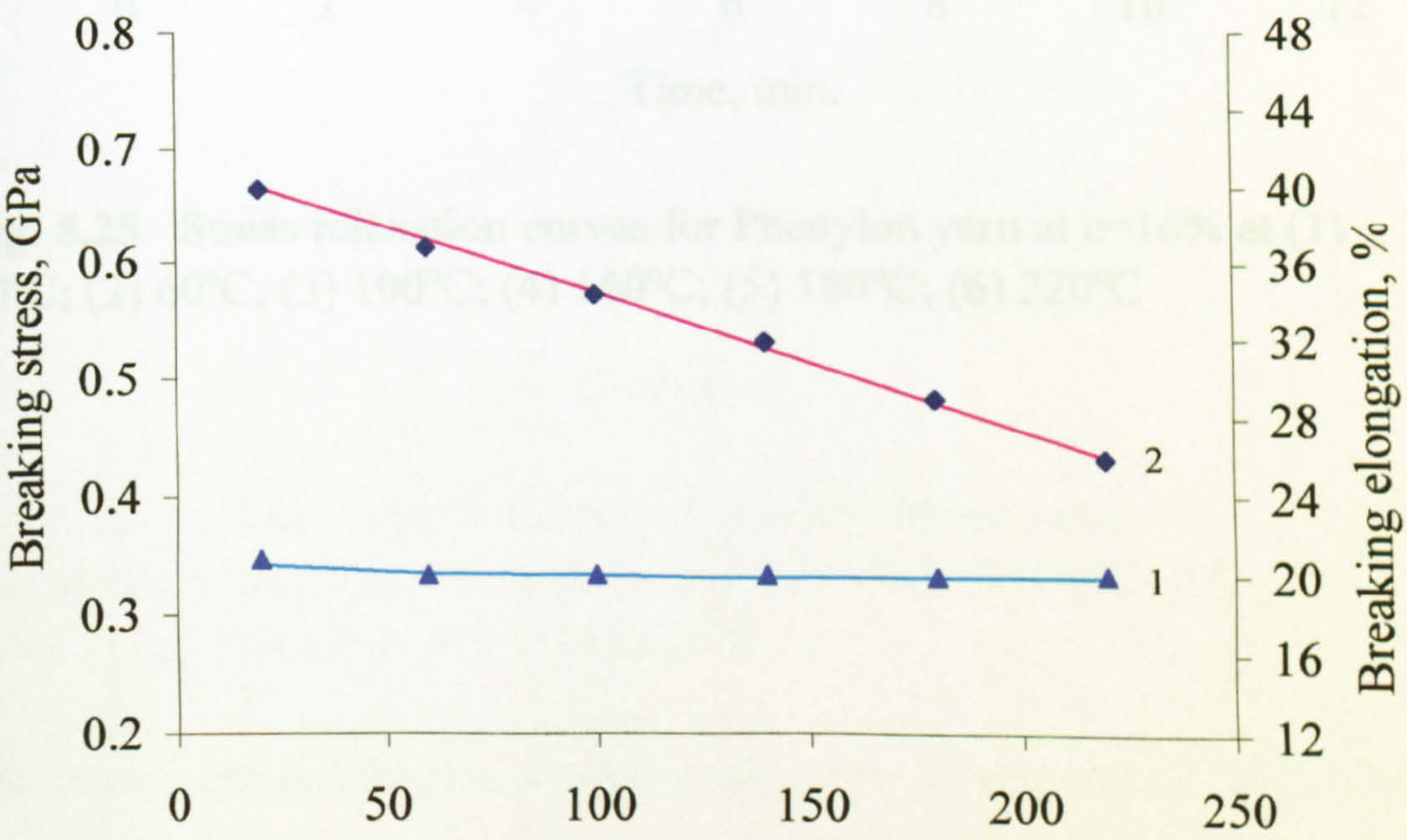

Fig. 5.24 Effect of temperature on (1) breaking elongation and (2) breaking stress of Phenylon yarn

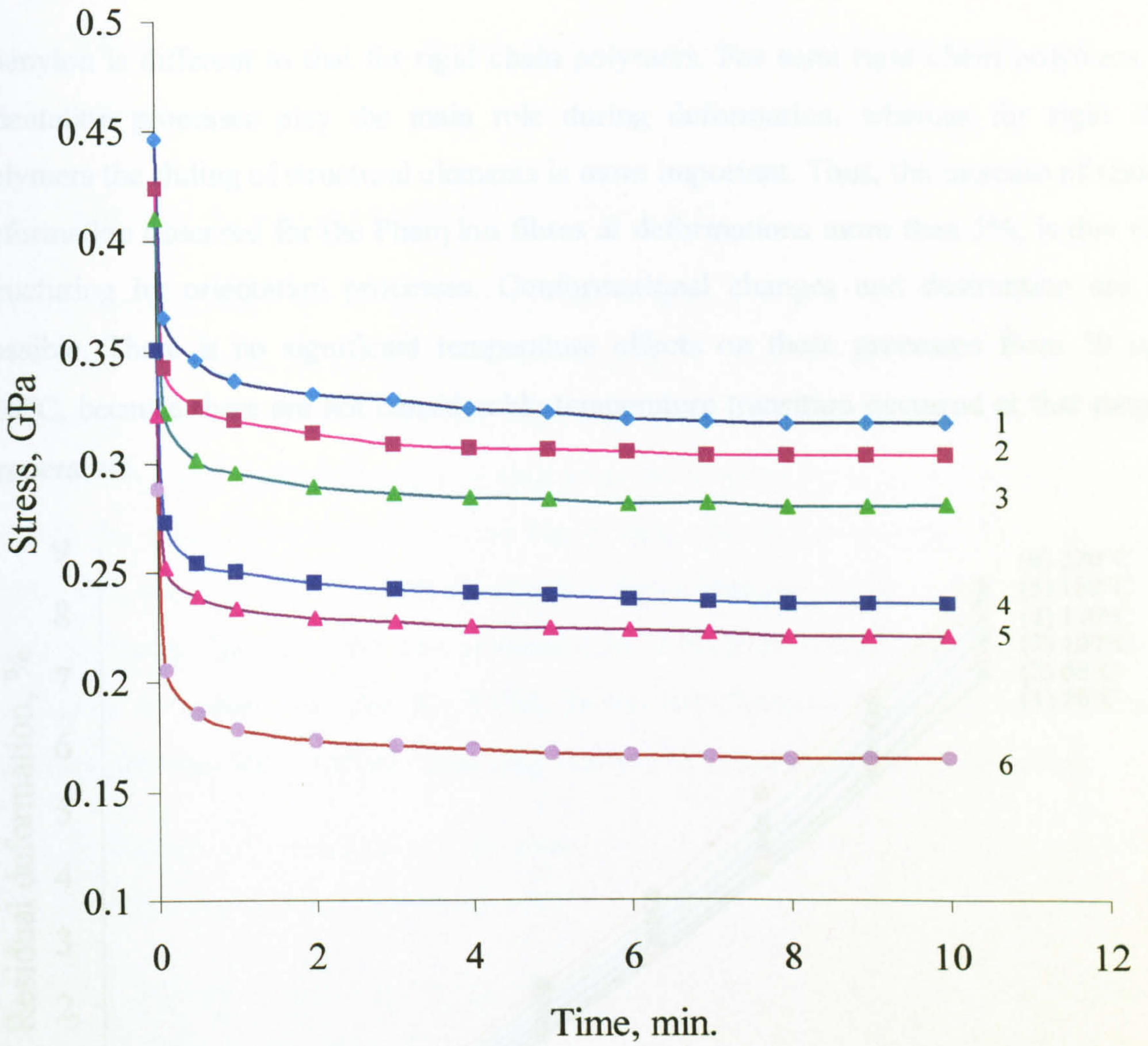

Fig. 5.25 Stress relaxation curves for Phenylon yarn at ε=16% at (1) 20°C; (2) 60°C; (3) 100°C; (4) 140°C; (5) 180°C; (6) 220°C

Phenylon is different to that for rigid chain polymers. For semi rigid chain polymers, the orientation processes play the main role during deformation, whereas for rigid chain polymers the sliding of structural elements is more important. Thus, the increase of residual deformation observed for the Phenylon fibres at deformations more than 5%, is due to re-structuring by orientation processes. Conformational changes and destruction are also possible. There is no significant temperature effects on these processes from 20 up to 220°C, because there are not considerable temperature transition occurred at that range of temperature.

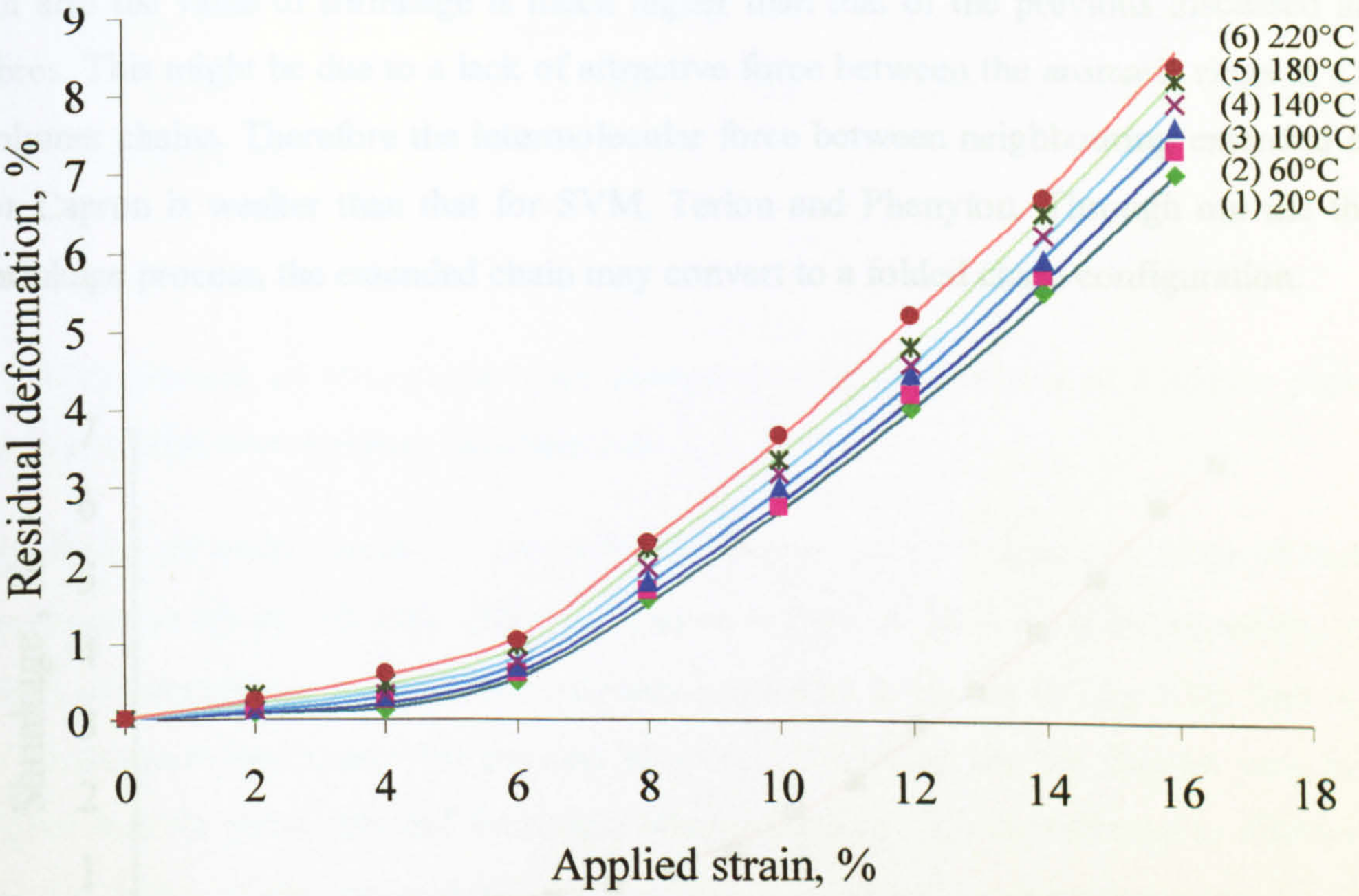

Fig. 5.26 Effect of applied strain on residual deformation for Phenylon yarn at different temperatures: (1) 20°C; (2) 60°C; (3) 100°C; (4) 140°C; (5) 180°C; (6) 220°C

It is also thought that the Phenylon yarn has a rather loose surface structure. An appreciable amount of moisture is present on the surface of the fibre and is easily removed and therefore does not have a significant influence on the intermolecular interaction of a fibre.

5.7 Effect of temperature on tensile properties of Capron yarn and their deformation

5.7.1 Thermal shrinkage properties of Capron yarn

The thermal shrinkage curve for Capron yarn is shown in Fig. 5.27. It is found that the percentage of shrinkage for Capron yarn increases quite significantly with increasing temperature, compared to the thermal shrinkage behaviour of aromatic polyamide yarns. Not only does the marked increase in shrinkage for Capron occur at a lower temperature, but also the value of shrinkage is much higher than that of the previous discussed aramid fibres. This might be due to a lack of attractive force between the aromatic rings in Capron polymer chains. Therefore the intermolecular force between neighbouring extended chains for Capron is weaker than that for SVM, Terlon and Phenylon. Through out the thermal shrinkage process, the extended chain may convert to a folded chain configuration.

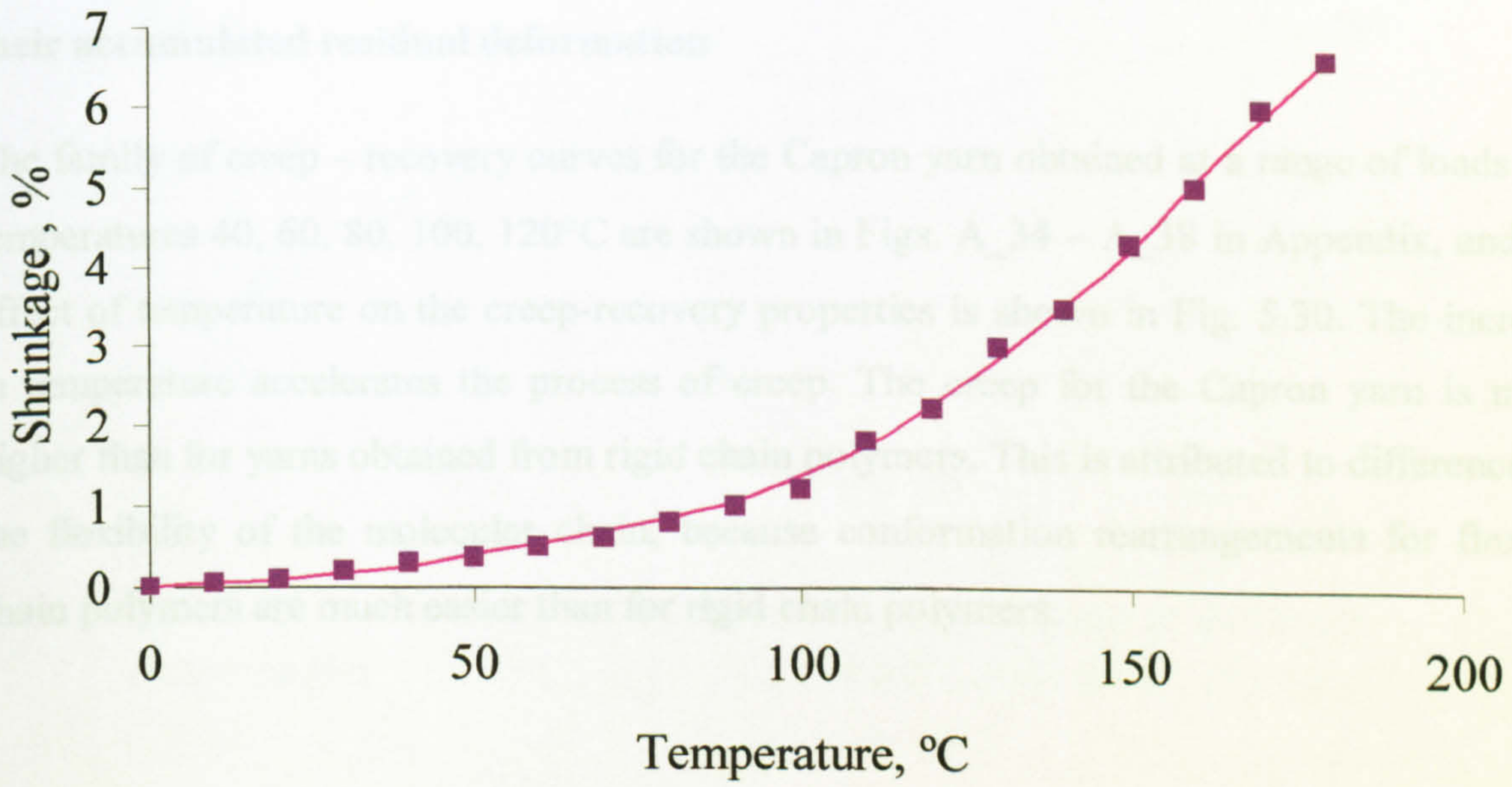

Fig. 5.27 Termo-mechanical curve of Capron yarn

5.7.2 Effect of temperature on the stress-strain curves of Capron yarn

The stress-strain curves of Capron yarn at temperatures 20, 40, 60, 80, 100 and 120°C are shown in Fig. 5.28. The stress-strain properties for Capron yarns at room temperature have been discussed in Section 3.5.1. With increasing temperature, the characteristic shape of the curve is retained to a temperature of 100°C, but shows a lower modulus and become almost linear at about 120°C. This might be due to an increase in the motility of chain segments at temperatures above 120°C. Fig. 5.29 shows that breaking stress of Capron yarn decreases over the range of temperature between 100°C and 120°C. At 120°C the strength decreases by approximately 50%. It is suggested that this is related to mechanical-destruction processes occurring as a result of heating. But the break elongation increases with increasing temperature.

5.7.3 Influence of temperature on creep-recovery properties of Capron yarn and their accumulated residual deformation

The family of creep – recovery curves for the Capron yarn obtained at a range of loads and temperatures 40, 60, 80, 100, 120°C are shown in Figs. A_34 – A_38 in Appendix, and the effect of temperature on the creep-recovery properties is shown in Fig. 5.30. The increase in temperature accelerates the process of creep. The creep for the Capron yarn is much higher than for yarns obtained from rigid chain polymers. This is attributed to differences in the flexibility of the molecular chain, because conformation rearrangements for flexible chain polymers are much easier than for rigid chain polymers.

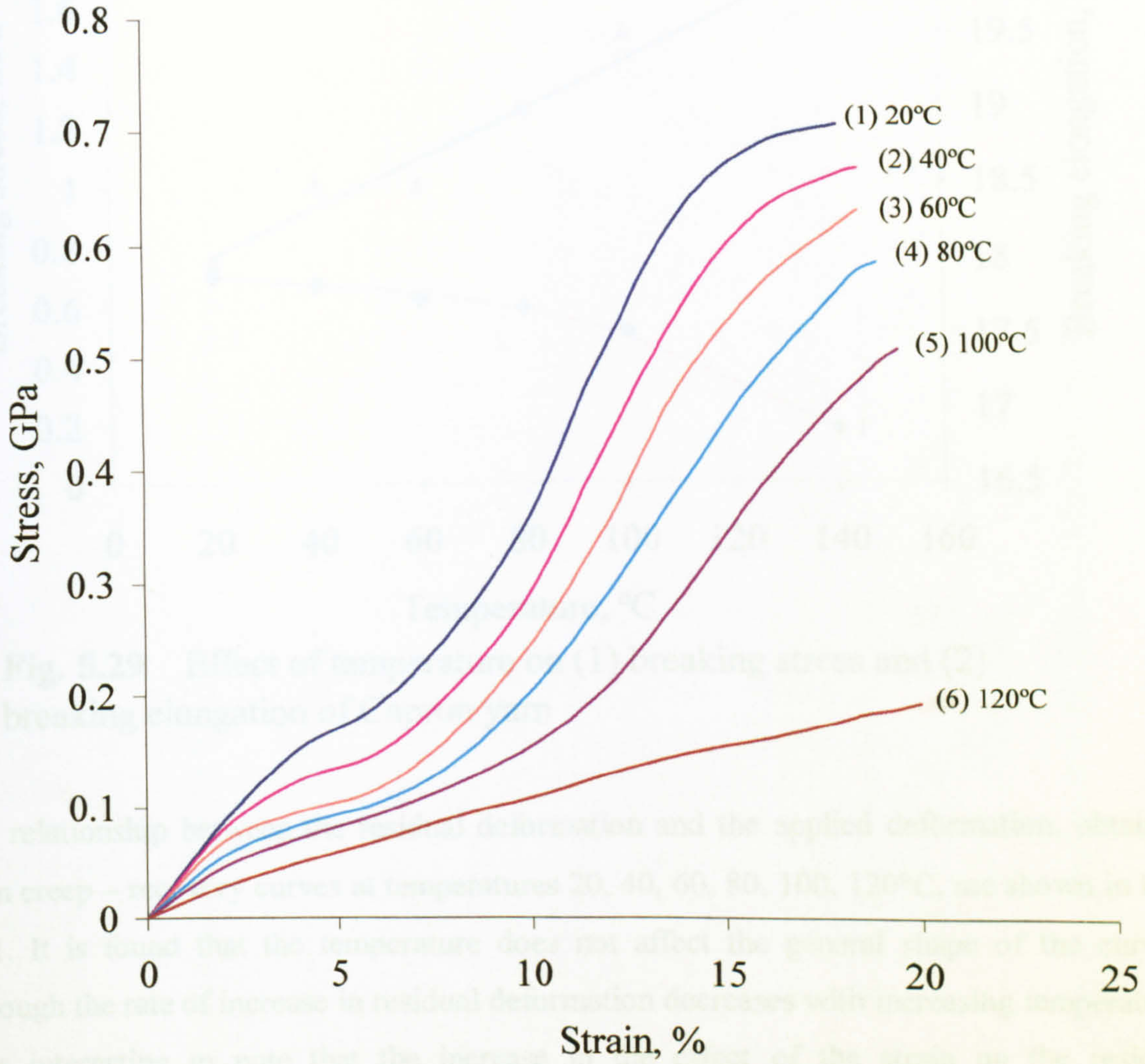

Fig. 5.28 Stress-strain curves of Capron yarn at different temperatures: (1) 20°C; (2) 40°C; (3) 60°C; (4) 80°C; (5) 100°C; (6) 120°C

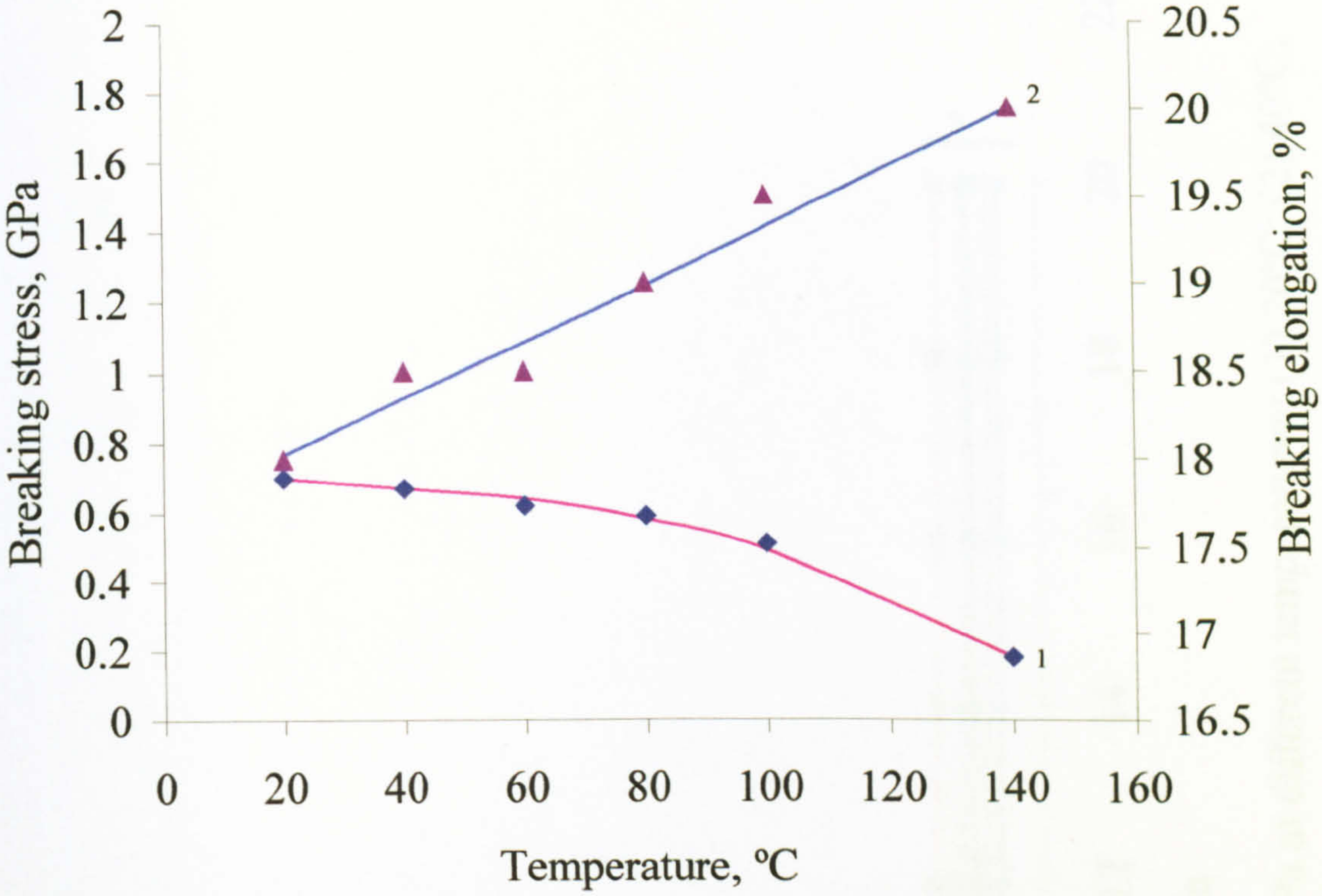

Fig. 5.29 Effect of temperature on (1) breaking stress and (2) breaking elongation of Capron yarn

The relationship between the residual deformation and the applied deformation, obtained from creep – recovery curves at temperatures 20, 40, 60, 80, 100, 120°C, are shown in Fig. 5.31. It is found that the temperature does not affect the general shape of the curves, although the rate of increase in residual deformation decreases with increasing temperature. It is interesting to note that the increase in the effect of the strain on the residual deformation begins at a bent 10-11% in all cases. Therefore, temperatures up to 120°C influence the value of the residual component rather than the nature of its accumulation.

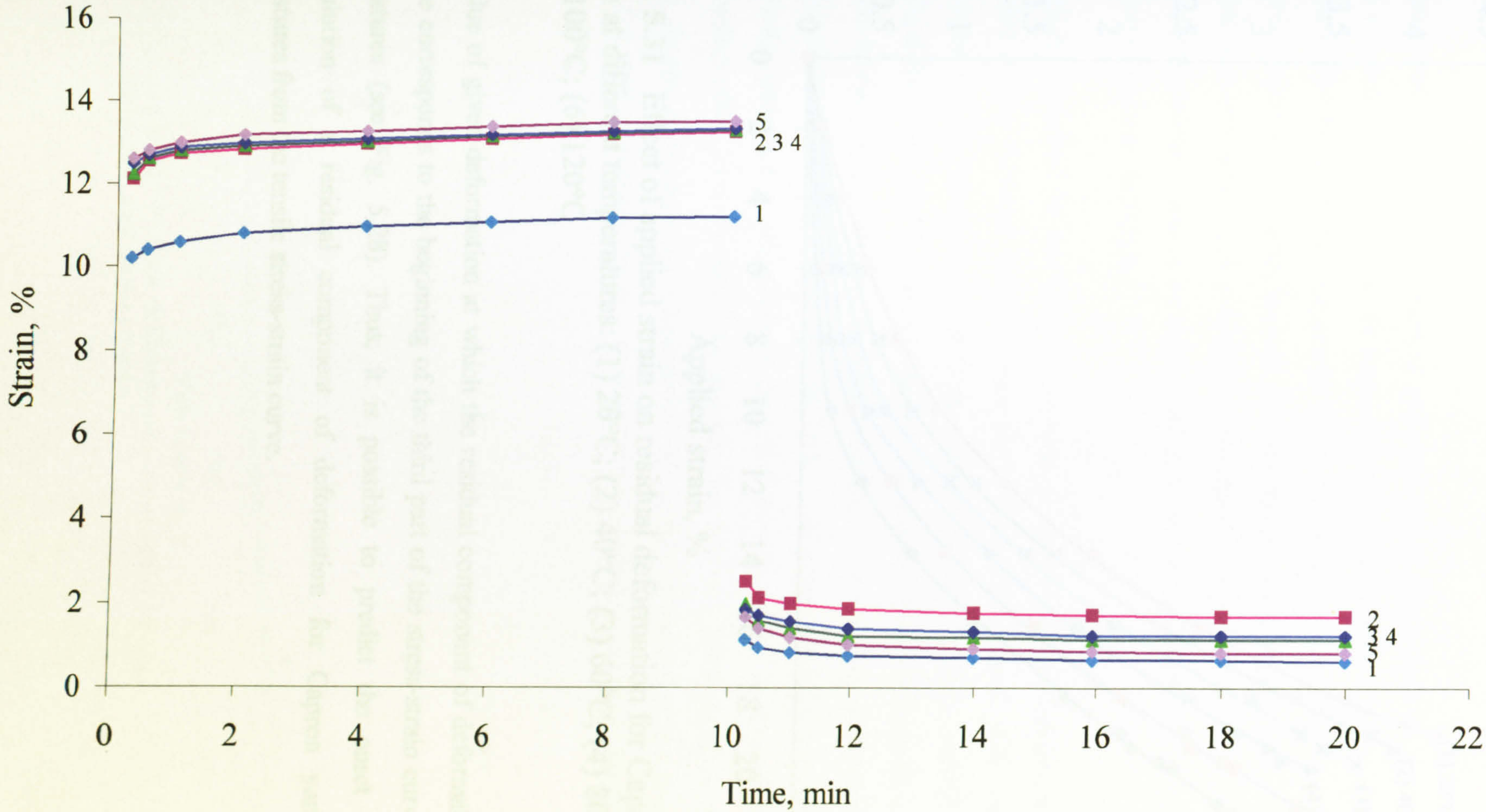

Fig. 5.30 Creep-recovery curves for Capron yarn at σ=0.49 GPa at different temperatures: (1) 20°C; (2) 40°C; (3) 60°C; (4) 80°C; (5) 100°C

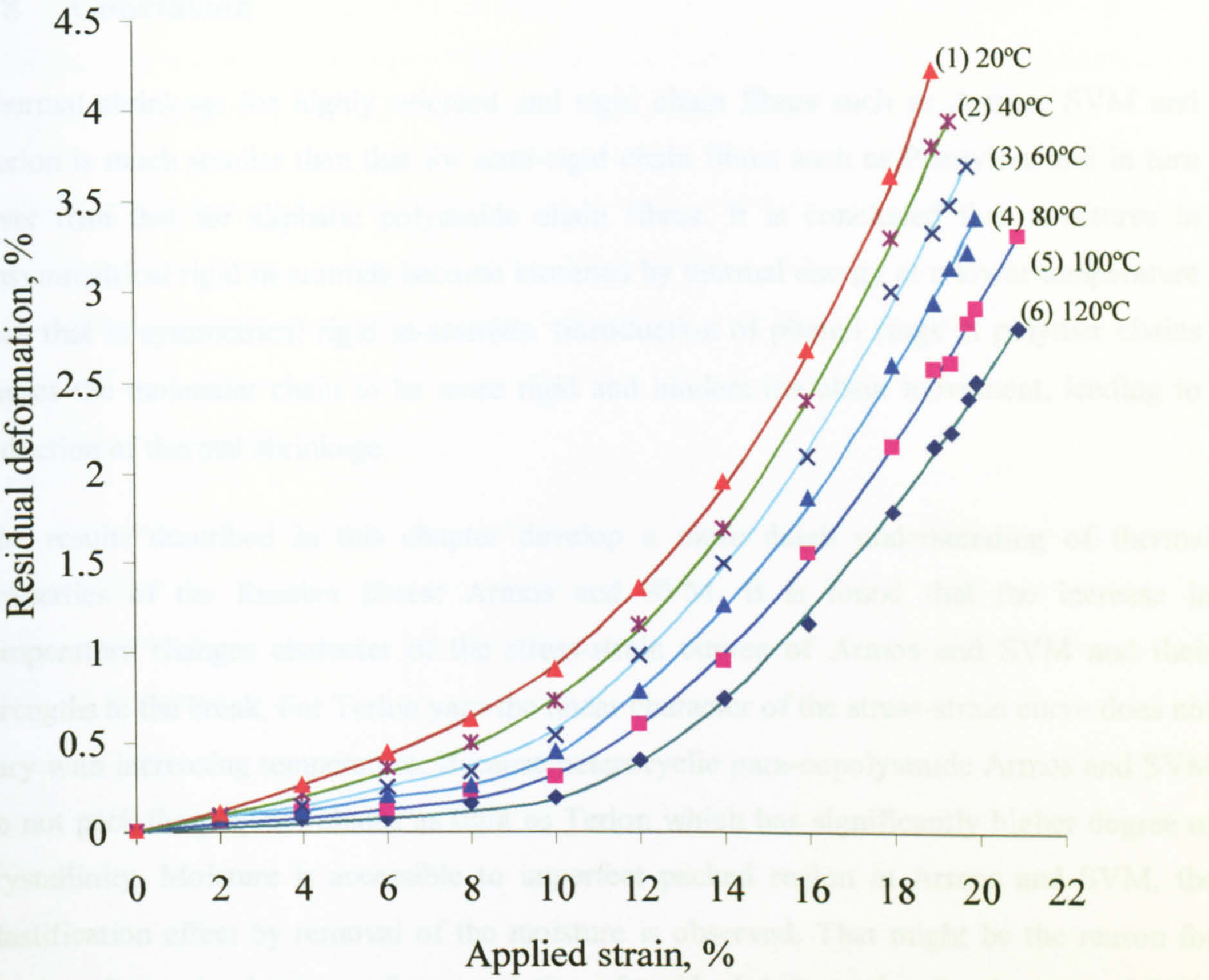

Fig. 5.31 Effect of applied strain on residual deformation for Capron yarn at different temperatures: (1) 20°C; (2) 40°C; (3) 60°C; (4) 80°C; (5) 100°C; (6) 120°C

The value of given deformation at which the residual component of deformation starts to increase corresponds to the beginning of the third part of the stress-strain curve at varying temperatures (see Fig. 5.28). Thus, it is possible to predict the onset of intensive accumulation of a residual component of deformation for Capron yarn at higher temperatures from the tensile stress-strain curve.

5.8 Conclusion

Thermal shrinkage for highly oriented and rigid chain fibres such as Armos, SVM and Terlon is much smaller than that for semi-rigid chain fibres such as Phenylon, and in turn laver than that for aliphatic polyamide chain fibres. It is concluded that structures in unsymmetrical rigid m-aramids become loosened by thermal energy at a lower temperature than that in symmetrical rigid m-aramids. Introduction of phenyl rings in polymer chains causes the molecular chain to be more rigid and hinders the chain movement, leading to reduction of thermal shrinkage.

The results described in this chapter develop a more detail understanding of thermal properties of the Russian fibres: Armos and SVM. It is found that the increase in temperature changes character of the stress-strain curves of Armos and SVM and their strengths to the break. For Terlon yarn the linear character of the stress-strain curve does not vary with increasing temperature. Because heterocyclic para-copolyamide Armos and SVM do not pack the polymer chains as tight as Terlon which has significantly higher degree of crystallinity. Moisture is accessible to unperfect packed region in Armos and SVM, the plastification effect by removal of the moisture is observed. That might be the reason for causing change in character of accumulation of residual deformation for Armos and SVM fibres. The most significant changes occur at temperatures from 80 up to 100°C.

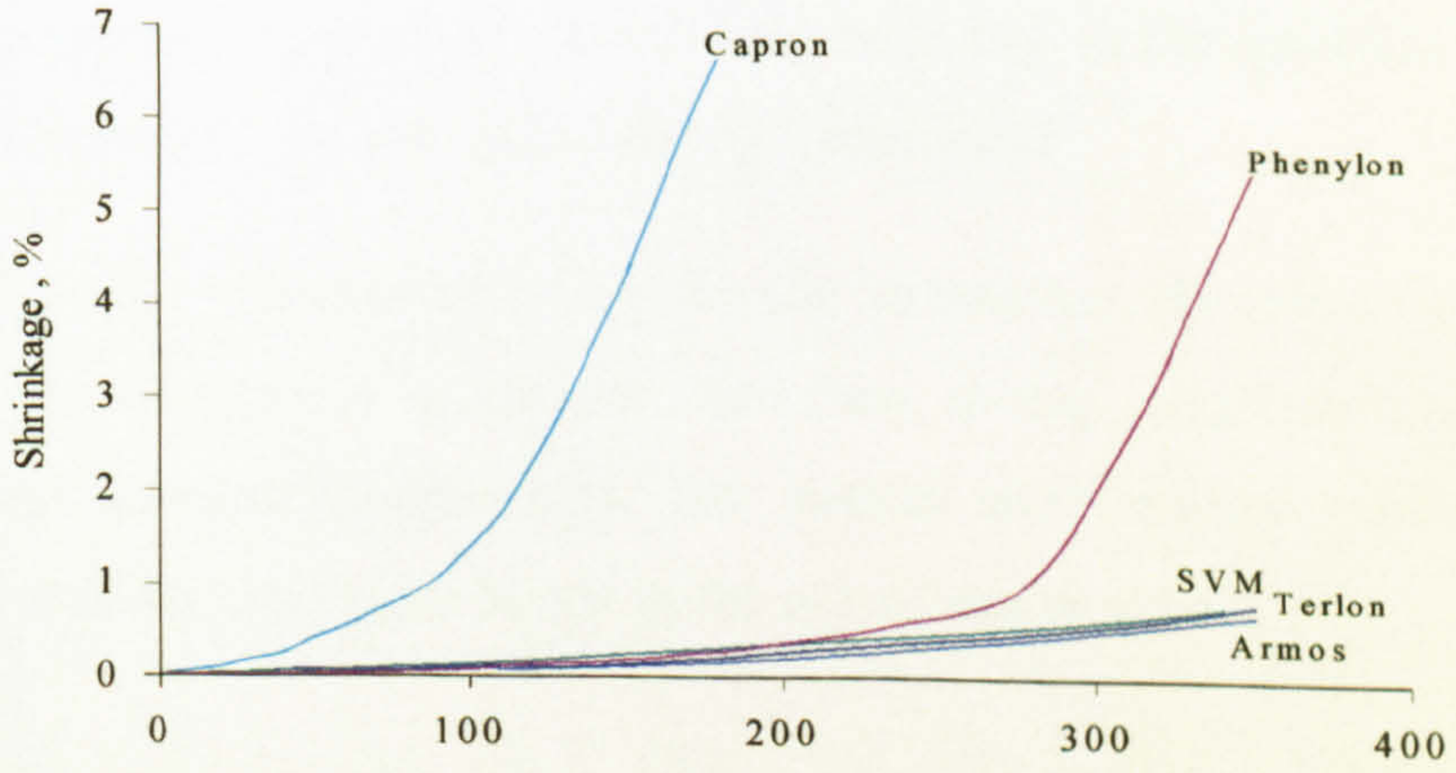

Fig. 5.32 Thermo shrinkage of Armos, SVM, Terlon, Phenylon, and Capron yarns

The accumulation of residual deformation for Terlon yarn at high temperatures is quite different than that for Armos and SVM yarns. It is due to difference in their structures and degree of crystallinity of Terlon compared to Armos and SVM.

Increase in temperature does not essentially influence in the nature of the stress-strain curve of Phenylon and Capron yarns. The strength for these yarns is diminished with increasing temperature. Accumulation of residual deformation for Phenylon and Capron yarns is similar. There is no essential change in the character of accumulation of residual deformation at elevated temperatures.

The mechanism of deformation for Phenylon is different to that for rigid chain polymers. For semi rigid chain polymers, the orientation processes play the main role during the earlier stages of deformation, whereas for rigid chain polymers the sliding of structure elements is more important.

CHAPTER 6

THE STUDY OF STRUCTURE OF POLYAMIDE AND POLYETHYLENE YARNS

6.1 Introduction

It is known that intermolecular interaction plays an essential role in the specific properties of polyamide fibres. An especially relevant role in the formation of intermolecular bonds for polyamide fibres is played by hydrogen bonds. Polyamide fibres always have some moisture in their structure, which can influence the intermolecular interaction in different ways. Moisture can cause breakage in the molecular structure by relaxing 'polymer - polymer' type intermolecular bonds. Water can also participate in the formation of hydrogen bridges, i.e. "polymer-water-polymer" type hydrogen bonds. The different mechanical properties of yarns e. g. stretching are related to changes in the intermolecular interaction.

It is most convenient to study the formation of hydrogen bonds by investigation of the absorption bands in the field of stretching vibrations of NH groups: 3300- 3440 cm^{-1}. In the case of NH···OC hydrogen bond formation the absorption band attributable to the stretching vibrations of NH groups is moved to a lower frequency area of the spectrum. Moreover the value of the shift indicates the strength of the hydrogen bond.

In order to analyse the influence of intermolecular interaction, the effects of moisture and stretching on the change of molecular structure during single-axis stretching was investigated using infrared spectroscopy. The method used enabled investigation of the presence of moisture and hydrogen bonds in the polyamide structure.

6.2 Experimental

6.2.1 Preparation of Samples

Yarn samples of Armos, SVM, Terlon, Phenylon, and Capron were treated in different ways prior to the physical analysis. Two types of samples were prepared by drying either at 105°C or in the desiccator at 20°C, respectively. Alternatively another two types of samples were prepared by stretching to a certain extension depending on the type of fibre for 10 min or by both drying and stretching. Conditions for preparation of samples are described in Table 6.1.

Table 6.1 Conditions for preparation of samples

Yarn samples prepared at different conditions		
1	Original yarns	conditioned at 20°C and 65 % r. h. for 30 days
2	Dried yarns at 105°C	dried at 105°C to constant weight
3	Stretched yarns	stretched to the certain extension for 10 min. 3% for Armos, SVM, Terlon and Polyethylene yarns; 14% for Capron yarn; and 19% for Phenylon yarn
4	Stretched and dried yarns	stretched and then dried as described for dried sample and stretched sample above
5	Dried yarn at room temp.	Dried at room temperature in the desiccator with silica gel to constant weight

6.2.2 Fourier Transform Infrared (FT-IR) analysis of polymer fibres

6.2.2.1 Identification of FT-IR bands

Armos, Terlon, SVM, Phenylon and Capron fibres were prepared in different ways as described in Section 6.2.1 before the FT-IR spectrum of the single fibre was carried out using a Spectra Tech. FT-IR 50XC, Nicolet with microscope IR-Plan TM.

FT-IR is widely used to provide detailed information about the structures of molecular compounds. Previous workers have examined a large number of spectra of known materials, to correlate specific vibrational absorption maxima with the responsible groupings. The reference data for the basic absorption bands related to bonds of polyamide and aromatic polymer material is presented in Table 6.2. Much more extensive and detailed correlations need take into account the intramolecular environment of each bond. The IR absorption is altered more or less extensively by the conditions under which the polymer is observed. The causes of these variations may be either instrumental or chemical in origin Armos, SVM, Terlon, Phenylon polymer fibres are mainly aromatic polyamides. Their main functional groups will be identified.

Table 6.2. Infrared positions of major bond vibrations in polyamides (Pavia, 1996).

Frequency (cm^{-1})	Type of Vibration
1600 and 1475	C=C Aromatic
3500 and 3100	N-H (stretch) Primary and secondary amides
1640~1550	N-H (bend) Amide
1670~1640	C=O (stretch) Amide
1350~1000	C-N (s) Amines
3650~3600 3500~3200	O-H Free H-Bonded
3150~3050 900~690 1465 3000~2850 2900~2800	C-H (stretch) Aromatics C-H (out-of plane bend) Aromatics C-H $-CH_2-$ (bend) C-H (stretch) Alkanes C-H Aldehyde

6.2.2.2 Estimate of the content of hydrogen bonds and moisture in the polymers

The FT-IR microscope can be successfully used to quantify the different components of individual fibres. There are many methods for quantitative processing of spectra, however they are all based on Beer-Lambert's law (Dehant, (1976).

$$\text{Transmission } T = I/I_0 = 10^{-\varepsilon cd}$$

Where I_0 = intensity of incident beam

I = intensity of light that has passed through a thickness of the material, d.

d = thickness of the penetration

c = concentration

ε = extinction coefficient

and $D = \varepsilon cd = \log_{10}(I_0/I)$

This is calculated by locating a straight base line across to the minima on either side of the absorption band and the vertical height from the horizontal axis to the point of intersection on the tangent (I_0) and that from the apex of the peak to the horizontal axis (I) (Figure 6.1)

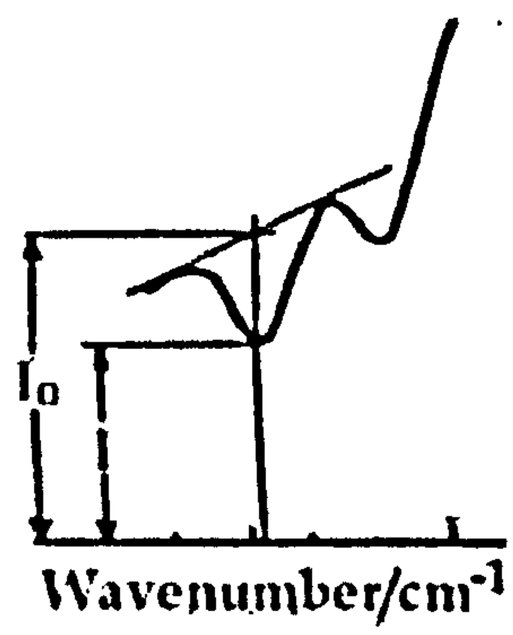

Fig. 6.1 Straight base line

In order to reduce the error due to any physical variations in the sample, it is necessary to select an absorption band of constant intensity as an internal standard. For aromatic polyamides, the band assigned to the stretching vibration of CH groups (3050 cm^{-1}) is chosen to be the internal standard. The intensity of this band depends on the type of fibre being studied and will vary between Armos, SVM, Terlon fibres due to differences in their chemical structure. However, comparison of the infrared spectra of original, dried, stretched and stretched dried yarns shows that the intensity of this band remains constant for each type of fibre. Therefore this band can be used as internal standard for calculations on each type of fibre.

Intermolecular interaction between the polymer chains is known to significantly influence the mechanical properties of a fibre (Pakhomov, 1999). Hydrogen bonds are dominant intermolecular force in aramid fibres such as Armos, SVM, Terlon and Phenylon. Therefore, the effects of stretching or drying processes on the degree of hydrogen bonding was preliminarily investigated by quantifying the IR transmission relating to hydrogen bonded and free NH groups. The ratio of hydrogen bonded and free NH groups can give information relating to the characterisation of the intermolecular interaction for treated fibres. The ratio of hydrogen bonded NH groups to free NH groups can be determined by the ratio of their absorbencies (or transmittance). This ratio is defined as the Degree of hydrogen bonding (DHB):

$$\text{Degree of hydrogen bonding (DHB)} = \frac{D_{(\text{hydrogen bonded N-H})}}{D_{(\text{free N-H})}}$$

As discussed in Chapters 1, 3, and 5 the hydrogen bonds between neighbouring chains can be either "polymer-H_2O-polymer" or "polymer-polymer" type. It is conceivable that the stretching or drying process might break the "polymer-H_2O-polymer" type of hydrogen bonding in the fibres. Therefore, the ratios of absorbance at 3500 cm^{-1} for hydrogen bonded

O-H and 3050 cm^{-1} for C-H (internal standard) were measured in order to estimate the moisture involved in hydrogen bonding.

6.2.3. Differential Scanning Calorimetry

Differential Scanning Calorimetry (DSC) was used to provide information about the polymer solid state and any transitions as a function of temperature using a Perkin Elmer DSC 4 instrument. The original and dried yarn samples, prepared as described in Section 6.2.1, were crimped in standard sample pans, but were not hermetically sealed. The measurements were made at a heating rate of 20°C/ min over the continuous temperature range from 20°C to around 450°C. A 100% N_2 atmosphere was used for measurements below zero.

6.2.4 Scanning Electron Microscopy (SEM)

Fibre surfaces of Armos, SVM, Terlon, Phenylon, and Capron were examined using a Leica Cambridge Stereoscan 360 scanning electron microscope (SEM). The sample yarns were stretched using the Instron at a speed of 1 mm/min to breaking point. The fibre breaking mechanism was investigated by SEM.

6.3 Results and Discussion

6.3.1 Research of moisture content and intermolecular interaction of SVM and Armos fibres by FT-IR method

Fig. 6.2 shows the infrared spectra of original SVM and Armos fibres. The spectra confirm that the chemical structures for SVM and Armos are very similar. The vibration modes of both of these fibres are due to intense amide vibrations. The intense band at 1646 cm^{-1} is attributed to conjugated amide and H-bonded C=O. The 1540 cm^{-1} band is due to the N-H bending. The small vibration next to these two bands is due to aromatic C=C stretch at about 1600 cm^{-1} and 1475 cm^{-1}. These peaks confirm the presence of aromatic rings. The C-N stretch from the carbonyl carbon of the amide is observed at 1400 cm^{-1}. The broad peak around 3300 cm^{-1} is a combination vibration due to the strongly hydrogen bonded N-

H stretching at 3300 cm^{-1}, nonhydrogen bonded N-H stretching at 3400 $cm^{-1}$and moisture O-H vibration at 3500 cm^{-1}. The shoulder at 2950 cm^{-1} is C-H vibration. Therefore, the Degree of hydrogen bonding (DHB) can be expressed as:

$$\text{Degree of hydrogen bonding (DHB)} = \frac{D_{(\text{hydrogen bonded N-H})}}{D_{(\text{free N-H})}} = \frac{D_{3300}}{D_{3400}}$$

The infrared spectrum of the original, stretched, dried, and stretched dried SVM yarn samples are shown in Fig. 6.3 and Armos in Fig. 6.4. Their absorbances ratio (D_{3500} / D_{3050}) for the moisture content and Degree of hydrogen bonding (DHB) are given in Table 6.3. According to the previous work on the FTIR test of synthetic fibres (Pandey, 1989), 6% variation within a single fibre might occur. Because only one test for each sample of fibre was carried out in the present FTIR experiments, this level of variation (6%) will be used for the margin of difference in the results.

Table 6.3. Moisture content and degrees of H-bonding for original and treated Armos and SVM fibres

Yarn Sample	SVM		Armos	
	moisture content D_{3500} / D_{3050}	DHB D_{3300} / D_{3400}	moisture content D_{3500} / D_{3050}	DHB D_{3300} / D_{3400}
Original	0.25	1.43	0.24	1.60
Stretched	0.23	1.43	0.22	1.60
Dried	0.16	1.43	0.20	1.33
Stretched dried	0.01	2.14	0.14	1.48

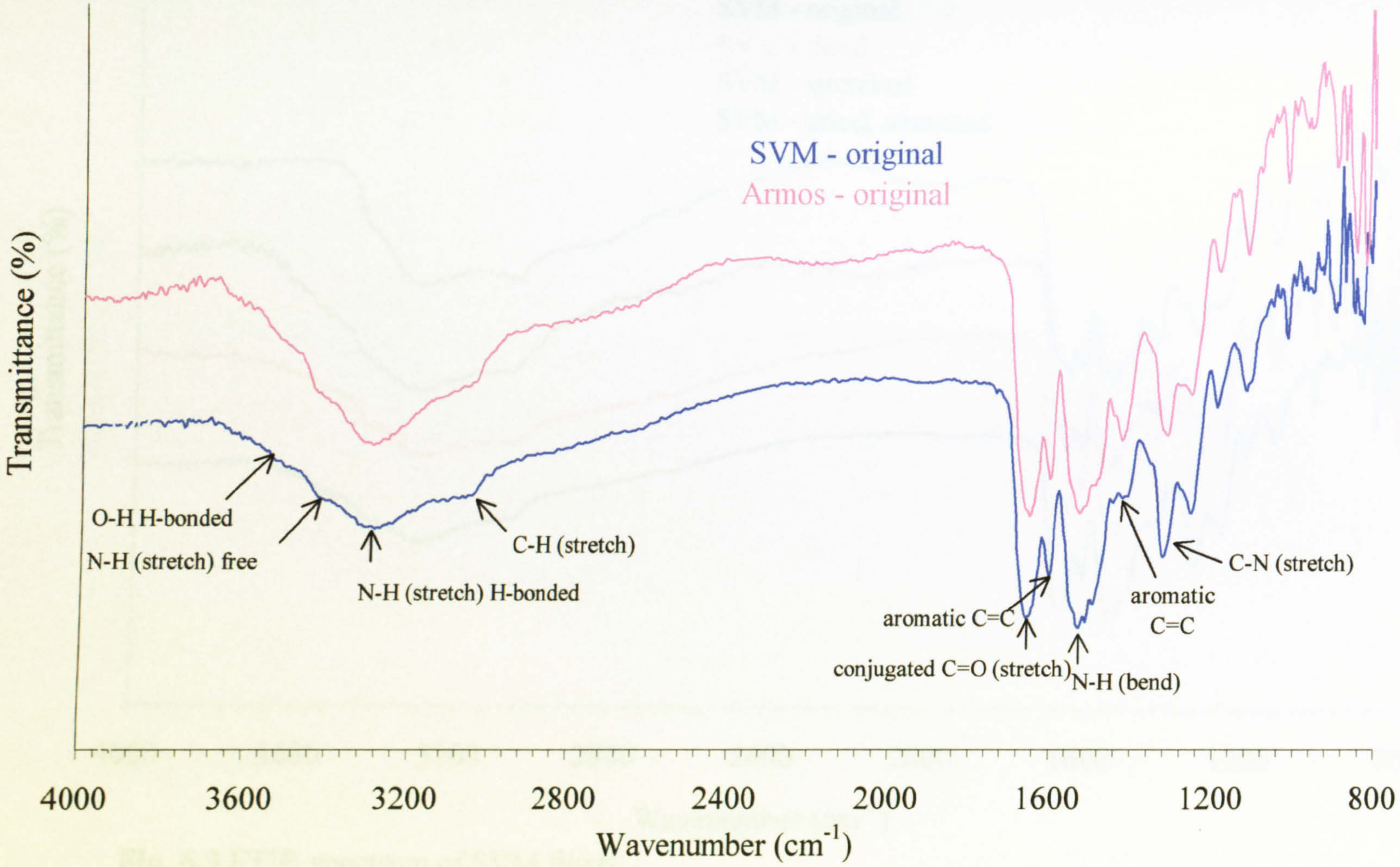

Fig. 6.2 FTIR spectrum of Armos and SVM original fibres

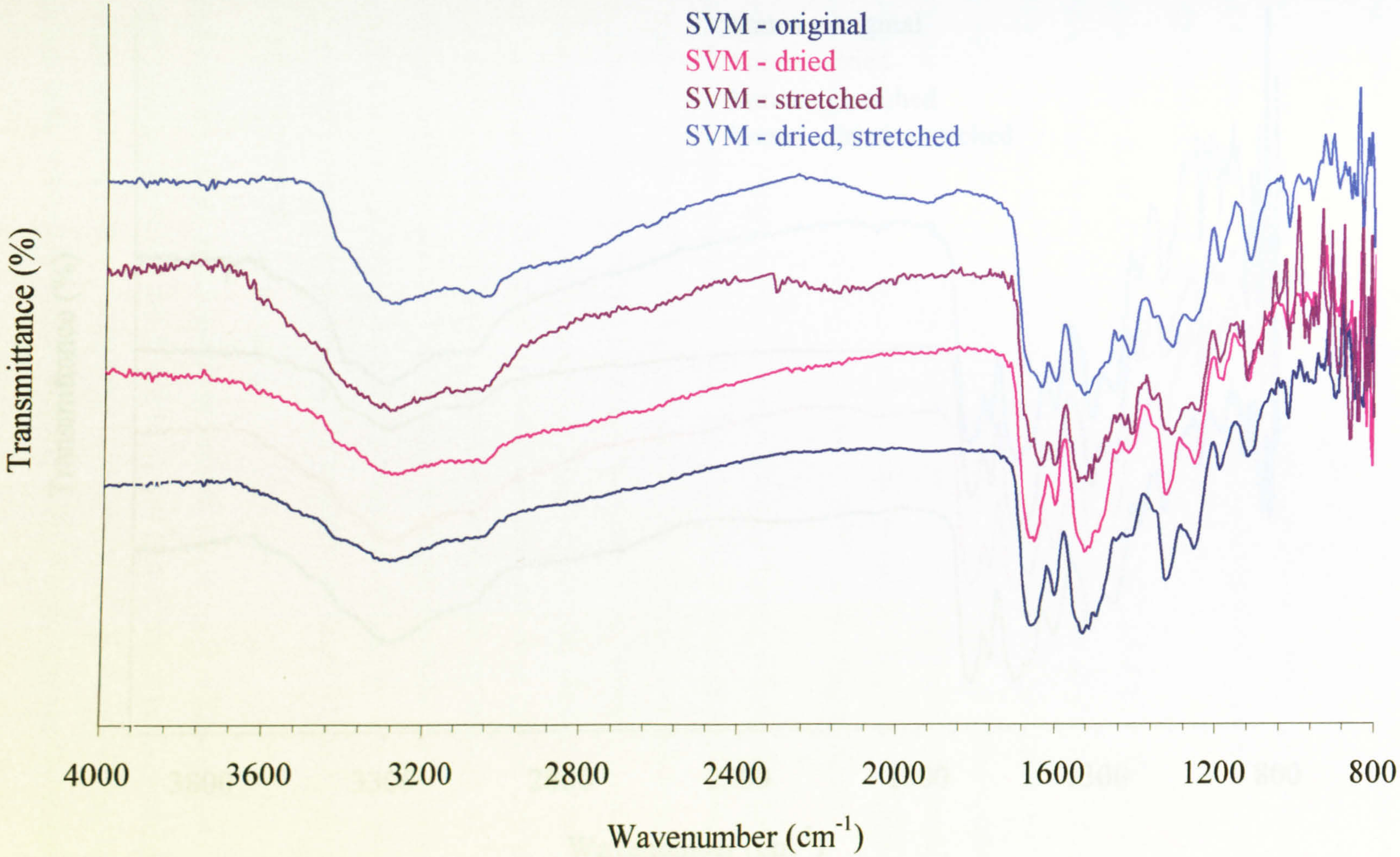

Fig. 6.3 FTIR spectrum of SVM fibres

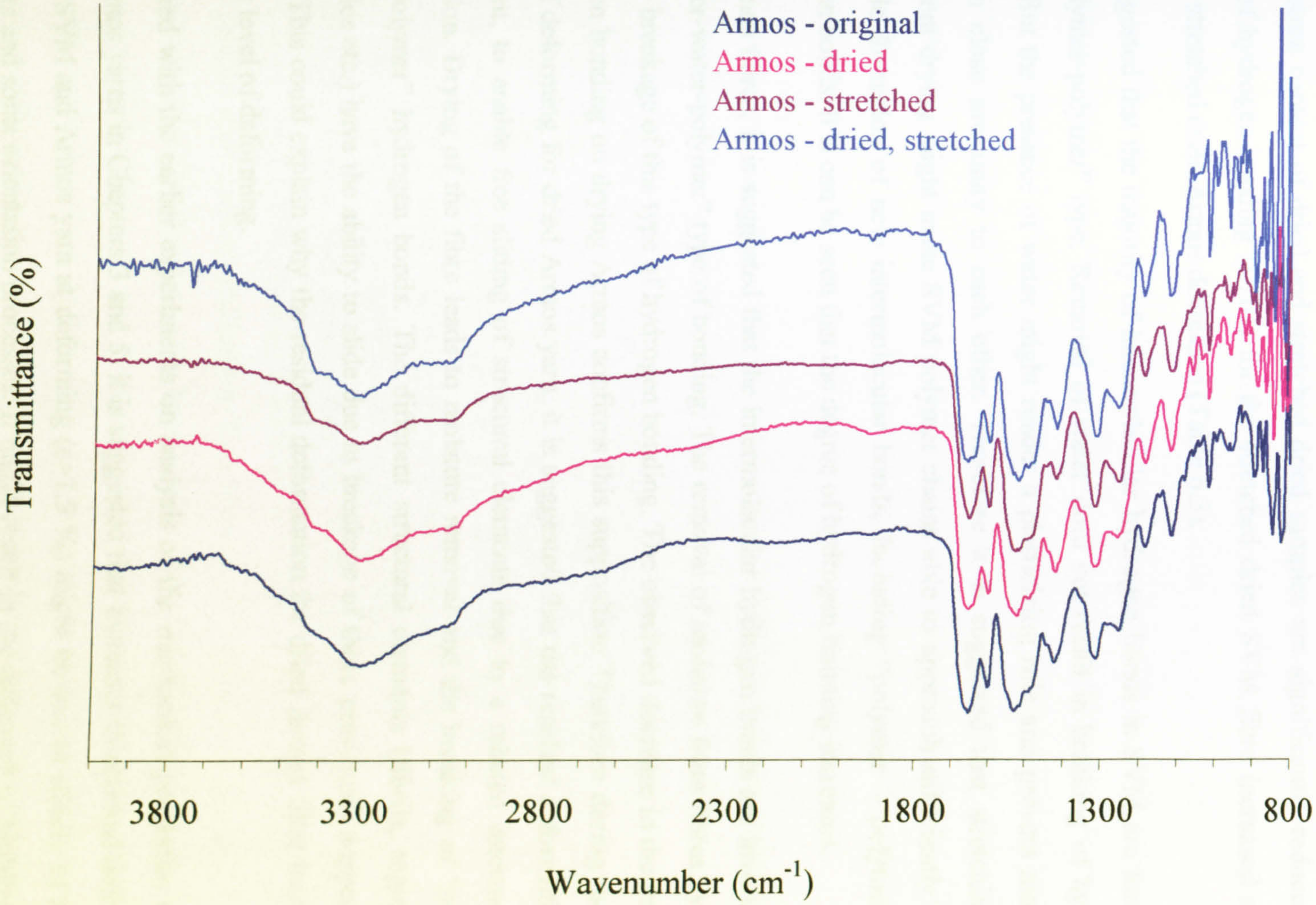

Fig. 6.4 FTIR spectrum of Armos fibres

Comparison of the infrared absorption spectrum for SVM and Armos fibres under different conditions shows that stretching does not cause a reduction in hydrogen bonded moisture contents or any change in the degree of hydrogen bonding (DHB) in the fibres. However the moisture content of dried and stretched dried samples are significantly reduced. The degree of hydrogen bonding (DHB) for the stretched dried SVM fibre increased and for dried or stretched dried Armos decreased (Table 6.3).

It is suggested that the majority of intermolecular hydrogen bonds in SVM are formed as the "polymer-polymer" type. Removal of water does not result in breaking of hydrogen bonds. But the presence of water might render a plasticizing role and prevent molecules being in close proximity to each other. Therefore it is suggested that stretching with subsequent drying might make SVM polymer chains able to approach sufficiently closely to enable formation of new intermolecular bonds, including "polymer – polymer" type hydrogen bonds. It is can be seen that the degree of hydrogen bonding increases.

For Armos fibres, it is suggested that the intermolecular hydrogen bonds are involved in a "polymer-water-polymer" type of bonding. The removal of moisture from fibres by drying leads to breakage of this type of hydrogen bonding. The observed decrease in the degree of hydrogen bonding on drying Armos confirms this supposition Therefore during the initial stage of deforming for dried Armos yarn, it is suggested that the residual deformations are sufficient, to enable free sliding of structural elements due to a relaxed intermolecular interaction. Drying of the fibre leads to moisture removal and the breaking of "polymer-water-polymer" hydrogen bonds. The different structural elements (fibrils, segments of molecules etc.) have the ability to slide due to breakage of these previously supportive H-bonds. This could explain why the residual deformation for dried Armos fibre increases at the first level of deforming.

Compared with the earlier experiments on analysis of the mechanical properties of SVM and Armos yarns in Chapters 3 and 5, it is suggested that increases in residual deformation for the SVM and Armos yarn at deforming (ε>1.5 %) might be due to sliding of structure elements and some orientation processes. It might result in the approach of building blocks

favouring the formation of the intermolecular interaction. But from the FT-IR results, it can be seen that an increase in the quantity of hydrogen bonds was not observed at deforming (ε>1.5%) with formation of essential plastic deformations. The nature of plastic deformations for these fibres is determined, initially, by the sliding of structural elements with subsequent breakage of old and formation of new intermolecular bonds. Orientation and conformation processes are also possible. It is conceivable that the different structural elements (fibrils, segments of molecules etc.) could also slide if only some of the intermolecular bonds were broken. But the FT-IR experiment did not show any change in the degree of hydrogen bonding on stretching for either fibre. Therefore it is suggested that at deforming (ε>1.5%) with formation of essential plastic deformations, not only does breakage of some bonds occur, but also new hydrogen bonds are formed. Thus the structural data obtained from the FT-IR study is in good agreement with the results of the mechanical properties study.

6.3.2 Research of moisture contents and intermolecular interactions of Terlon and Phenylon fibres by FT-IR method

Figs. 6.5 and 6.6 show the effects of the drying and stretching processes on the infrared spectra of Terlon and Phenylon fibres respectively. The IR vibration characteristics of these fibres are very similar to those of SVM and Armos, because they are all aromatic polyamides with similar chemical groups. It is found that the band contributing the hydrogen bonded N-H stretching was shifted from 3300 cm^{-1} (for SVM and Armos) to 3330 cm^{-1} (for Terlon). It is suggested that the hydrogen bonds on N-H groups within the Terlon fibre are weaker than those within the SVM and Armos fibres. According to Beliaev's *et al.*, work (1978), hydrogen bonding is weakened by a tendency of phenylene rings to parallel pack upon crystallization. This tendency is accompanied by the increase in H···O distance. It is also found that the band around 3330 cm^{-1} for Terlon is much sharper than that for SVM and Armos, and the shoulder at 3400 cm^{-1} (attributed to non H-bonded N-H) in the spectrum of the Terlon fibre is less pronounced. This testifies to a higher degree of crystallinity for the Terlon yarn. The crystallinity for Terlon can reach 80% while SVM and Armos have a semi-crystalline structure.

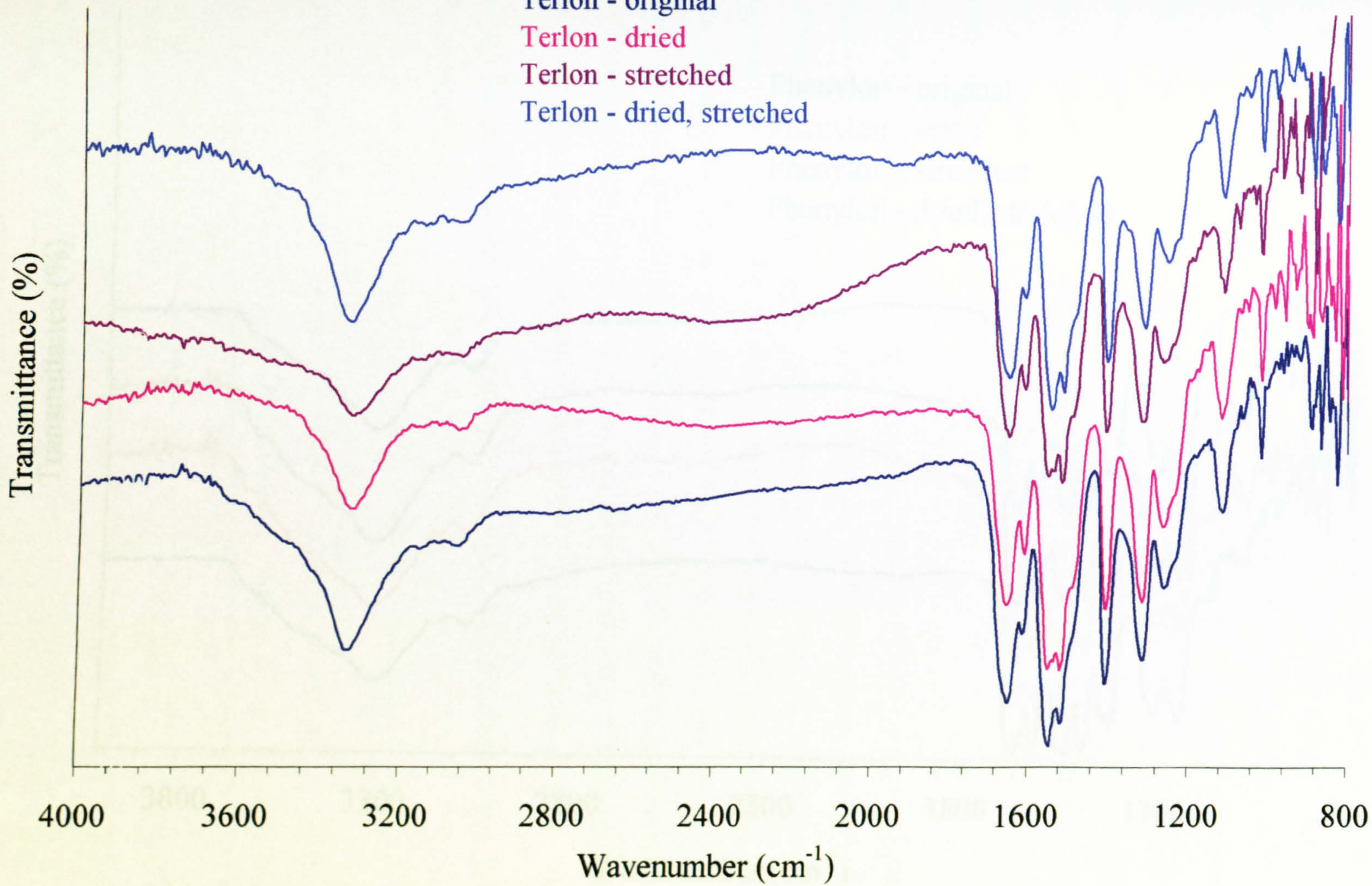

Fig. 6.5 FTIR spectrum of Terlon fibres

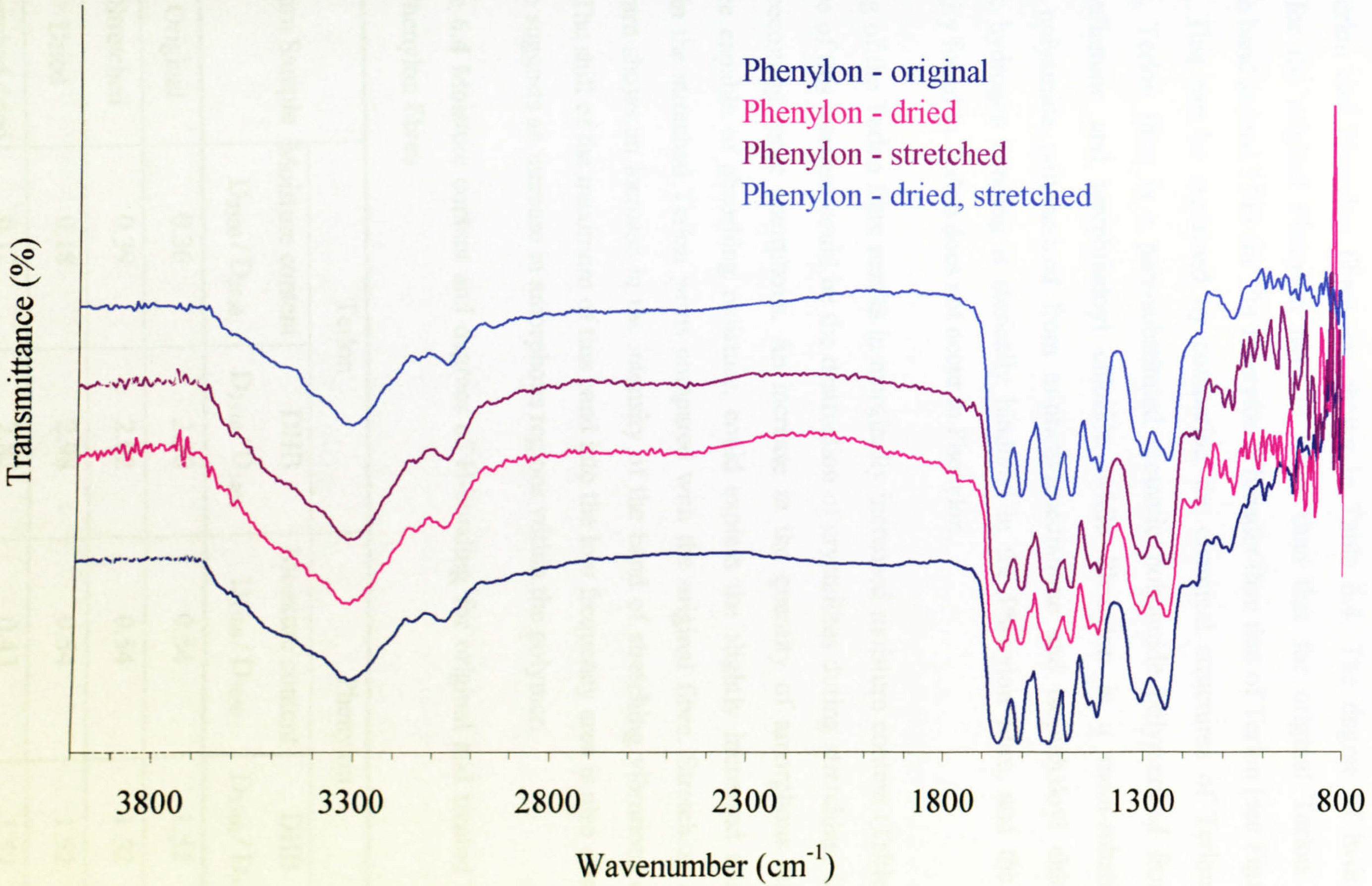

Fig. 6.6 FTIR spectrum of Phenylon fibres

The absorption ratios D_{3500}/D_{3050} and the degrees of hydrogen bonding for original and treated Terlon and Phenylon fibres are shown in Table 6.4. The degree of hydrogen bonding for the original Phenylon fibre is lower than that for original Terlon. The absorption band around 3300 cm^{-1} for Phenylon is broader than that of Terlon (see Figs. 6.5 and 6.6). This can be explained by comparing the chemical structures of Terlon and Phenylon. Terlon fibre is a para-substituted aromatic polyamide polymerized from p-phenylenediamine and terephthaloyl chloride, while Phenylon is a meta-substituted aromatic polyamide polymerized from m-phenylenediamine and isophthaloyl chloride. Therefore hydrogen bonding is sterically hindered in the Phenylon fibre, and the high crystallinity found in Terlon does not occur in Phenylon.

Stretching of the Terlon fibre results in marginally increased moisture content (Table 6.4). The cause of this increase could be the destruction of crystallites during stretching, i.e. the sample becoming more amorphous. An increase in the quantity of amorphous regions, which are capable of absorbing moisture, could explain the slightly increased moisture content in the stretched Terlon yarns compared with the original fibre. Stretching of the Terlon yarn shows an increase in the intensity of the band of stretching vibrations of NH groups. The shift of the maximum of this band into the low frequency area is also observed. This also suggests an increase in amorphous regions within the polymer.

Table 6.4 Moisture content and degrees of H-bonding for original and treated Terlon and Phenylon fibres

Yarn Sample	Terlon		Phenylon	
	Moisture content D_{3500}/D_{3050}	DHB D_{3330}/D_{3400}	Moisture content D_{3500}/D_{3050}	DHB D_{3300}/D_{3400}
Original	0.36	2.30	0.54	1.52
Stretched	0.39	2.02	0.54	1.52
Dried	0.18	2.98	0.54	1.52
Stretched dried	0.12	2.82	0.43	1.52

The drying of the Terlon yarn results in a decrease of moisture content but an increase in the degree of hydrogen bonding. It is suggested that drying promotes the approach of structural elements or polymer chains within the amorphous regions, and subsequent formation of new "polymer – polymer" type hydrogen bonds.

For the stretched dried Terlon sample, the quantity of moisture is further reduced, but the degree of hydrogen bonding DHB does not significantly change compared to the dried sample. If drying results in an increase in the degree of H-bonding, as described above, and stretching causes a decrease in the degree of H-bonding, then the two processes may be competitive.

Table 6.4 shows that concomitant drying and stretching of Phenylon fibre does not result in a significant change of hydrogen bonded moisture content, and the degree of intermolecular hydrogen bonding remains constant. It is thought that the bonded moisture is contained mainly in closed polymer cavities of molecules (so-called "dissociation traps"), and is therefore difficult to remove. Phenylon has very loose surface structure, as a consequence the presence of surface moisture is characteristic of this fibre. Therefore it is suggested that water and the hydrogen bonds in this case do not exert a significant influence on the properties of a fibre obtained from semi rigid chain polymer, compared to fibres obtained from rigid chain polymers. This is in agreement with data on the analysis of the mechanical properties of Phenylon fibre. Increasing the temperature of Phenylon yarn does not result in a change in the accumulation of residual deformation, and does not change significantly the value of the residual component. Thus, comparing with para-aramid fibres, an increase of temperature up to 220°C does not render a strong influence on the mechanical properties and structure of the Phenylon yarn.

6.3.3 Research of moisture content and intermolecular interaction of Capron fibre by FT-IR method

The IR spectra for untreated, stretched, dried and stretched dried Capron fibre respectively are shown in Fig. 6.7. Capron is an aliphatic polyamide, therefore its IR spectrum differs

from those of the previously reviewed aromatic polyamides. It can be seen that there are peaks of vibration absorptions at 1650 cm^{-1} for amide C=O; 1550 cm^{-1} for N-H bending; 1450 cm^{-1} and 1250 cm^{-1} for CH_2 scissoring and wagging bending; and 1400 cm^{-1} for C-N stretch from the carbonyl carbon of the amide. But the aromatic C=C absorption at 1610 cm^{-1} and 1510 cm^{-1}, seen previously for the aromatic polyamide fibres, is absent. The sharp peaks at 2870 cm^{-1} and 2920 cm^{-1} are due to CH_2 symmetric and asymmetric stretches.

The intense band at 3300 cm^{-1} with a weak shoulder at about 3200 cm^{-1} characterises amide stretching of NH groups, bonded by hydrogen bonds. A band at 3200 cm^{-1} is assigned to strongly hydrogen bonded NH groups, the band at 3300 cm^{-1} to weakly hydrogen bonded NH groups. Therefore an estimation of the intermolecular interaction is given by the ratio of the absorbance for strongly hydrogen bonded NH groups to the absorbance for weakly associated NH groups (d):

$$d = \frac{D_{(\text{strongly hydrogen bonded N-H})}}{D_{(\text{weakly hydrogen bonded N-H})}} = \frac{D_{3200}}{D_{3300}}$$

The band assigned to the stretching vibrations of CH_2 groups at 2870 cm^{-1} was used as internal standard for the measurement of the moisture content.

The absorbances ratio (D_{3500} / D_{2870}) representative of the moisture content and Degree of hydrogen bonding (DHB) for Capron fibre are given in Table 6.5. It is found that the moisture content for Capron yarn after stretching does not change. The value of d can be seen to decrease after stretching suggesting an increase in weakly associated NH groups. The cause of this hydrogen bond easing is thought to be due to the mechanical destruction of the intermolecular interaction grid and breaks in the main molecular chain of the polymer at applied deformation >10-11%.

After drying the moisture content decreases, but the ratio of strongly hydrogen bonded NH groups to weakly hydrogen bonded NH groups almost is not changed.

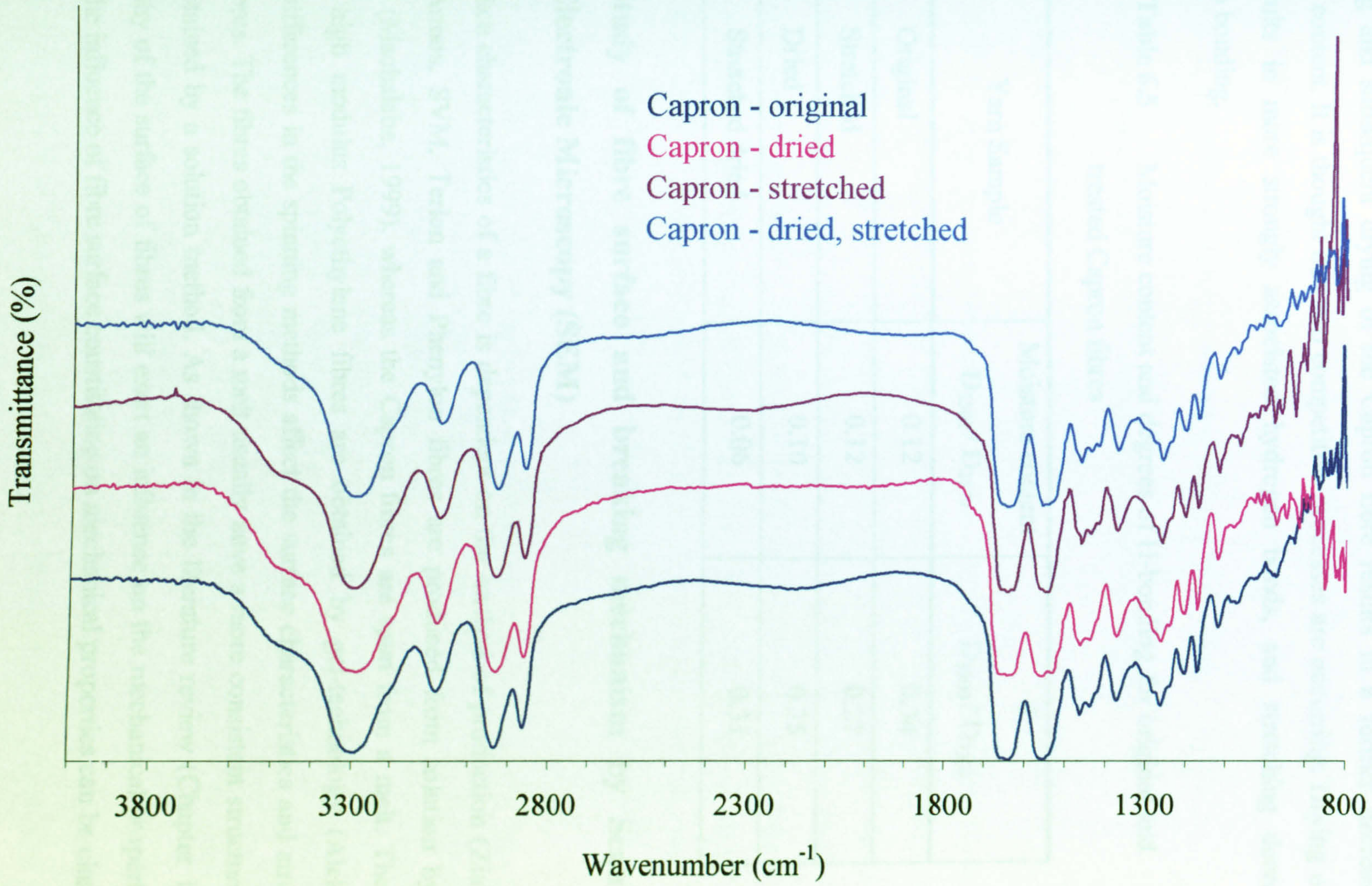

Fig. 6.7 FTIR spectrum of Capron fibres

Stretching and subsequent drying of the Capron fibre results in a further decrease in moisture content. It is thought that two competitive processes are occurring. Drying of the fibre results in more strongly associated hydrogen bonds, and stretching decreases hydrogen bonding.

Table 6.5 Moisture content and degrees of H-bonding for original and treated Capron fibres

Yarn Sample	Moisture content D_{3500}/D_{2870}	d D_{3200}/D_{3300}
Original	0.12	0.34
Stretched	0.12	0.27
Dried	0.10	0.35
Stretched dried	0.06	0.31

6.4 Study of fibre surface and breaking mechanism by Scanning Electronic Microscopy (SEM)

The surface characteristics of a fibre is dependent on the method of production (Ziabicki, 1976). Armos, SVM, Terlon and Phenylon fibres are produced from solution by wet spinning (Machalaba, 1999), whereas the Capron fibres are spun from a melt. The high strength high modulus Polyethylene fibres are obtained by gel-technology (Alekseev, 1994). Differences in the spinning methods affect the surface characteristics and structure of the fibres. The fibres obtained from a melt usually have a more consistent structure than fibres obtained by a solution method. As shown in the literature review (Chapter 1), the topography of the surface of fibres will exert an influence on the mechanical properties of fibres. The influence of fibre surface constitution on mechanical properties can be classified into:

- The presence of defects, microcracks, pollutants, fragments of a settling bath and lubricant, dressing etc., on the surface of fibre, that usually results in deterioration of mechanical properties of yarns and fibres;

- Breakage of fibres due to defective centres emanating from the fibre surface;

- The adhesive properties of fibres depending on the surface condition

6.4.1 Topography of fibres

Armos and SVM fibres in many respects are similar. The similarity of their surfaces is reflected by the SEM images in Fig.6.8. The fibrillar structure of these fibre surfaces is not observed as clearly as is the case for Phenylon (Fig. 6.9), however macrofibrilar aggregates which create a corrugated relief on their surfaces are visible (Fig. 6.8). These macrofibrils have a spindle-shaped appearance. Stretching of the fibres does not render any influence on the surface condition for Armos and SVM fibres. The SEM pictures reveal many white spots on the surface of dried Armos and SVM fibres. It is thought that the removal of moisture increases the tendency to build up static charges which might affect gold coating. (Fig. 6.8 c, f).

The SEM images of Terlon and Phenylon fibre surfaces are shown in Fig.6.9. The Terlon fibre has a smooth surface with unremoved fragments of dust, lubricant and dressing (Fig. 6.9 a-c). As shown by Sukhanova, (2000) the fibril structure of these fibres is observed only in the core of the fibre, the fibre has smooth skin surface layer (Sukhanova, 2000; Yudin *et al.*, 1997). By comparison Phenylon fibre has very obvious fibril structure on the surface. The loosely packaged macrofibrils have a spindle-shaped appearance (Fig. 6.9 d-f). as is the case for the dried Armos and SVM fibres, it is thought the dried Phenylon fibres might also have higher electrostatic properties.

From Fig 6.10 (a) and (b) it can be seen that the surface of the Capron fibre is smooth. However it is possible to note the presence of some features on the surface, due to salt crystals, remaining after special processing of the yarn.

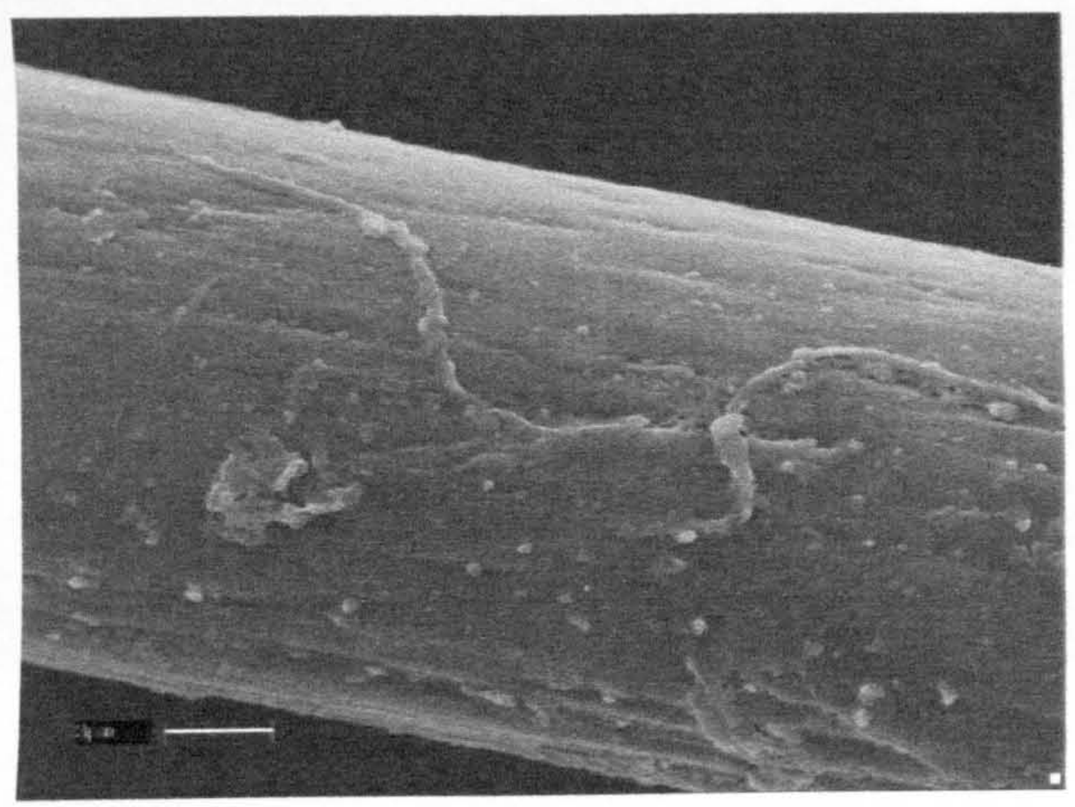

Armos (a) original fibre

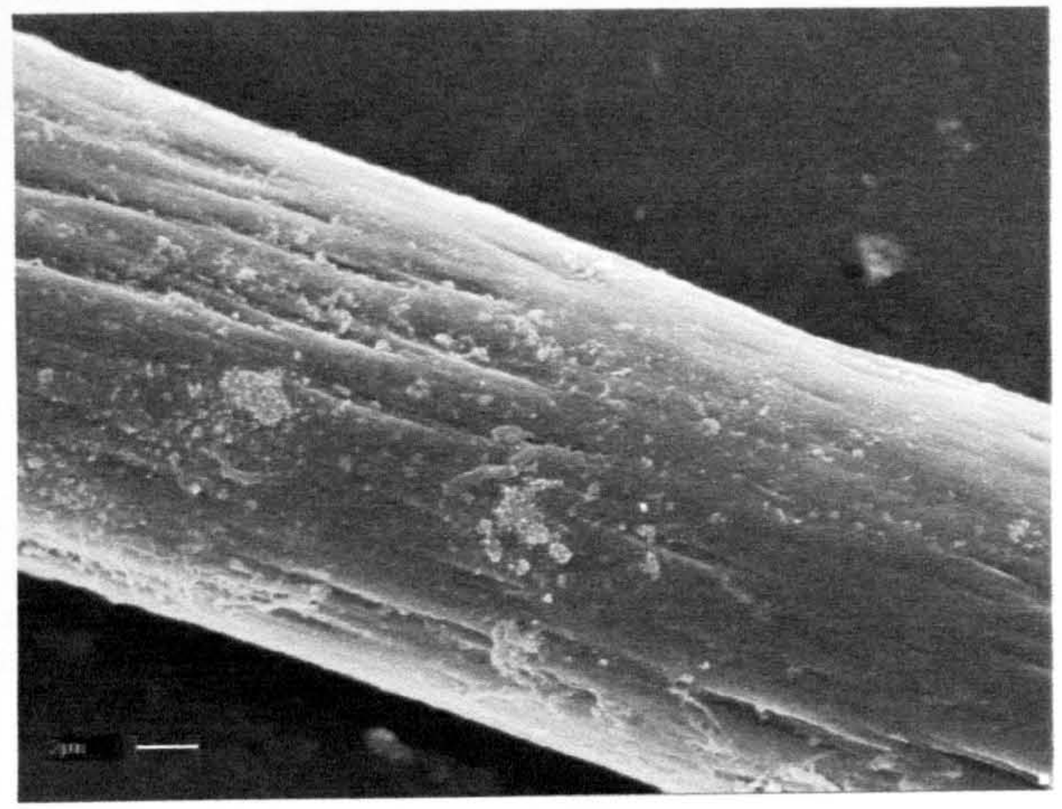

(b) stretched fibre

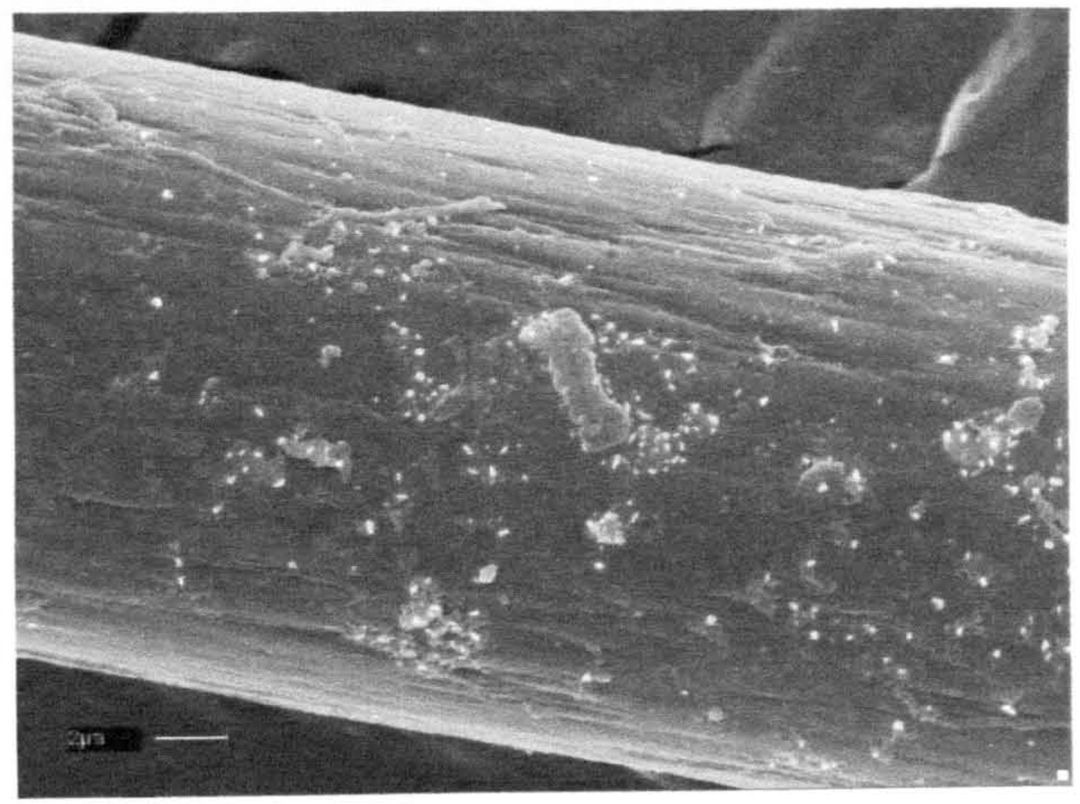

(c) dried fibre

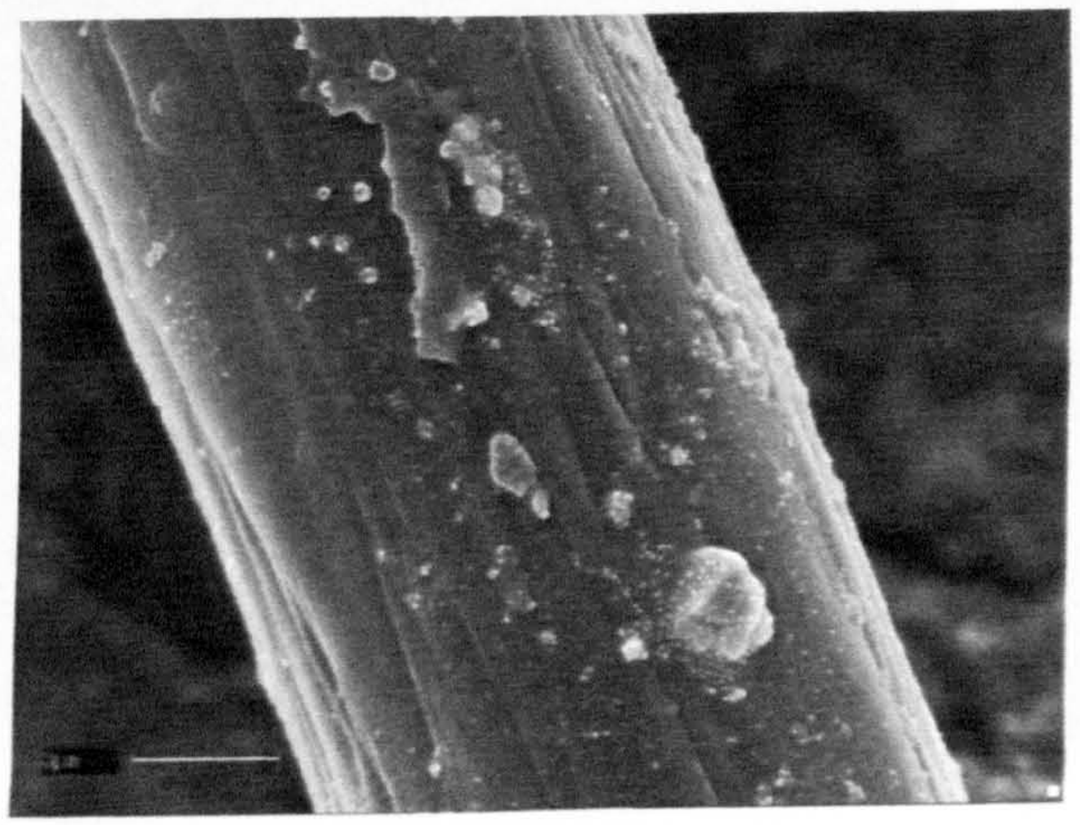

SVM (d) original fibre

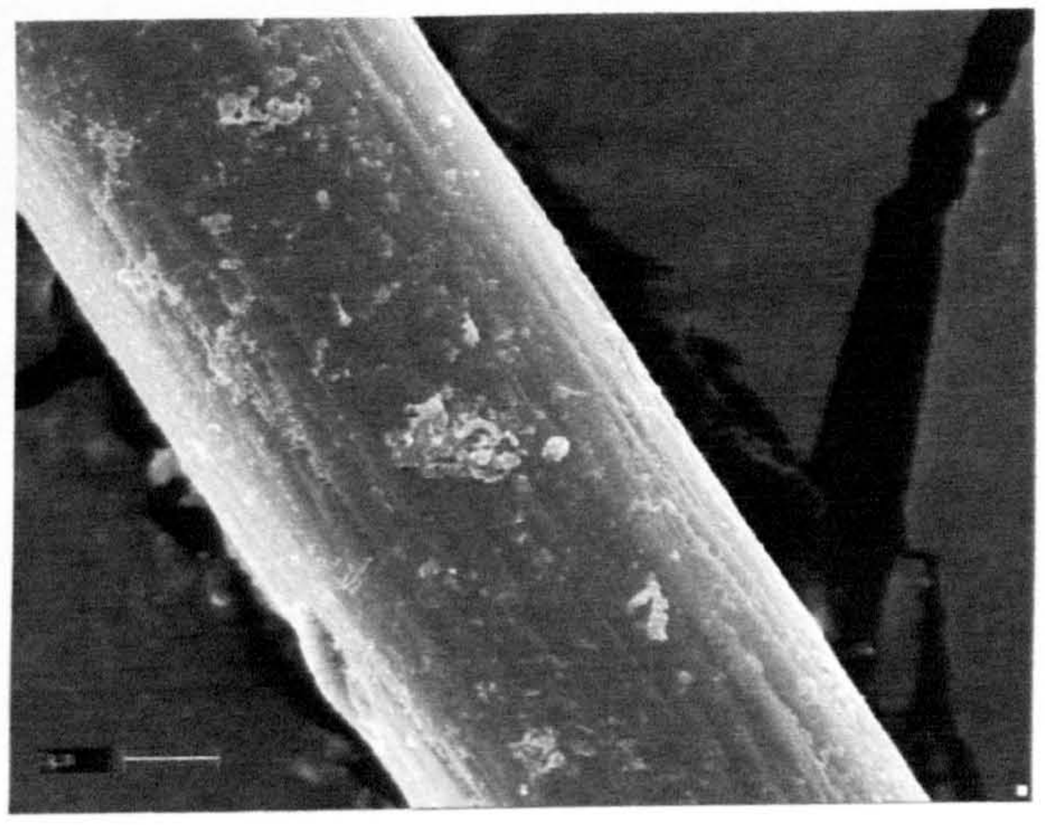

(e) stretched fibre

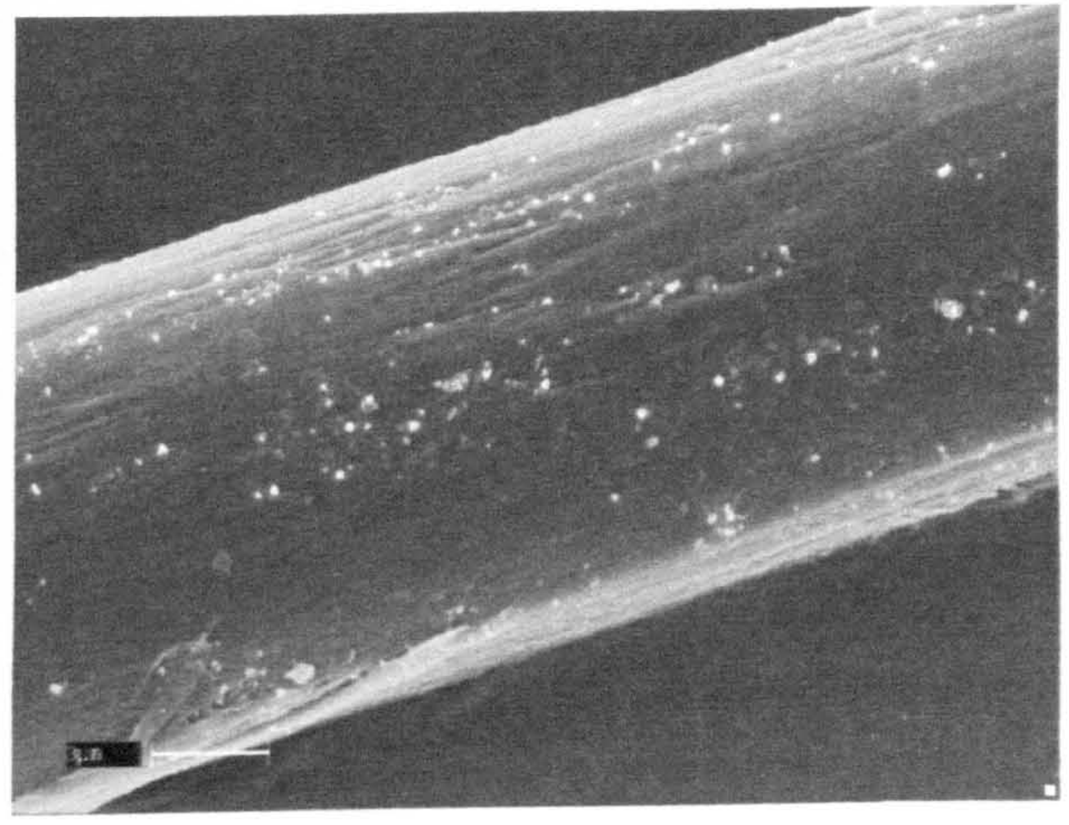

(f) dried fibre

Fig. 6.8 SEM pictures of Armos and SVM fibre surfaces

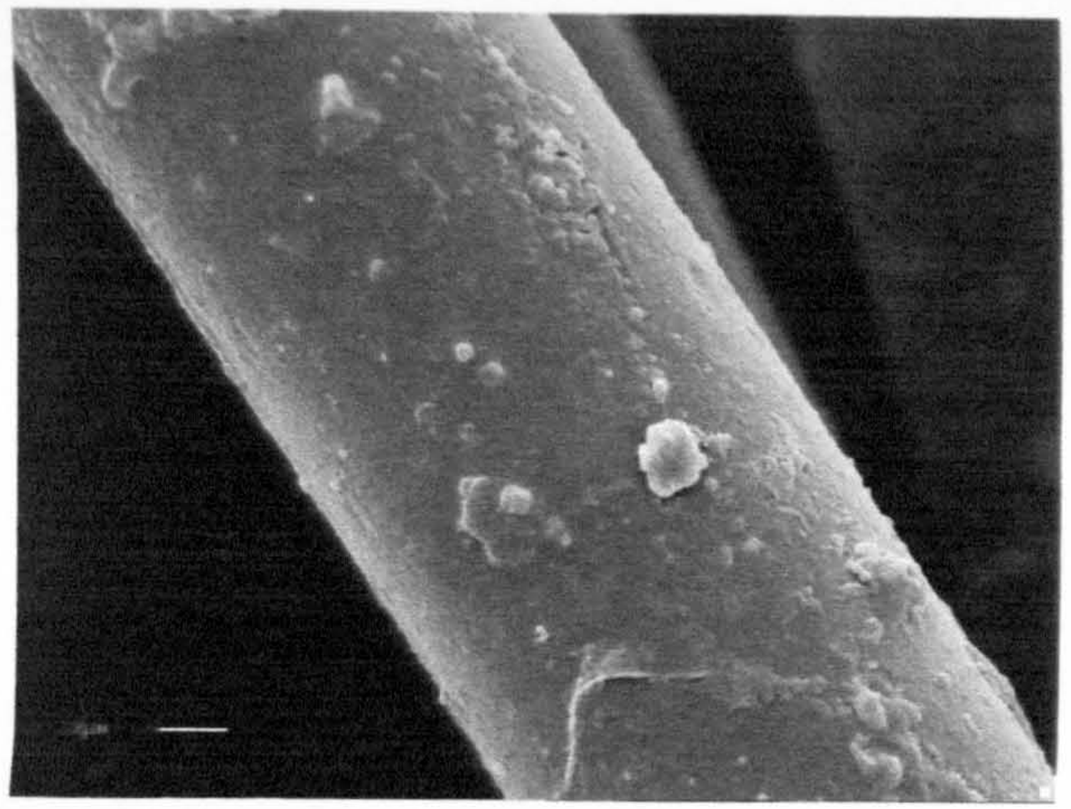

Terlon (a) original fibre

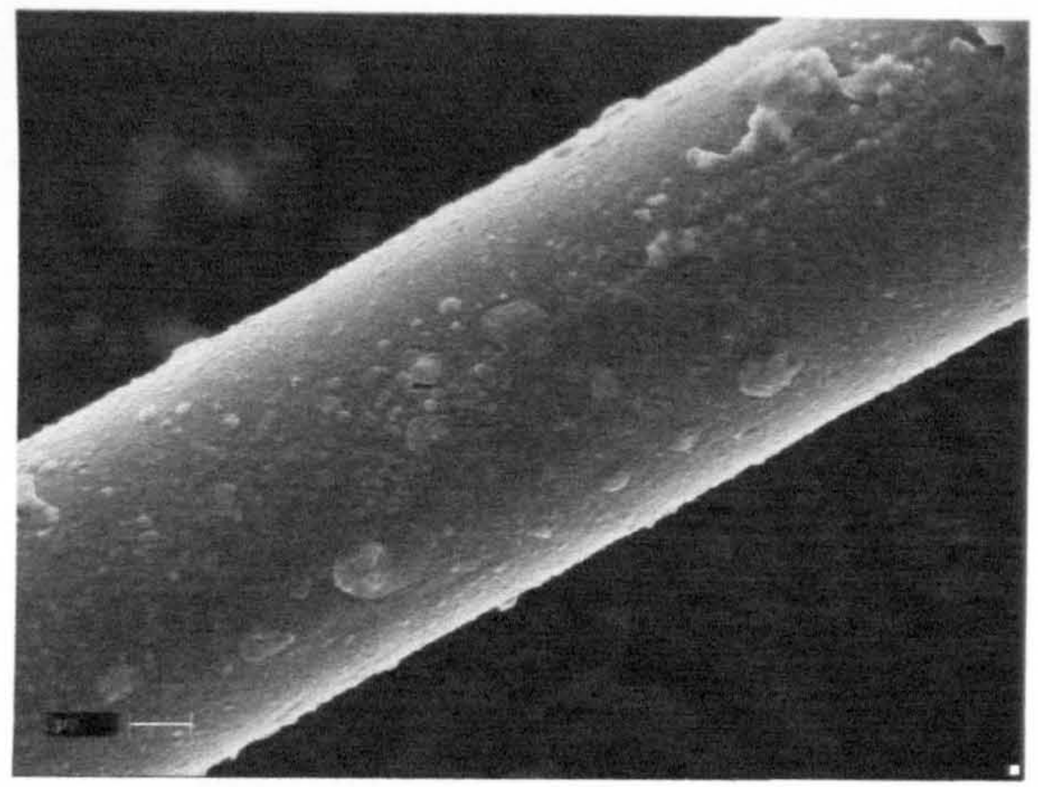

(b) stretched fibre

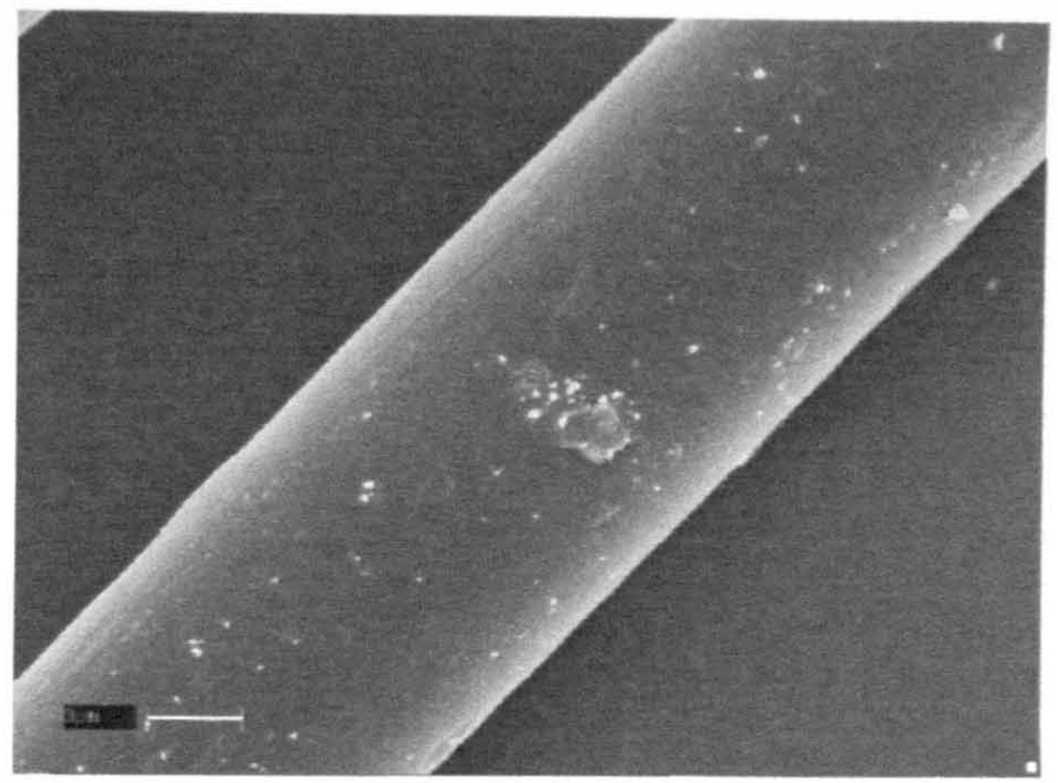

(c) dried fibre

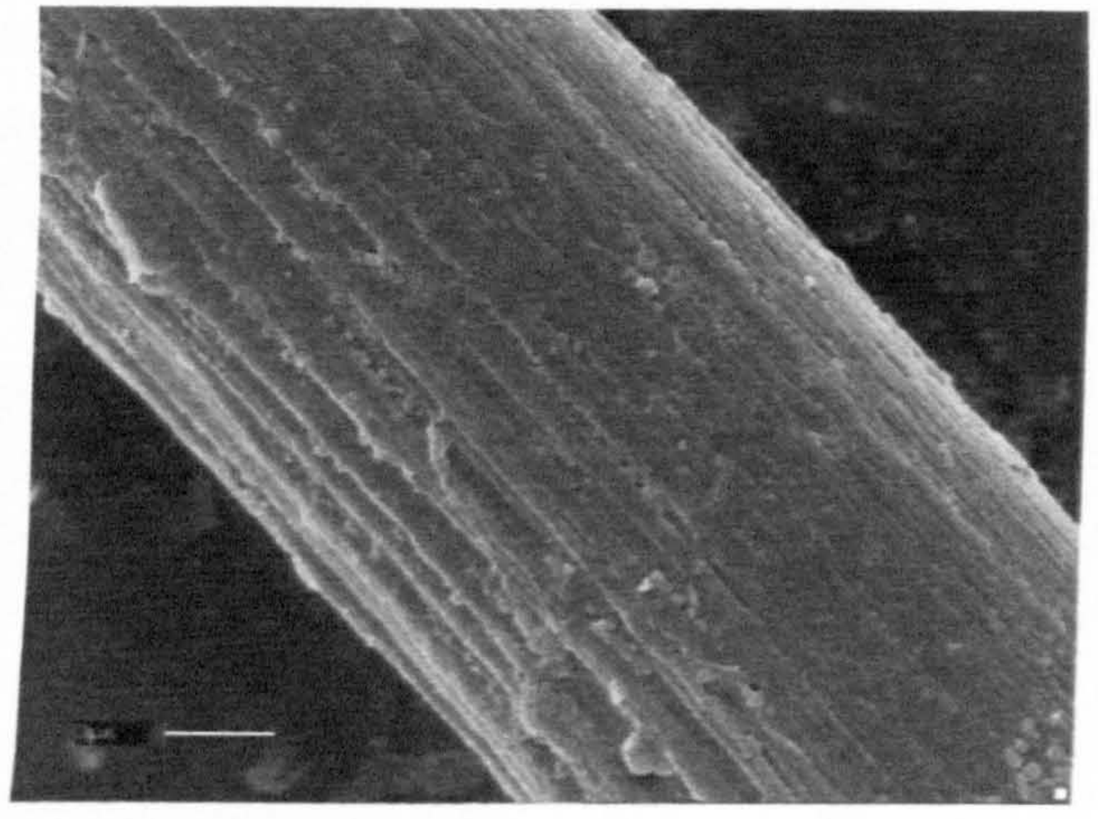

Phenylon (a) original fibre

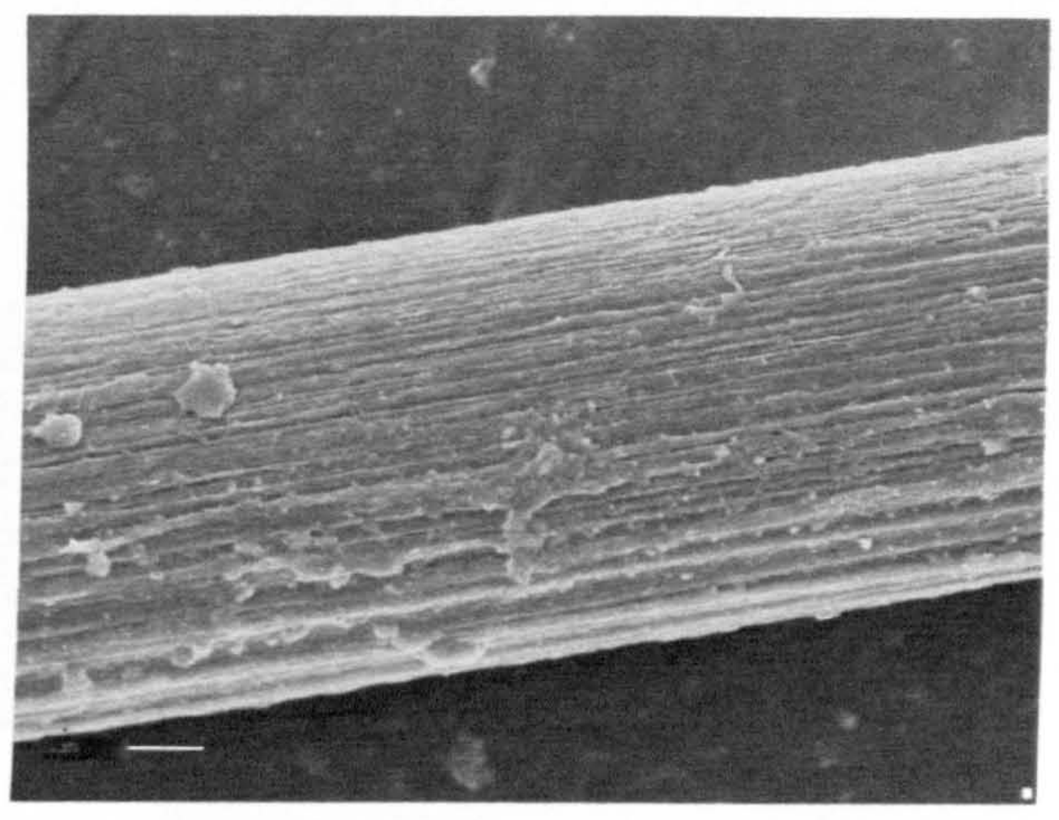

(b) stretched fibre

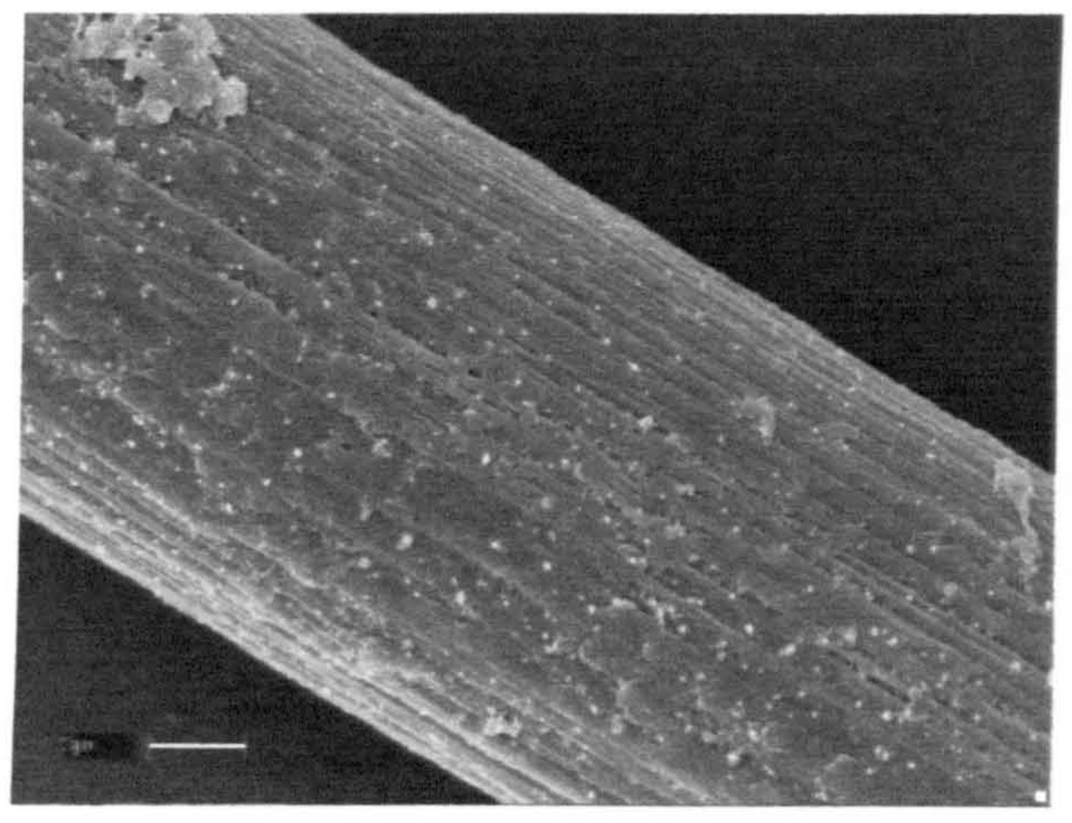

(c) dried fibre

Fig. 6.9 SEM pictures of Terlon and Phenylon fibre surfaces

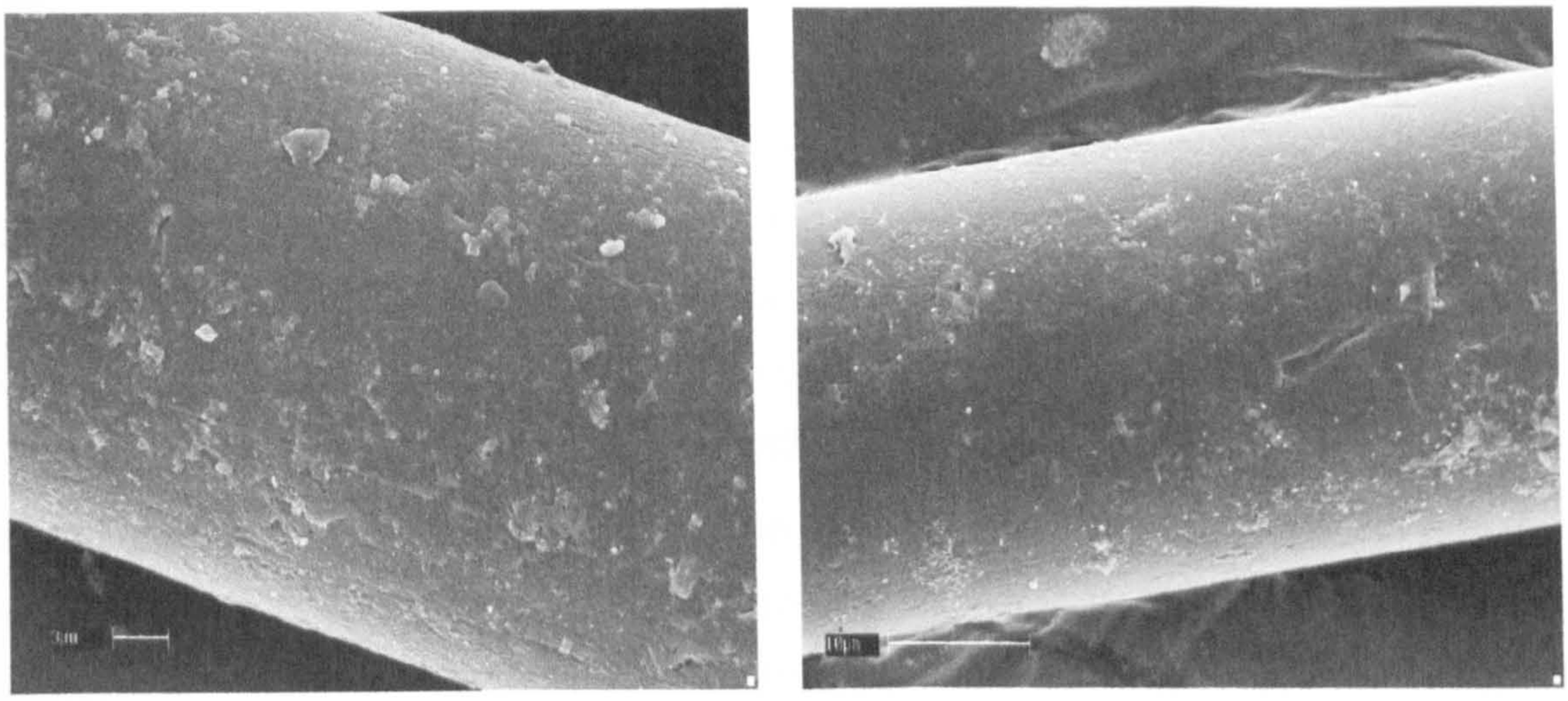

Capron (a) Original fibre (b) Stretched fibre

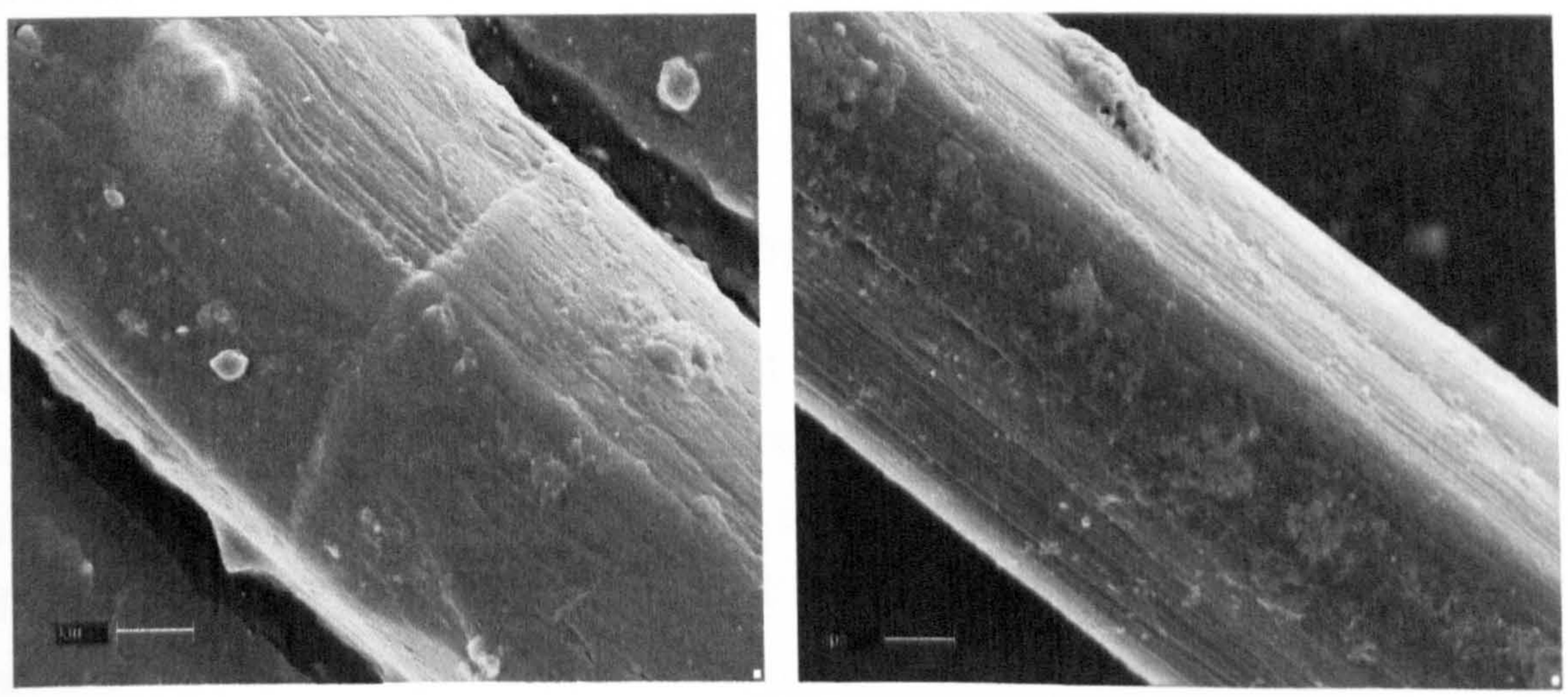

Polyethylene (c) Original fibre (d) Stretched fibre

Fig.6.10 SEM pictures of Capron fibre untreated (a) and stretched (b) and Polyethylene untreated (c), stretched (d)

Polyethylene fibre, similar to the Phenylon fibre has a clearly fibrilar surface. However in this case fibrils have the shape resemble belt formations (Fig. 6.10 c). The SEM images of the Polyethylene fibre also clearly show folds on the surface of the fibre, these are the so-called "bands of kink". The formation of kink-bands for Polyethylene has been reviewed in several reports (Marikhin, 1981; Marikhin, 1984). As shown by Marikhin, (1984) the high orientation of macromolecules in amorphous areas of high-strength Polyethylene fibres results in the highly anisotropic crystalline properties of these materials. In such materials, compression, bending and other kinds of deformation lead to the formation of kink-bands. The emergence of the kink-bands is connected with the presence of structural formations such as the microfibrils, most critical being the contacts of microfibrils tips, which serve as the initial loci of oriented polymer breakage (Marikhin, 1981). In the present study kink-bands were caused by the compression and bending processes during production of the fibre, attributable to orientation stretching.

6.4.2. Study of fibre breaking mechanism by SEM

Structural heterogeneity and defects present in oriented polymer fibres cause breaks of chains to occur in areas of greatest defects, resulting in the formation of microcracks. Such microcracks occurs in less oriented areas of the structure, i.e. in amorphous regions. Microcracks in the most defective areas of the structure may grow significantly during further stretching or merge with one another. The formation of a main crack will occur in the weakest part of a sample, and result in the final breakage of the sample. Fig. 6.11 shows that cracks occur before fibre breakage.

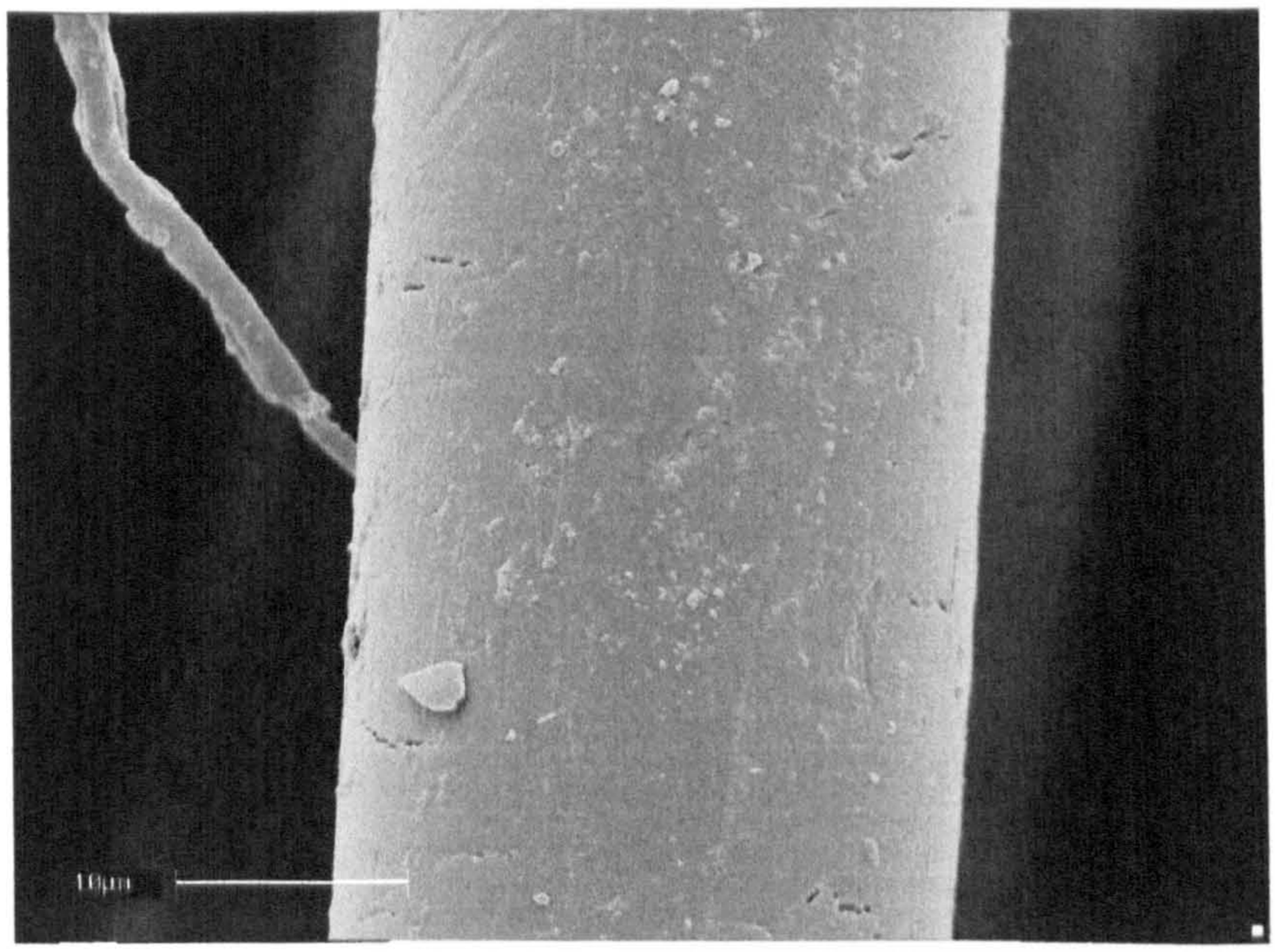

Fig. 6.11 SEM picture of fibre surface of Polyethylene just prior to breaking

Fig. 6.12 (a)-(c) shows breakage of fibre structures observed by SEM when fibres are subjected to force and stretched beyond the limit of breakage. It can be seen that fibres of Armos, SVM and Terlon fibrillate and eventually split along the longitudinal fibre direction during the process of breakage. The fibrilisation of SVM is clearly shown in Figure 6.13.

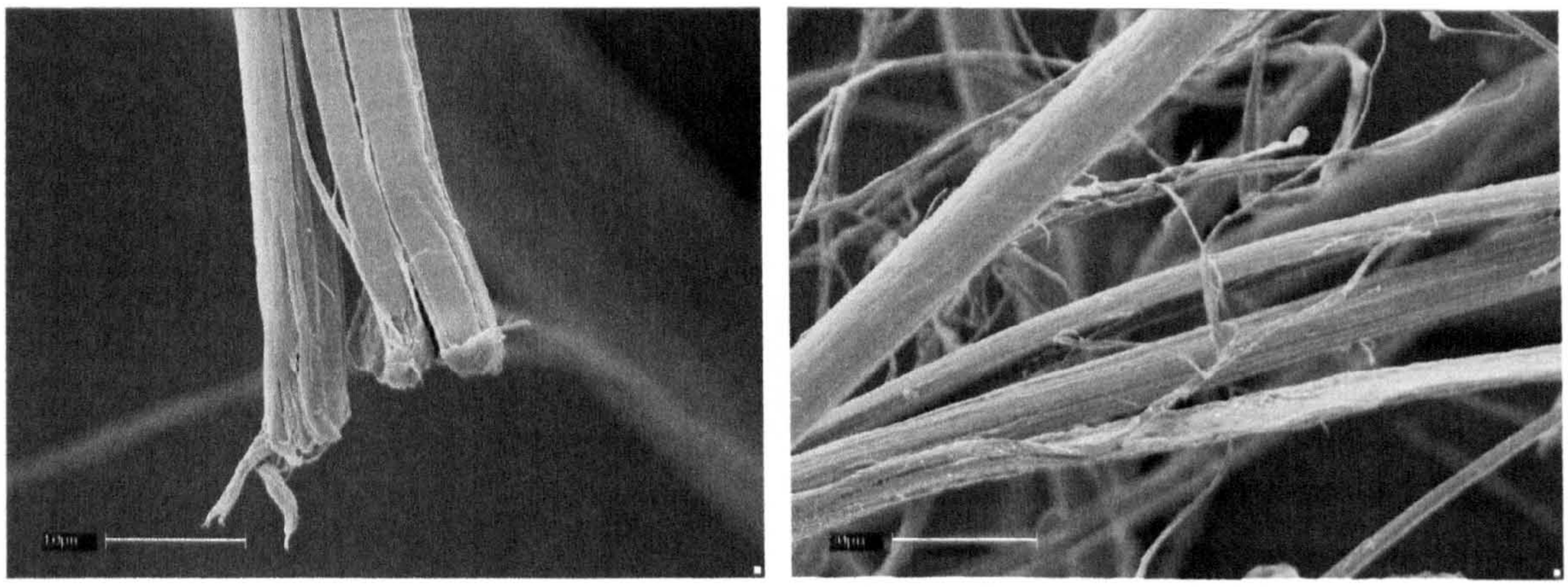

(a)

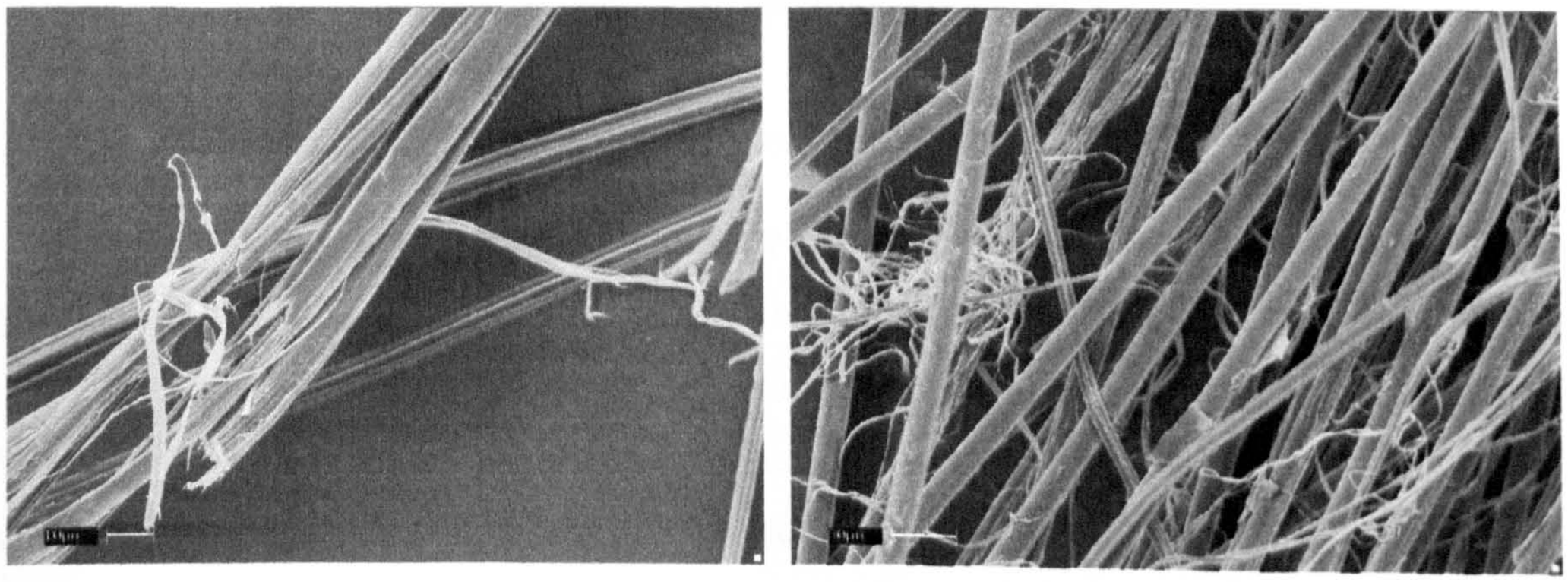

(b)

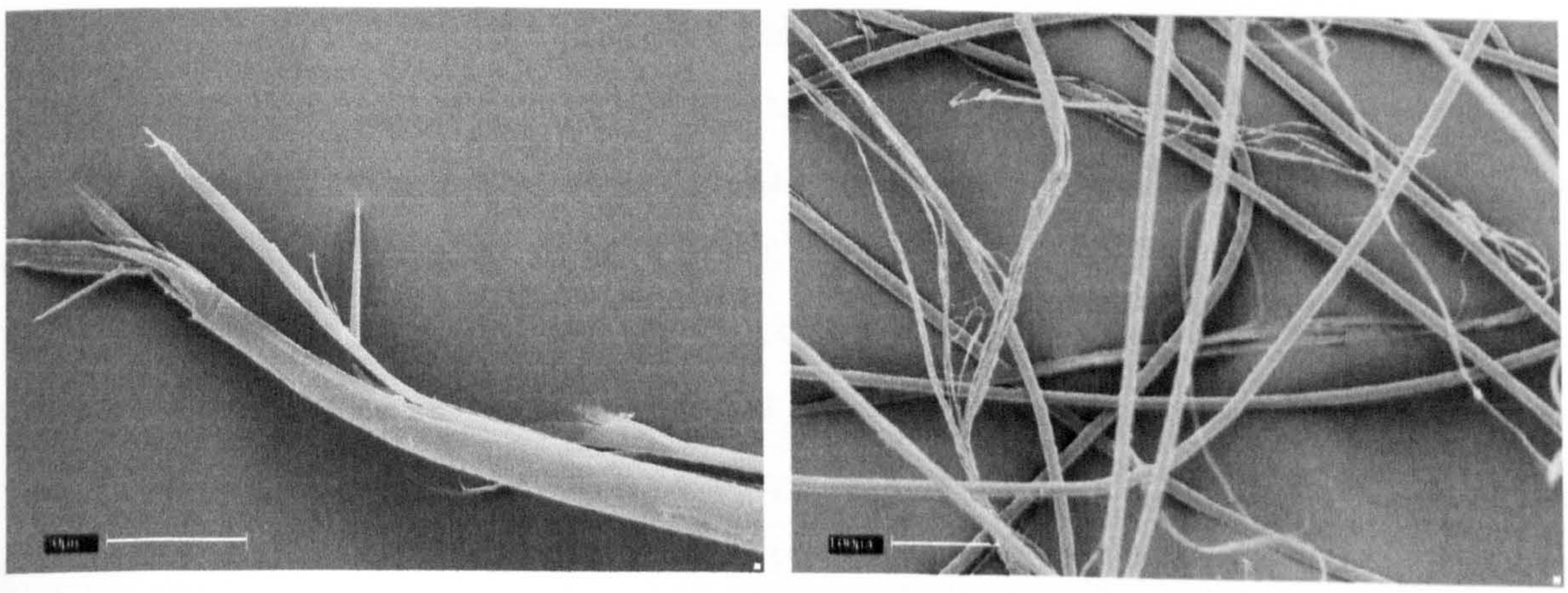

(c)

Fig. 6.12 SEM pictures of fibres after break: (a) Armos fibre; (b) SVM fibre; (c) Terlon fibre

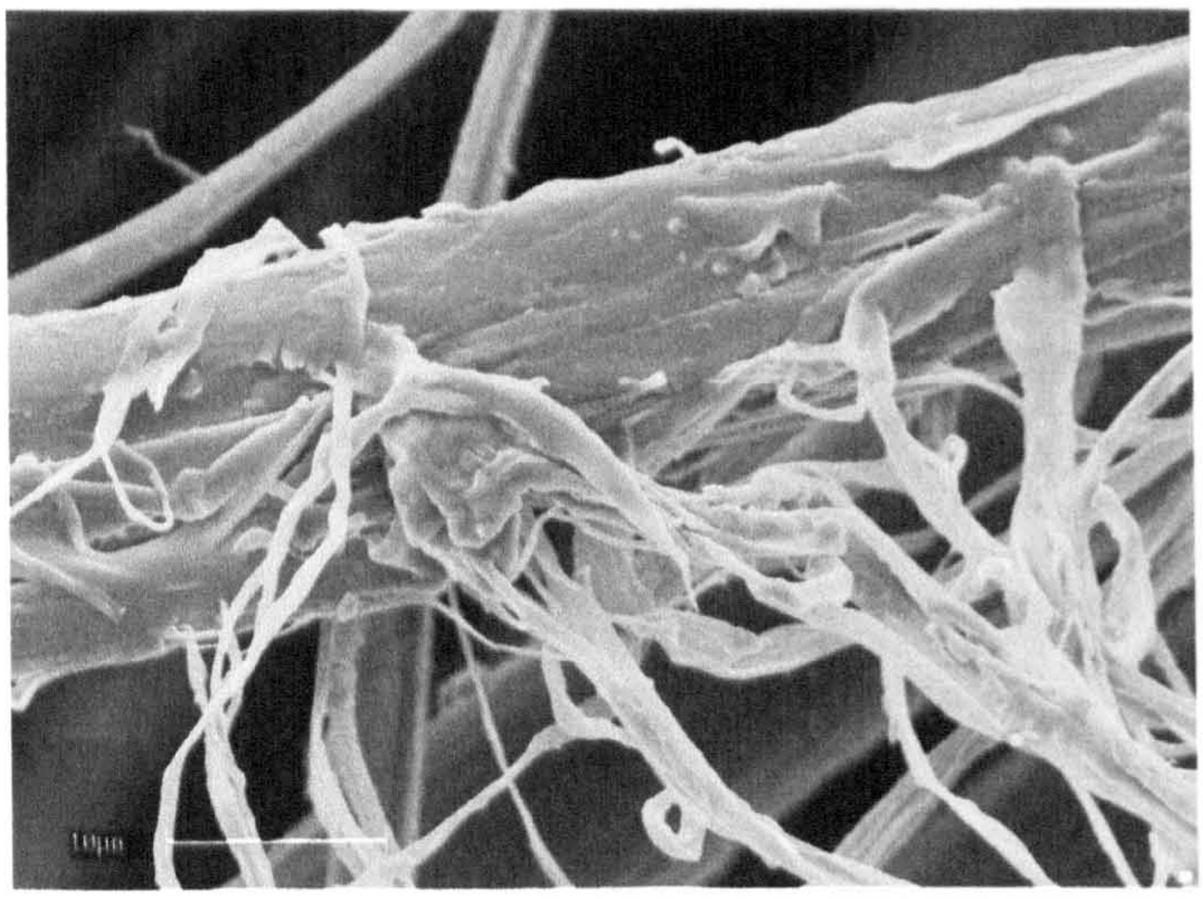

Fig. 6.13 SEM picture of fibre surface of SVM just prior to breaking

It is clearly seen that the fibres split at the point of breakage. However Phenylon, Capron and Polyethylene fibres exhibit different behaviour, and the breaking mechanism is different to the previous discussed para-aramides. The fibre ends after breakage for Phenylon and Capron are very sharp, and no fibrilisation has occurred (Fig. 6.14 a, b). Because the polymer chains in these fibres do not pack very closely, there are a large number of amorphous regions. Any cracks quickly extend throughout amorphous regions in the fibre. However it is found that fibre breaks cause explosion at the breaking point for Polyethylene fibre. This can be explained by significant local overstressing near to the zone of fibre breakage resulting in large deformations, which then relax after the break. This causes sudden distortions at the breaking point, and the formation of a "mushroom cap" at the breaking ends of the fibres (Fig. 6.14 c). Kirienko *et al* (1971) suggested that at the breaking point of the fibre some melting can occur. The reason for such melting might be due to the large amount of energy released at the moment of the break. Because Gel-spun Polyethylene fibre has high strength, melting temperature is not rather high, the energy released at the moment of break is sufficiently to cause melting of the fibre in the breaking area. The characteristics of crack formation depends on the structure of a fibre. A schematic representation of different types of break is shown in Fig. 6.15, and is in good agreement with previous work by Perepelkin (Perepelkin 1978 and 1985).

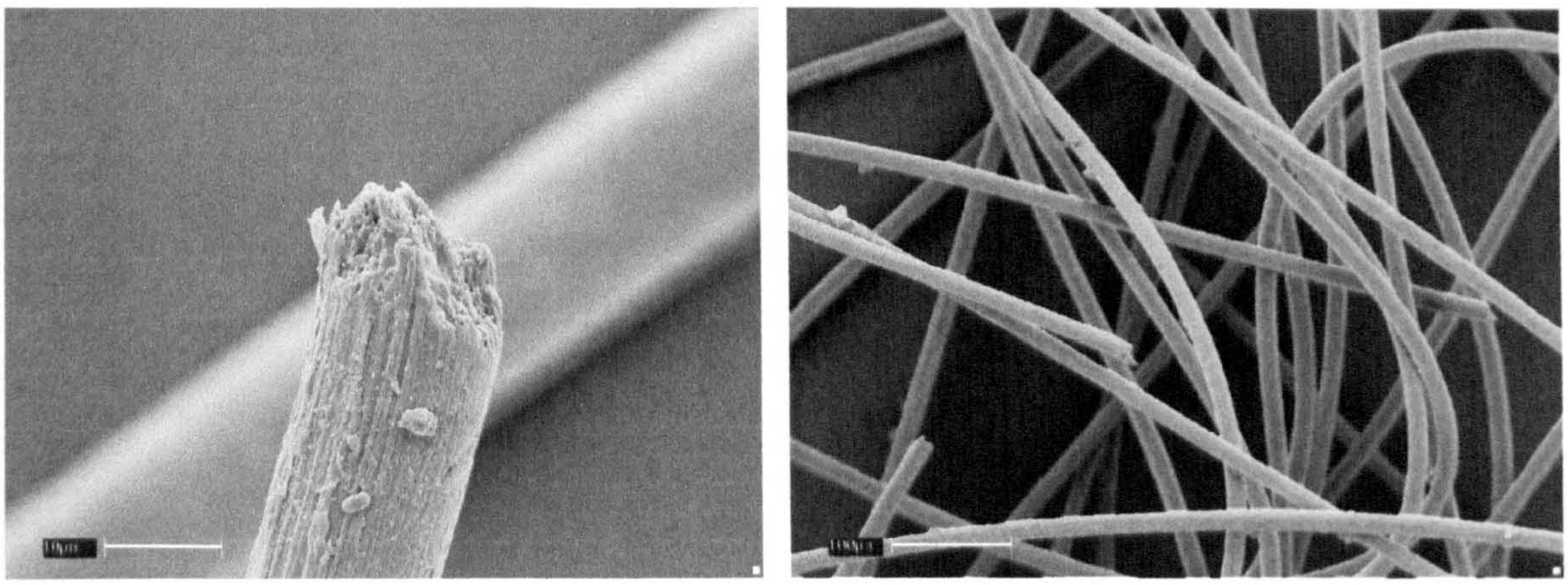

a)

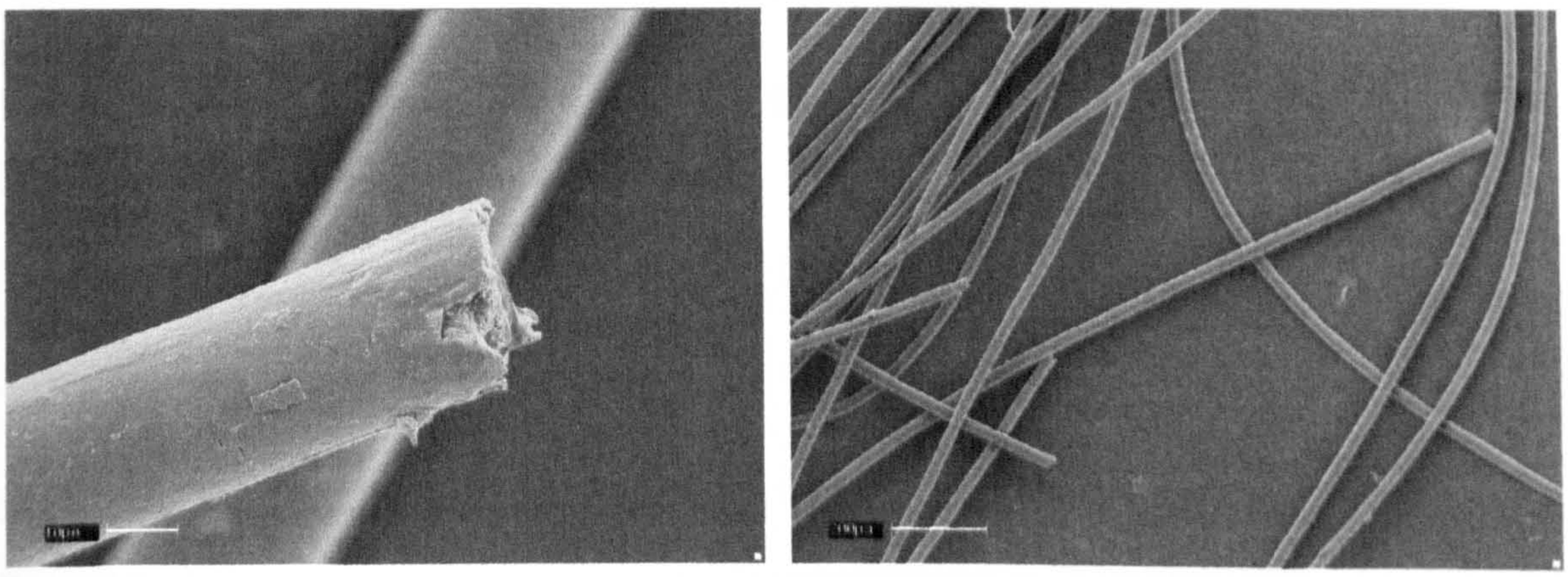

b)

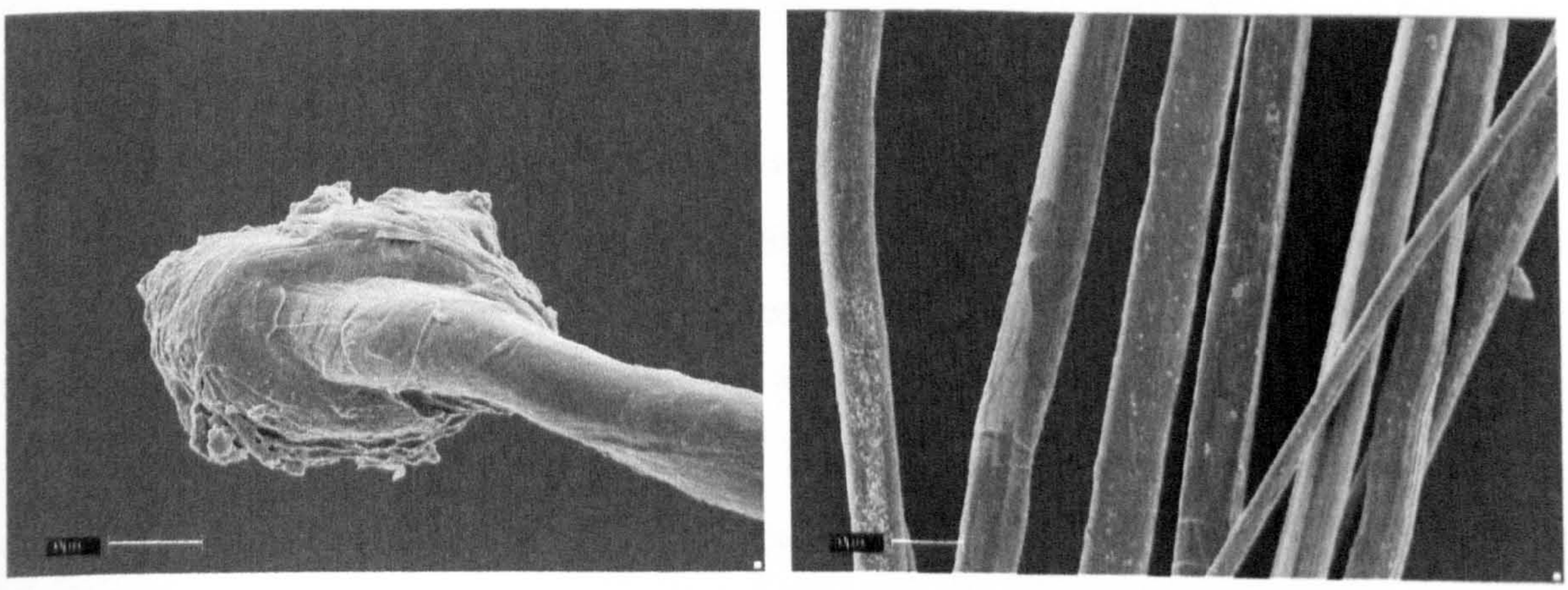

c)

Fig. 6.14 SEM pictures of fibres after break: (a) Phenylon fibre; b) Capron fibre; c) Polyethylene fibre

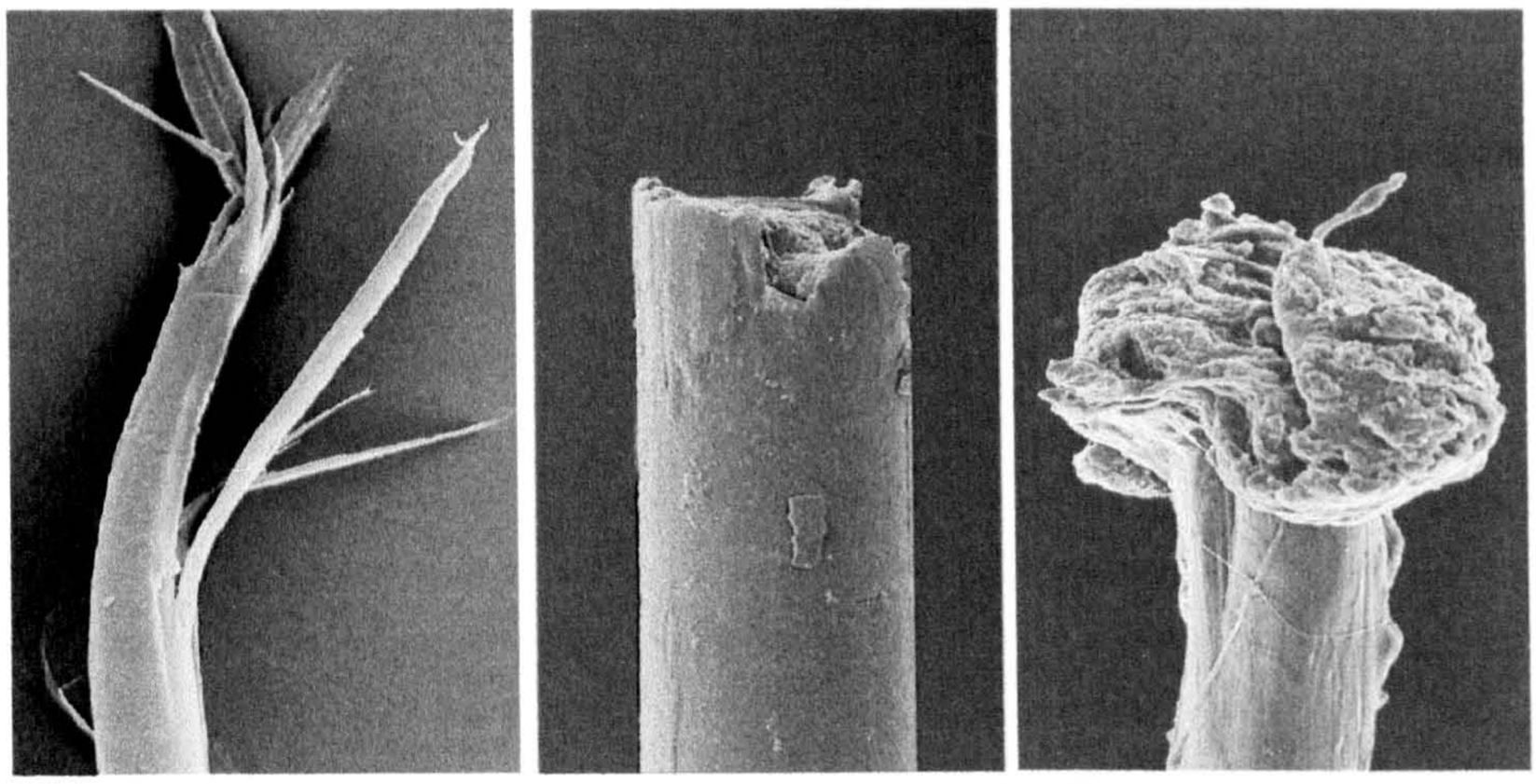

Fig. 6.15 Different types of fibre break a) The break with fibrillisation; b) The graduated break; c) The break with a thickening

6.6 Research of changes in fibre structure by a differential scanning calorimetry method

Differential Scanning Calorimetry (DSC) was carried out on SVM, Armos, Terlon, Phenylon, Capron and Polyethylene samples conditioned at 20°C and 65% r.h. or dried in a desiccator at room temperature respectively. Figs. 6.16-6.21 show the thermograms of original and dried SVM, Armos and Terlon. There are very small peaks around 90 to 130°C for the original samples. These peaks may be due to the vaporisation of water, because there are no corresponding peaks around that temperature for the dried samples. There are no glass transition temperatures for these rigid aromatic polyamides. This is due to the fact that the motility of large size and rigid molecular chains is hindered at lower temperatures. Glass transition for rigid chain polymers usually perceive first sings of the restricted motility which is different from motility in flexible chain polymers. Such first sing is not detected by the method of differential scanning calorimetry. It also shows that these aramides are very resistant to heat and only begin to decompose and char at temperature in excess of 400°C. This is due to specialities of their structure.

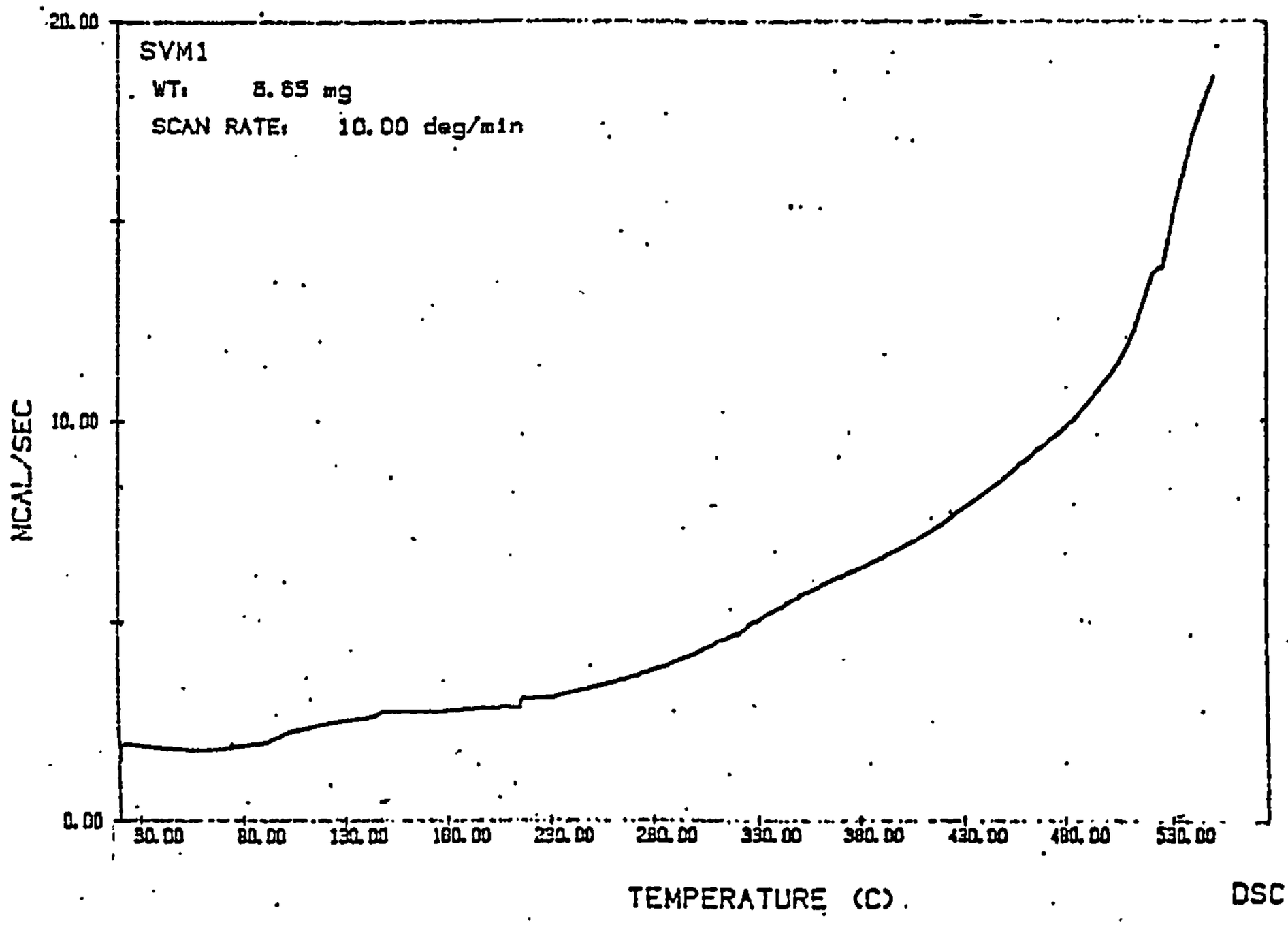

Fig. 6.16 DSC picture of original SVM fibre

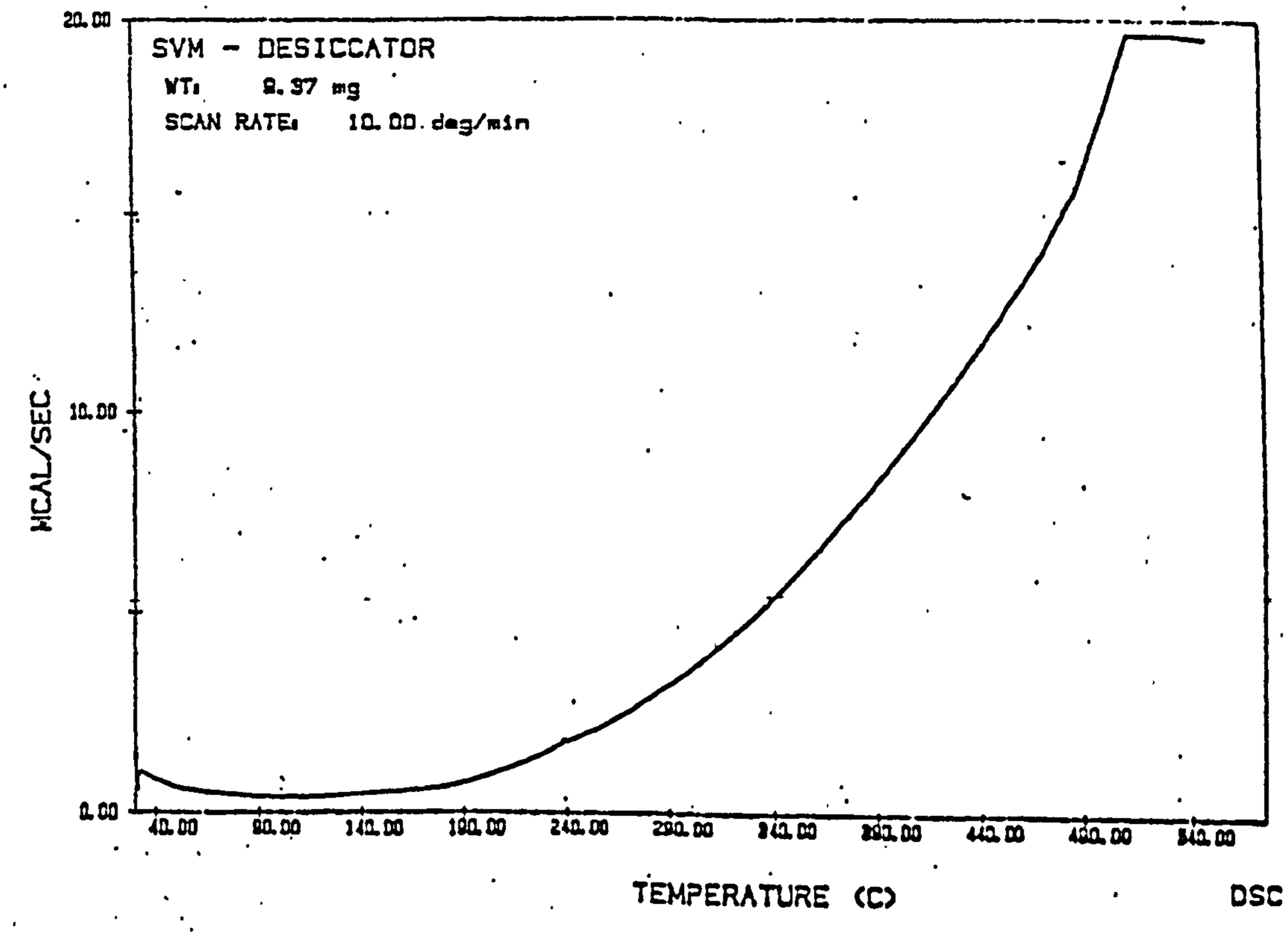

Fig. 6.17 DSC picture of SVM fibre dried at desiccator

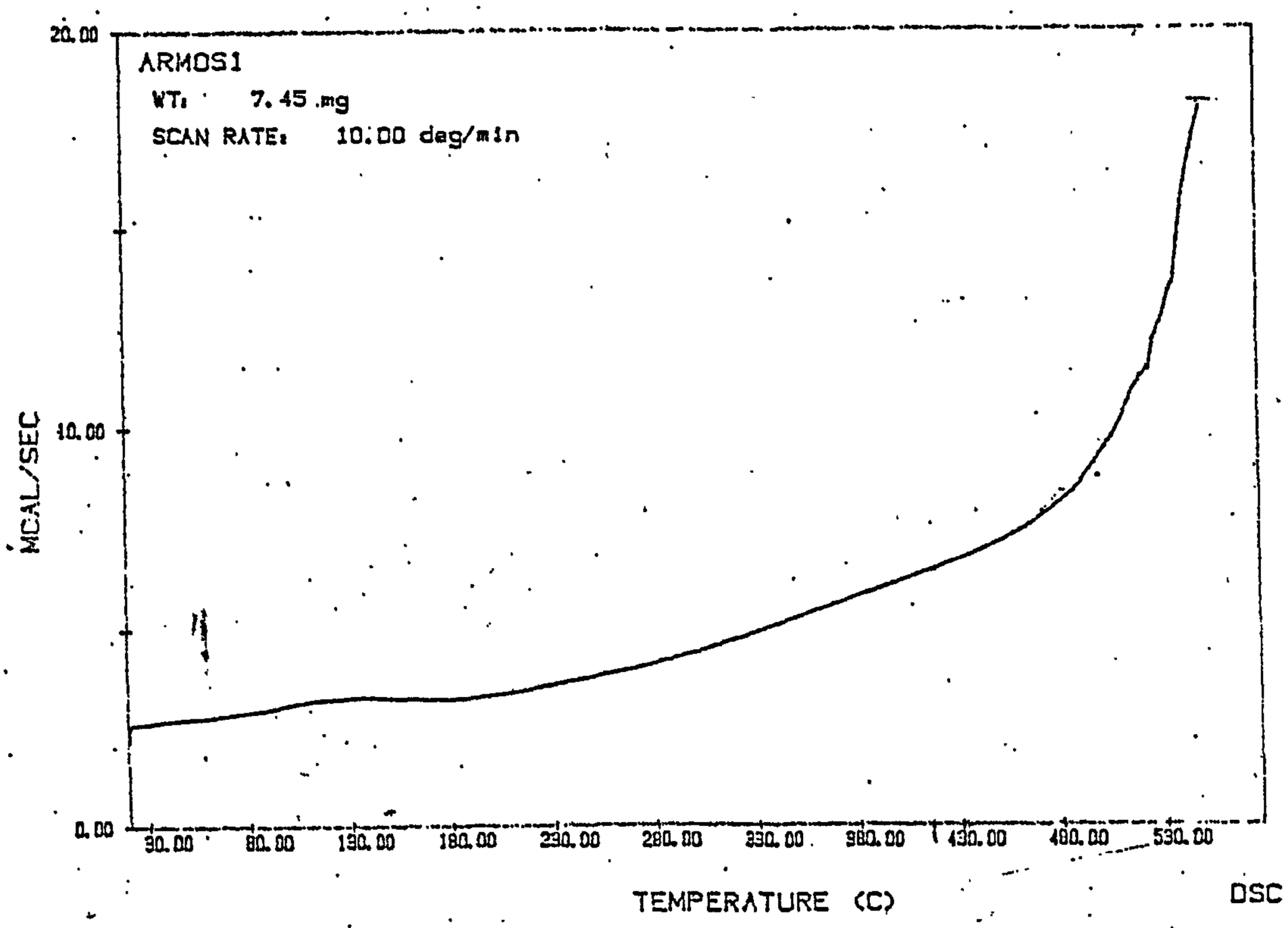

Fig. 6.18 DSC picture of original Armos fibre

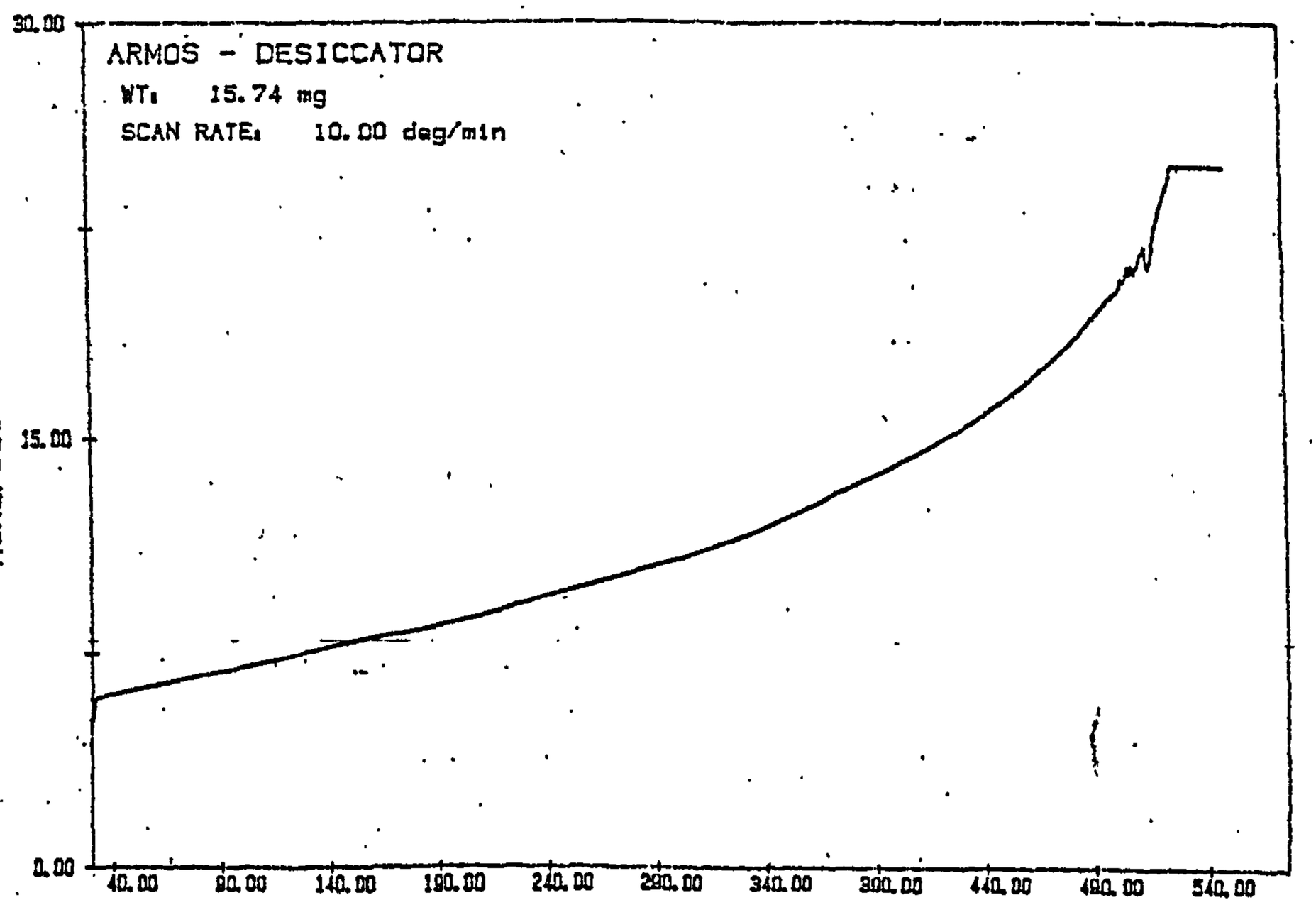

Fig. 6.19 DSC picture of Armos fibre dried at desiccator

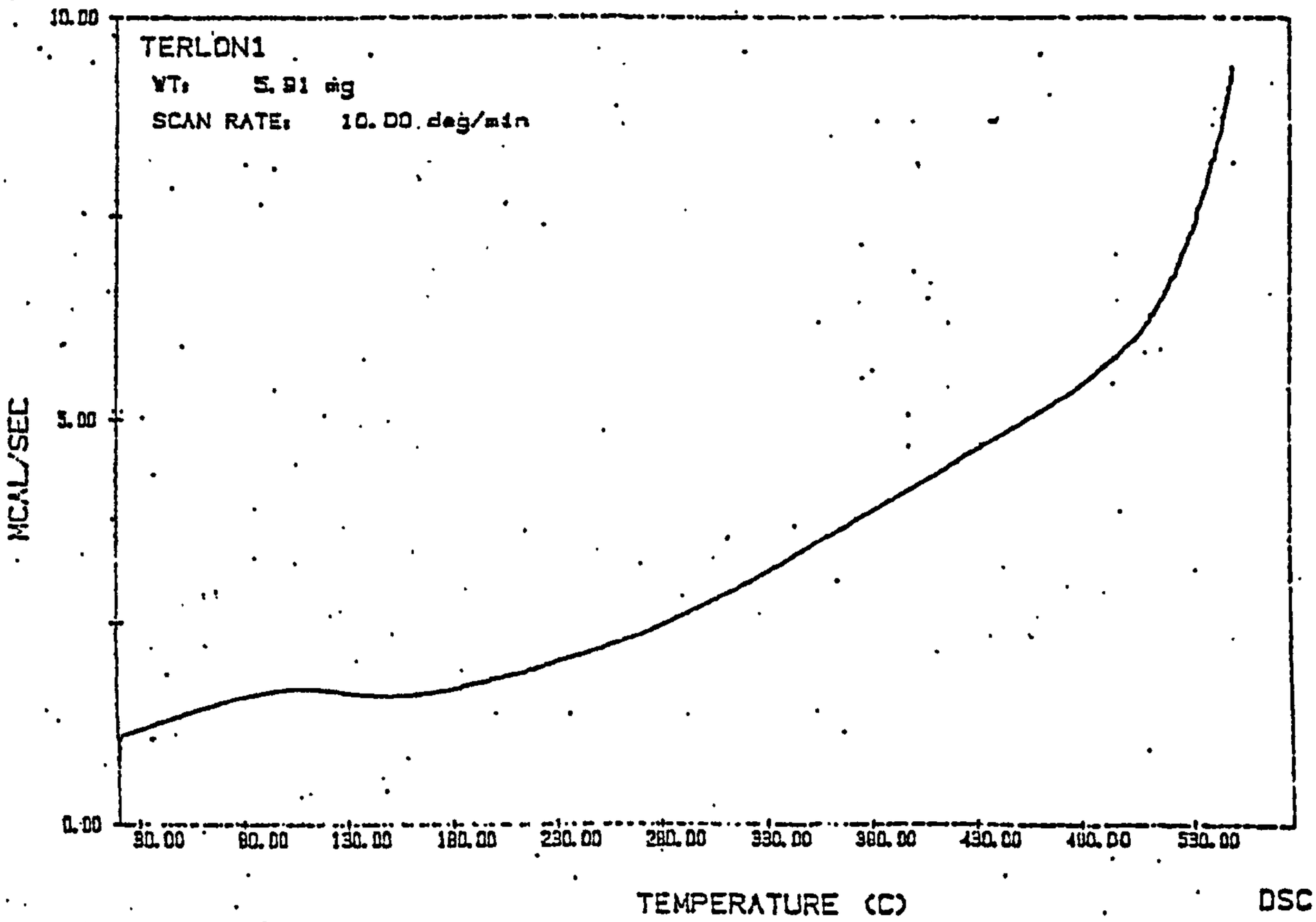

Fig. 6.20 DSC picture of original Terlon fibre

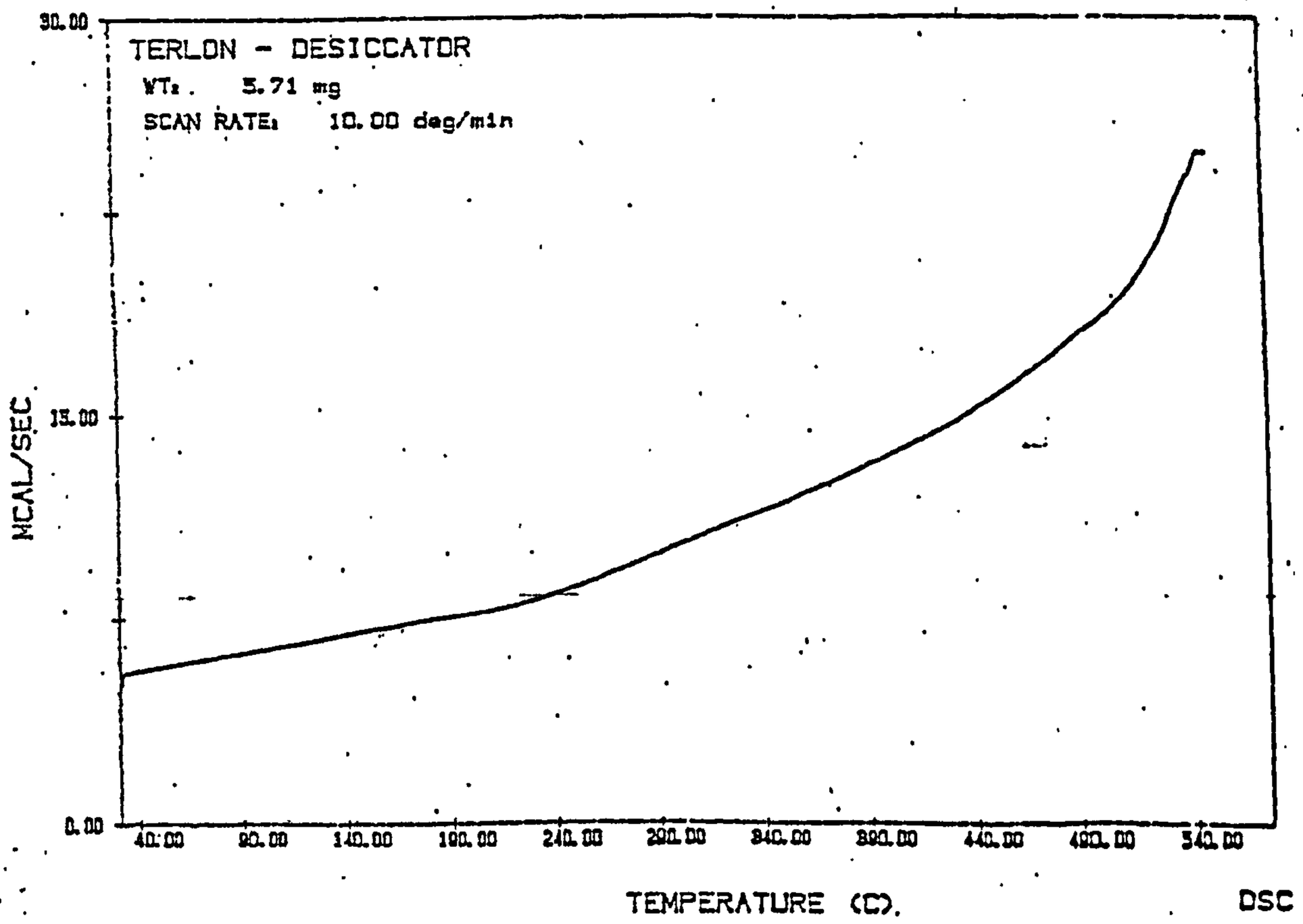

Fig. 6.21 DSC picture of original Terlon fibre dried at desiccator

Fig. 6.22 and 6.23 show the thermograms of original and dried Phenylon. The peak observed around 80-120°C in the thermogram of the original sample is due to moisture vaporisation. Comparing with the Terlon sample, the peak for Phenylon appears at a lower temperature than that for Terlon. This is due to the different chemical structure of the fibres. The SEM pictures of these fibre surfaces show that the Terlon fibre has a very smooth surface whilst the Phenylon fibre has many striations which would trap moisture in the fibre. Moisture located on the surface is easily vapourised. Phenylon is a meta-substituted aromatic polyamide whilst Terlon is para-substituted aromatic polyamide. Phenylon therefore has a reduced capability for close packing of chains and thus decreased intermolecular attraction force, than Terlon. This explains the fact that Phenylon starts to decompose at 405°C, and Terlon melts at 500°C. From Fig. 6.22, it can be seen that there is small shoulder around 280 to 380°C which might be due to glass transition.

Thermograms of Capron and Polyethylene fibre samples are shown in Figs. 6.24-6.26. These fibres are obtained from flexible polymers. From the literature, the glass transition temperature for Capron is approximately 40-65°C (Kudriyavtsev *et al.*, 1976). The peak around 65°C in thermogram of Fig. 6.21 might be due to the combination of glass transition and moisture vaporisation, as the glass transition temperature of dried Capron is lower at 35-40°C. The melting points for Capron and Polyethylene are 231°C and 140°C respectively. The difference can be explained by the fact that Capron has hydrogen bonds between the flexible polymer chains while Polyethylene only has Wan der Waals force between the neighbouring flexible chains. The higher the intermolecular attractive force, the greater the resistance to heat.

6.7 Conclusion

FTIR shows that new fibre Armos is very similar to SVM in chemical structure. Investigation of degree of hydrogen bonding and H-bonded moisture by FTIR was preliminarily carried out. The results can explain some change in mechanical properties due to the treatment condition.

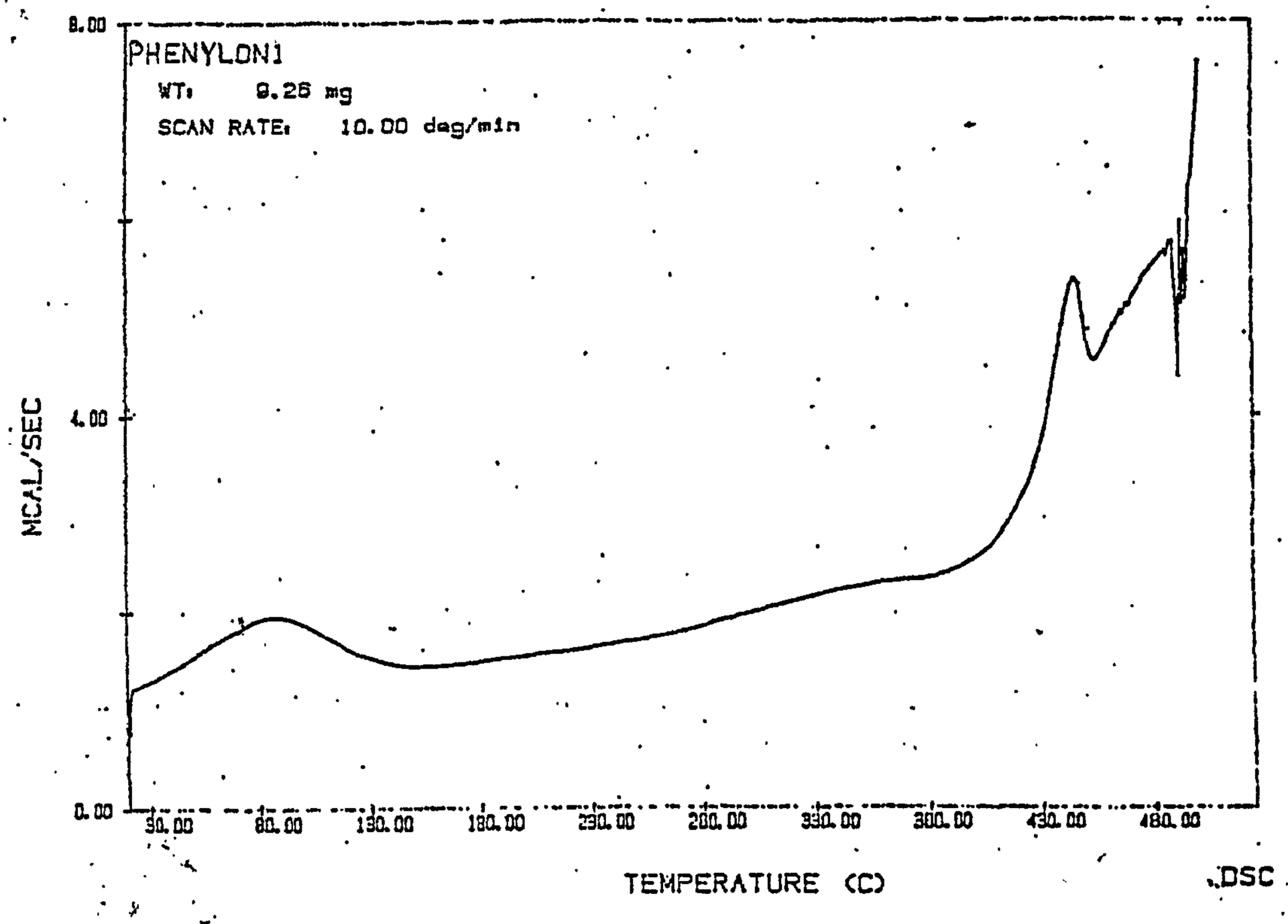

Fig. 6.22 DSC picture of original Phenylon fibre

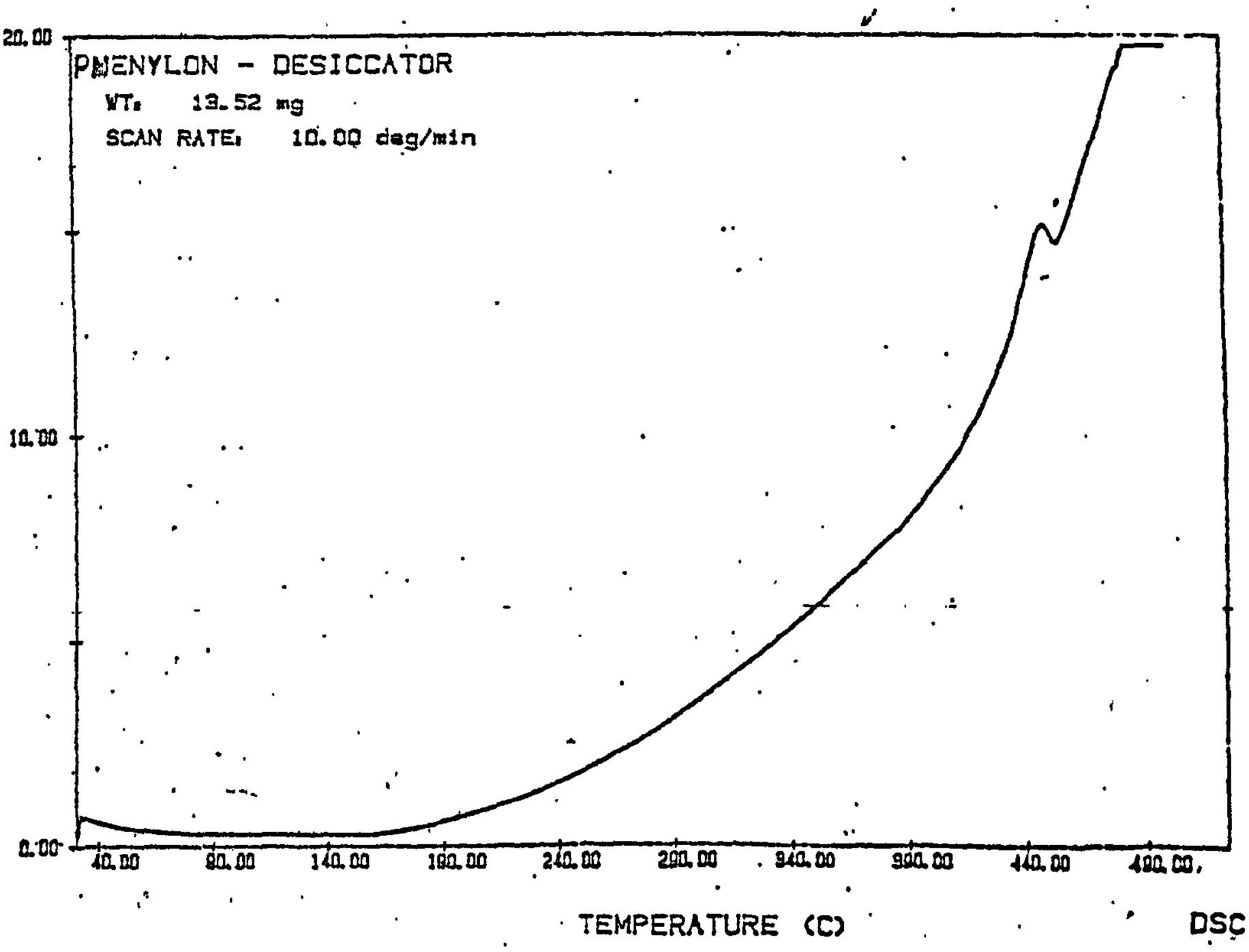

Fig. 6.23 DSC picture of original Phenylon fibre dried at desiccator

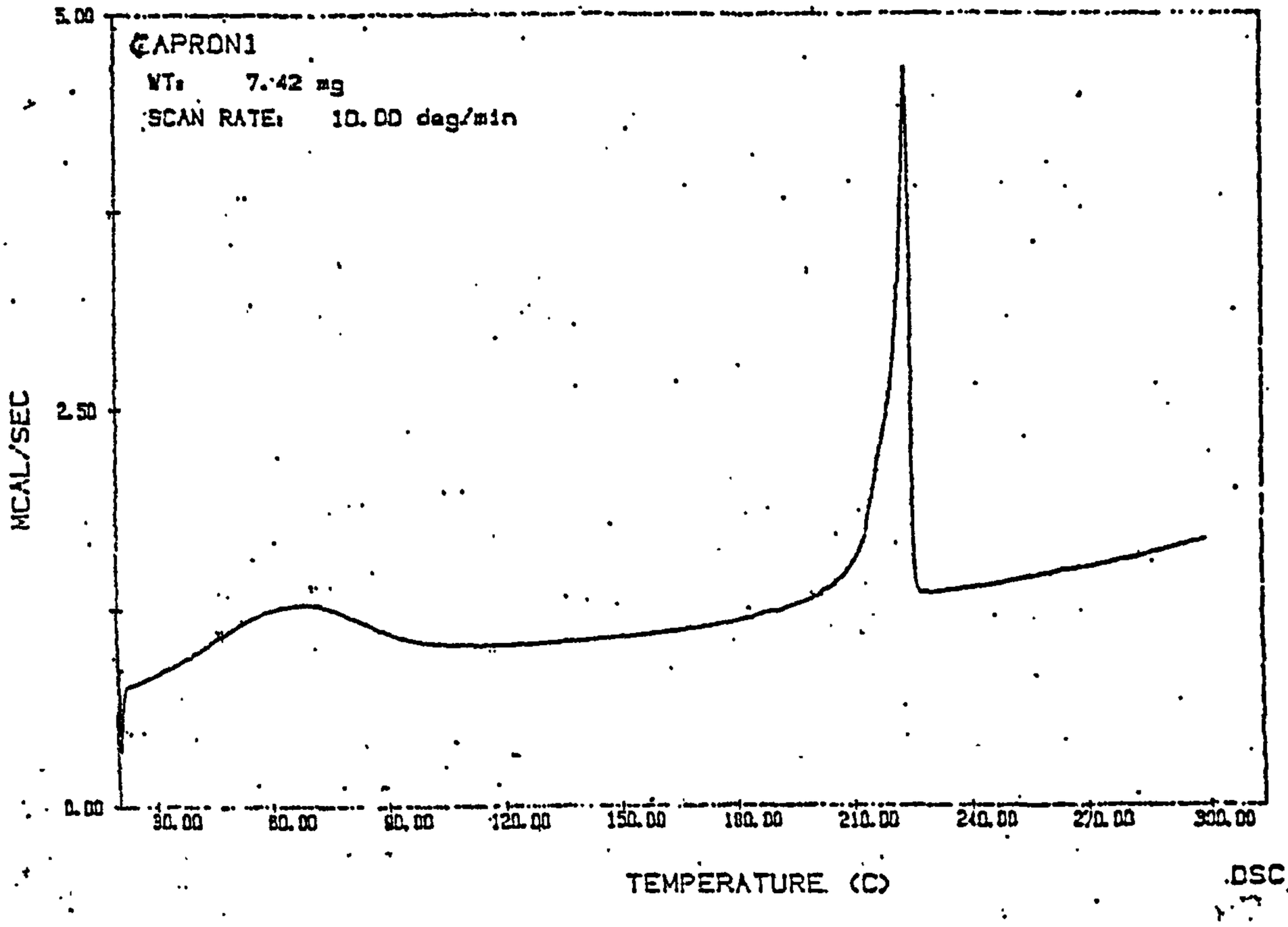

Fig. 6.24 DSC picture of original Capron fibre

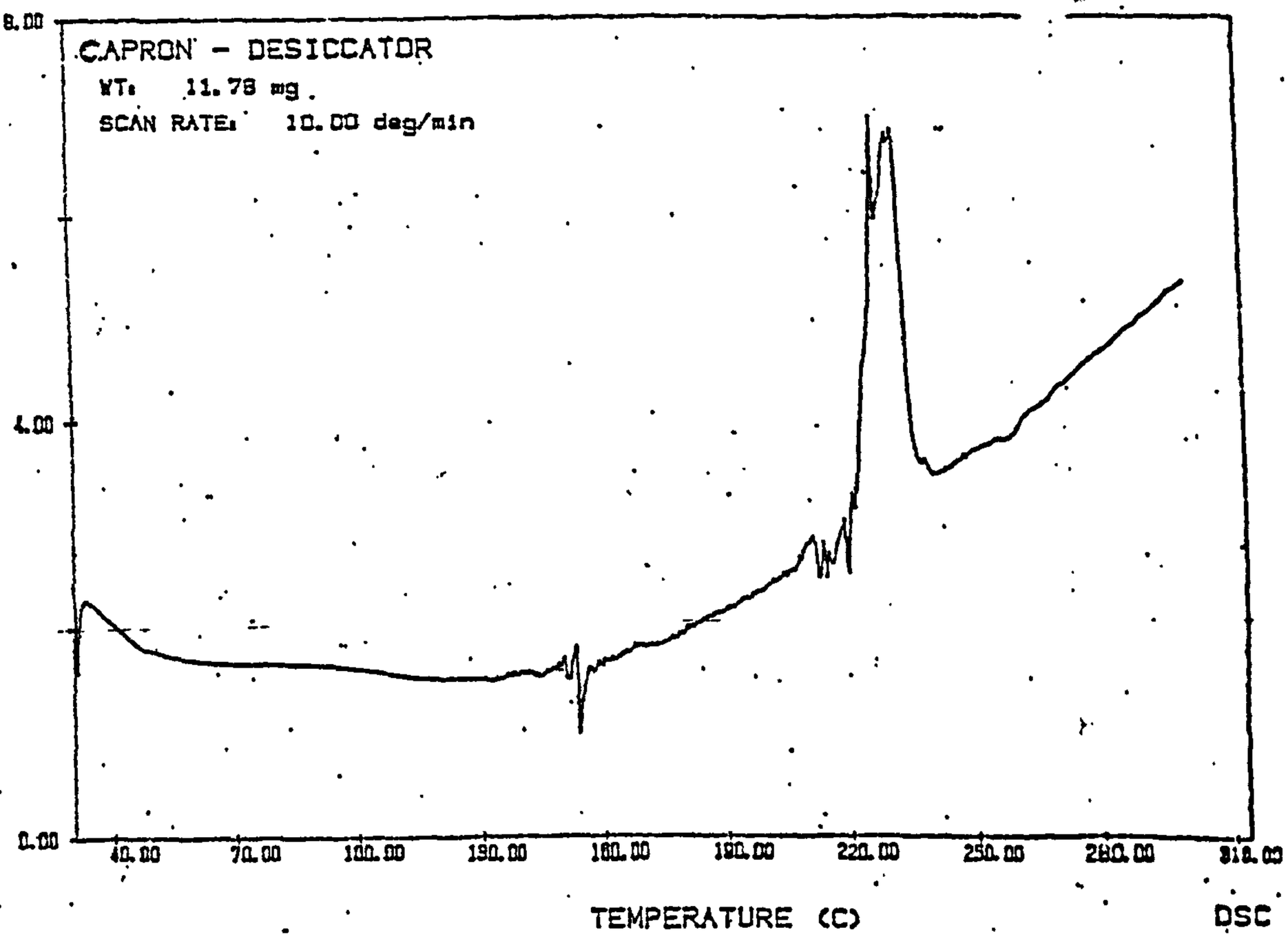

Fig. 6.25 DSC picture of original Capron fibre dried at desiccator

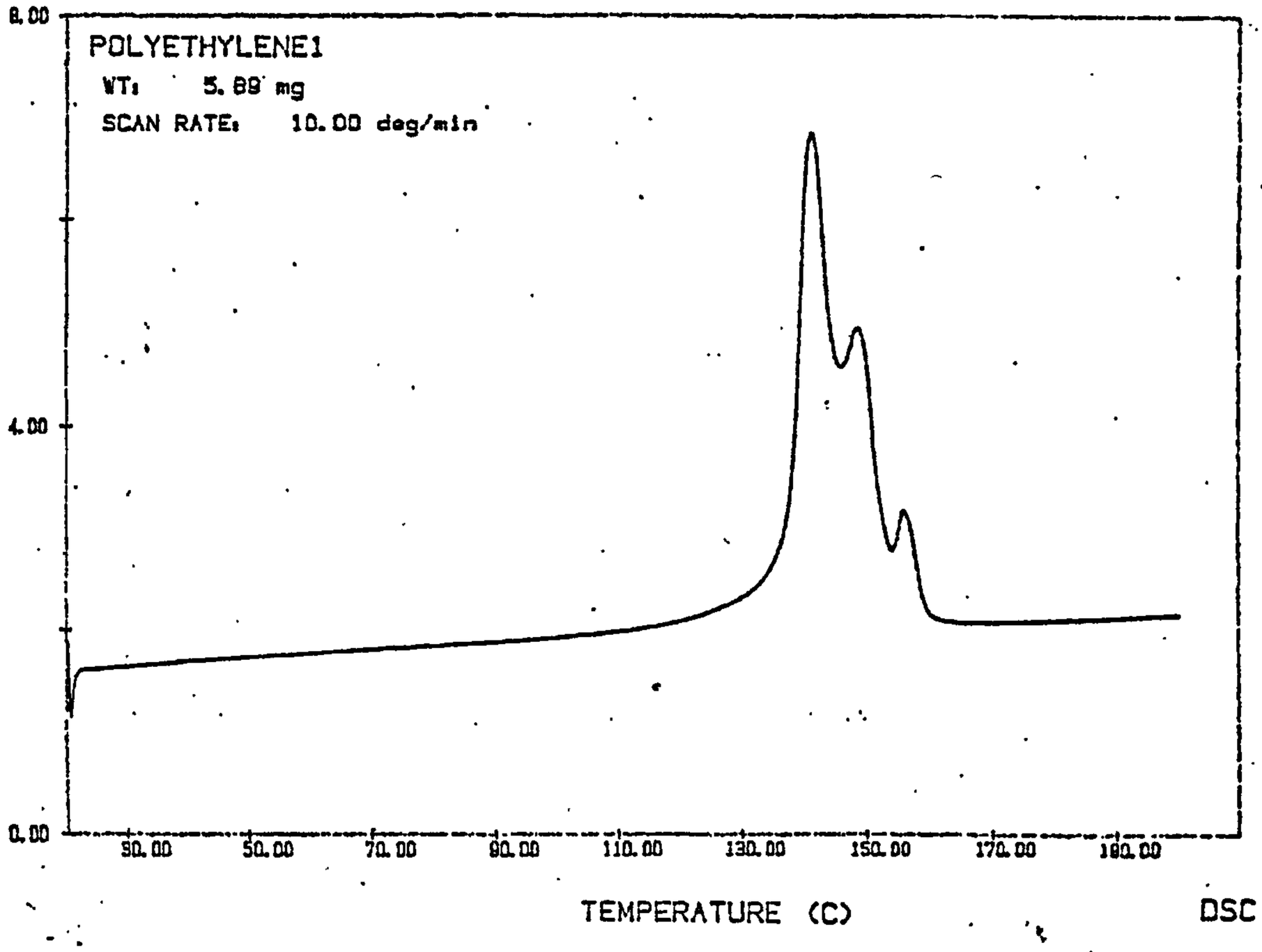

Fig. 6.26 DSC picture of original Polyethylene fibre

It is confirmed that the water molecules might be involved in intermolecular H-bonding in the "polymer-water-polymer" type for Armos fibres. But intermolecular H-bonding in SVM is mainly in "polymer-polymer" type.

Stretching of the Terlon yarn results in an increase of H-bonded moisture content. This might be due to partial disrupter of crystalline areas. For Phenylon fibres, the moisture is contained mainly in dissociation traps within the fibre. Dehumidification is possible after concomitant stretching and drying due to the mechanical breakage of dissociation traps upon stretching. It is thought that the presence of moisture and nature of hydrogen bonds do not exert a significant influence on the structure and properties of Phenylon fibre.

Study of fibre breaking mechanism by SEM shows that breakage characteristics are different between rigid chain polymer, semi- or flexible chain polymer and gel-spun polyethylene. Fibrillation occurs during breakage of Armos, SVM and Terlon fibres. The graduated break is characteristic for Phenylon and Capron fibres. The PE fibre breakage is accompanied a thickening. A schematic representation of different types of break is given.

DSC experiments show that the rigid aromatic polyamide fibres are very resistant to heat. SVM, Armos and Terlon fibres decompose at very higher temperature around 500°C. No glass transition temperature is detected. That is due to the fact that the motility of large size and rigid molecular chains is hindered at normal temperature. Phenylon (semi-rigid m-aramid fibre) starts to decompose at 405°C. Flexible chain polymers such as Capron and Polyethylene fibres have glass transition temperature before melting. The higher the intermolecular attractive force and chain rigid, the greater the resistance to heat.

CHAPTER 7

GENERAL CONCLUSIONS

Synthetic polyamide fibres have been widely studied, especially aromatic polyamide fibres become of major interest as super high strength, rigid and thermally stabled. Mechanical properties of fibres highly depend on their structure including rigidity, crystallinity and orientation. The analysis and comparison of deformation and strength properties of polyamide yarns formed from rigid chain polymers (Armos, SVM and Terlon), semi rigid chain polymers (Phenylon) and flexible chain polymers (Capron) provide more information towards the understanding of structure-property relationships. Polyethylene differs from aliphatic polyamides which have amide groups, that are capable of forming intermolecular hydrogen bonds between adjacent polymer chains. Therefore Polyethylene yarn is also used for comparison. Table 7.1 summarizes some information about these fibres. Investigation has focused on the interaction between the intermolecular chains of rigid; or semi rigid; and flexible polymer fibres.

Table 7.1 Characteristics of polymer yarns

Fibres	Polymer chains			Orientation	Crystallinity
Terlon, Kevlar	Aromatic	Symmetrical	Rigid	High	High
SVM, Armos	Aromatic	Symmetrical	Rigid	High	Para
Phenylon	Aromatic	unsymmetrical	Semi-Rigid	normal	Partial
Capron	Aliphatic	Symmetrical	Flexible	normal	Partial
Gel-spun Polyethylene	Aliphatic	Symmetrical	Flexible	High	High

Polyamide fibres such as Armos, SVM, Terlon, Phenylon and Capron present different characteristic in chemical structure and performance in mechanical properties (see Table 7.2). Terlon (poly(p-phenylene terephthalamide)) fibre has very highly symmetrical para-aramid structure with parallel, densely packed chains and leads to high crystallinity. In consequence, Terlon has a high elastic modulus and a low breaking strain. However the

chemical structure for Phenylon fibres is meta-aramid and unsymmetrical. The meta links hinder a high degree of structural organization. It can not be packed as clearly as the rigid chain polymers. In consequence, Phenylon shows mechanical behaviour typical of a partially crystalline polymer and similar to that of aliphatic polyamides such as Capron. Armos and SVM also show high strength and high modulus due to their rigid aromatic copolymer chains which are highly oriented. The chain rigidity for Armos and SVM might be higher than that for Terlon. It is concluded that chain stiffness obviously affects the initial modulus. The other major factors such as extension of polymer chains, orientation and possibility of symmetrical structure directly affect on strength and modulus of polymer fibres. It is noticed that Terlon has very high degree of crystallinity while Armos and SVM have only semi-crystalline in structure, but breaking strength and initial modulus for Armos and SVM are higher than that for Terlon.

Table 7.2 Mechanical properties of yarns

Fibres	Strength to break, GPa	Elongation to break, %	Initial modulus, GPa
Armos	3.9	4.6	113
SVM	3.3	4.5	112
Terlon	2.5	3.5	72
Phenylon	0.7	22.0	11
Capron	0.7	18.0	6
Polyethylene	1.9	4.7	63

Gel-spun Polyethylene fibres are produced from a flexible chain polymer but with highly oriented structure. Only Van der Waals forces operated between the polymer chains in polyethylene. Although the Van der Waals forces are weaker than hydrogen bonds with which polyamide is associated, the rigidity of gel-spun Polyethylene fibre is much higher than that of Phenylon and Capron, and approaching to that of Terlon. It is concluded that the rigidity of fibres is mainly contributed by extension and orientation of symmetrical polymer chains leads to extremely high level of molecular alignment along the fibre axis.

Influence of preliminary stretching on the mechanical properties of fibres is very dependent on the structure of the fibre, including polymer chain extension, orientation and crystallinity. Terlon fibres has a very highly symmetrical para-aramid structure which leads to high orientation and crystallinity. Preliminary stretching is not able to further improve the orientation, so the character of the stress-strain curves for Terlon is not influenced by preliminary stretching. SVM and Armos are heterocyclic para-copolyamide. The structure of this copolymer is characterised by less regularity and less rigidity in comparison with poly-p-phenylene terephthalamide. It is for this reason that the strength and rigidity of Armos and SVM yarns increases after preliminary stretching.

Preliminary stretching of Phenylon yarns changes the nature of the stress-strain curves due to the rearrangement of the supermolecular structure which occur during the elongation process. The preliminary stretching does not result in a significant change of strength. But for Capron yarns preliminary stretching improves orientation but also causes partial breaking chemical bonds in molecular chains, resulting in the influence on the stress-strain curves.

Study of creep-recovery properties of polyamide fibres shows that irrecoverable residual deformation for the rigid chain polymers is developed within a very short initial period of time (15 seconds) after the load is applied. But for semi-rigid or flexible chain polymer fibres, the residual deformation is developed during the whole time that the load is applied.

Aromatic polyamide fibres have high temperature resistance. They have the potential to be used at elevated temperature. Current work has developed a more detailed understanding of the thermal properties of polyamide fibres. It is found that an increase in temperature causes change in character of the stress-strain curves of Armos and SVM. Their strengths of break decrease with increasing temperature. For Terlon yarn, the linear character of the stress-strain curve still remains when temperature increases.

The effect of temperature on the character of accumulation of residual deformation for some polyamide yarns is significant. Fig. 7.1 shows the relationship between residual deformation and applied strain at room temperature. The corresponding relationship at 100°C is shown in

Fig. 7.2. The significant changes in the character of accumulation of the residual deformation for Armos occur at temperatures from 80 up to 100°C. Because heterocyclic para-copolyamide Armos do not pack the polymer chains as tight as Terlon which has a significantly higher degree of crystallinity. Moisture is accessible to amorphous region in Armos, the plastification effect by removal of the moisture is observed. This might be the reason for the change in character of the accumulation of residual deformation for Armos fibres. The effect of temperature on SVM fibres is similar.

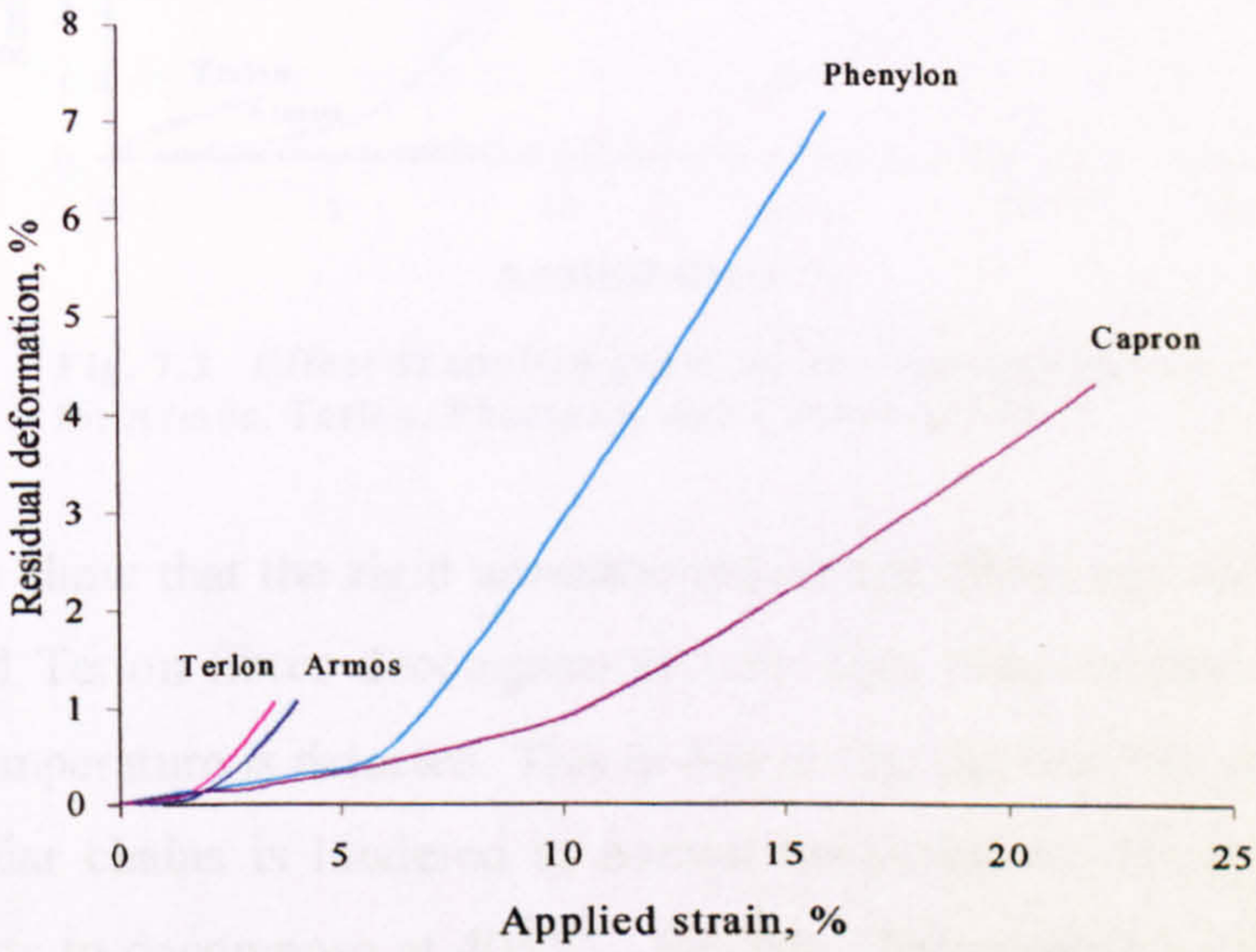

Fig. 7.1 Effect of applied strain on residual deformation for Armos, Terlon, Phenylon, and Capron

The mechanical properties of polyamide fibres are influenced by moisture which is associated with intermolecular interaction. Polyamide fibres contain a certain level of moisture. The location of moisture within the fibres depends on the fibre structures. They can be trapped in the microviods in the fibres or associated with hydrogen bonds between neighboring chains or crystallites. Heterocyclic para-copolyamide Armos and SVM do not pack the polymer chains as tight as Terlon which has significantly higher degree of crystallinity. Moisture is accessible to amorphous regions in Armos and SVM, the plastification effect by removal of the moisture is observed. This might be the reason for the change in character of the accumulation of residual deformation for Armos and SVM

fibres. The most significant changes occur at temperatures from 80 up to 100°C. There is no significant influence on Terlon.

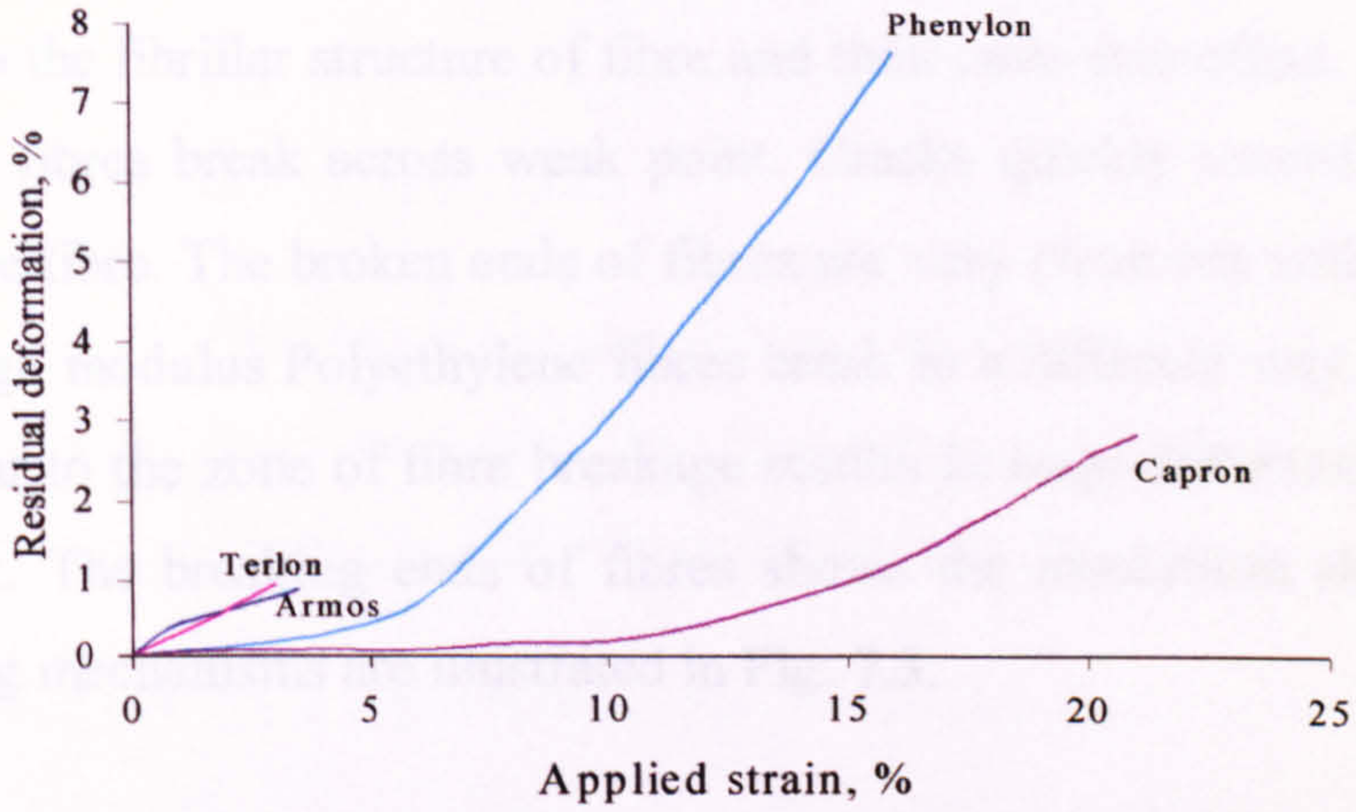

Fig. 7.2 Effect of applied strain on residual deformation for Armos, Terlon, Phenylon, and Capron at 100°C

DSC experiments show that the rigid aromatic polyamide fibres are very resistant to heat. SVM, Armos and Terlon fibres decompose at very high temperatures around 500°C. No glass transition temperature is detected. This is due to the fact that the motility of large size and rigid molecular chains is hindered at normal temperatures. Phenylon (semi-rigid m-aramid fibre) starts to decompose at 405°C. Flexible chain polymers such as Capron and Polyethylene fibres have glass transition temperature before melting. Aromatic rings in polymer chains increase the polymer rigidity. The higher the intermolecular attractive force and chain rigid, the greater the resistance to heat.

Table 7.3 The thermal characteristics of some polymer fibres

Fibres	Glass transition temperature	Melting or decomposing temperature
Terlon	-	about 500°C (decomposing)
Armos	-	about 450°C (decomposing)
SVM	-	about 450°C (decomposing)
Phenylon	330°C	about 405°C (decomposing)
Capron	65°C	210°C
Polyethylene	-	140°C

The breaking mechanism of polyamide fibres and high strength Polyethylene were investigated using SEM. These fibres can be classified into three groups according to the way the fibres break. Rigid chain aramid fibres break with fibrillation, the fibre splits are significant due to the fibrillar structure of fibre and their core-skin effect. Semi- or flexible chain polyamide fibres break across weak point. Cracks quickly extended in amorphous regions across the fibre. The broken ends of fibres are very clean cut without fibrillisation. High strength high modulus Polyethylene fibres break in a different way. Significant local overstressing near to the zone of fibre breakage results in large deformations and relaxing during the break. The breaking ends of fibres shows the mushroom shape. These three different breaking mechanisms are illustrated in Fig. 7.3.

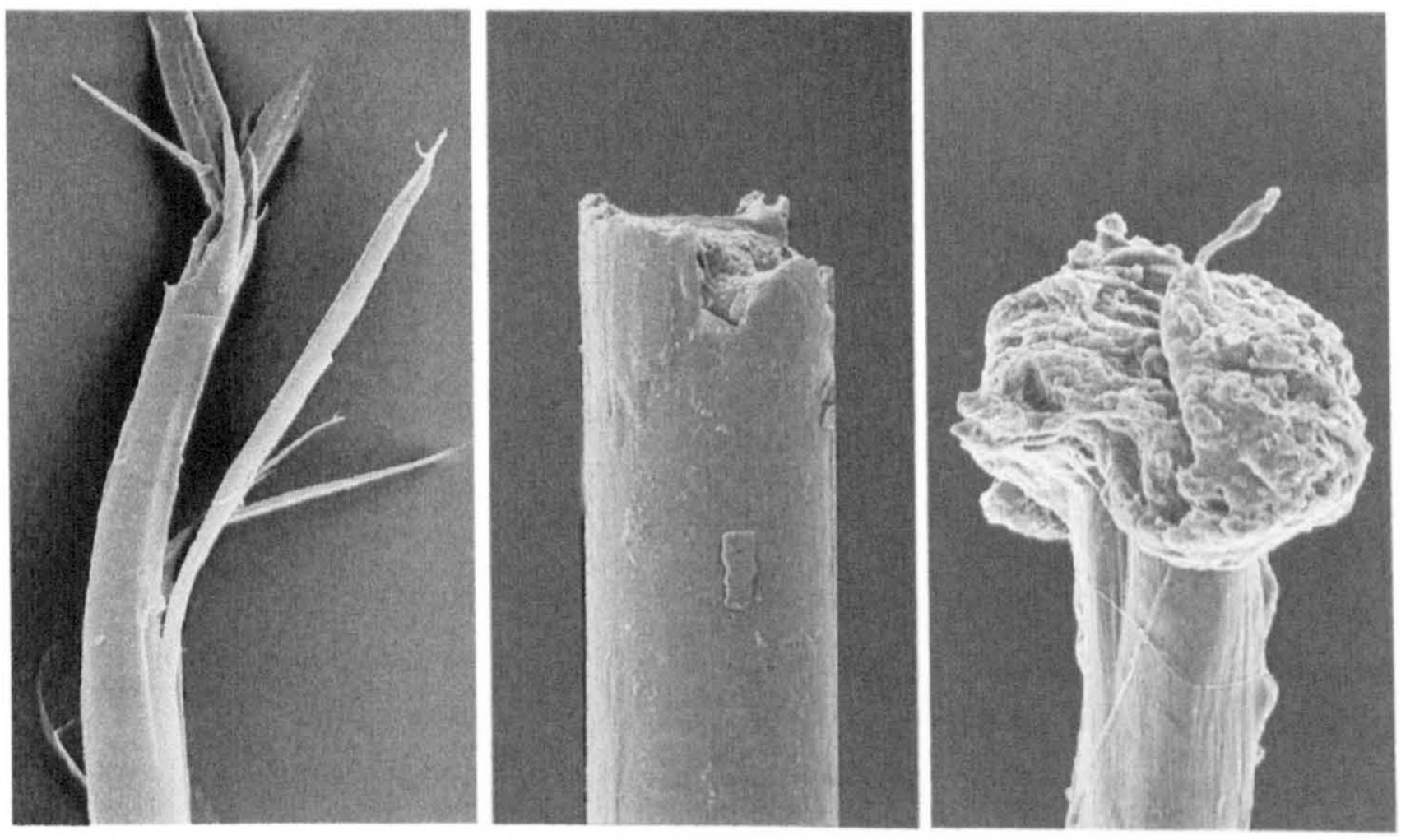

Fig. 7.3 Different types of fibre break a) The break with fibrillisation; b) The graduated break; c) The break with a thickening

References

ALEKSEEV, V.G. (1994) The Obtaining of High Strength High Modulus Yarn from Supermolecular Polyethylene. PhD thesis, Saint-Petersburg State University of Technology and Design, Saint-Petersburg, 128p.

AVROROVA, L.V., GVOZDEV, V.V., and DADASHEVA, B.Sh. (1993) To Question of Use of High Strength Aramide Fibres for Protection of Environment. *Khimicheskie volokna*, (5), pp.55-56. (reprinted in US: Fibre Chemistry. 1993, (5)).

ASKADSKII, A.A. (1973) *The deformation of polymers*, Moskow, Khimiya. 448p.

ASKADSKII, A.A., MUZILEV, S.V., DVALISHVILI, G.I., and KUDRIYAVTSEV, G.I. (1990) Influence of Thermo Ageing on Strength and Relaxation Properties of High Modulus Fibres Based on Aromatic Polymers. *The 5th international symposium on chemical fibres*. Kalinin, 1, pp.124-129.

BAKEEV, N.F., ZUBOV, U.A., KABANOV, V.A. *et al.*, (1986) The Specialities of Structure of High Modulus Oriented Crystallite Flexible Chain Polymers. *The abstracts of 4th international symposium on chemical fibres*. VNIISV, Kalinin, l, (1), pp.26-39.

BECHT, J., DE VRIES, K.L. and KAUSCH, H.H. (1971) On Some Aspects of Strength of Fibres. *European Polymer Journal*, 7, pp.105-114.

BELIAEV, A.A., KRASNOV, E.P., and STEPAN'YIAN, A.E. (1978) Intermolecular Interaction in Aromatic Polyamides. *Vysokomolekulyarnye soedineniya*, A 20, (2), pp.386-390.

BELOKUROVA, A.P. and REITLINGER, S.A. (1978) About Temperature Dependence of Water Penetrating and Sorption ability of Polymers. *Izvestiya VUZov, Khimiya i khimicheskaiya tehnologiya*, (9), pp.1362-1365.

BIGG, D.M. (1988) Mechanical Property Enhancement Semicrystalline Polymers - A Review. *Polym. Eng. Sci.*, 28, July, (13), pp.830-840.

BLUMSHTEIN, A. (1981) *The Liquid-Crystall Order of Polymers,* Moskow, Mir. 352p.

BODOR, G. (1984) Morphology and Tensile Property relations of High-Strength/High-Modulus Polyethylene Fiber. *J. Polym. Sci. Part B: Polym Phys.*, 22, pp.1541-1543.

BUDNITSKII, G.A. (1990) Reinforcing fibres for composites. *Khimicheskie volokna,* (2), pp.5-13. (reprinted in US: Fibre Chemistry. 1990, (2)).

DEHANT, I., DANTS, R., KIMMER, V., and SHMOLKE, R. (1976) *Infrared Spectroscopy of Polymers.* Translation from German by Arhangelskii V.V., Edit Oleinik E.F., Moskow, Khimiya. 472p.

DEOPURA, B.L., SENGUPTA, A.K., and VERMA, A. (1983) Effect of Moisture on Physical Properties of Nylon. *Polym. Commun.*, 24, September, pp.287-288.

DOBB, M.G., JOHNSON, D G. and SAVILLE, B.P. (1977) Supramolecular Structure of high-Modulus Polyaromatic Fiber (Kevlar 49). *J. Polym. Sci., Polym. Phys.*, 15, pp.2201-2211.

DOBB, M.G., JOHNSON, D.J., MAJEED, A., and SAVILLE, B.P. (1979) *Polym.* 20, pp.1284.

DOBB, M.G., ROBSON, R.M., and ROBERTS, A.H. (1993) The Ultraviolet Sensitivity of Kevlar 149 and Technora Fibres. *J. Mater. Sci.*, 28, pp.785-788.

DUOBINIS, N. (1993) Structure and Properties of Aromatic Polyamide and Polyimide Fibers Commercially available in the Former USSR. *Tex. Res. J.*, 63, (9), pp.99-103.

EISENBERG, D. and KAUZMANN, W. (1969) *The Structure and Properties of Water*, London, *Oxford: U. P.* 296p.

FELTHAM, P. (1966) *Deformation and Strength of Materials*, London, Butterworths. 135p.

FRANK, B., FRUBING, P., and PISSIS, P. (1996) Water Sorption and Thermally Stimulated Depolarization Currents in Nylon-6. *J. Polym. Sci., Part B: Polym. Phys.*, 34, pp.1853-1860.

FUKUDA, M., OCHI, M., MIYAGAWA, M., and KAWAI, H. (1991) Moisture Sorption Mechanism of Aromatic Polyamide Fibers: Stoichiometry of the Water Sorbed in Poly (para-phenylene Terephthalamide) Fibers. *Text. Res. J.*, 61, (11), pp.668-680.

GORDEEV, S.A. (1992) The Deformation and Strength Properties of Polyethylene Yarns. PhD thesis, Saint-Petersburg State University of Technology and Design, Saint-Petersburg, 168p.

GREBENNIKOV, S.F., KYNIN, A.T. *et al.*, (1984) Gisterezis Phenomenon at Steam Sorption by Polymers. *Zurnal prikladnoi khimii*, 87, (11). pp.2114-2116.

GUL, V.E. (1979) *Structure and Mechanical Properties of Polymers,* Moskow, Vysshaiya Shkola. 352p.

HARAGUCHI, K., KAJIYAMA, T., and TAKAYANAGI, M. (1979) Uniplanar Orientation of Poly (p-phenylene terephthalamide) Crystal in Thin Film and Its Effect on Mechanical Properties. *J.Appl.Polym.Sci.*, 23, (3), pp.903-914.

HARGET, P.J. and OCSWALD, M.J. (1977) Amorphous Content in Polymer, In: THERM. METHODS POLYM. ANAL. EAST. ANAL. SYMP. *Proceedings of the 17th-(Edited by S. W. Shalaby): Franklin Inst., Philadelphia, Pa.* pp.23-33.

HEARL, J.W.S. (1963) The Development of Ideas of Fine Structure. In: HEARL, J.W.S. and PETERS, R.H. ed. *Fibre structure*, Manchester, London, Butterworths. pp. 209-234.

HINDERLICH, A.M. and ABDO, Sh. M. (1989) Relationship between Crystalline Structure and Mechanical Properties in Kevlar 49 Fibres. *Polym. Commun.*, 30, (6), pp.184-186.

HOOGSTEEN, W., KORMELINK, H., BRINKE, G.T., and PENNINGS, A.J. (1988) Gel-spun Polyethylene Fibres. *J. Mater. Sci.*, 23, (10), pp.3467-3474.

HUDOSHEEV, I.F., TOKAREV, A.V., and KUDRIYAVTSEV, G.I. (1981) About Forecast of Thermo Ageing of High Strength High Modulus Fibres. In: *Proceedings of the 5th conference on composites materials*, Moskow, 1, pp.152-153.

HUDOSHEEV, I.F., TSUMAN, E.P., LEVITES, L.M. *et al.*, (1982) Strength and Thermal Properties of Nontwisted Fibre Vniivllon. *Khimicheskie volokna*, (2), p.38. (reprinted in US: Fibre Chemistry. 1982, (2)).

KARGIN, V.A. and SLOMINSKII, G.L. (1967) *The Brief Essay about Physics and Chemistry of Polymers*, Moskow, Khimiya. 232p.

KATZ, H. S. and MILEWSKI, V. (1978) *Handbook of Fillers and Reinforcements for Plastics*, New York, Cincinnati, Atlanta, Dallas, San Francisco, London, Toronto, Melbourne, Van Nostrand Reinhold Comparny. 652 p.

KELLER, A. (1963) The Crystallinity of High Polymers. In: HEARL, J.W.S. and PETERS, R.H. ed. *Fibre structure*, Manchester, London, Butterworths. pp.332-385.

KETTLE, G.J. (1977) Variation of the Glass Transition Temperature of Nylon-6 with Changing Water Content. *Polym.*, 18, July, pp.742-743.

KIRIENKO, O.F., MARIKHIN, V.A., and MYASNIKOVA, L.P. (1971) Fractographic Study of spreading of macrocrack in oriented capron. *Mechanics of Composite Materials*.(4), pp. 645-648.

KOITOVA, J.Y. (1992) The Development of Tests and Research of Moister Influence on Physical and Mechanical Properties of Thermo Resistance Chemical Fibres and Yarns, PhD

thesis. Saint-Petersburg University of Technology and Design, Saint-Petersburg, Russia, 185p.

KOITOVA, J.Y., PEREPELKIN, K.E., KYNIN, A.T., and LEBEDEVA, G.G. (1993) Sorption Properties of Thermo Resistance Yarns based on Aromatic Polymers. *Khimicheskie volokna*, (2), pp.37-39. (reprinted in US: Fibre Chemistry. 1993. (2)).

KOLLROSS, P. and OWEN, A.J. (1982) The Influence of Hydrogen Bonding on Mechanical Anisotropy in Oriented Nylon-12. *Polym.*, 23, June, pp.829-833.

KONKIN, A.A. (1978) *Thermo, Heat Resistance and Unfired Fibres*, Moskow, Khimiya. 421p.

KOZLOV, P.V. and PAPKOV, S.P. (1982) *Physical and Chemical Basis of Polymer Plastification*, Moskow, Khimiya. 223p.

KUDRIYAVTSEV, G.I., NOSOV, M.P., and VOLOKHINA, A.V. (1976) *Polyamide Fibres*, Moskow, Khimiya. 264p.

KUDRIYAVTSEV, G.I., VARSHAVSKII, V.Ya., SHETININ, A.M., and KASAKOV, M.E. (1992) *Reinforcing Chemical Fibres for Composite Materials*, Moskow, Khimiya. 236p.

KUNUGI, T., AKIYAMA, I., and HASHIMOTO, M. (1982) Mechanical Properties and Superstructure of High-Modulus and High-Strength Nylon-6 Fibre Prepared by the Zone-Annealing Method, *Pol.*, 23, July, pp.1199-1203.

KURZEMNIEKS, A.H. (1979) Deformation Properties of the Structure of Organic Fibres Based on *Para*-Polyamides. *Mekhanika kompozitsionnykh materialov*, (1), pp.10-14. (reprinted in US: Mechanics of Composite Materials. 1979, (1)).

KURZEMNIEKS, A.H. (1980) Effect of Moisture on the Structure and Properties of an Organic Fibre. *Mekhanika kompozitsionnykh materialov*, (5), pp.40-43. (reprinted in US: Mechanics of Composite Materials. 1980, (5)).

KUZ'MIN, V.N. (1988) Structure, properties and features of breaking of organic reinforce fibres. PhD thesis. Saint-Petersburg, Institute of Light and Textile industry. 161p.

KVEDER, S.M. and RIJAVEC, T. (1994) Dynamic Mechanical Properties, Superstructure, and Texturability of PA 6.6 Partially Oriented Yarns. *Tex.Res.J.*, 64, 9, pp.495-500.

LEE, K.G., BARTON, R., SHULTZ, JR., and J.M. (1995) Structure and Property Development in Poly(p-phenylene trephthalamide) During Heat Treatment Under Tesion, *J.Polym.Sci., Polym.Phys.*, 13, pp.1-14.

LEWIN, M. and PEARSE, E.M. (1985) Polyamide Fibers. In: *Handbook of Fiber Science and Technology*. 4, (2), pp.74-161.

MACHALABA, N.N. (1999) The Modern *p*-Aramide Fibres. The Role of Tver'Him Volokno JSC in Armos Fibre Production. *Khimicheskie volokna*, (3), pp.3-10. (reprinted in US: Fibre Chemistry. 1999, (3)).

MANDELKERN, L. (1964) *Crystallization of Polymers*, New York, San Francisco, Toronto, London, McGraw-Hill Book Company. 359p.

MARIKHIN, V.A., and MYASNIKOVA, L.P. (1977) *The Supermolecular Structure of Polymers*, Moskow, Khimiya. 240p.

MARIKHIN, V.A., MYASNIKOVA, L.P., and PELZBAUER, Z. (1981) Formation of Kink-bands during the Orientation Drawing of Linear Polyethylene. *Vysokomolekulyarnye soedinenia*, A 23, (9), pp.2108-2116.

MARIKHIN, V.A., MYASNIKOVA, L.P., ZENKE, D., HIRTE, R., and WEIGEL, P. (1984) Particularly Strong and Rigid Fibres from Polyethylene. *Vysokomolekulyarnye soedinenia*, B 26, (30), pp.210-214.

MATVEEV, V.S., BUDNITSKII, G.A., MASHINSKAIYA, G.P. *et al.* (1993) Structure-Mechanical Characteristics of Aramide Fibres for Armours Waistcoat. *Khimicheskie volokna*, (5), pp.55-56. (reprinted in US: Fibre Chemistry. 1993, (5)).

McNAUGHTON, J.L. and MORTIMER, C.T. (1975) *Differential Scanning Calorimetry,* The Perkin-Elmer Corporation, Norwalk, Connecticut 06856. Printed in thr United State of America. 43p.

MORTON, W.E. and HEARL, J.W.S. (1975) *Physical Properties of Textile Fibres,* 2nd Ed. London, The Textile Inst. 660p.

NORTHOLT, M.G. (1981) The Structure and Mechanical Properties of Poly(p-phenylene terephthalamide) Fibre. *The British Polym. J.* 13, June, pp.64-65.

PAKHOMOV, P.M. and SHABLYGIN, M.V. (1982) Orientation Strengthening of Flexible-Chain and Rigid-Chain Polymers. *Vysokomolekulyarnye soedineniya*, A 24, (5), pp.1020-1026.

PAKHOMOV, P.M., SHABLYGIN, M.V., TSOBKALLO, E.S., and CHEGOLYA, A.S. (1986) Interpreting the Extesion Curve of Oriented Polymers. *Vysokomolekulyarnye soedineniya,* A 28, (3), pp.558-563.

PAKHOMOV, P.M., EGOROV, E.A., ZIZENKOV, V.V., and CHEGOLIYA, A.S. (1990) Micro Processes during Deformation of Oriented Polymers. *Vysokomolekulyarnye soedineniya,* A 32, (1), pp.136-142.

PAKHOMOV, P.M. (1999) *The Conformation Structure and Mechanical Properties of Polymers*, Tver, Tverskoi gosudarstvennii universitet. 234p.

PANDEY, G.C. (1989) Fourier Transform Infrared Microscopy for the Determination of the Composition of Copolymer Fibres: Acrylic Fibres. *Analyst.,* February, 114, pp.231-232.

PARKER, J.P. and LINDERMEYER, P.H. (1977) On the Crystal Structure of Nylon 6, *J. Appl. Polym. Sci.*, 21, pp.821-837.

PAULING, L. (1960) *The Nature of Chemical Bonds and the Structure of Molecules and Crystals,* 3rd ed. Ithaca; London, Cornell U.P; Oxford U.P. 644p.

PAVIA, D.L., LAMPMAN G.M., and KRIZ G.S. (1996) Introduction to Spectroscopy: A Guide for Students of Organic Chemistry. W.B. Saunderers Company. Philadelphia. London. Toronto.

PENN, L. and MILANOVICH, F. (1979) Raman Spectroscopy of Kevlar 49 Fibre. *Polymer*, 20, January, pp.31-36.

PENN, L., (1979) Physicochemical Properties of Kevlar 49 Fiber. *J. Appl. Polym. Sci.*, 23, pp.59-73.

PENNINGS, A.J. (1967) Fractination of Polymers by Crystallsation from Solutions *J. Poly. Sci. Part C,* (16), pp.1799-1812.

PENNINGS, A.J., VAN DER HOOFT, R.J., POSTEMA, A.R. *et al.,* (1986) High-Speed Gel-Spinning of Ultra-High Molecular Weight Polyethylene. *Polymer Bull.* 16, pp.167-174.

PEREPELKIN, K.E. (1966) About theoretical and ultimate elastic and strength properties of chemical fibres. *Khimicheskie volokna*, (2), p.3.

PEREPELKIN, K.E. and CHEREISKII, Z.U. (1977) Ultimate values of Mechanical Properties of New Varieties of Highly-Oriented Polymer Materials. *Mekhanika polimerov*, (6), pp.1002-1010.

PEREPELKIN, K.E. (1978) *Physic and Chemistry Basis of Spinning of Chemical Fibres*, Moskow, Khimiya. 320p.

PEREPELKIN, K.E. (1985) *The structure and properties of fibres,* Moskow, Khimiya. 208p.

PEREPELKIN, K.E. (1987) Structural features of Highly-Oriented Reinforcing Fibres and their Effect on Ultimate Mechanical Properties. *Mekhanika kompozitsionyikh materialov*, (3), pp.387-395. (reprinted in US: Mechanics of Composite Materials. 1987, (3)).

PEREPELKIN, K.E. (1992) Fibres and fibrous Materials for Reinforcing Composites with Extreme Characteristics. *Mekhanika kompozitsionyikh materialov*, (3), pp.291-306. (reprinted in US: Mechanics of Composite Materials. 1992, (3)).

PEREPELKIN, K.E., BARANOVA, S.A., GUROVA, E.U., and KYNIN, A.T. (1993) The Complex Assessment of Thermo Resistance Aromatic Yarns. *Khimicheskie volokna*, (6), pp.43-47. (reprinted in US: Fibre Chemistry. 1993, (6)).

PEREPELKIN, K.E., BARANOVA, S.A., and GUROVA, E.U. (1995) Influence of Thermo Ageing on Defection of Super Strength *p*-aromatic Yarns –Armos and SVM. *Khimicheskie volokna*, (1), pp.34-38. (reprinted in US: Fibre Chemistry. 1995, (1)).

PEREPELKIN, K.E., MACHALABA, N.N., and BUDNITSKII, G.A. (1999[a]) Armos-the Russian High-Performance Fiber: Comparison with other *p*-Aramide Fiber Types. *Chemical fibers international*, 49, May, pp.211-214.

PEREPELKIN, K.E., MACHALABA, N.N., and BUDNITSKII, G.A. (1999[b]) A New Russian High-Performance Fibre. *Textile Asia*, July, pp.38-41.

PREVORSEK, D.C., BUTLER, R.H., KWON, Y.D., LAMB, G.E.R., and SHARMA, R.K. (1977) Influence of Fiber Properties on Wrinkling Behavior of Fabrics. Part VII: Effects of Morphology on Fiber Properties. *Text. Res. J.*, February, pp.107-126.

PREVORSEK, D.C. (1989) Ultimate Poperties Unaxial Systems. In: *Encyclopedia of polymer science and engineering*, 2nd edition. Supplement volume, pp.803-821.

PULLMAN, B. (1978) *Intermolecular Interactions: From Diatomics to Biopolymers*, Chichester, New York, Brisbane, Toronto, John Wiley and Sons. 447p.

RADUSCH, H.J., STOLP, M., and ANDROSH, R. (1994) Structure and Temperature-Induced Structural Changes of Various Polyamides. *Polym.*, 35, (16), pp.3568-3571.

REIMSCHUESSEL, A.C. and PREVORSEK, D.C. (1976) Domain Structure of Nylon 6 Fibers, *J. Polym. Sci., Part B: Polym Phis.*, 14, pp.485-498.

RIEWALD, P.G. (1980) Ropes and Cables from Aramid Fibers for Ocean Systems. *Amer. Inst. of Chem. Eng. Symposium Series*, 76, (194), pp.134-147.

RIEWALD, P.G., DHINGRA, A., and CHERN, T. (1987) Recent Advaces in Aramid Fibre and Composite Technology, *The International Conference on Composite Materials, London, July.*

RIYAUZOVA, A.N., GRUZDEV, V.A., KOSTROV, U.A., SIGAL, M.B., AIZENSHTEIN, E.M., TSIPERMAN, V.L., and HODAKOVSKII, M.D. (1974) *The Technology of Chemical Fibre Production*, Moskow, Khimiya. 512p.

ROWLEND, S. P. (1980) *Water in polymers*. Washington, American Chemical Socienty, ACS Symposium Series 127. 597p.

SAIJO, K., ARIMOTO, O., HASHIMOTO, T., FUKUDA, M., and KAWAI, H. (1994) Moisture Sorption Mechanism of Aromatic Polyamide Fibres: Diffusion of Moisture into Regular Kevlar as Observed by Time-Resolved Small-Angle X-ray Scattering Technique. *Polym.*, 35, (3), pp.496-503.

SAVITSKII, A.V., GORSHKOVA, I.A., DEMICHEVA, V.P., FROLOVA, I.L., and SHMIKK, G.N. (1984) Model for the Stress Reinforcement of Polymers and the Production of High-Strength Polyethylene Fibres. *Vysokomolekulyarnye soedineniya*, A 26, (9), pp.1801-1808.

SAVITSKII, A.V., ANDREEVA, G.N., GORSHKOVA, I.A. *et al.*, (1989) Influence of Drawing Conditions on Strength Properties of Fibres from High Molecular Polyethylene. *Vysokomolekulyarnye soedineniya,* A 31, (9), pp.1865-1871.

SHABLYGIN, M.V. and PAKHOMOV, P.M. (1979). Spectroscopic Study of the Hydrogen Bond in Aromatic Polyamides. *Vysokomolekulyarnye soedineniya,* B 21, (8), pp.612-616.

SHORIN, S.V., SUGAK, V.N., TOKAREV, A.V., and KOMISSAROV, V.I. (1999) The Method of High Strength High Modulus Yarns Production. *Partent of Russian Federation.* 2143504 C1.

SHUSTER, M.P. (1988) The Using of NMR Method for Research of Changes of Aramide Fibres Properties under Action of Moisture and other Medium. *Proceedings of the 12th Scientific conference of textile materials*, Kiev, pp.66-67.

SIKORSKI, J. (1963) Surface Structure. In: HEARL, J.W.S. and PETERS, R.H. ed. *Fibre structure*, Manchester, London, Butterworths. pp. 391-421.

SLUTSKER, A.I. (1974) Oriented condition of polymers. In: *The polymer encyclopaedia*, Moskow, Sovetskaiya Entsiklopedia. 2, pp.515-528.

SMITH, P. and LEMSTRA, P.J. (1980) Ultra-High Strength Polyethylene Filaments by Solution Spinning/Drawing. *Polym.*, 21, (11), pp.1341.

SMOOK, J. and PENNINGS, A.J. (1982) The Effect of Temperature and Deformation Rate on the Hot-Drawing Behavior of Porous High-Molecular-Weight Polyethylene Fibers. *J.Appl. Polym. Sci.* 27, (6), pp.2209-2228.

SOKOLOV, L.B., GERASIMOV, V.D. *et al.*, (1975) *Thermostabile Aromatic Polyamides*, Moskow, Khimiya. 256p.

SPRINGER, H., OBAID, A.A., PRABAWA, A.B., and HINRICHESEN, G. (1998) Influence of Hydrolytic and Chemical Treatment on the Mechanical Properties of Aramid and Copolyaramid Fibers. *Text. Res. J.*, 68, (8), pp.588-594.

STALEVICH, A.M., TIRANOV, V.G., and SLUTSKER, G.Ya. (1981) Temperature/Force Relationship of the Viscoelastic Effects in Highly-Oriented Yarns from Aromatic Polyamide. *Khimicheskie volokna*, (10), pp.31-33. (reprinted in US: Fibre Chemistry. 1981, (10)).

STARKWEATHER, H.W. (1980) In: ROWLAND S.P. ed. *Water in polymers*, ASC Symposium Series 127, Washington, DC.

STARKWEATHER, H.W. and BARKLEY, J.R. (1981) *J. Polym. Sci. Part B: Polym. Phys.*, 19, pp.1211.

STOECKEL, T.M., BLASIUS, J., and CRIST, B. (1978) Chain Rupture and Tensile Deformation of Polymers. *J. Polym. Sci. Part B: Polym. Phys.*, 16, pp.485-500.

SUKHANOVA, T.E. (2000) Structure Forming and Morphology of Oriented Polyimides and Fibre Composites Based on its. Doctor of Science thesis, Saint-Petersburg, Russian Academy of Science, Institute of high molecular compounds.

TADOKORO, H. (1979) *Structure of Crystalline Polymers*, New York – London, John Wiley a. Sons. 465p.

TERMONIA, Y. and SMITH, P. (1986) Theoretical Study of the Ultimate Mechanical Properties of poly(p-phenylene-terephthalamide) Fibres. *Polym.* 27, December, pp.1845-1849.

The theory of FT-IR. *by A subsidiary of Thermo Instrument Systems, Inc., a Thermo Electron company Nicolet Instrument Corporation.*

TIRANOV, V.G., STALEVICH, A.M., SOKOLOVA, T.S., and VOLOKHINA, A.V. (1976) Effect of Drawing Temperature on Properties of Heat Resistant Fibre Terlon. *Khimicheskie volokna*, (1), pp.28-29. (reprinted in US: Fibre Chemistry. 1976, (1)).

Total Coverage in FT-IR Microscopy.

TSOBKALLO, E.S. (1988) Relationship between creep and recovery processes and molecular-destruction processes for filmier polyethylene yarn. *Izvestiya VUZov, Tehnologiya legkoi promishlennosti*, (5), pp.62-66.

TSOBKALLO, E.S. (1996) Determination of character of accumulation of residual deformation by the stress-strain curve of oriented synthetic yarns. *Phisiko-khimiya polimerov*, Tver, pp.77-81.

TSOBKALLO, E.S., GROMOVA, E.S., TIRANOV, V.G. (1997) Residual component of deformation of oriented synthetic yarns with different rigidity. *Khimicheskie volokna*, (3), pp.27-29. (reprinted in US: Fibre Chemistry. 1997, (3)). p.27-29.

TSOBKALLO, E.S., NACHINKIN, O.I., and KVARATSHKELIYA, V.A. (1998) The Ifluence of Preliminary Stretching on Deformation and Strength Properties of High Strength Yarns. *Khimicheskie volokna*, (3), pp.30-33. (reprinted in US: Fibre Chemistry. 1998, (3)).

TUGOV, I.I. and KOSTRIKINA, G.I. (1989) *Chemistry and Physics of Polymers*, Moskow, Khimiya. 432p.

VANDERSCHUEREN, J. and LINKENS, A. (1978) Water-Dependent Relaxation in Polymers. Study by the Thermally Stimulated Current Method. *Macromol.*, 11, (6), pp.1228-1233.

VOLKOV, A.V., ARZHAKOV, A.S., VOLYNSKII, A.L., and BAKEEV N.F. (1990) Mechanical Properties and Structure of Nylon 6 Modified with Oxyaromatic Compounds. *Vysokomolekulyarnye soedineniya*, A 32, (7), pp.489-494.

VOLOKHINA, A.V., OGNEV, V.I., PRONICHKINA, I.K., SOKOLOVA, T.S., KIRILLOV, V.A., KOVALEV, V.K., MOREV, V.S., and POROSHIN, G.V. (1993) Using of Terlon Fibre for Ecological Purposes. *Khimicheskie volokna,* (5), pp.53-54. (reprinted in US: Fibre Chemistry. 1993, (5)).

VOLOKHINA, A.V. (1997) High Strength Synthetic for Reinforcing of Thermoplastic Organic Plastics for Construction Purposes. *Khimicheskie volkna,* (3), pp.44-52. (reprinted in US: Fibre Chemistry. 1997, (3)).

WANG, J.Z., DILLARD, D.A., and WARD, T.C. (1992) Temperature and Stress Effects in the Creep of Aramid Fibers Under Transient Moisture Conditions and Discussions on the Mechanisms. *J. Polym. Sci., Part B: Polym. Phis.*, 30, pp.1391-1400.

WANG, J.Z., GHOTRA, J.S., PRITCHARD, G., and ROSE, R.G. (1997) The Mechanical Properties of Particulate-Filled Aramide and Polyethylene Laminate. *Polymer International*, 42, (3), pp.241-244.

WARD, I. M. (1971) The Mechanical Properties of Solid Polymers. London, New York, Sydney, Toronto, John Wiley and Sons Ltd. 375p.

WARD, I. M. (1986) Recent Studies of Physical Properties of Highly Oriented PE. *Brit. Polym. J.*, 18, (4), pp.216-220.

WARNER, S.B. (1995) *Fiber Science*. New Jersey, Prentice Hall, Inc. A Division of Simon and Schuster, Inc. Englewood Cliffs. 316p.

WU, Z., ZHANG, A., CHENG, S.Z.D., HUANG, B., and BAOJUN, Q. (1990) Changes in Crystal Structure Parameters and Thermal Mechanical Properties of Poly(p-Phenylene Terephthalamide) fibers Under Different Annealing Conditions. *J. Polym. Sci., Part B: Polym. Phys.*, 28, pp.2565-2583.

YANG, H.H. (1989) *Aromatic High-Strength Fibers*, N.-Y., Intersci. Publ., 873p.

YANG, H.H. (1993) *Kevlar Aramide Fiber*, N.-Y., Intersci. Publ., 198p.

YUDIN, V.E., SUKHANOVA, T.E., VILEGZHANINA, M.E., LAVRENTIEV, V.K., MIKHAILOV, G.M., OPRITS, Z.G., ZAITSEV, B.A., POPOVA, E.N., and MIKHAILOV, A.A. (1997) Effect of the Organic Fibre Morphology on Mechanical Behaviour of Composites. *Mekhanika kompozitsionnykh materialov*, 33, (5), pp.656-669. (reprinted in US: Mechanics of Composite Materials. 1997, (5)).

ZARIN, A.V., KOLONISTOV, V.G., PEREPELKIN, K.E. *et al.*, (1983) Specialities of Influence of Moisture on High Oriented Chemical Fibres. *Proceedings of the 4th conference of young scientist and specialists*. Kalinin, pp.10-11.

ZARIN, A.V. (1991) The Development of Research Methods of Properties of Chemical Yarns, which are Used for Reinforcing of Composite Materials, PhD thesis, Saint-Petersburg science research institute of chemical fibres and composite materials, Saint-Petersburg, 173p.

ZAZULINA, Z.A., DRUZININA, T.V., and KONKIN, A.A. (1985) *The Bases of Chemical Fibre Technology*, Moskow, Khimiya. 304p.

ZIABICKI, A. (1976) *Fundamental of Fibre Formation. The Science of Fibre Spinning and Drawing*, Jonh Wiley and Sons, London, New York, Sydney, Toronto. 488p.

ZVEREV, M.P. (1973) Polyolephene and polystirol fibres. In: *Carbo-chain synthetic fibres*, Moskow, Khimiya, pp.491-589.

ZUBOV, U.A., CHVALUN, S.N., and BAKEEV, N.F. (1986) The Structural Specialities of High Oriented Polyethylene. *Proceedings of the 4th international symposium on chemical fibres*. VNIISV, Kalinine, 1, pp.19-26.

APPENDIX

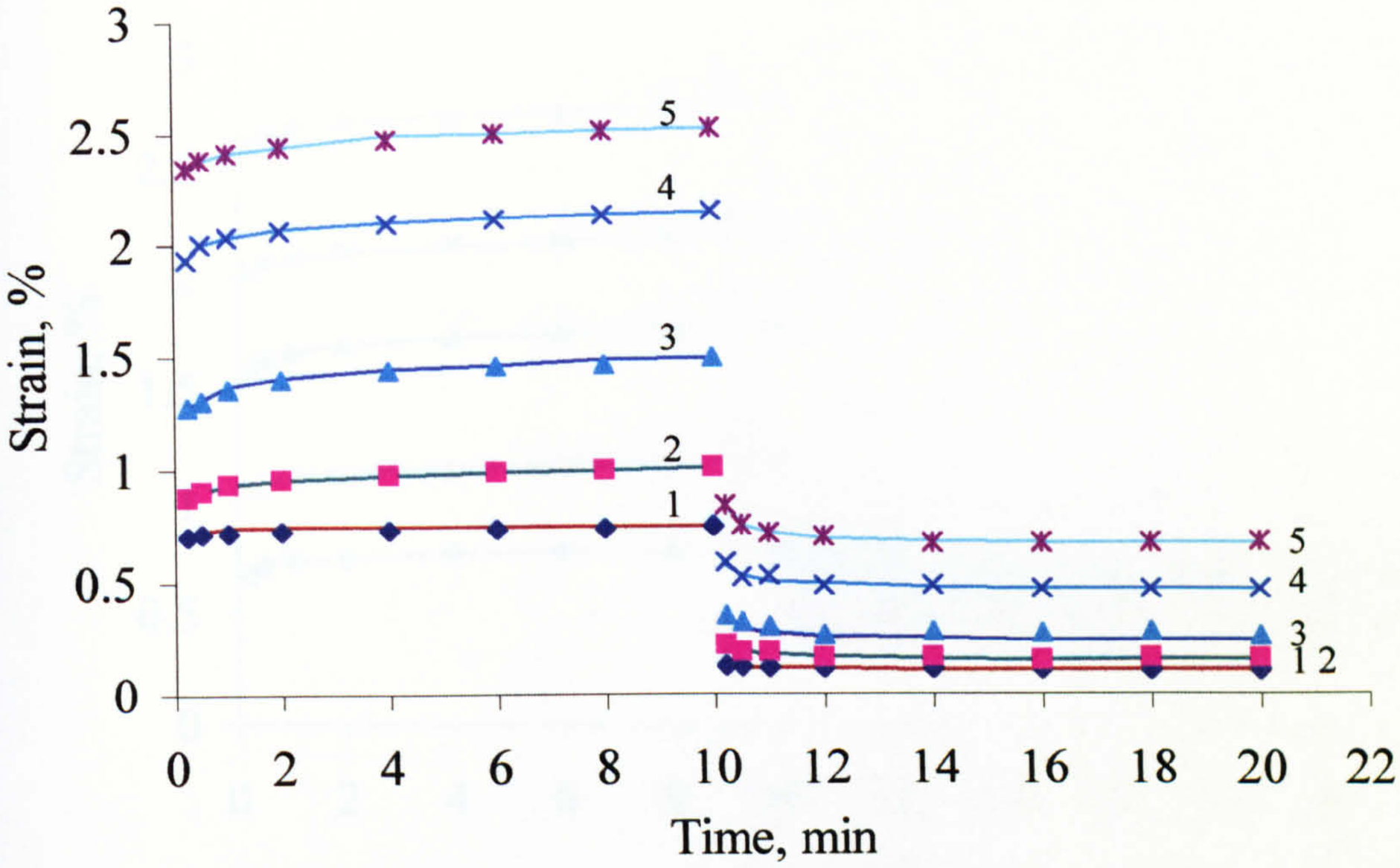

Fig. A_1 The family of creep-recovery curves for armos yarn at 60 °C at σ: (1) 0.65 GPa; (2) 0.83 GPa; (3) 1.35 GPa; (4) 1.74 GPa; (5) 2.12 GPa

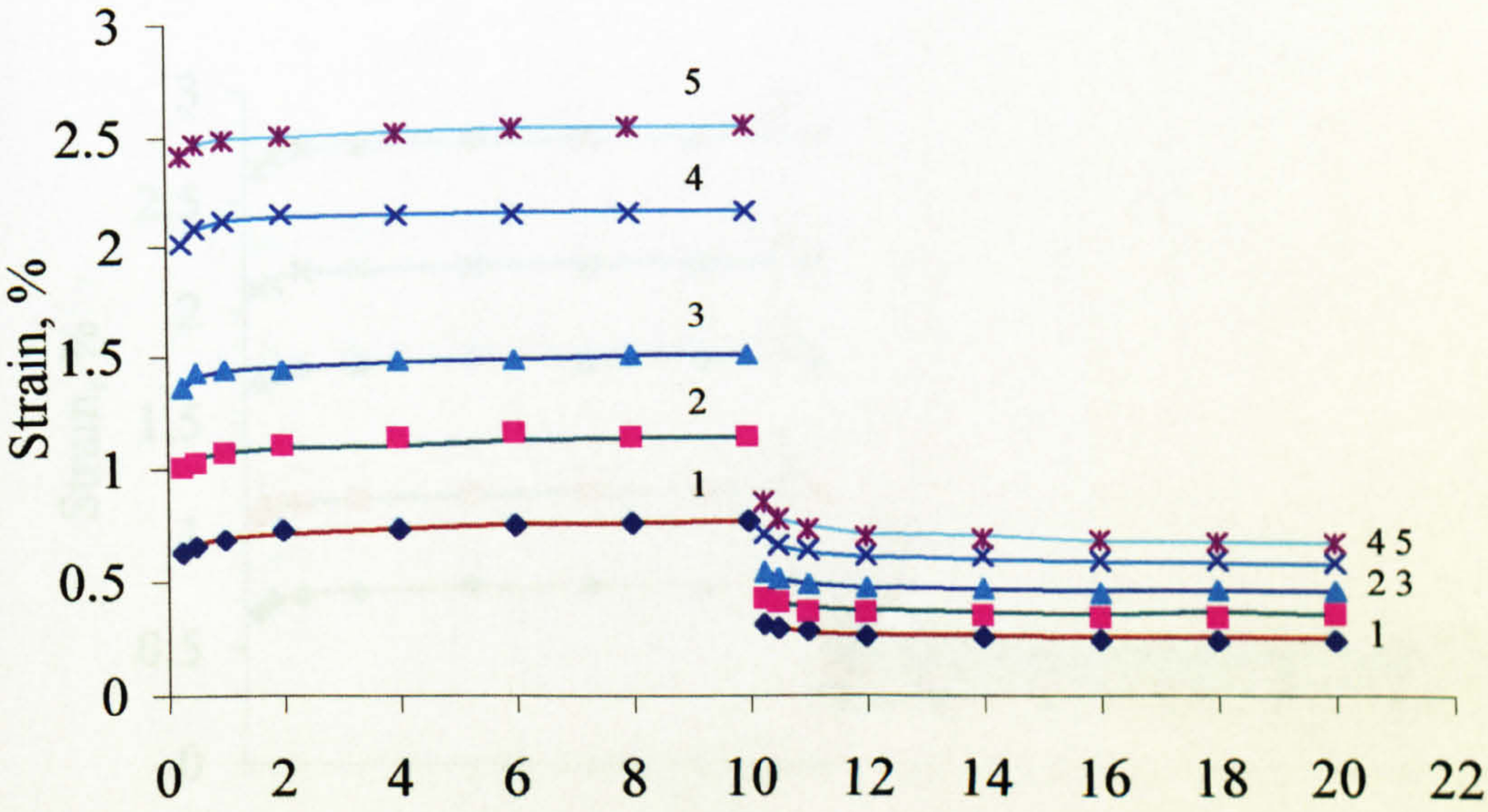

Fig. A_2 The family of creep-recovery curves for armos yarn at 80 °C at σ:(1) 0.65 GPa; (2) 0.83 GPa; (3) 1.35 GPa; (4) 1.74 GPa; (5) 2.12 GPa

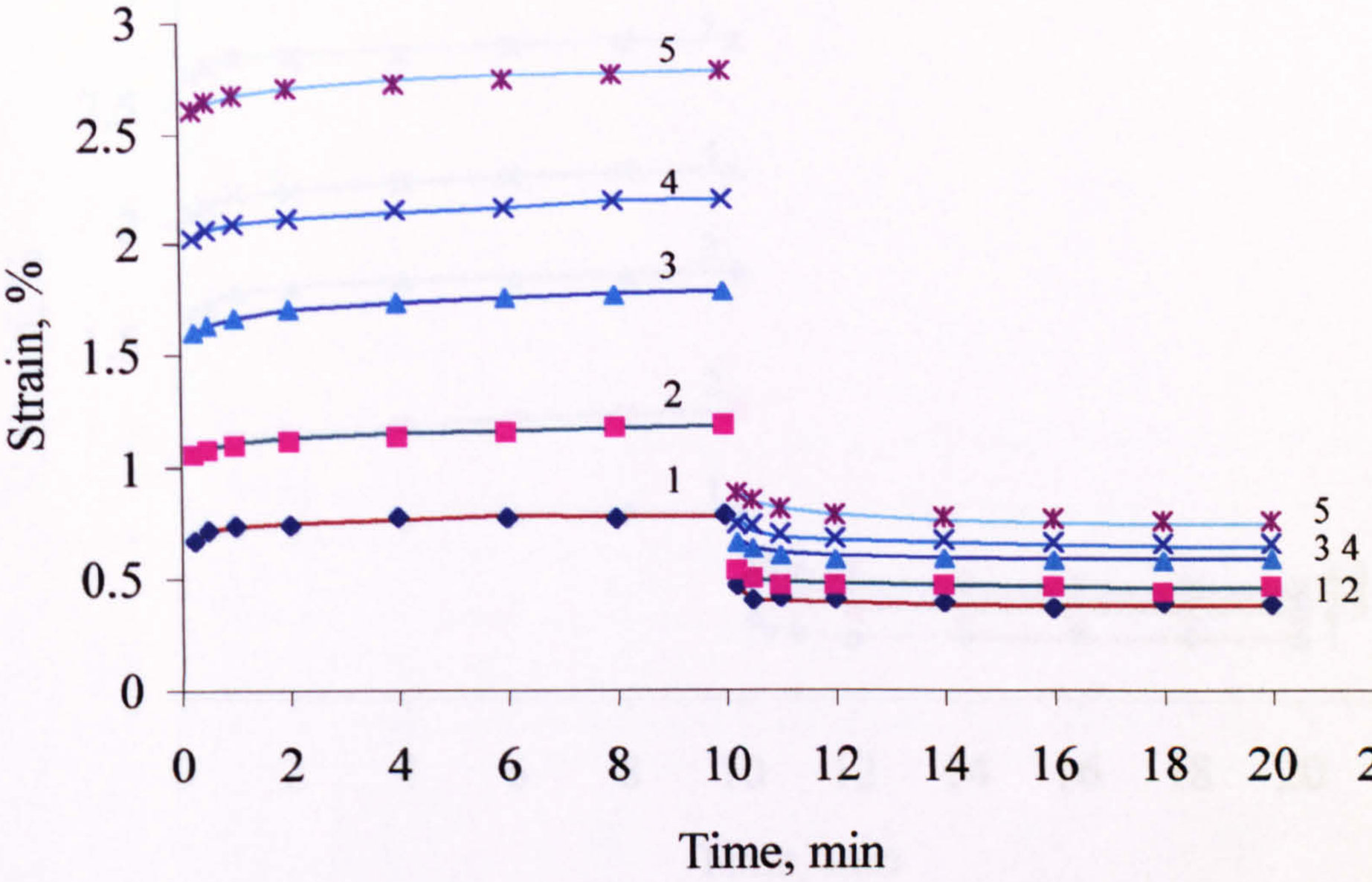

Fig. A_3 The family of creep-recovery curves for armos yarn at 100°C at σ:(1) 0.65 GPa; (2) 0.83 GPa; (3) 1.35 GPa; (4) 1.74 GPa; (5) 2.12 GPa

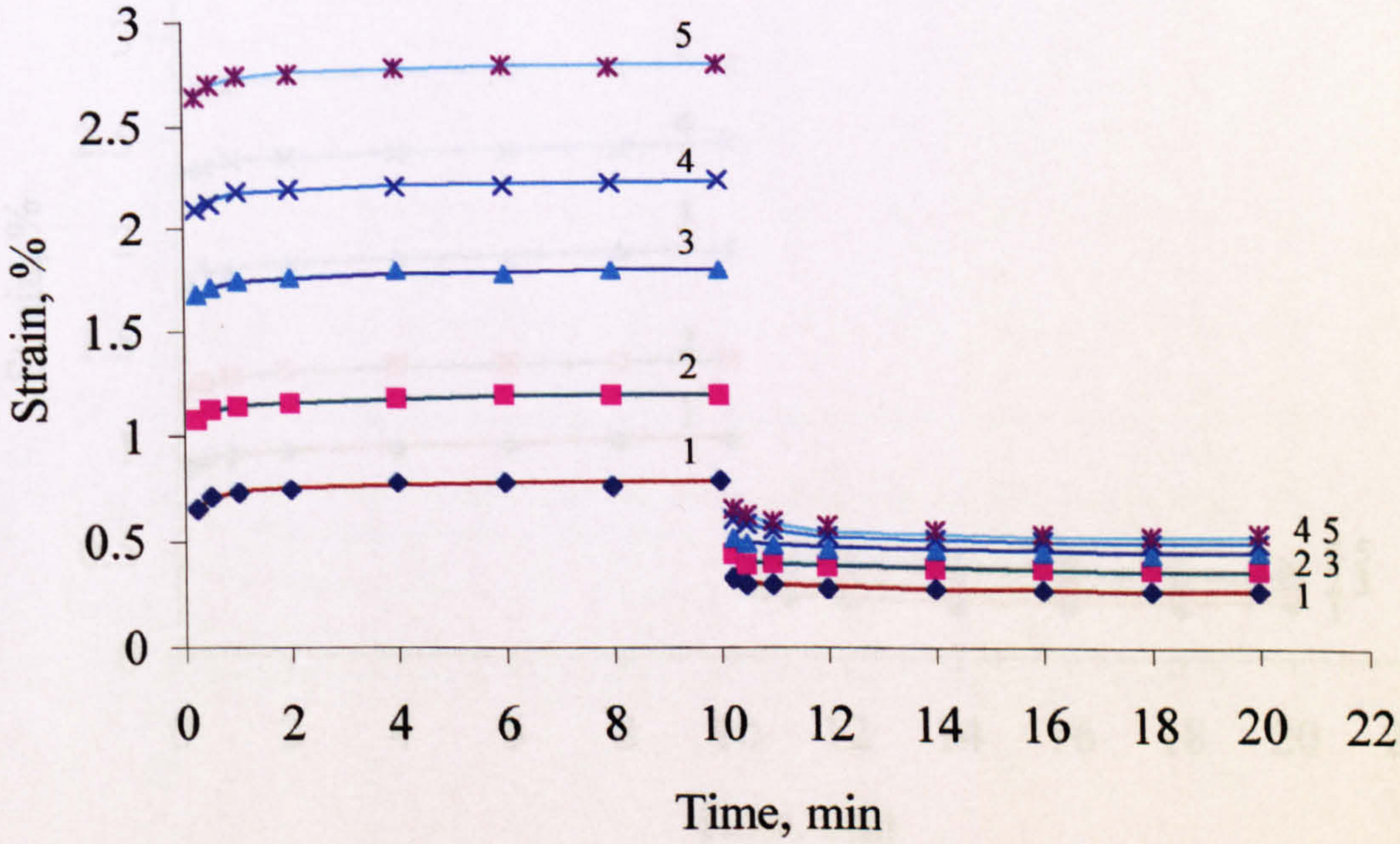

Fig. A_4 The family of creep-recovery curves for armos yarn at 140 °C at σ:(1) 0.65 GPa; (2) 0.83 GPa; (3) 1.35 GPa; (4) 1.74 GPa; (5) 2.12 GPa

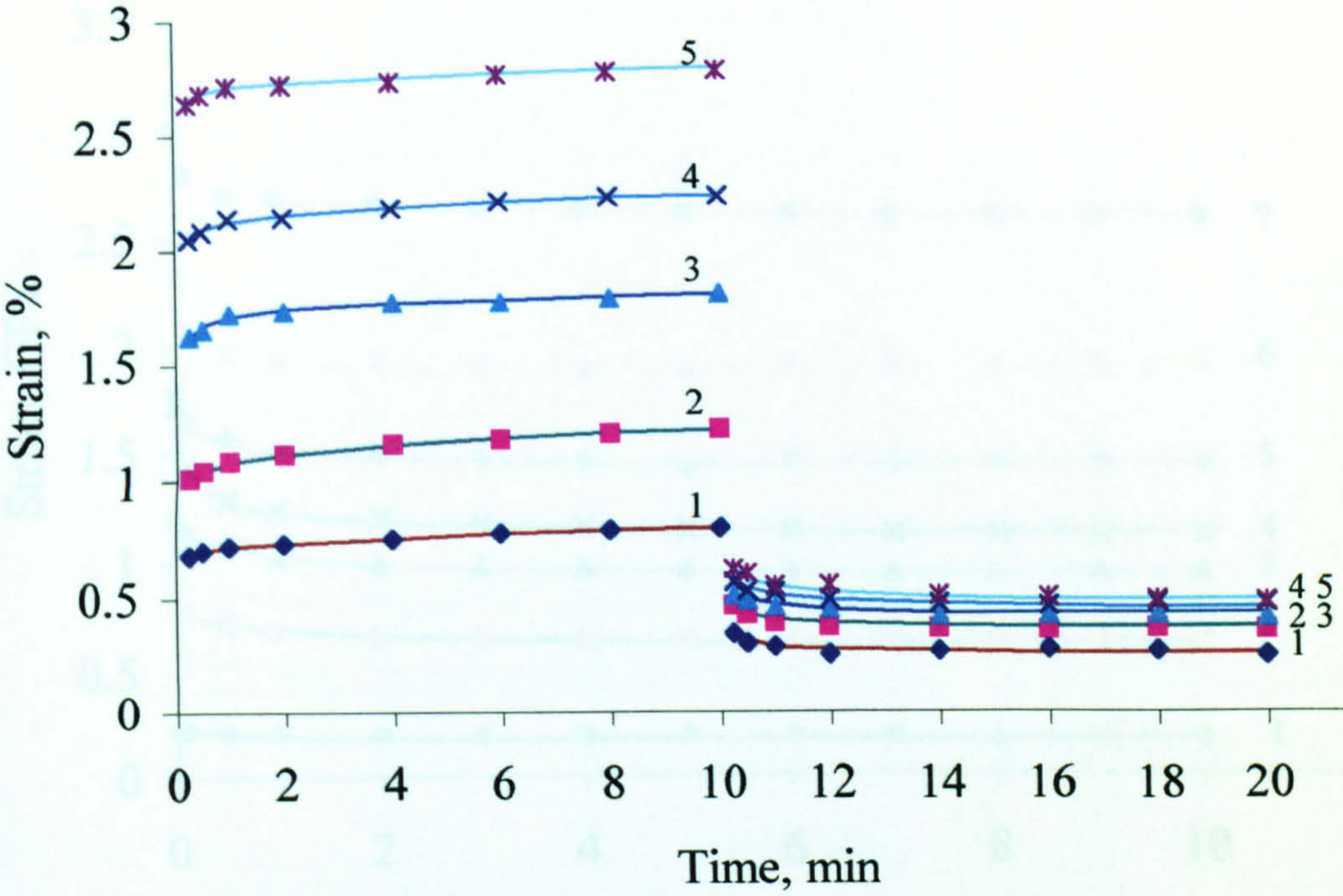

Fig. A_5 The family of creep-recovery curves for armos yarn at 180 ℃ at σ:(1) 0.65 GPa; (2) 0.83 GPa; (3) 1.35 GPa; (4) 1.74 GPa; (5) 2.12 GPa.

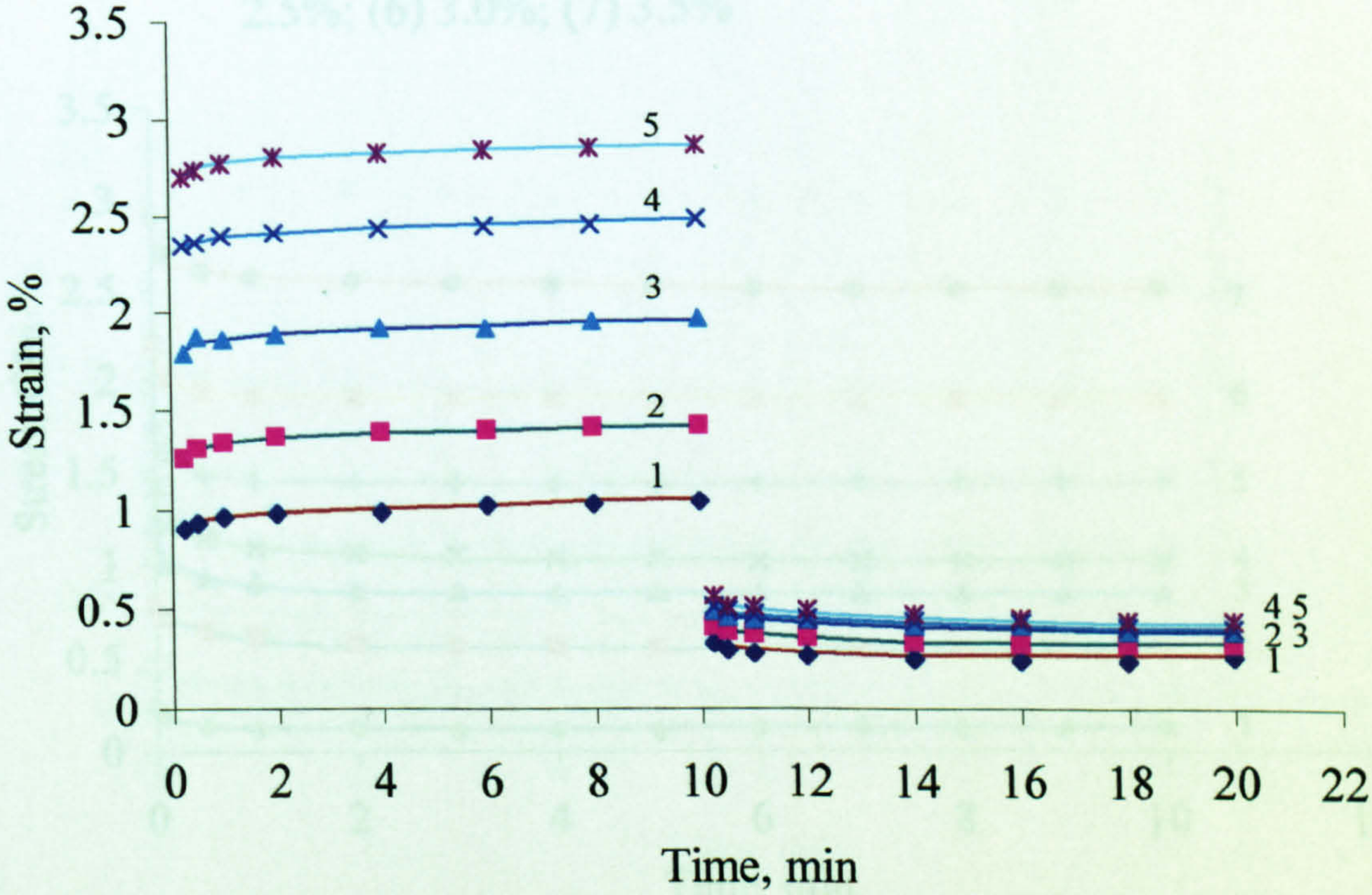

Fig. A_6 The family of creep-recovery curves for armos yarn at 20 ℃ at σ: (1) 0.65 GPa; (2) 0.83 GPa; (3) 1.35 GPa; (4) 1.74 GPa; (5) 2.12 GPa

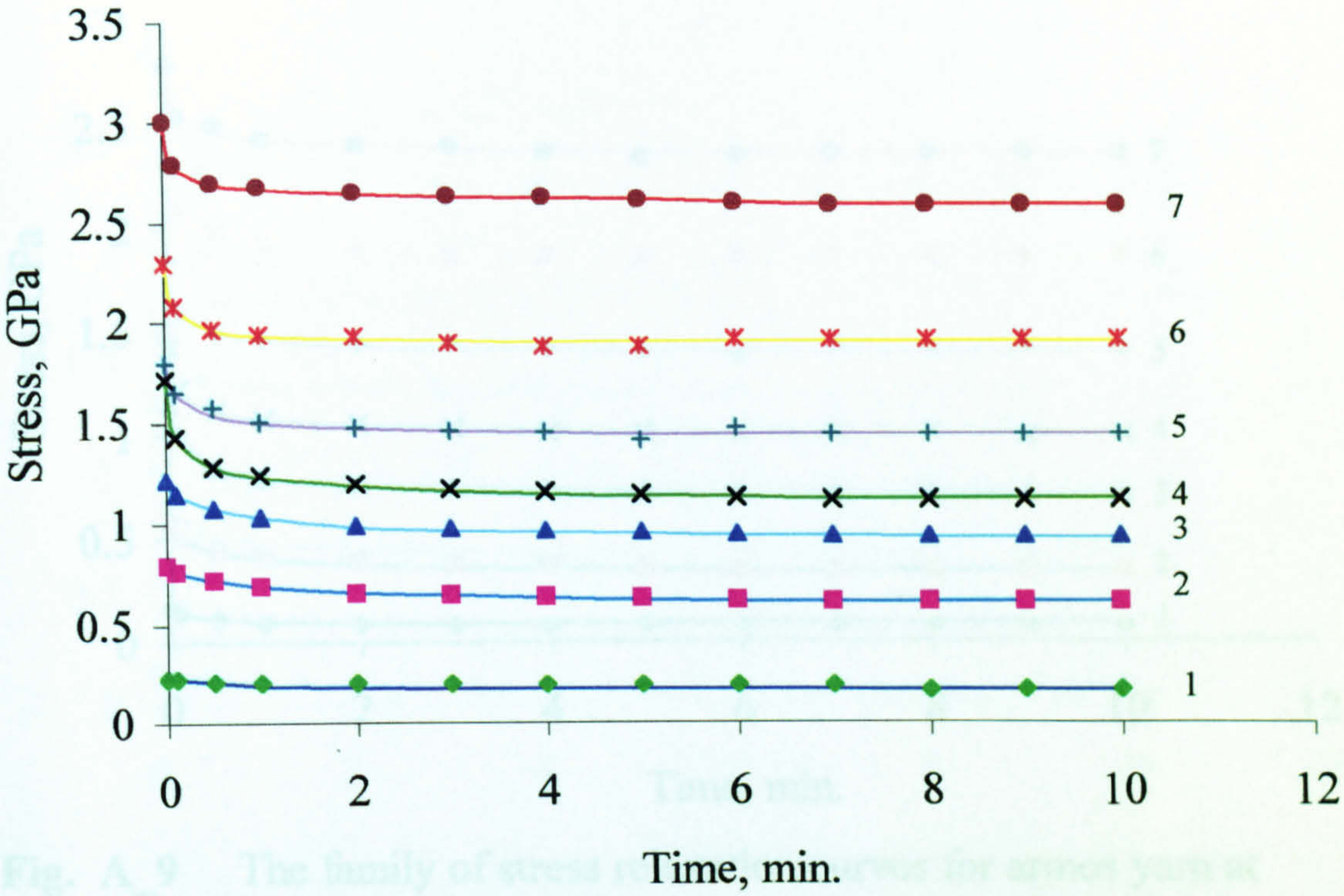

Fig. A_7 The family of stress relaxation curves for armos yarn at 60°C at ε: (1) 0.5%; (2) 1.0%; (3) 1.5%; (4) 2.0%; (5) 2.5%; (6) 3.0%; (7) 3.5%

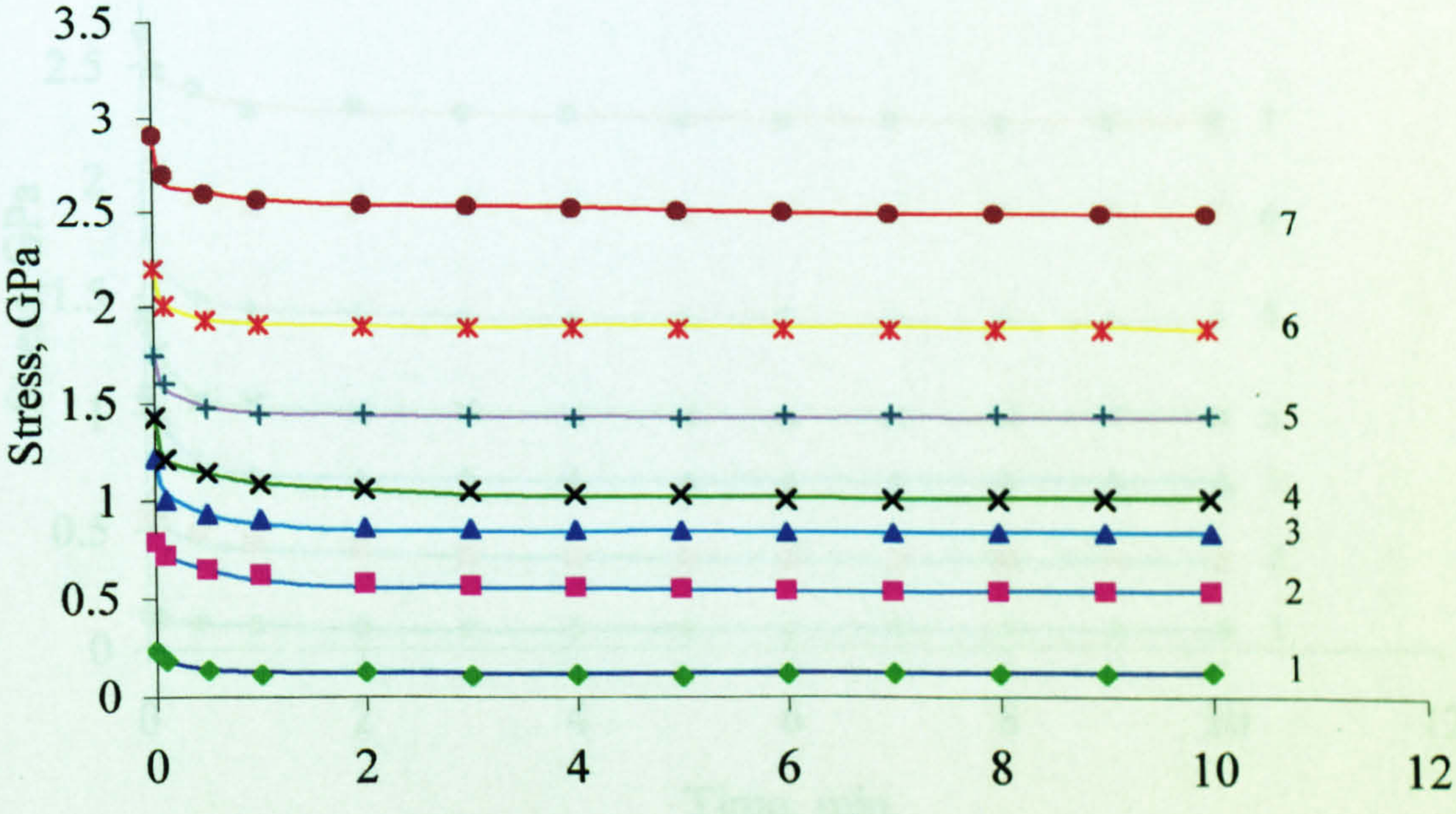

Fig. A_8 The family of stress relaxation curves for armos yarn at 80°C at ε: (1) 0.5%; (2) 1.0%; (3) 1.5%; (4) 2.0%; (5) 2.5%; (6) 3.0%; (7) 3.5%

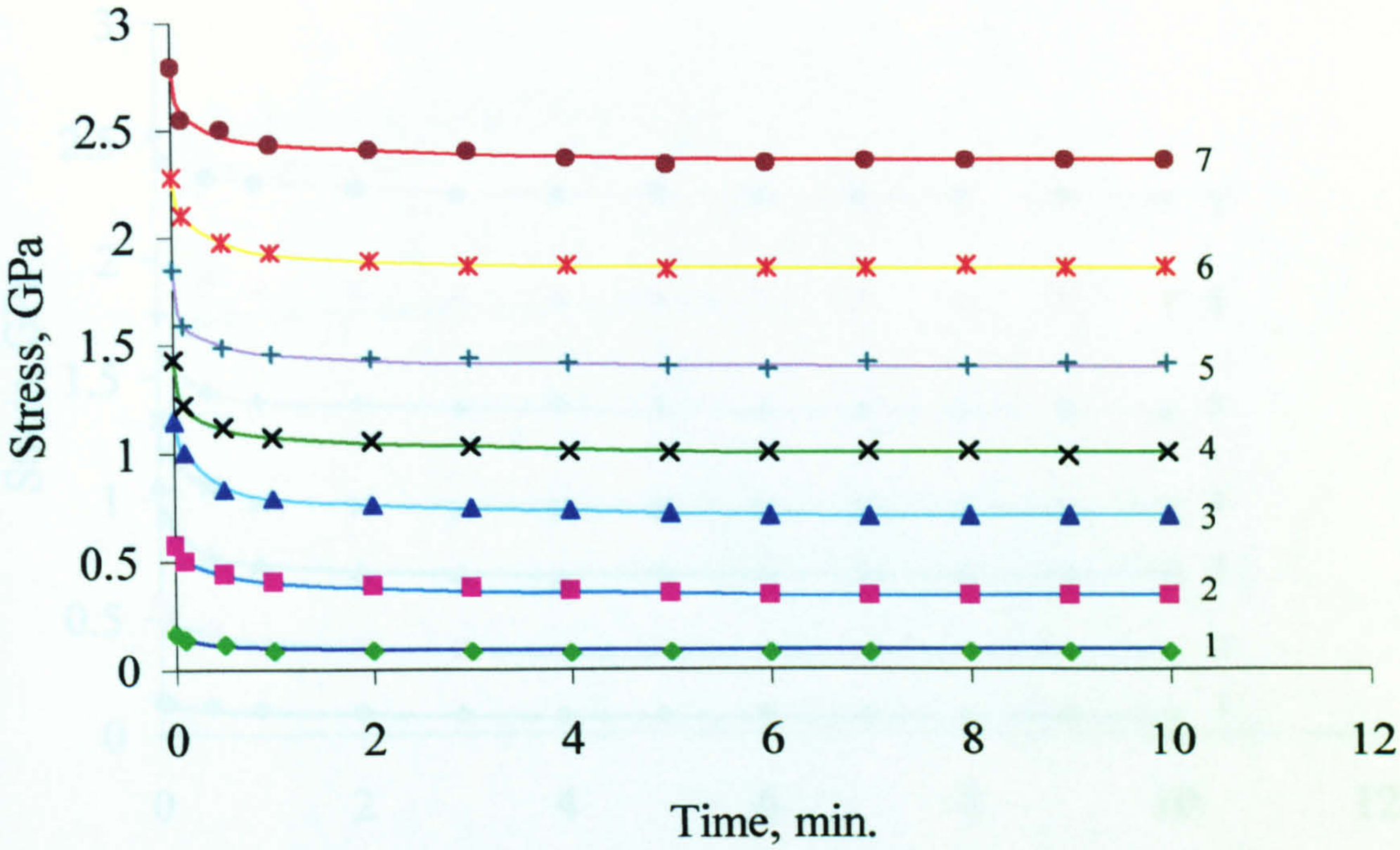

Fig. A_9 The family of stress relaxation curves for armos yarn at 100°C at ε: (1) 0.5%; (2) 1.0%; (3) 1.5%; (4) 2.0%; (5) 2.5%; (6) 3.0%; (7) 3.5%

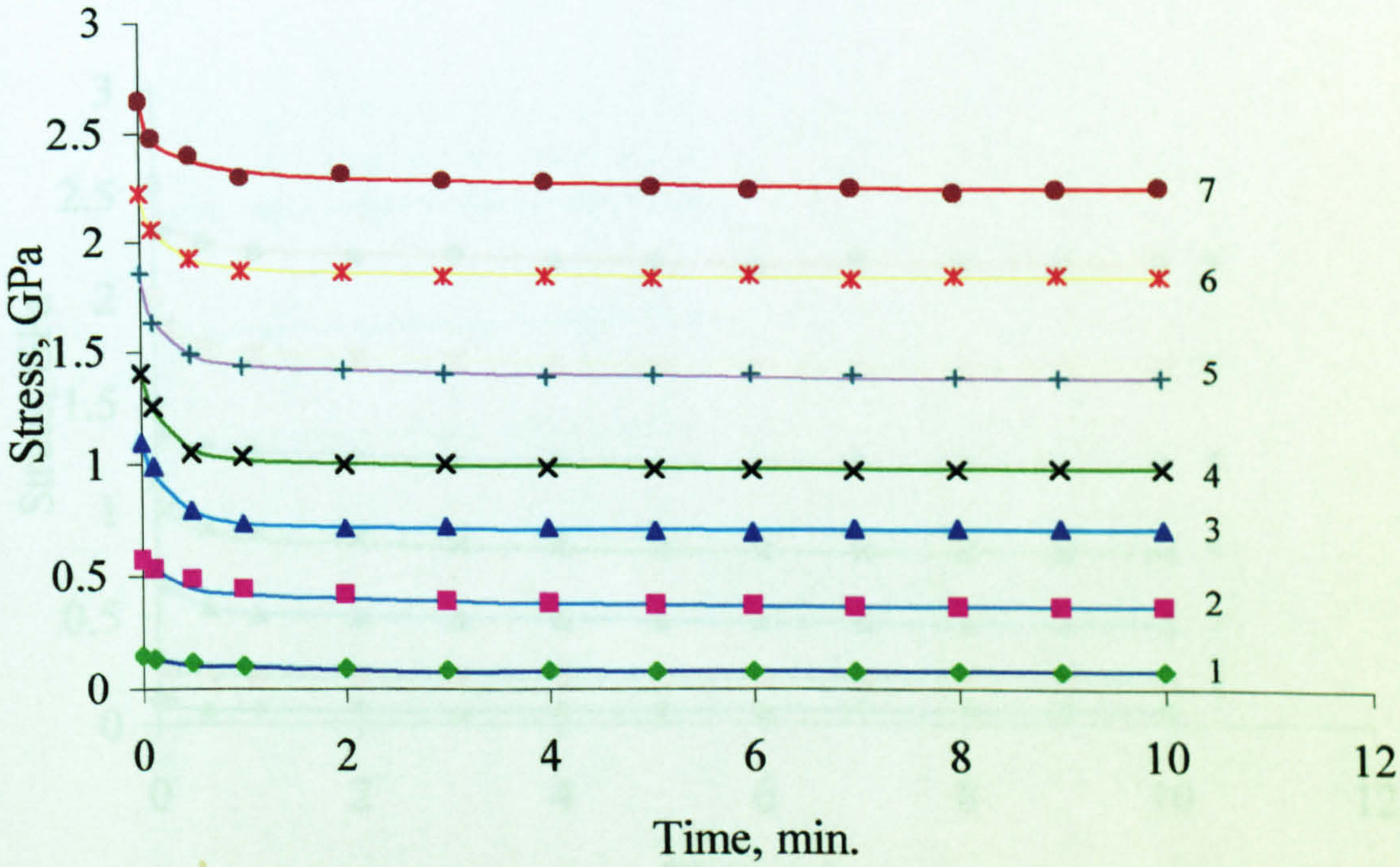

Fig. A_10 The family of stress relaxation curves for armos yarn at 140°C at ε: (1) 0.5%; (2) 1.0%; (3) 1.5%; (4) 2.0%; (5) 2.5%; (6) 3.0%; (7) 3.5%

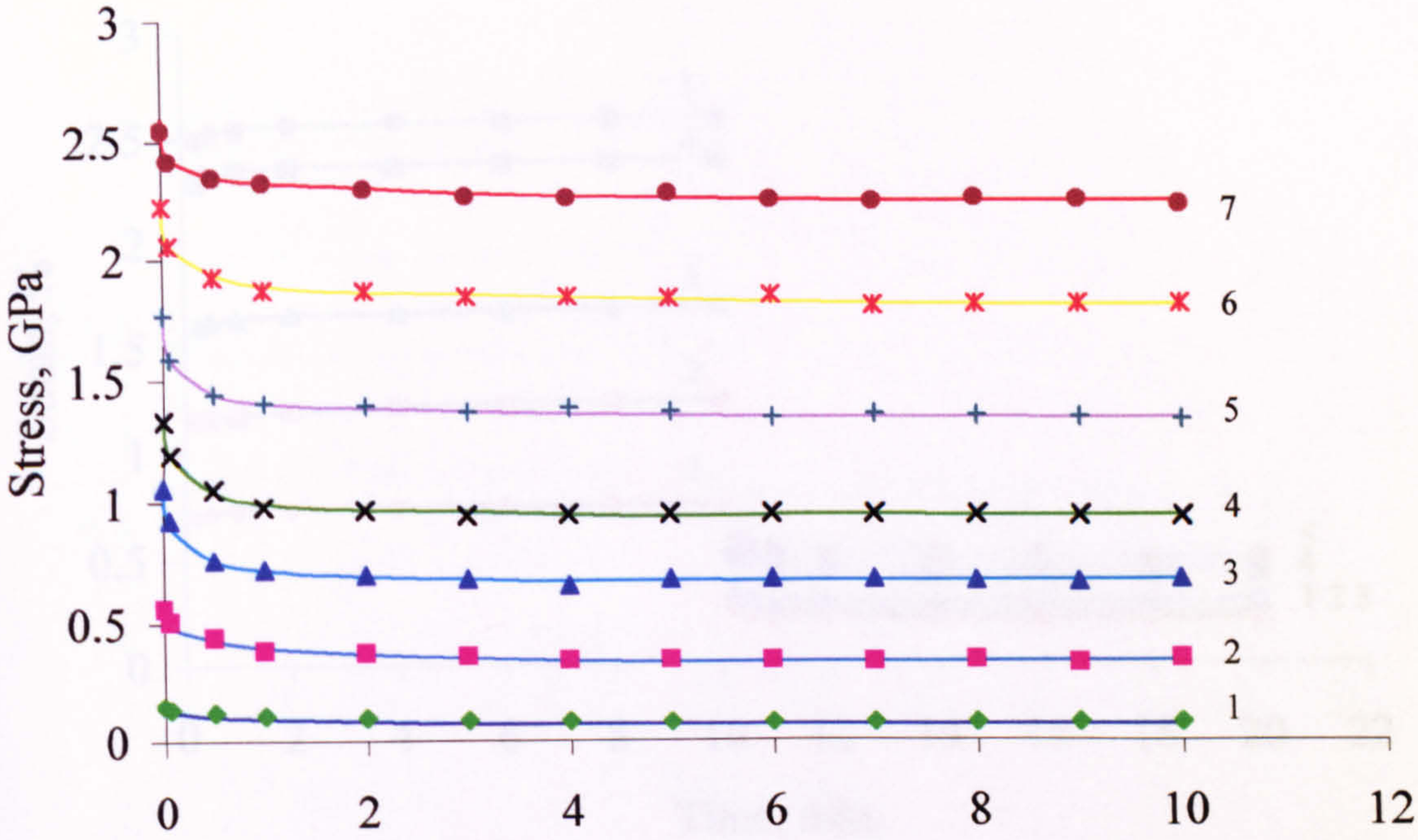

Fig. A_11 The family of stress relaxation curves for armos yarn at 180°C at ε: (1) 0.5%; (2) 1.0%; (3) 1.5%; (4) 2.0%; (5) 2.5%; (6) 3.0%; (7) 3.5%

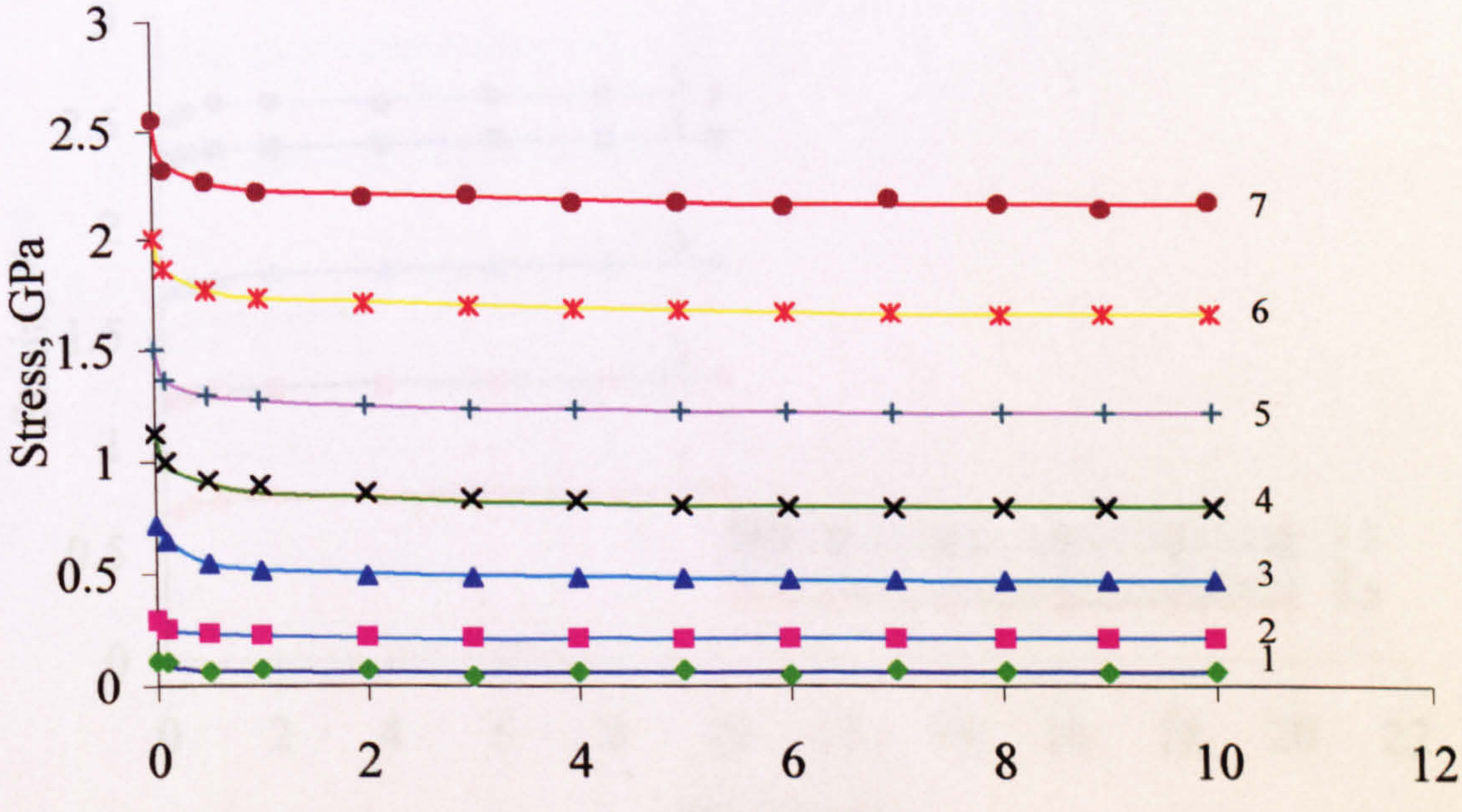

Fig. A_12 The family of stress relaxation curves for armos yarn at 220°C at ε: (1) 0.5%; (2) 1.0%; (3) 1.5%; (4) 2.0%; (5) 2.5%; (6) 3.0%; (7) 3.5%

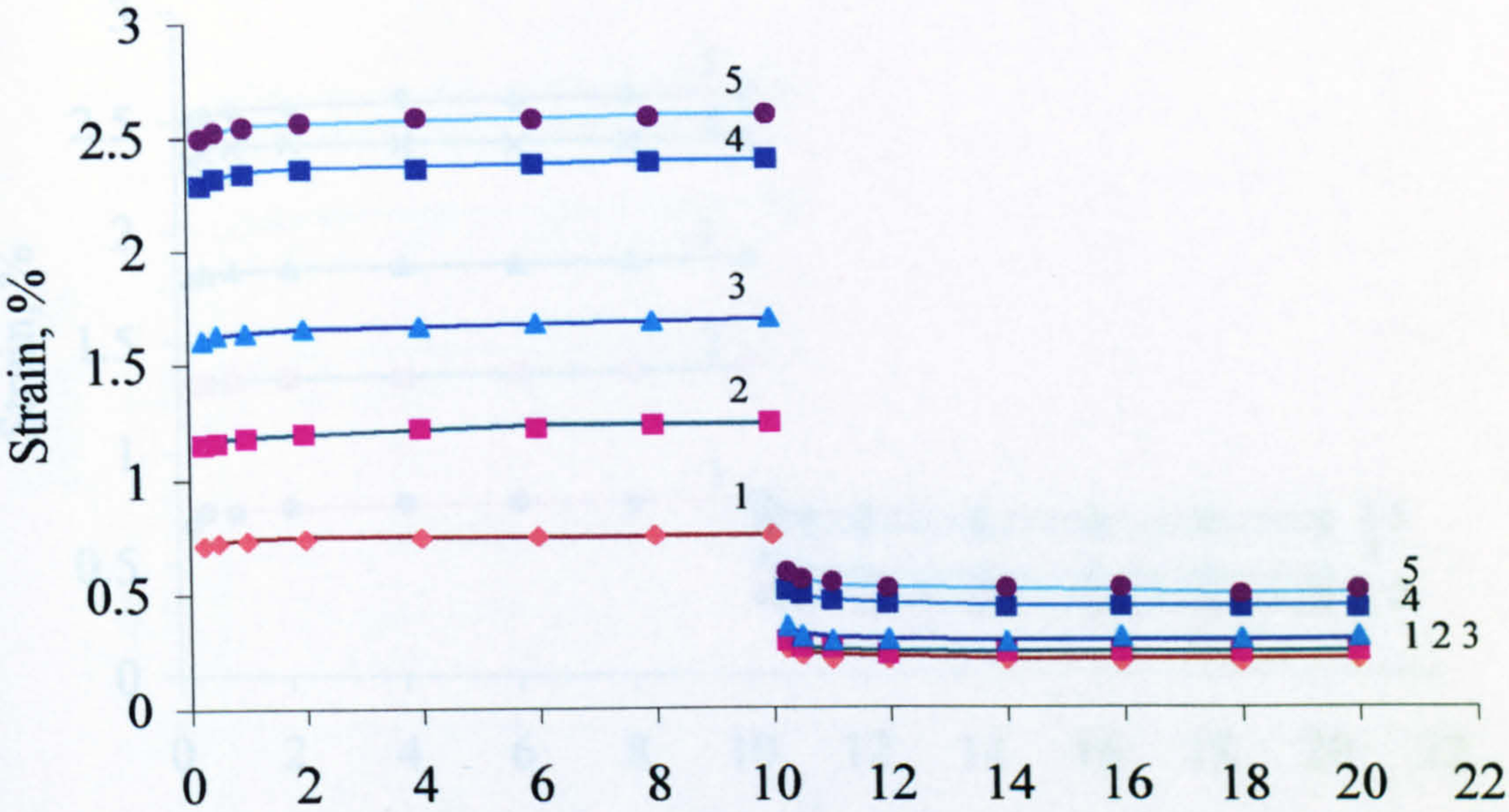

Fig. A_13 The family of creep-recovery curves for dried armos yarn at 20 ℃ at σ: (1) 0.74 GPa; (2) 1.28 GPa; (3) 1.79 GPa; (4) 2.37 GPa; (5) 2.52 GPa

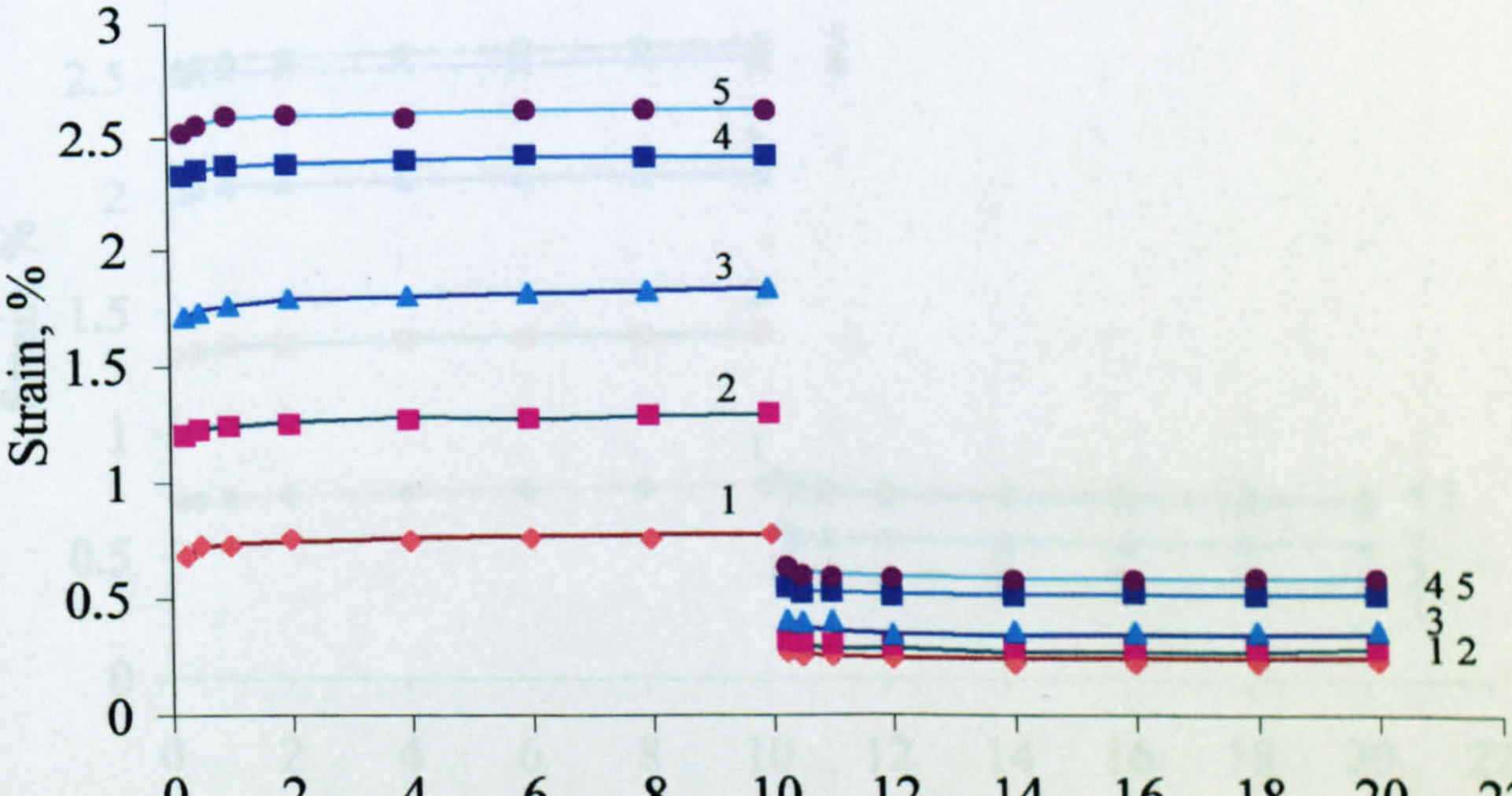

Fig. A_14 The family of creep-recovery curves for dried armos yarn at 60 ℃ at σ:(1) 0.74 GPa; (2) 1.28 GPa; (3) 1.79 GPa; (4) 2.37 GPa; (5) 2.52 GPa

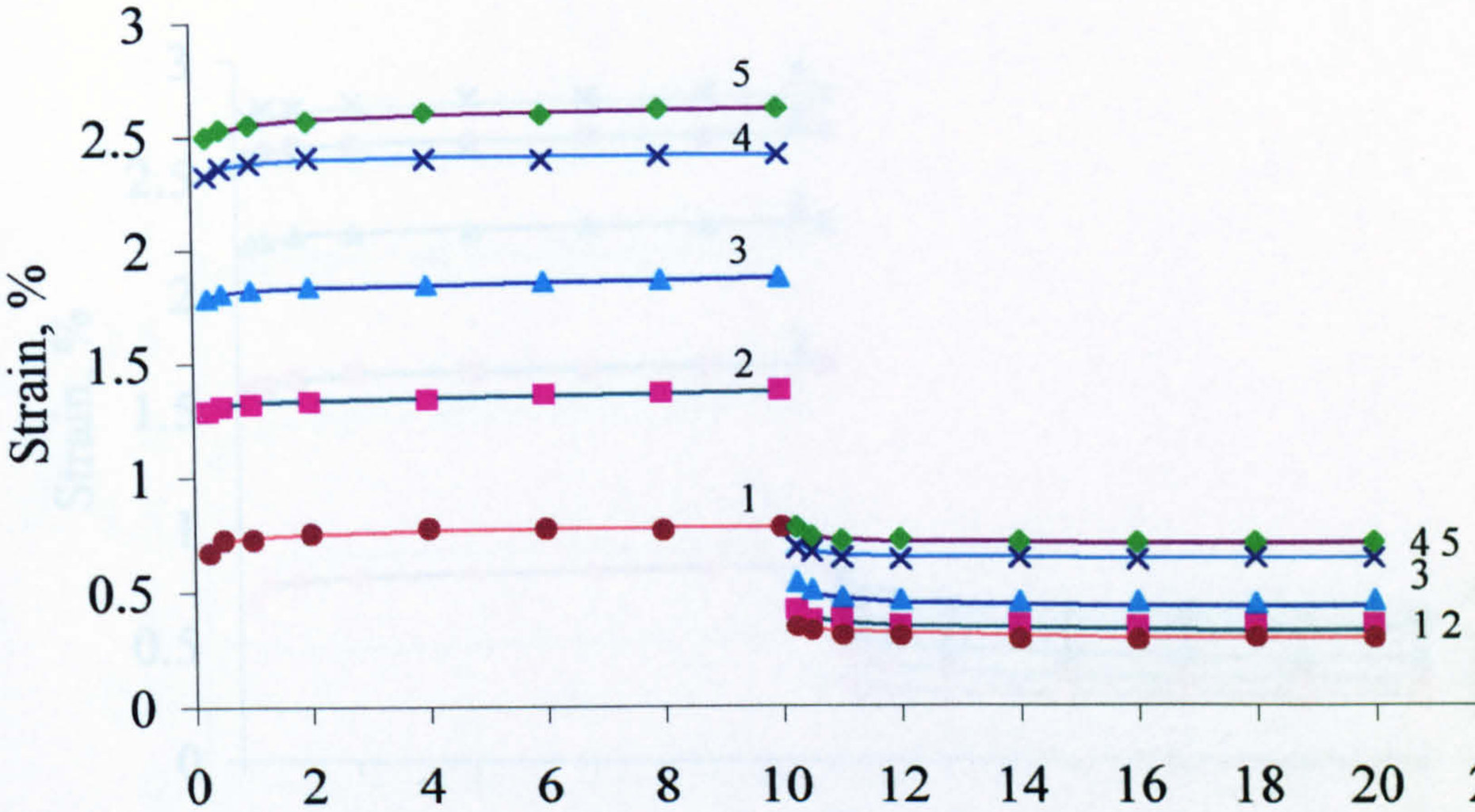

Fig. A_15 The family of creep-recovery curves for dried armos yarn at 100 ℃ at σ: (1) 0.74 GPa; (2) 1.28 GPa; (3) 1.79 GPa; (4) 2.37 GPa; (5) 2.52 GPa

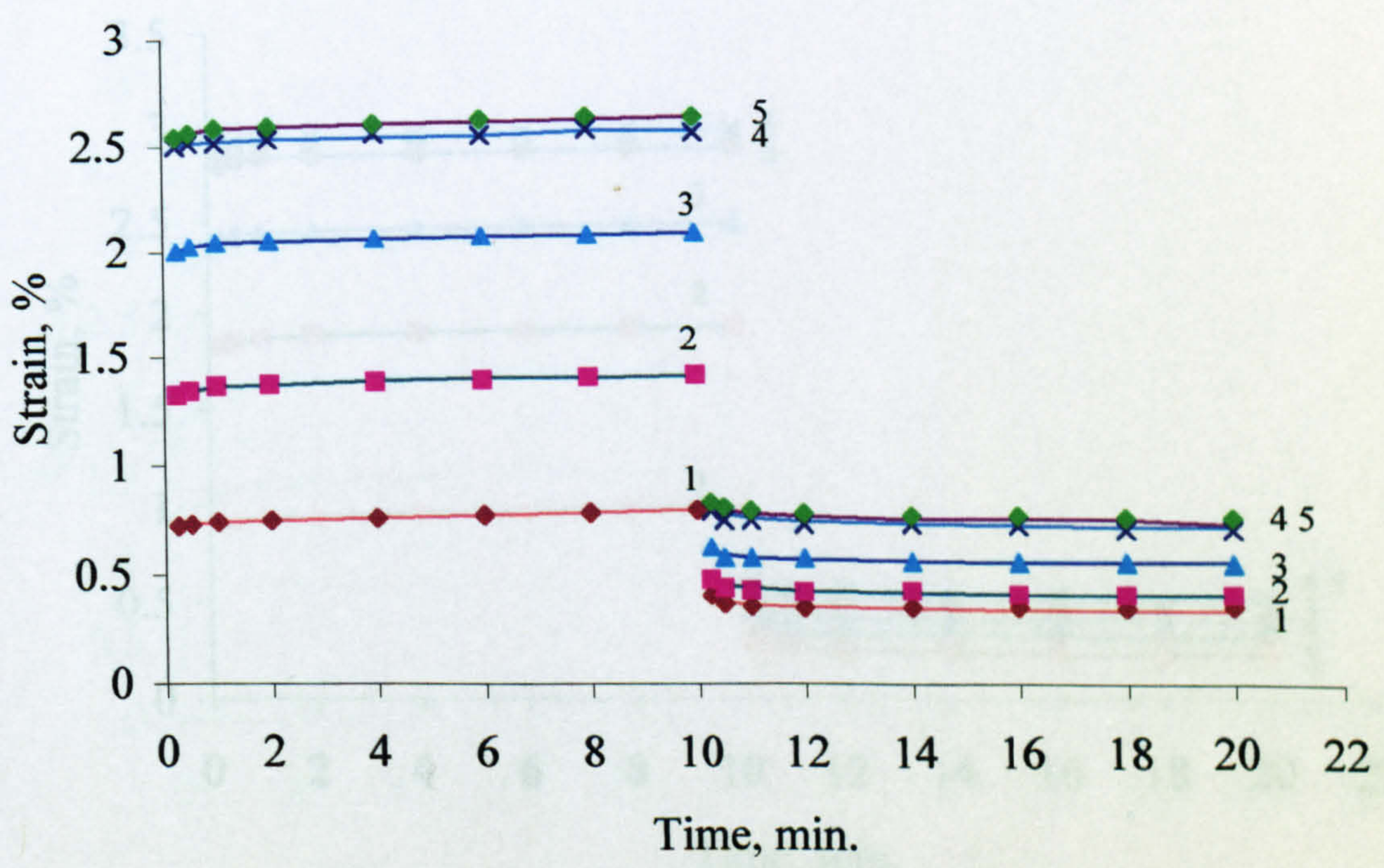

Fig. A_16 The family of creep-recovery curves for dried armos yarn at 140 ℃ at σ: (1) 0.74 GPa; (2) 1.28 GPa; (3) 1.79 GPa; (4) 2.37 GPa; (5) 2.52 GPa

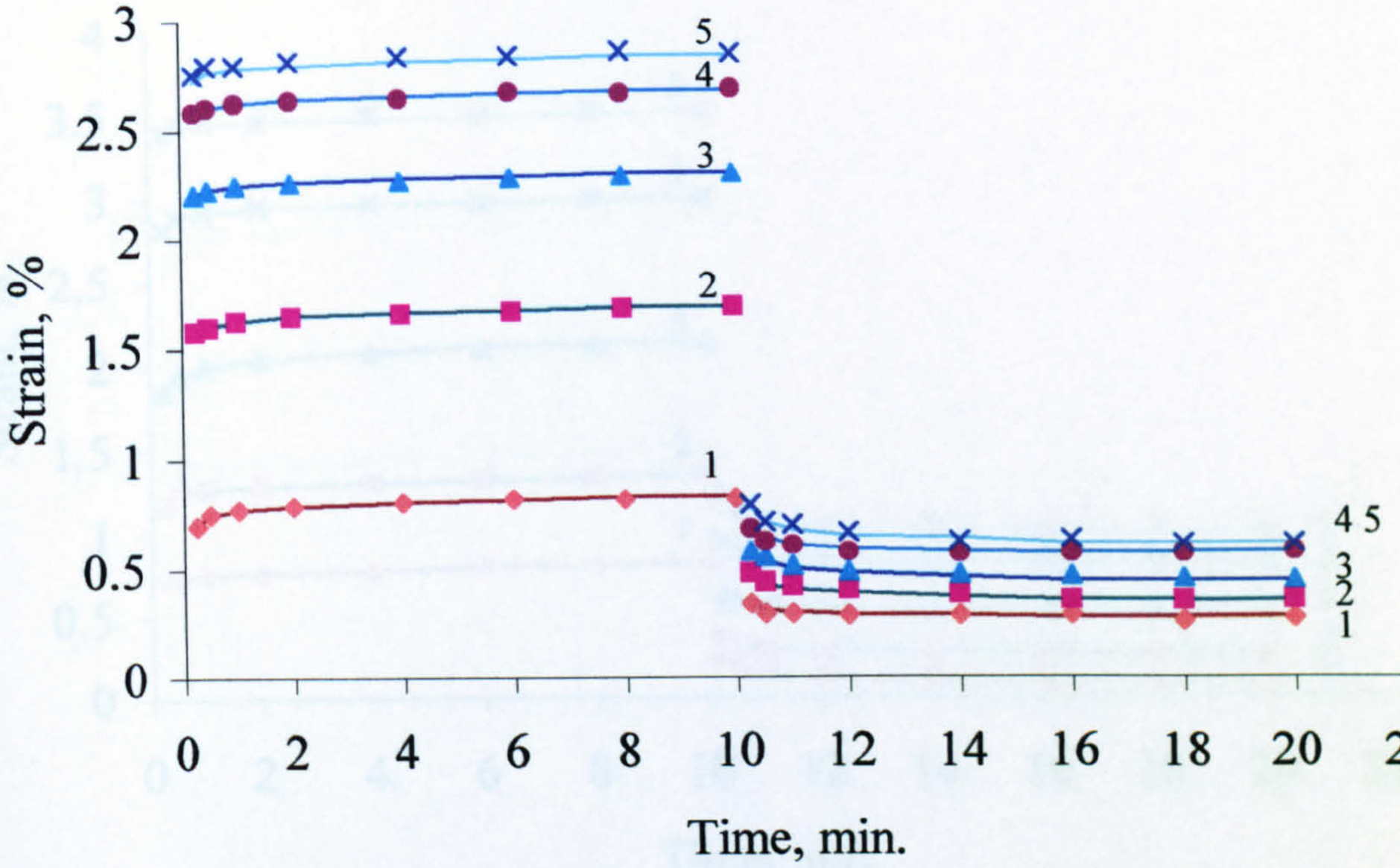

Fig. A_17 The family of creep-recovery curves for dried armos yarn at 180 °C at σ: (1) 0.74 GPa; (2) 1.28 GPa; (3) 1.79 GPa; (4) 2.37 GPa; (5) 2.52 GPa

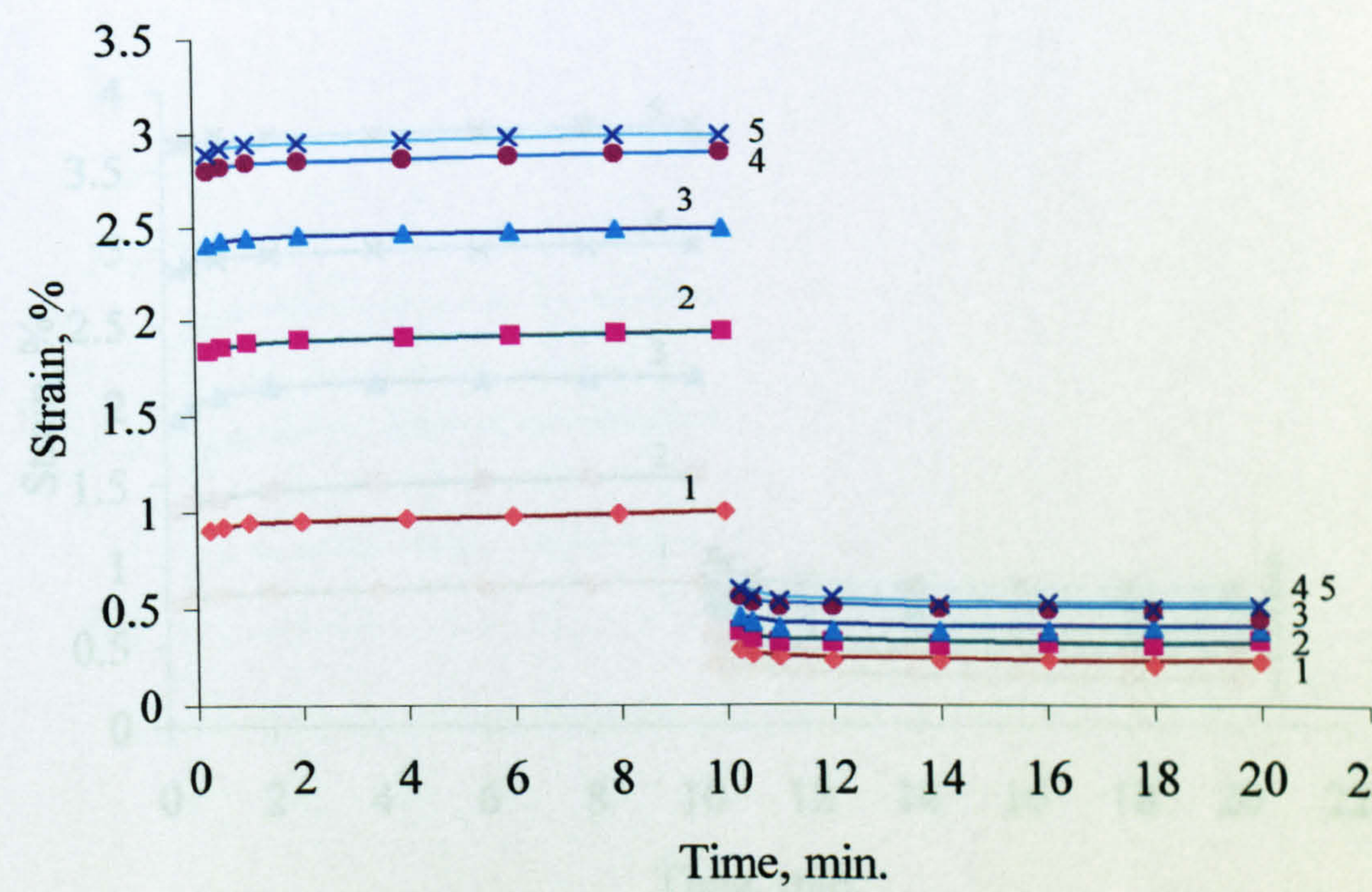

Fig. A_18 The family of creep-recovery curves for dried armos yarn at 220 °C at σ: (1) 0.74 GPa; (2) 1.28 GPa; (3) 1.79 GPa; (4) 2.37 GPa; (5) 2.52 GPa

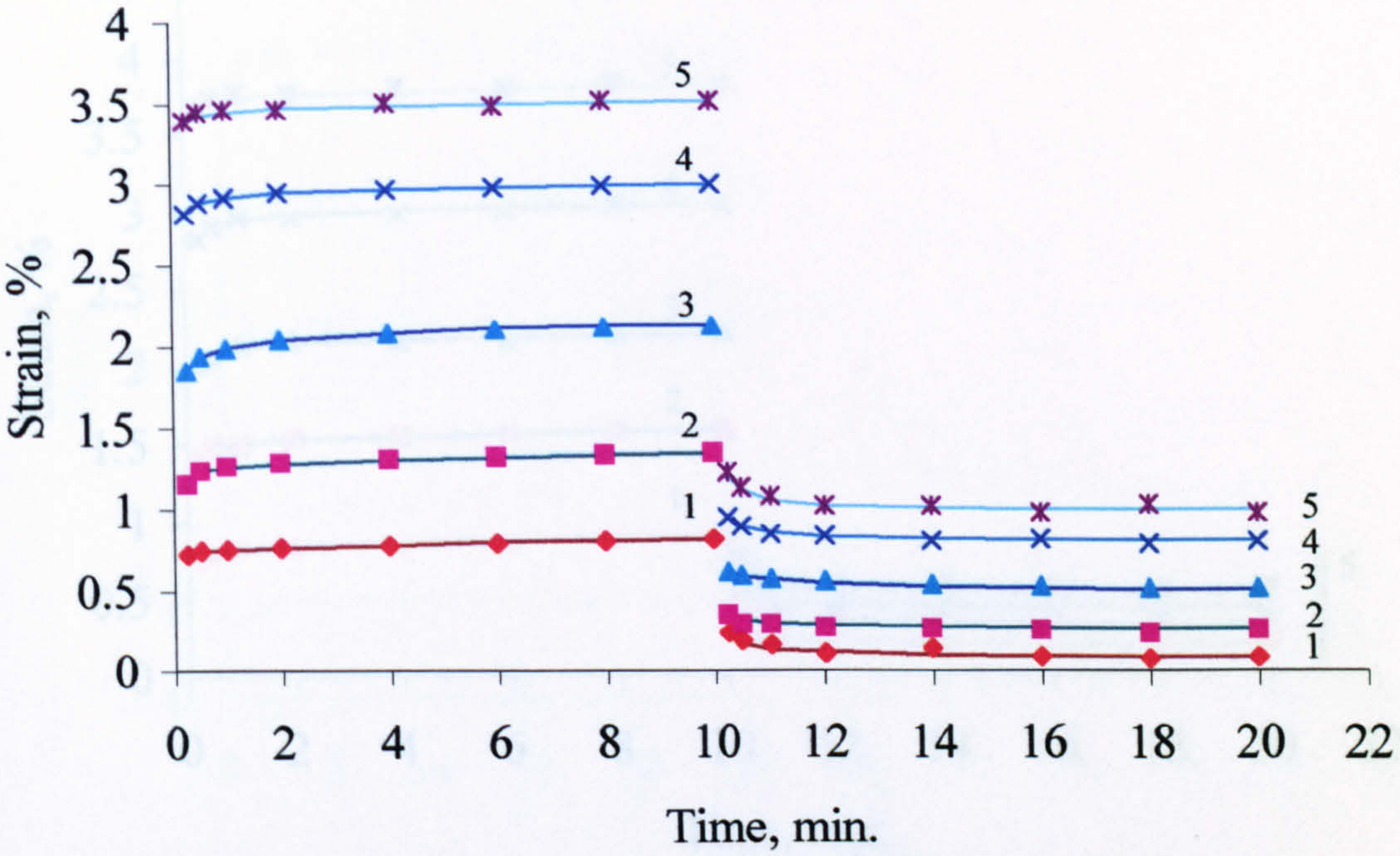

Fig. A_19 The family of creep-recovery curves for SVM yarn at 60 °C at σ: (1) 0.62 GPa; (2) 1.23 GPa; (3) 1.66 GPa; (4) 1.96 GPa; (5) 2.52 GPa

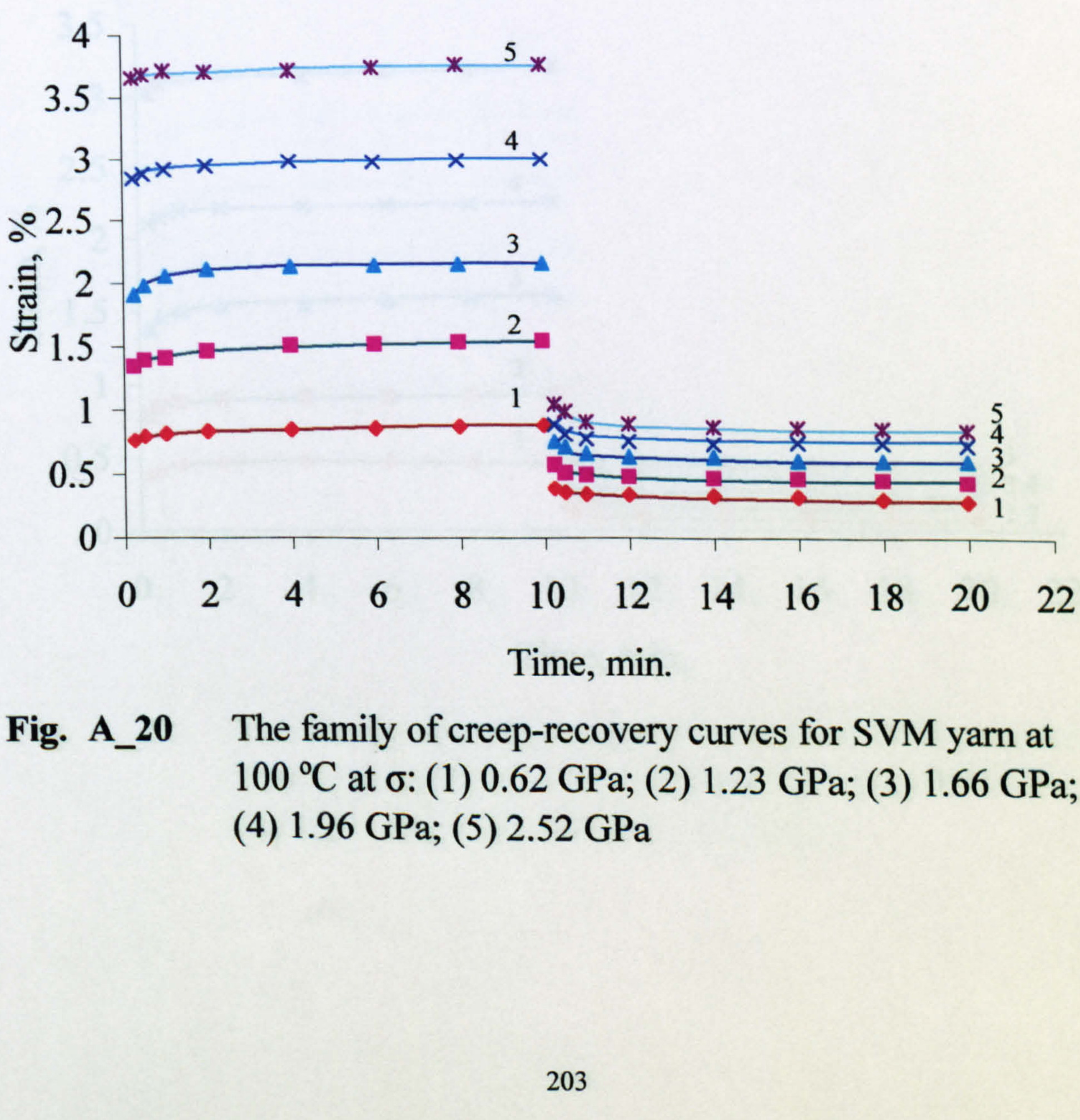

Fig. A_20 The family of creep-recovery curves for SVM yarn at 100 °C at σ: (1) 0.62 GPa; (2) 1.23 GPa; (3) 1.66 GPa; (4) 1.96 GPa; (5) 2.52 GPa

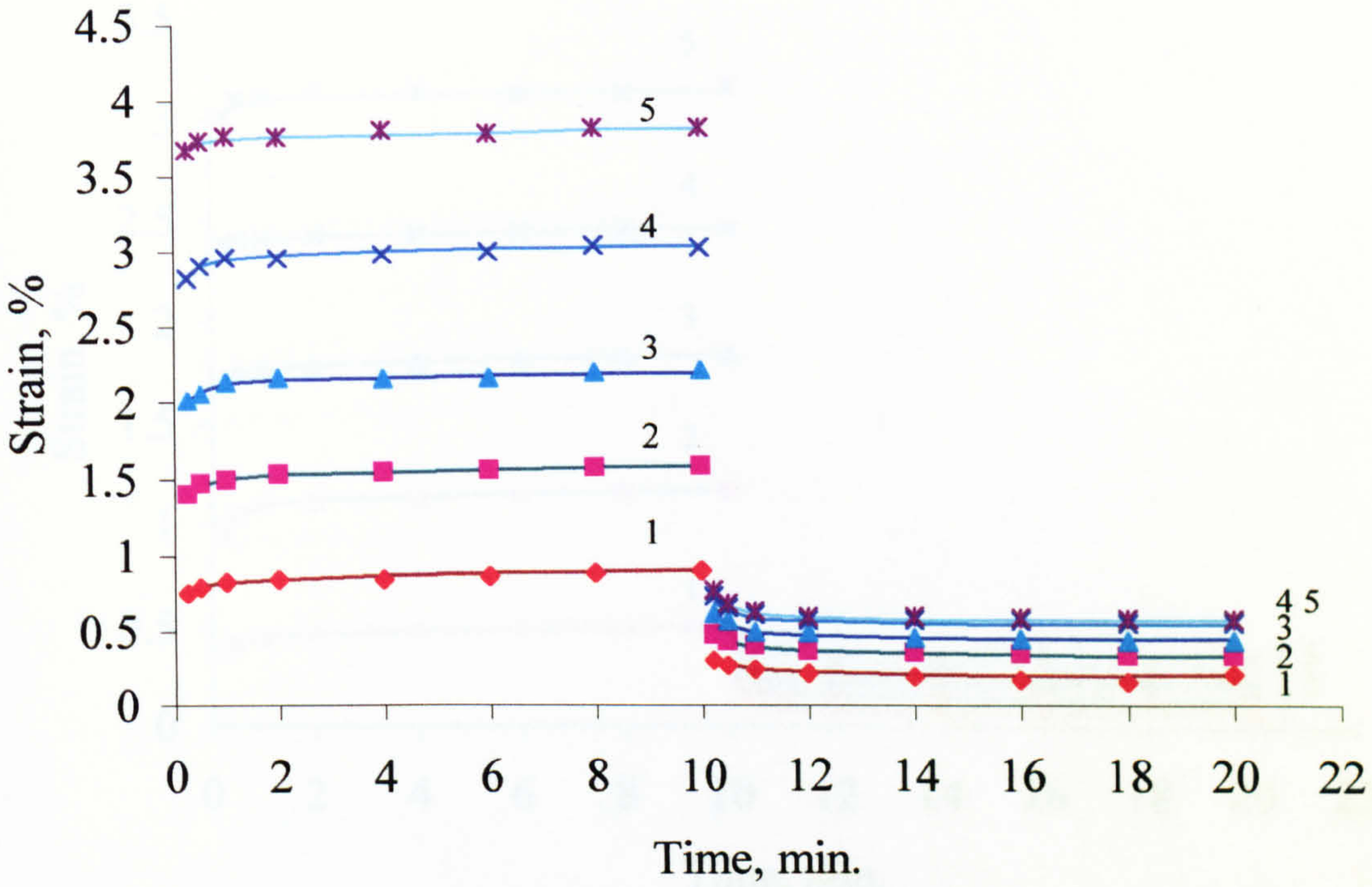

Fig. A_21 The family of creep-recovery curves for SVM yarn at 140 °C at σ:(1) 0.62 GPa; (2) 1.23 GPa; (3) 1.66 GPa; (4) 1.96 GPa; (5) 2.52 GPa

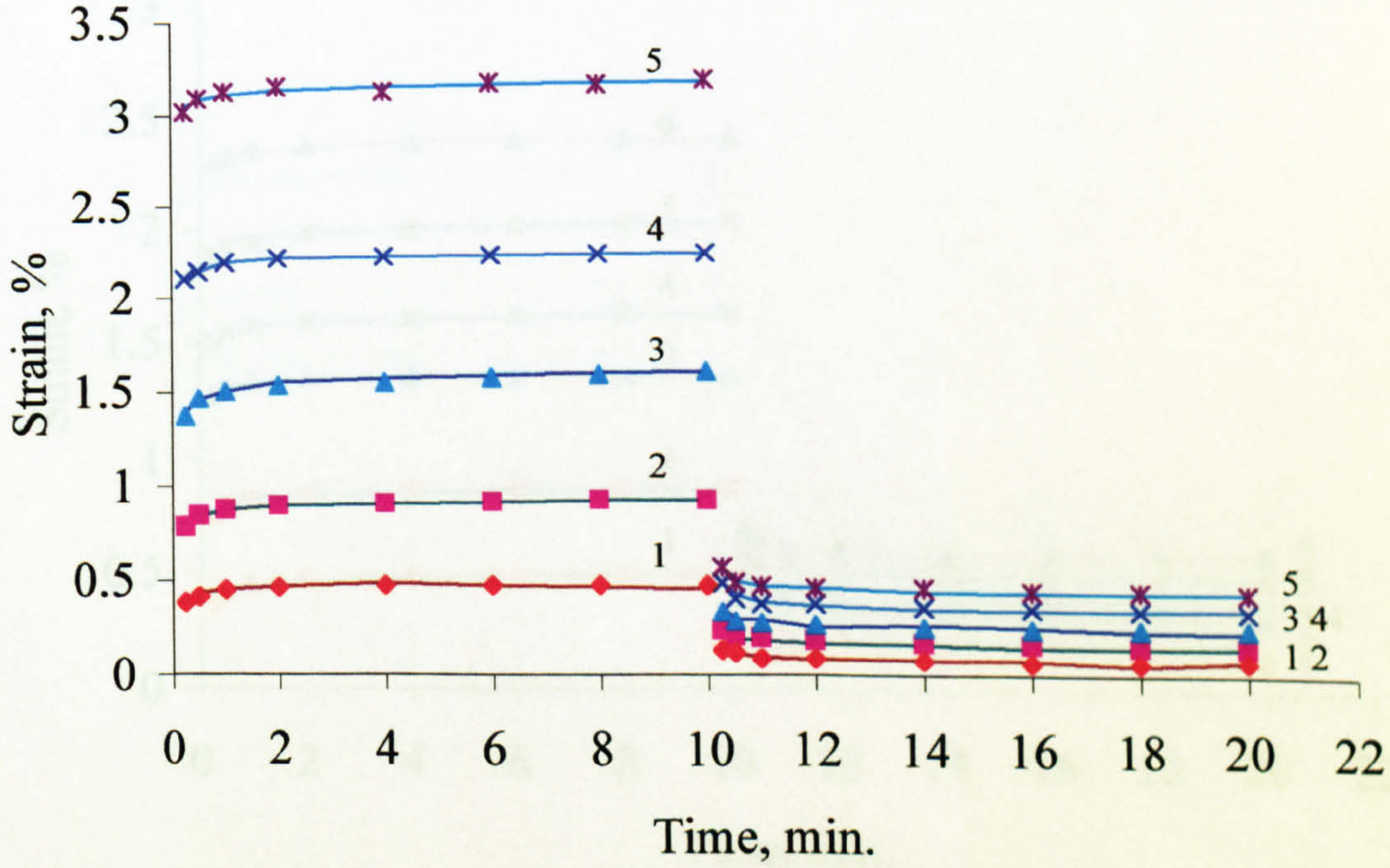

Fig. A_22 The family of creep-recovery curves for SVM yarn at 180 °C at σ: (1) 0.24 GPa; (2) 0.62 GPa; (3) 0.94 GPa; (4) 1.29 GPa; (5) 1.96 GPa

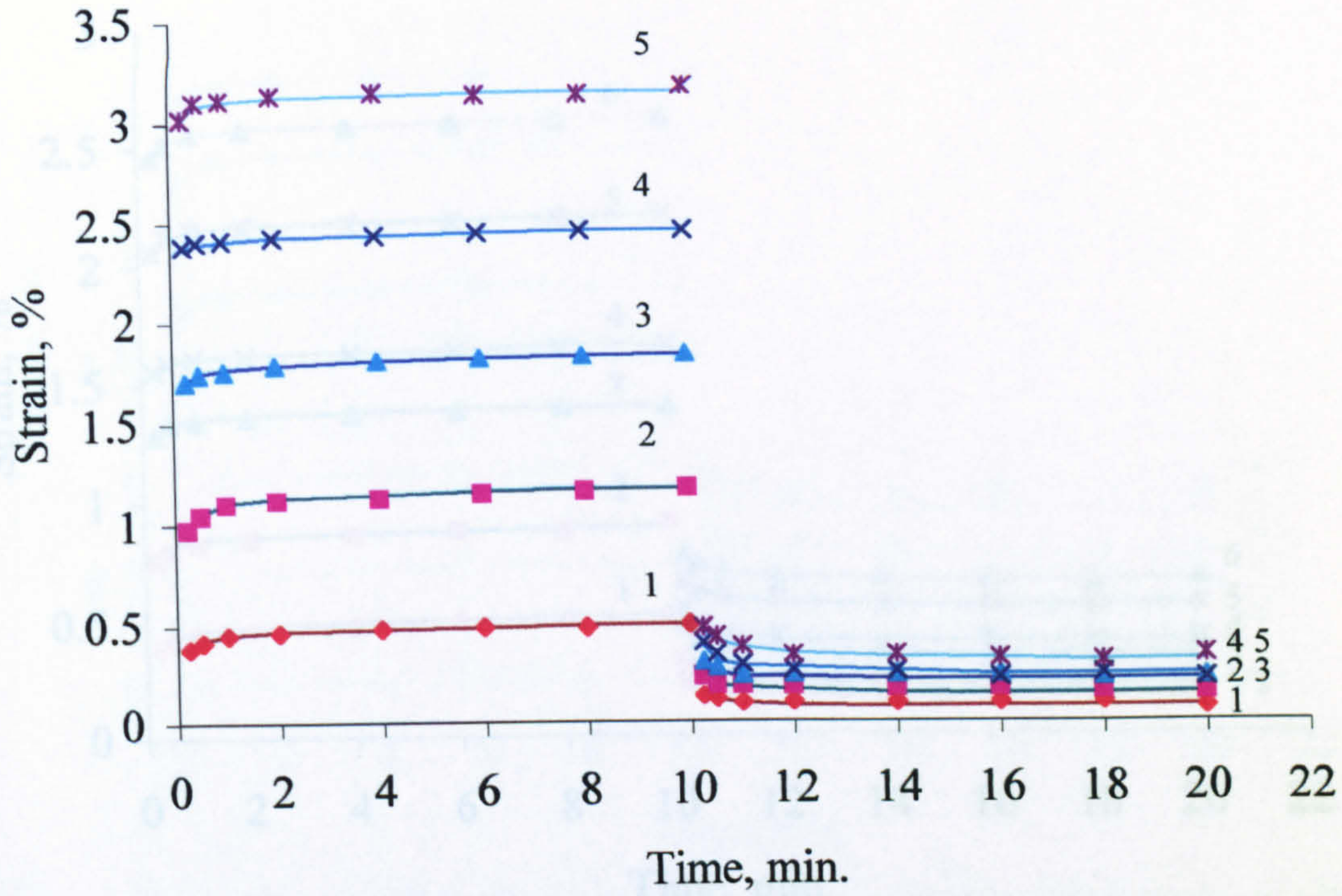

Fig. A_23 The family of creep-recovery curves for SVM yarn at 220 °C at σ: (1) 0.24 GPa; (2) 0.62 GPa; (3) 0.94 GPa; (4) 1.29 GPa; (5) 1.96 GPa

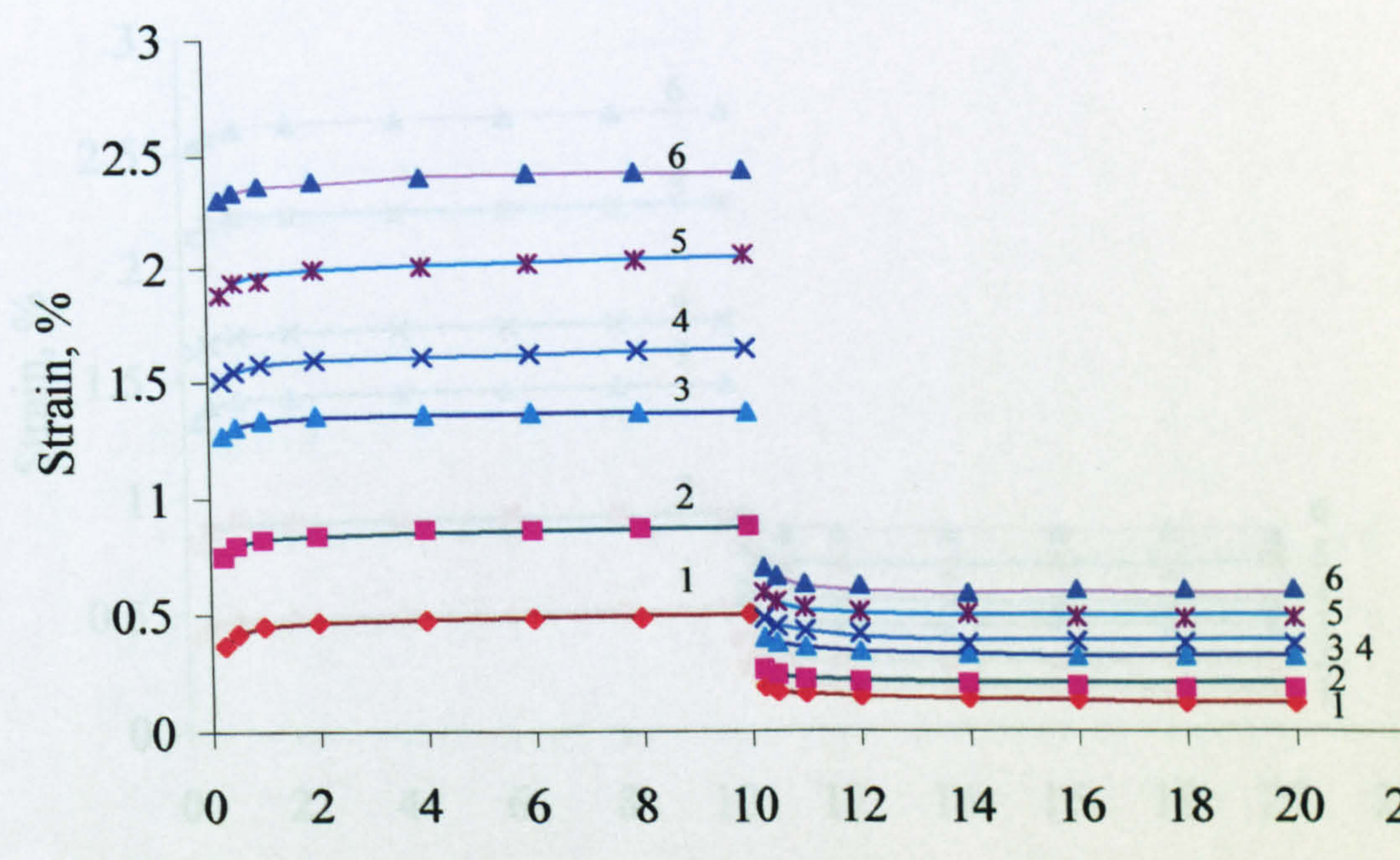

Fig. A_24 The family of creep-recovery curves for terlon yarn at 60 °C at σ: (1) 0.25 GPa; (2) 0.50 GPa; (3) 0.74 GPa; (4) 0.99 GPa; (5) 1.23 GPa; (6) 1.54 GPa

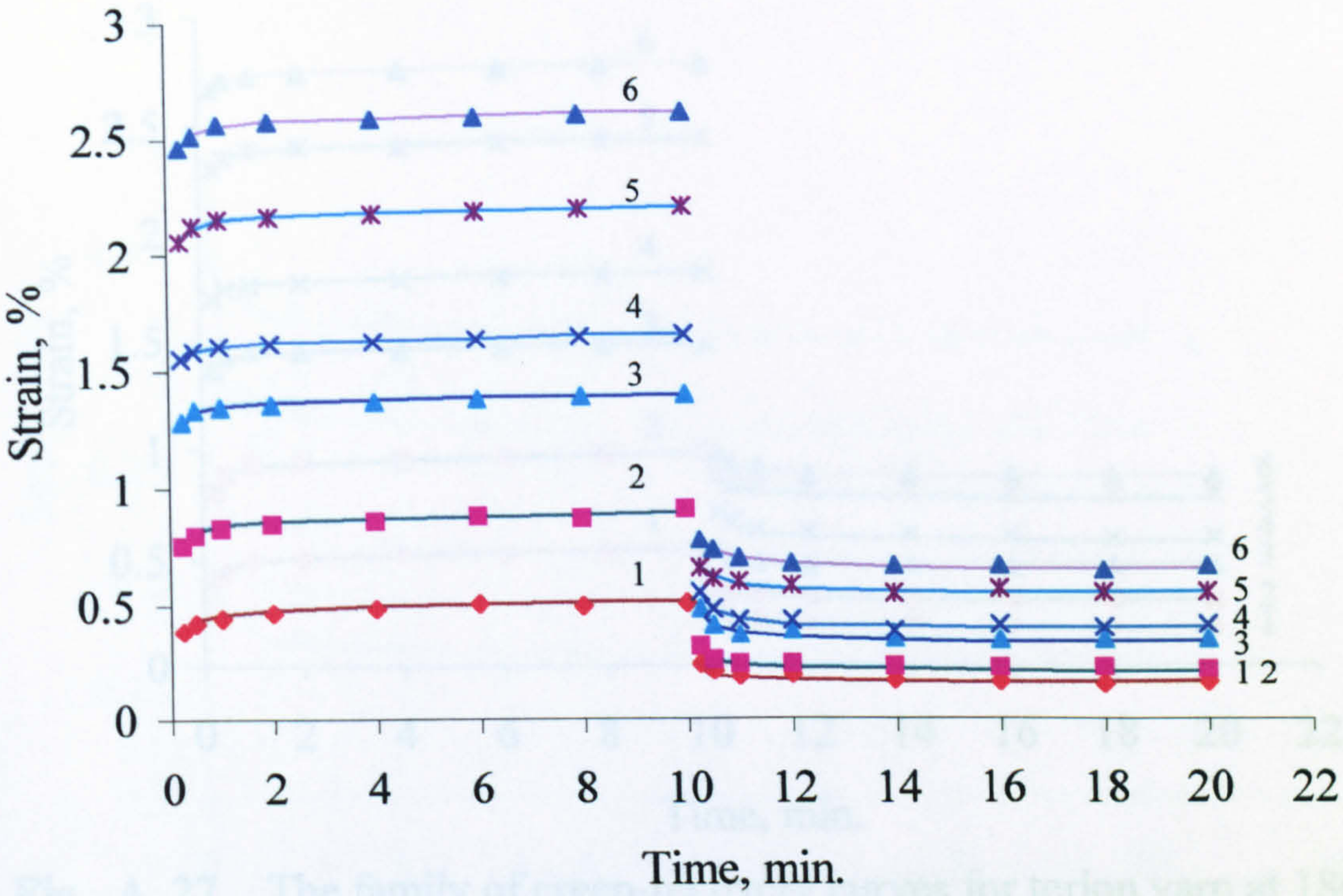

Fig. A_25 The family of creep-recovery curves for terlon yarn at 100 °C at σ: (1) 0.25 GPa; (2) 0.50 GPa; (3) 0.74 GPa; (4) 0.99 GPa; (5) 1.23 GPa; (6) 1.54 GPa

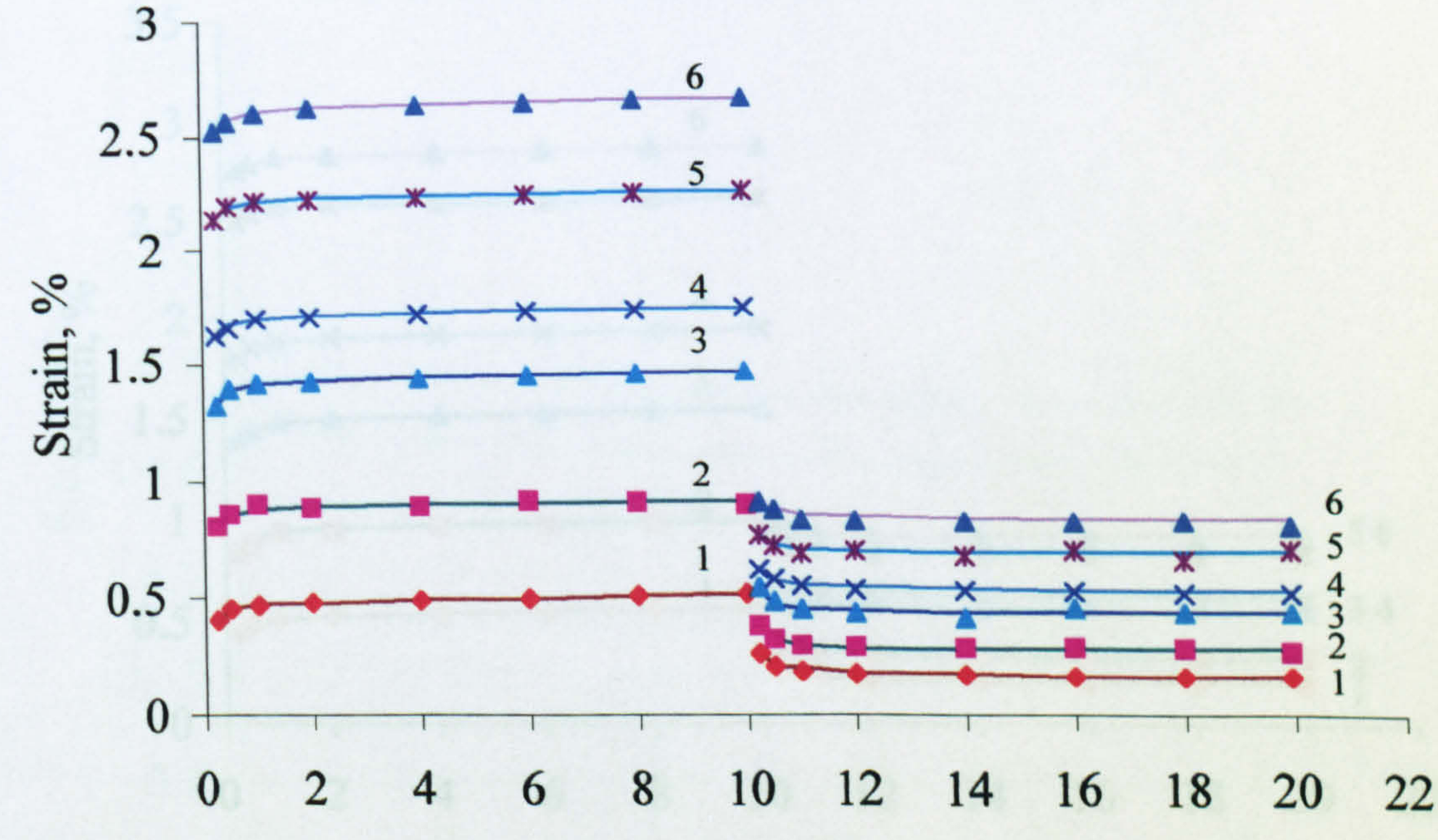

Fig. A_26 The family of creep-recovery curves for terlon yarn at 140 °C at σ: (1) 0.25 GPa; (2) 0.50 GPa; (3) 0.74 GPa; (4) 0.99 GPa; (5) 1.23 GPa; (6) 1.54 GPa

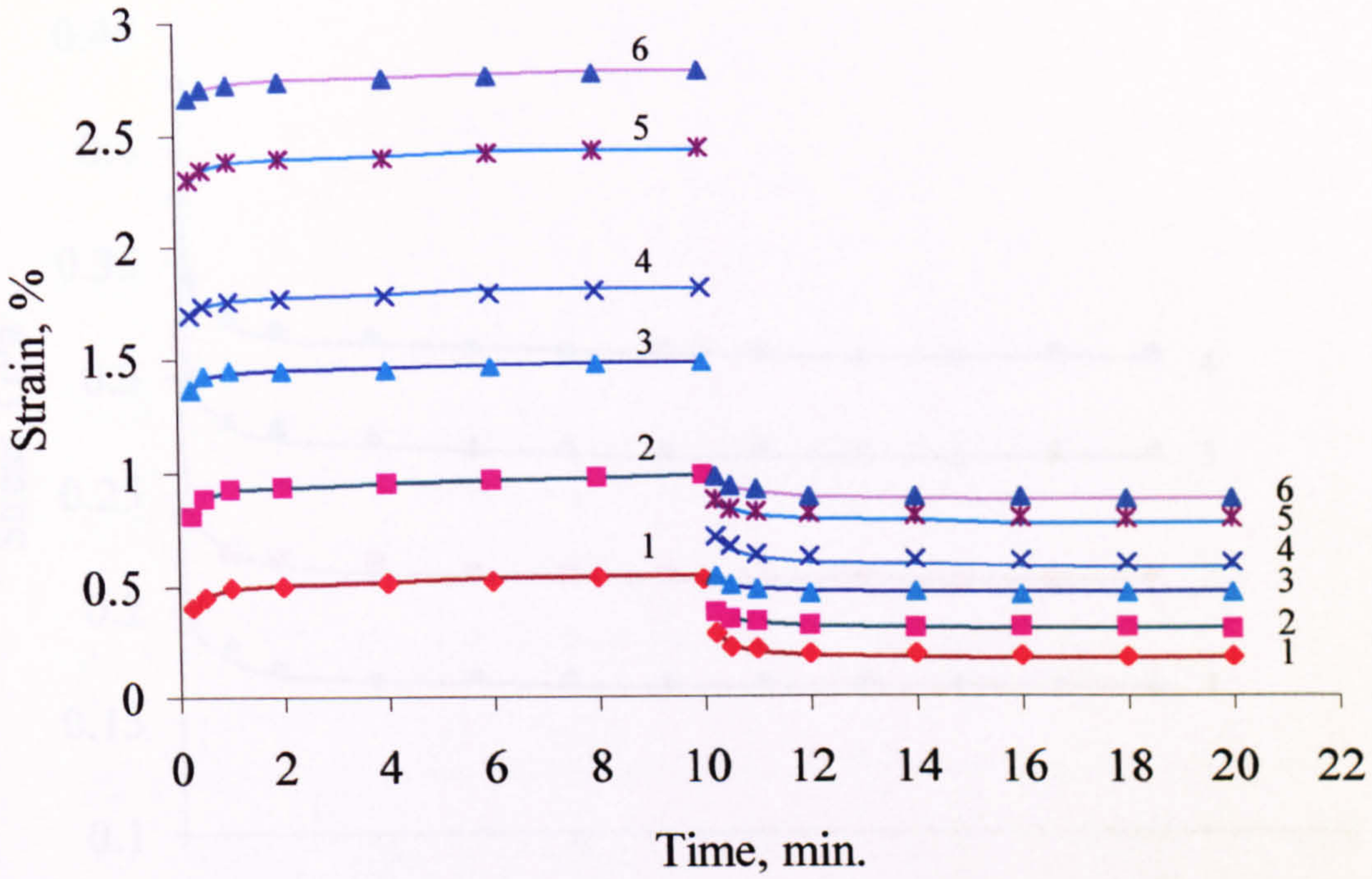

Fig. A_27 The family of creep-recovery curves for terlon yarn at 180 ℃ at σ: (1) 0.25 GPa; (2) 0.50 GPa; (3) 0.74 GPa; (4) 0.99 GPa; (5) 1.23 GPa; (6) 1.54 GPa

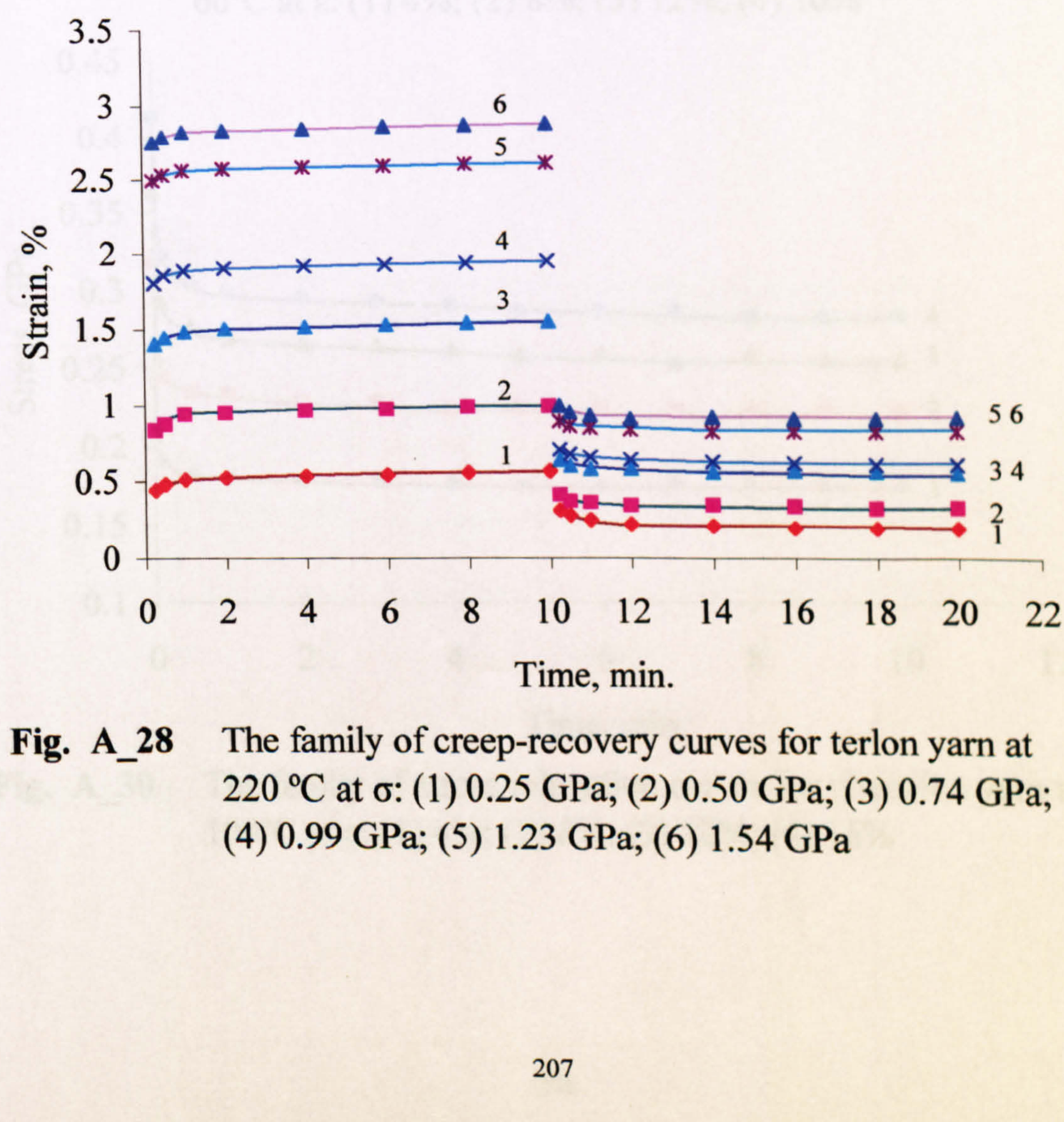

Fig. A_28 The family of creep-recovery curves for terlon yarn at 220 ℃ at σ: (1) 0.25 GPa; (2) 0.50 GPa; (3) 0.74 GPa; (4) 0.99 GPa; (5) 1.23 GPa; (6) 1.54 GPa

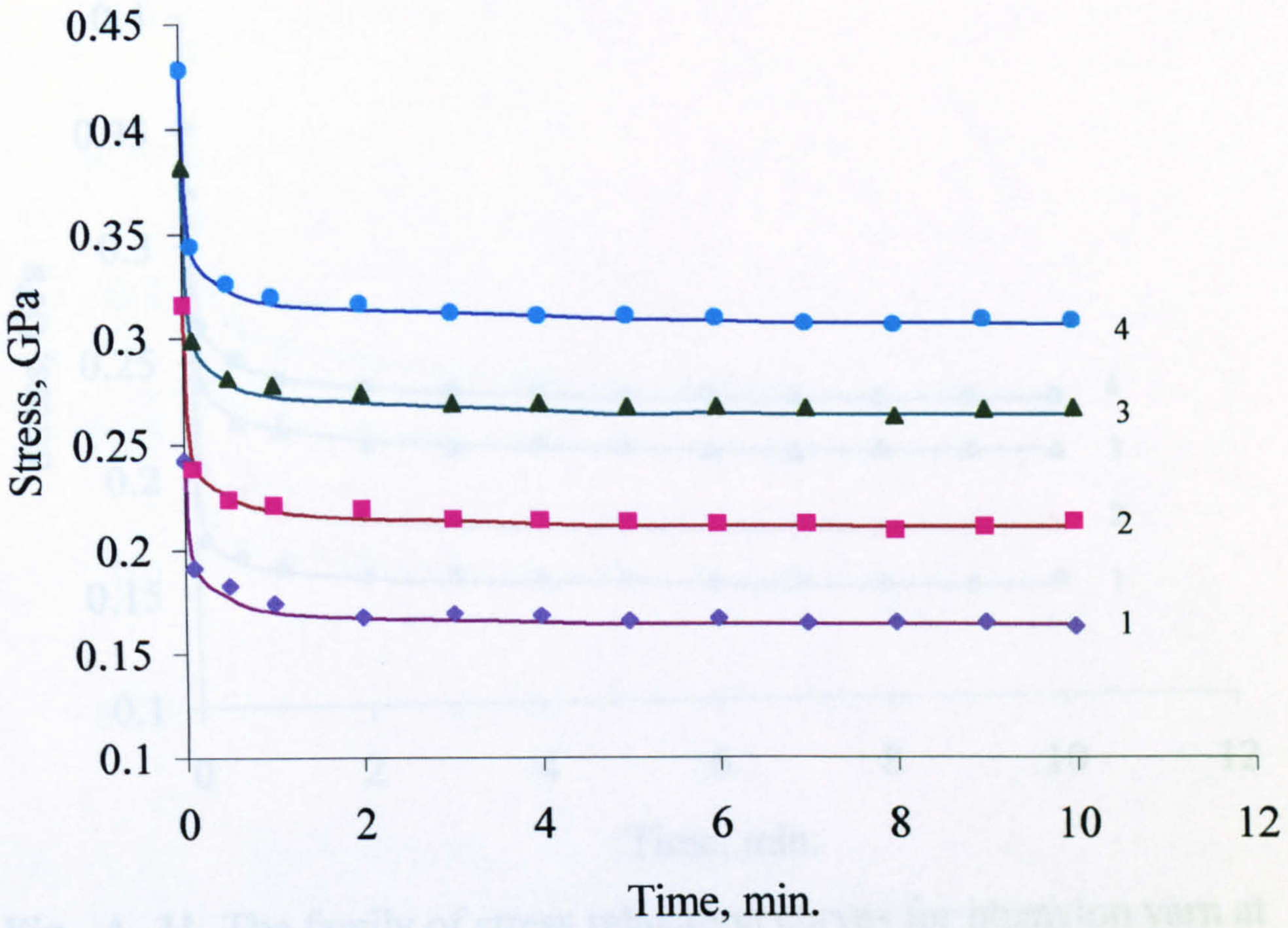

Fig. A_29 The family of stress relaxation curves for phenylon yarn at 60°C at ε: (1) 4%; (2) 8%; (3) 12%; (4) 16%

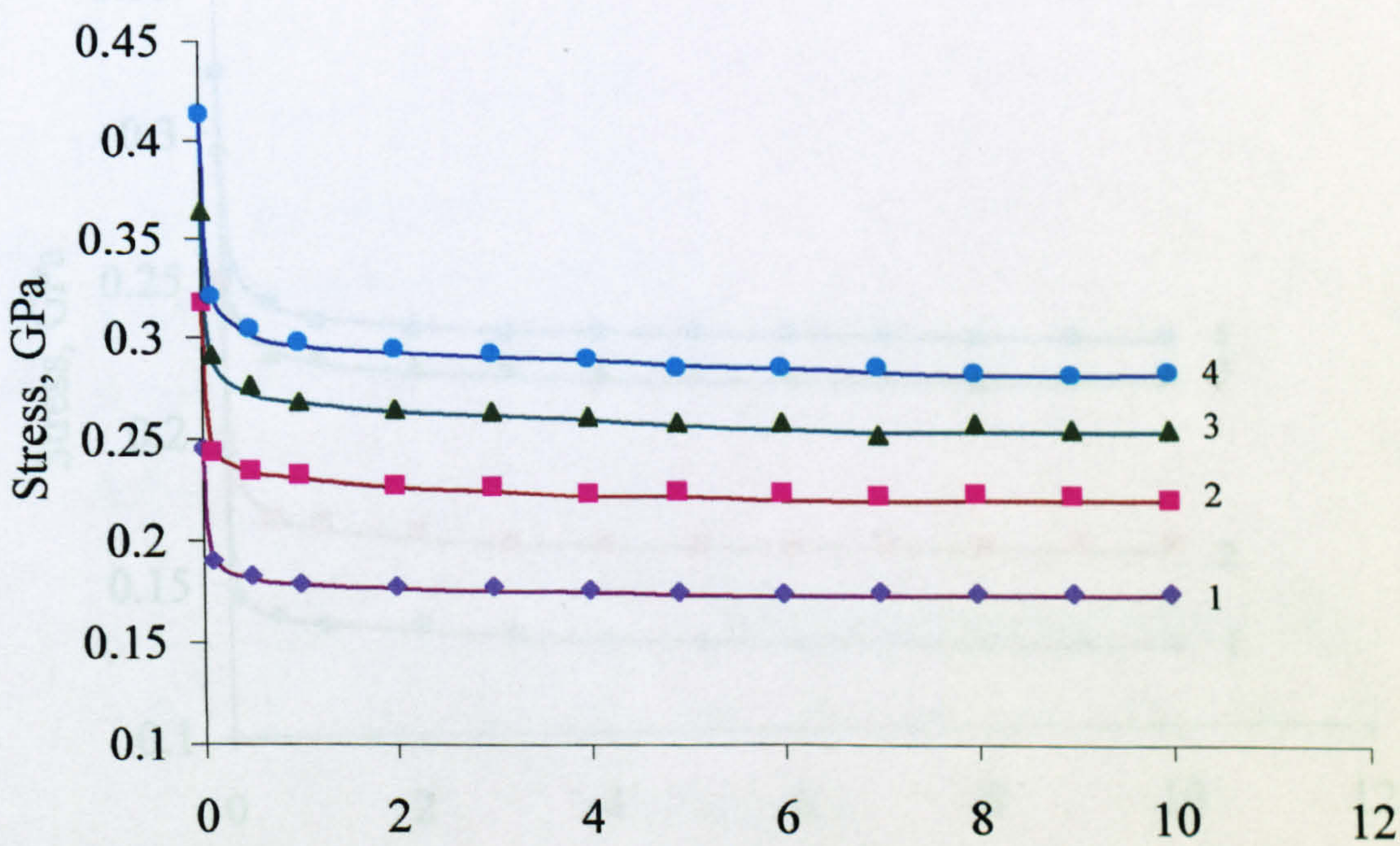

Fig. A_30 The family of stress relaxation curves for phenylon yarn at 100°C at ε: (1) 4%; (2) 8%; (3) 12%; (4) 16%

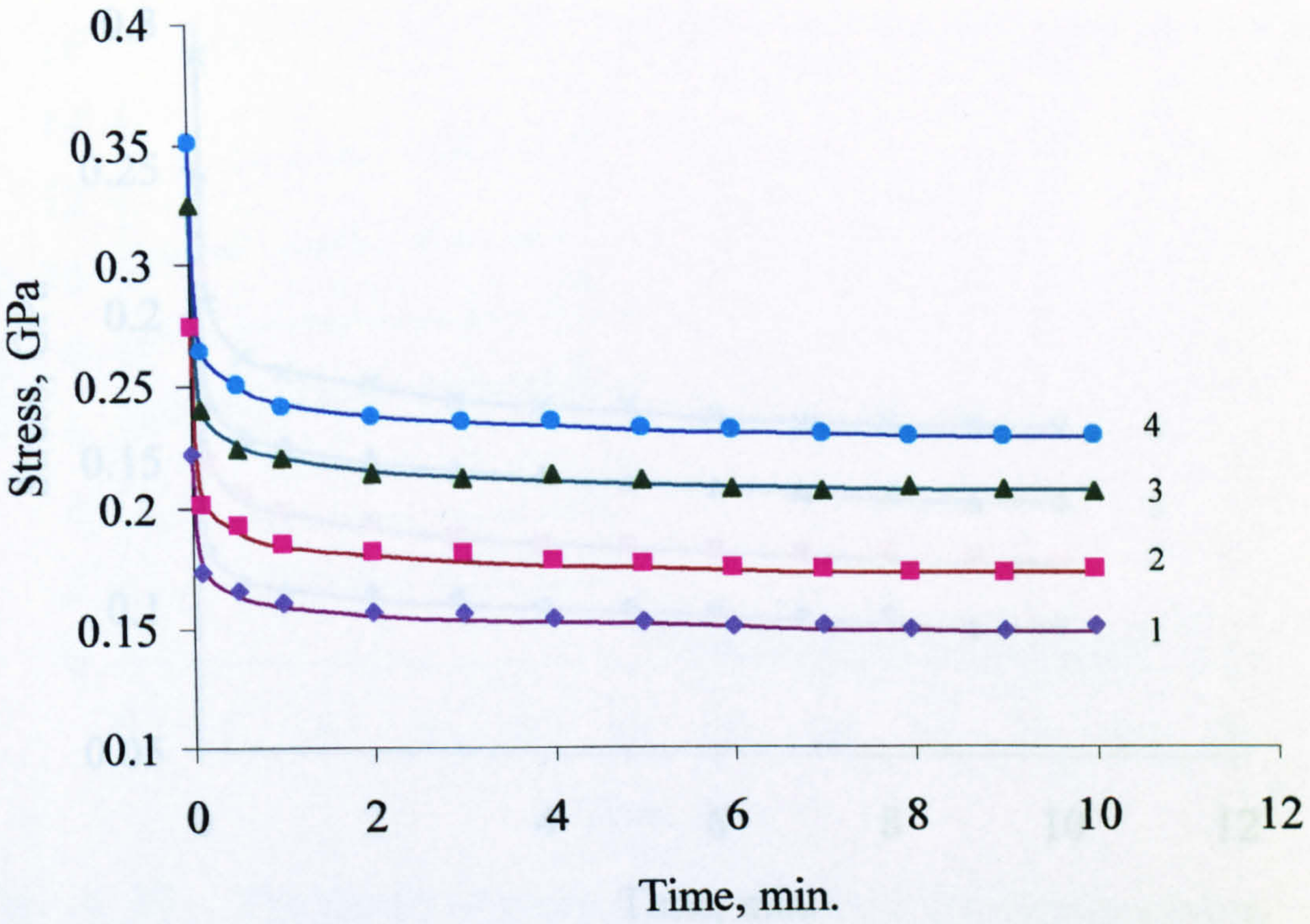

Fig. A_31 The family of stress relaxation curves for phenylon yarn at 140°C at ε: (1) 4%; (2) 8%; (3) 12%; (4) 16%

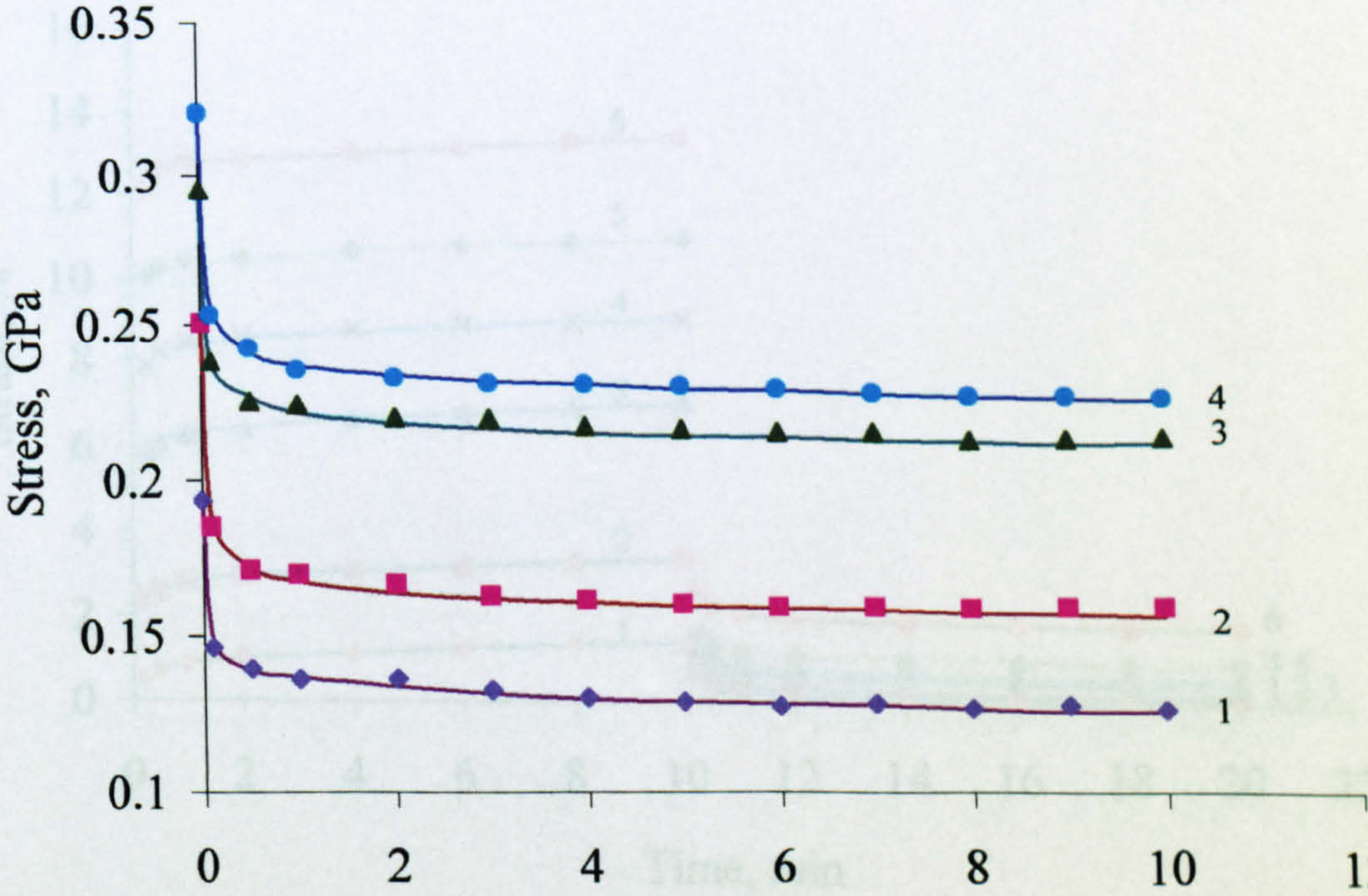

Fig. A_32 The family of stress relaxation curves for phenylon yarn at 180°C at ε: (1) 4%; (2) 8%; (3) 12%; (4) 16%

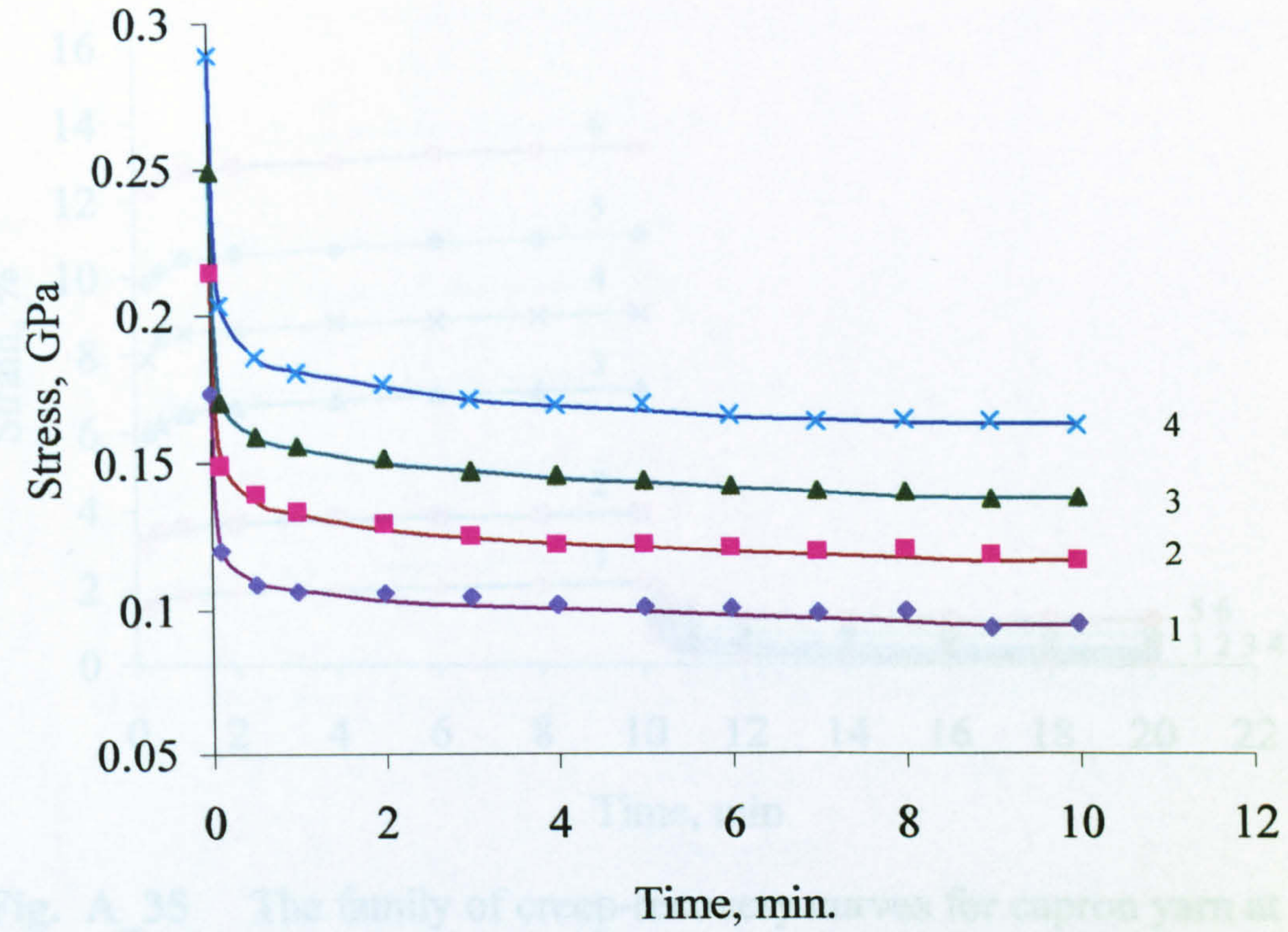

Fig. A_33 The family of stress relaxation curves for phenylon yarn at 220°C at ε: (1) 4%; (2) 8%; (3) 12%; (4) 16%

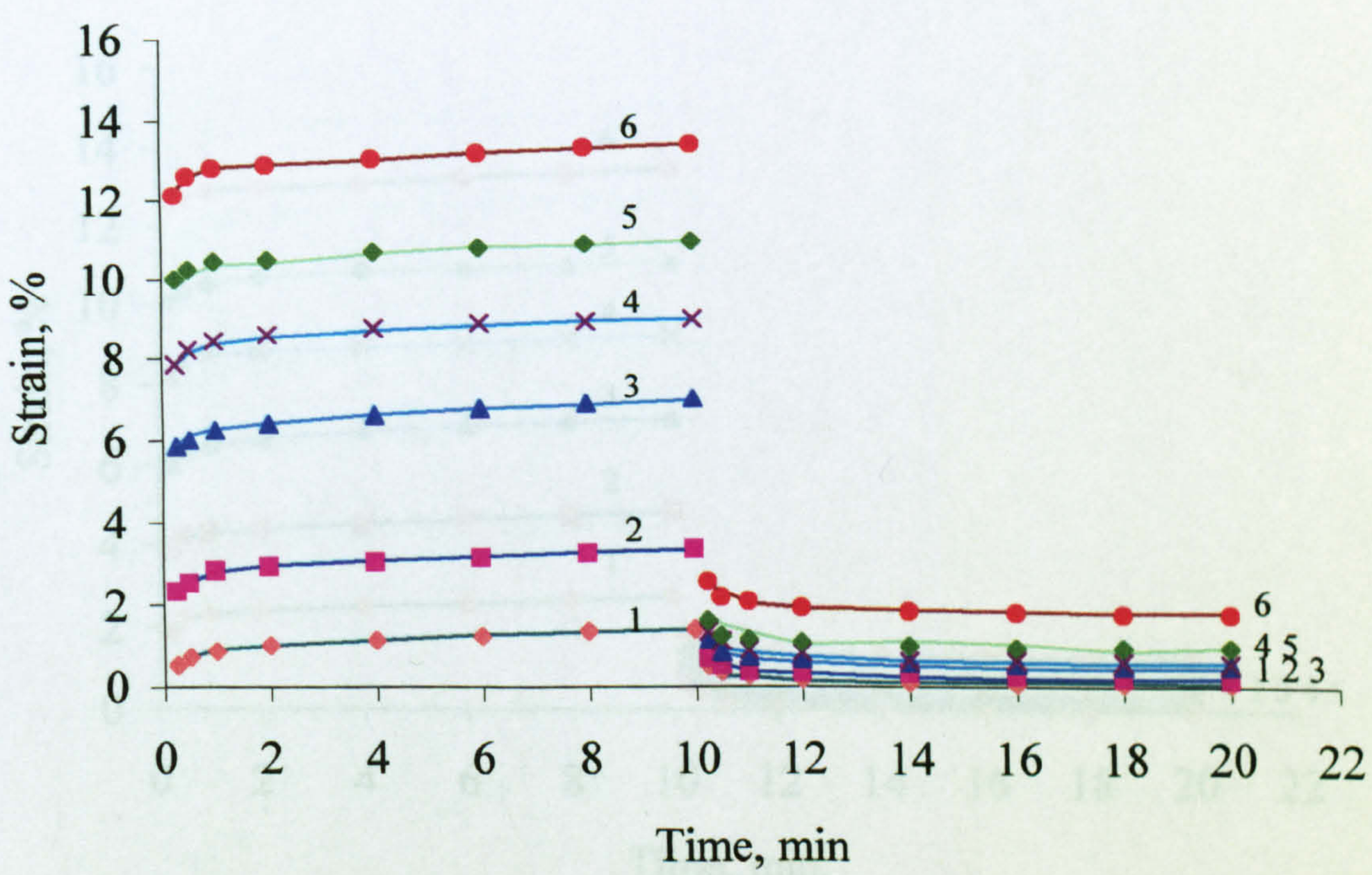

Fig. A_34 The family of creep-recovery curves for capron yarn at 40 °C at σ: (1) 0.08 GPa; (2) 0.12 GPa; (3) 0.16 GPa; (4) 0.24 GPa; (5) 0.32 GPa; (6) 0.49 GPa

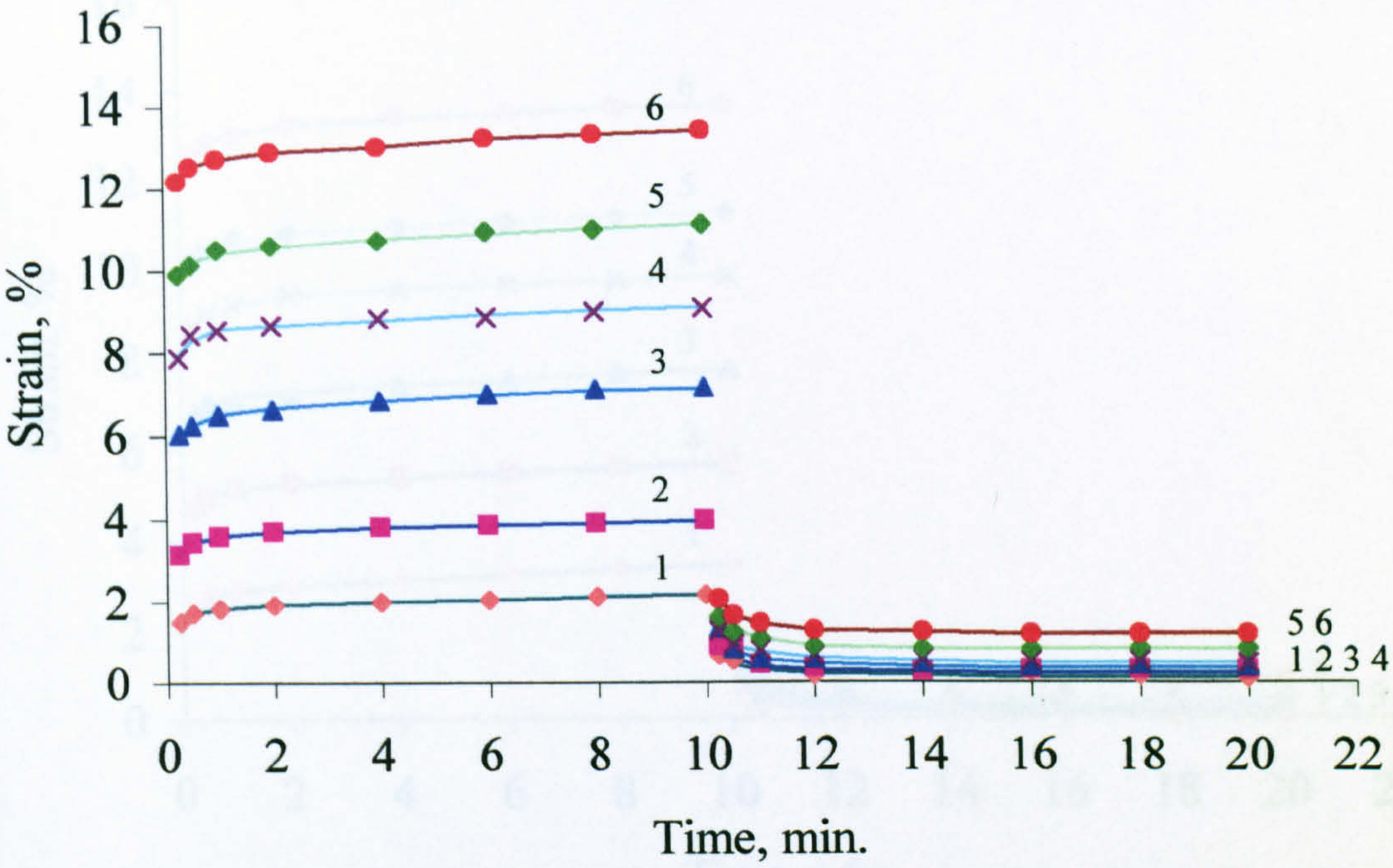

Fig. A_35 The family of creep-recovery curves for capron yarn at 60°C at σ: (1) 0.08 GPa; (2) 0.12 GPa; (3) 0.16 GPa; (4) 0.24 GPa; (5) 0.32 GPa; (6) 0.49 GPa

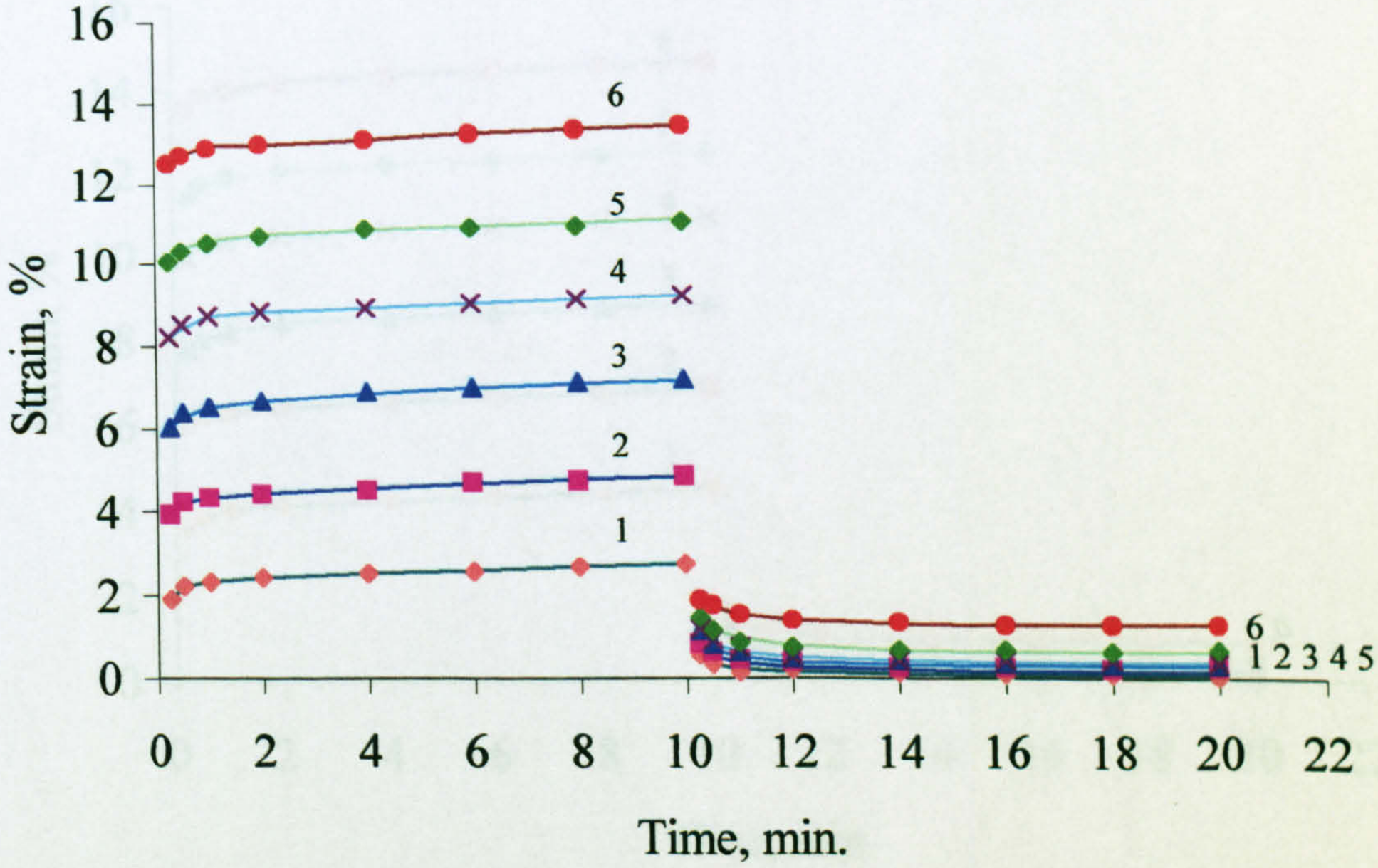

Fig. A_36 The family of creep-recovery curves for capron yarn at 80 °C at σ: (1) 0.08 GPa; (2) 0.12 GPa; (3) 0.16 GPa; (4) 0.24 GPa; (5) 0.32 GPa; (6) 0.49 GPa

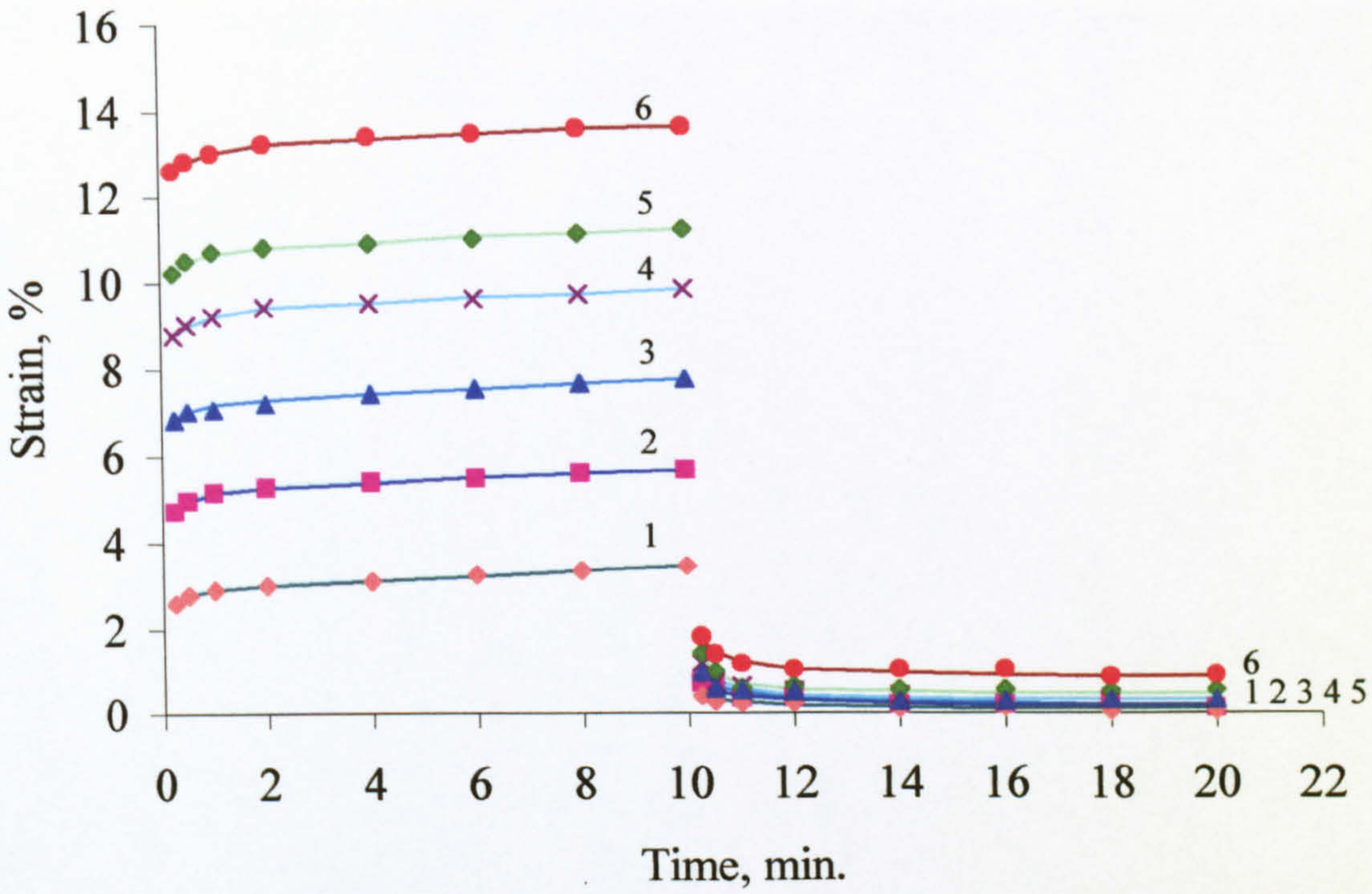

Fig. A_37 The family of creep-recovery curves for capron yarn at 100°C at σ: (1) 0.08 GPa; (2) 0.12 GPa; (3) 0.16 GPa; (4) 0.24 GPa; (5) 0.32 GPa; (6) 0.49 GPa

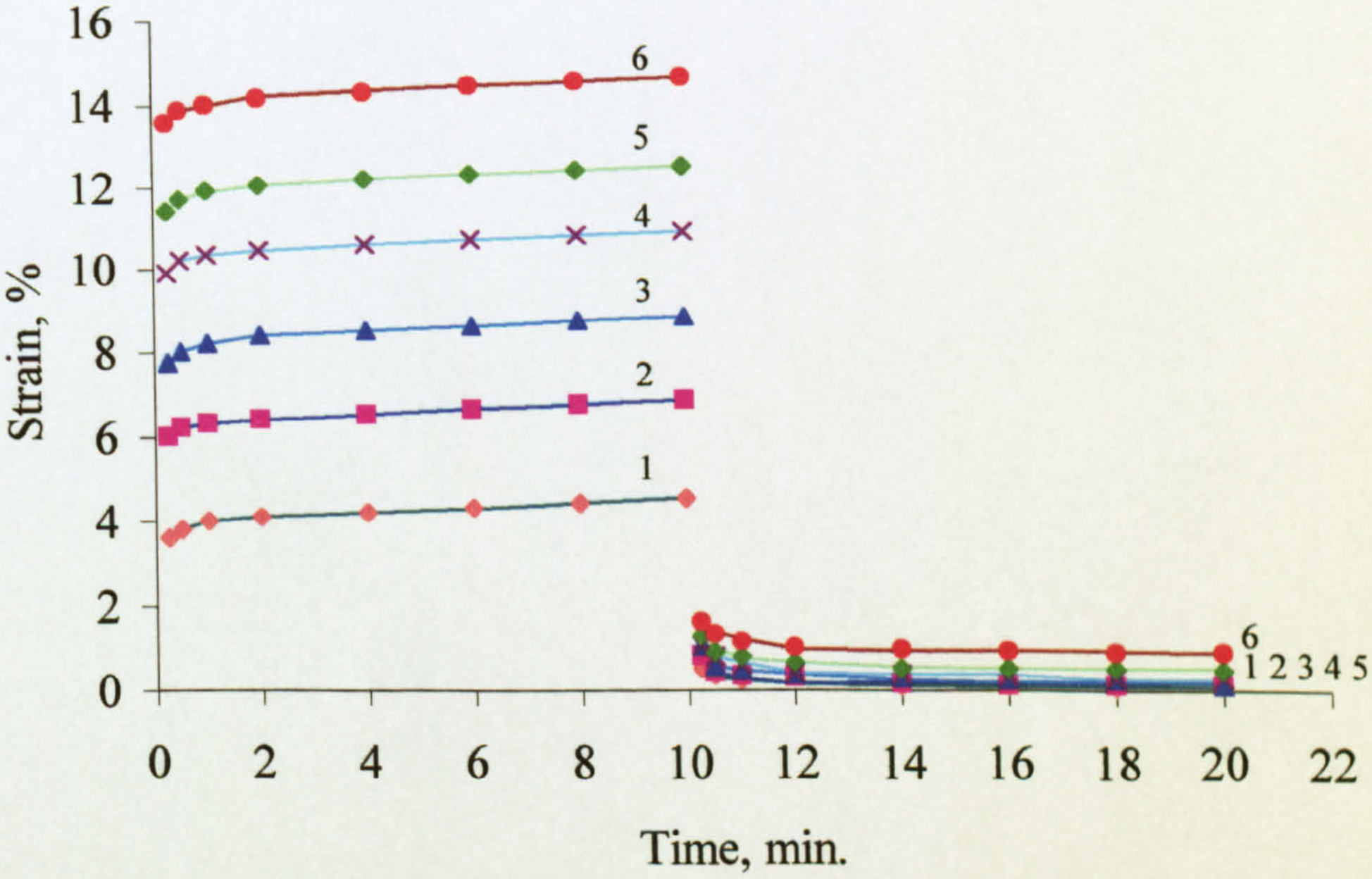

Fig. A_38 The family of creep-recovery curves for capron yarn at 120°C at σ: (1) 0.05 GPa; (2) 0.07 GPa; (3) 0.09 GPa; (4) 0.10 GPa; (5) 0.12 GPa; (6) 0.19 GPa